Behaviour Based Autonomy for Single and Multiple Spacecraft

Gianmarco Radice

Thesis submitted to the Department of Aerospace Engineering of the Faculty of Engineering, University of Glasgow, for the Degree of Doctor of Philosophy.

Gianmarco Radice, December 2002

"With autonomy we declare that no sphere is off limits. We will send our spacecraft to search beyond the horizons, accepting that we can not directly control them, and relying on them to tell the tale"

Bob Rasmussen, New Millennium Autonomy Team

Abstract

Current research in space systems engineering has highlighted the requirement for increasingly autonomous spacecraft and planetary rovers to meet the stringent needs of future missions. The purpose of this thesis is to present a new approach in the concept and implementation of single and clustered micro-spacecraft. The one true "artificial agent" approach to autonomy requires the micro-spacecraft to interact in a direct manner with the environment through the use of sensors and actuators. As such, there is little computational effort required to implement such an approach, which is clearly of great benefit for limited micro-satellites. Rather than using complex world models, which have to be updated, the agent is allowed to exploit the dynamics of its environment for cues as to appropriate actions to take to achieve mission goals. The particular artificial agent implementation used here has been borrowed from studies of biological systems, where it has been used successfully to provide models of motivation and opportunistic behaviour. The so called "cue-deficit" action selection algorithm considers the micro-spacecraft to be a non linear dynamical system with a number of observable states. Using optimal control theory, rules are derived which determine which of a finite repertoire of behaviours the satellite should select and perform. The principal benefits of this approach is that the micro-spacecraft is endowed with self-sufficiency, defined here to be the ability to achieve mission goals, while never placing itself in an irrecoverable position.

Acknowledgements

After all these years I have got quite a list of people who contributed in some way or other to this thesis, and I would like to take this opportunity to thank them.

Colin, my supervisor, for continuous enthusiasm, inspiration and friendship, and without whose help this work would not have been finished.

I am grateful to many people, past and present, in the Department of Aerospace Engineering for their friendship and assistance. Among them Angus, Jason, Eric, Richard, Brian, Mark, Ryan, Martin, Frank, Stefano and Miguel.

The people of the Space Systems Engineering group: Mal, Gareth, Teri and Spencer for their comments, suggestions and ideas.

Emily and Helen for helping out with all things a student needs helping out with.

To all those people who have made Glasgow a very special place over all these years: Fraser, Norton with Sean, Scott with Karen Lucy and Kitty, Brian, Hersh, Jonny, Ian with Estelle, Kev. Baby Jesus, Wavey, Dave, Shmucky, Craig, Jeremy and Phil.

All the friends from back home: Giangi "JJ", Seba "Siepe", Davide "The Head", Cristiano "Crisalide Lionheart", Carlo, Andrea and Luisello; the email banter is always great.

I would like to thank my parents, Ferdinando and Valeria who have always supported and encouraged me throughout the years, my sister Alessia and my in-law family Anna, Gianni and Sergio for their support and love.

Last but not least I would like to dedicate this work to my wife Ilaria, in more ways than one my better half, and my daughter Matilde, my little angel. You are my greatest motivation.

Contents

List of Figures

CHAPTER ONE: INTRODUCTION TO SPACECRAFT AUTONOMY

CHAPTER TWO: STATE SPACE APPROACH TO BEHAVIOURISM

CHAPTER THREE: FROM ETHOLOGY TO ROBOTICS

CHAPTER FOUR: POTENTIAL FUNCTIONS

CHAPTER FIVE: ORBITAL AND SPACECRAFT MODEL

CHAPTER SIX: SINGLE SPACECRAFT

CHAPTER SEVEN: CLUSTERED SPACECRAFT

List of Tables

CHAPTER SIX: SINGLE SPACECRAFT

CHAPTER SEVEN: CLUSTERED SPACECRAFT

CHAPTER I

INTRODUCTION TO SPACECRAFT AUTONOMY

1.1 PREFACE

The development of autonomy technologies is the key to three vastly important strategic technical challenges facing future spacecraft missions. The reduction of mission operation costs, the continuing return of quality science products through increasingly limited communications bandwidth and the launching of a new era of solar system exploration, characterised by sustained presence and in depth scientific studies. New deep space missions, coupled with the challenge to do things "faster, better, cheaper" have highlighted the need for increasingly more autonomous spacecraft. Spacecraft autonomy will bring significant advantages by improving resource management, increasing fault tolerance and simplifying payload operations. Also, when considering the communication delays in deep space missions, the requirement for autonomy becomes clear. Ground stations and controllers will not be able to communicate and control distant spacecraft in real-time to guarantee pointing precision and safety. There is the need therefore to provide autonomous and semi-autonomous computational capabilities to enable and enhance further deep space missions.

This thesis will propose an autonomous action selection methodology applicable to a variety of autonomy problems. The approach considered in this work

provides a method for action selection that balances the demands of the satellite users – gathering or transmitting data – and the actions necessary to guarantee the survival of the spacecraft – charging the battery and thermal control. The study is presented firstly with an examination of the theories and applications behind behaviour oriented agents consisting of Chapters 2 and 3. A background in control theory using potential functions and the general application of this algorithm is examined in Chapter 4. The description of the environmental and spacecraft model is given in Chapter 5. The extensions of the methods, introduced in the earlier chapters, to a control algorithm capable of controlling single and clustered spacecraft satellite are discussed in Chapters 6 and 7. Finally conclusions and recommendations are drawn in Chapter 8.

1.2 ESTABLISHING A VIRTUAL PRESENCE IN SPACE

Recently, renewed motives for space exploration have been offered to the scientific community, thanks to a series of discoveries that suggest the possibility of life in space. While still controversial, the best known example is the Martian meteorite ALH84001, discovered in 1996, which analysed at fine resolution showed "*native microfossils, mineralogical features characteristic of life, and evidence of complex organic chemistry*" [McKay et al. 1996]. More recently, after much speculation [Lewis 1971, Reynolds et al. 1983], the Galileo mission has provided encouraging evidence that Europa, one of Jupiter's sixteen known moons, might have an ocean of liquid water under a layer of ice, stimulating ideas that life might possibly exist in such an environment [Kerr 1997, McKinnon 1997, Zimmerman 1997]. If the search for life on Mars is to be a fossil hunt, the hunt for life on Europa will be for

low level life. Extending a virtual presence in space to confirm or deny these findings requires new means of exploration that have higher performance and lower costs than traditional missions. Planetary missions such as Galileo or Cassini have budgets exceeding several billion dollars, and ground crews of over 100 personnel.

The Mars Pathfinder mission introduced a shift within NASA towards lighter and cheaper missions, operated by small ground teams [Cook 1998]. The viability of this concept was demonstrated in the summer of 1998 when the Mars Pathfinder landed on Mars and enabled the Sojourner micro-rover to land on the surface of the red planet [Mishkin et al. 1998], Figures 1.1 and 1.2.

Figure 1.1 Pathfinder and Sojourner on Mars

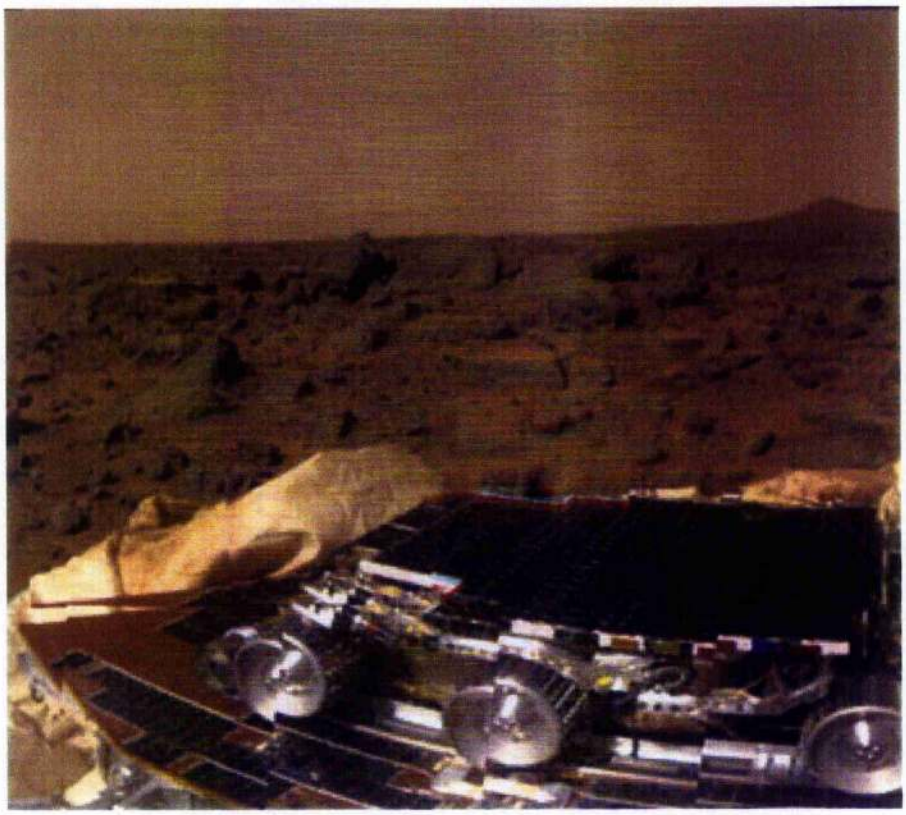

Figure 1.2 Sojourner rover leaving Pathfinder to explore Mars

Pathfinder and Sojourner although successful, lack the on-board intelligence necessary to achieve the goals of more challenging missions. Future Mars rovers are expected to operate for over one year, emphasizing the need for the development of remote agents that are capable of continuously and robustly interacting with an unknown environment. A current project under consideration at the NASA Lewis and NASA Ames research centres is the development of a solar aeroplane to survey the Martian surface. Given the thin CO_2 atmosphere on Mars, an aeroplane flying a few hundred feet above the Martian surface is equivalent to a terrestrial plane flying more than 30 km above sea level. Developing an aeroplane that can autonomously survey Mars over long periods of time, while negotiating the harsh Martian climate, requires the creation of remote agents that are able to accurately model and quickly adapt to their environment.

A second example, which motivates new space science missions, is the discovery of the first planet around another star. This discovery raises the question of the existence of Earth-like planets somewhere in the universe [Mayor and Queloz 1995]. To meet this challenge NASA is developing a series of interferometric telescopes, which identify and categorize planets by measuring a "wobble" in the star, around which the planets are orbiting [Dallas 1998]. This can be achieved by placing three optical units onto three separate spacecraft, extending the technology challenge to the development of multiple, tightly co-ordinated remote agents.

A final example is the question of the possibility of life under Europa's frozen surface. In February of 1998, the Galileo mission identified features that lead to the conclusion that Europa may have subsurface oceans, hidden under an icy layer. To explore this ocean, NASA is currently considering an ice penetrator (cryobot) and submarine (hydrobot) that could navigate beneath Europa's surface [NASA 1999], Figure 1.3.

Figure 1.3 Hydrobot exploring Europa's ocean.

This hydrobot would need to operate autonomously within an environment that is completely unknown. This is perhaps the greatest challenge which autonomous systems must face: to be situated in an environment of which little, if nothing at all is known, to face unprecedented conditions and dangers, hours away from a possible remote human intervention. Another suggestion for the exploration of Europa is the "Arthur C. Clarke" mission, which proposes the utilisation of a fleet of self-organising imaging microbot explorers [Buckland and Johnson 1999].

Taken together these examples of small explorers, including micro-rovers, aeroplanes, formation flying interferometers, cryobots and hydrobots, provide an extraordinary opportunity to develop remote agents that will assist in establishing a virtual presence in space, on land, in the air and under the sea of other worlds.

1.3 NEW MILLENNIUM PROGRAMME

As highlighted above, the level of on-board autonomy necessary for future missions is unprecedented. Coupled with this is the challenge of achieving such capabilities at a fraction of the cost and design time of previous missions. With the creation of the New Millennium Program in 1995, NASA has put forth the challenge of reducing mission costs, while at the same time improving space technologies and scientific return [JPL 1996]. To successfully meet these new standards four major challenges must be met. Firstly, the spacecraft must carry out autonomous operations for long periods of time with no human intervention. This requirement stems from a variety of sources including the cost and limitations of deep space communication. Secondly, autonomous operations must guarantee success through tight deadlines and

resource constraints. Tight deadlines derive from orbital dynamics and rare celestial events, while limited resources, such as power or propellant, must be carefully managed throughout the mission. Thirdly, spacecraft operations will have to be highly reliable. The harsh environment of space may cause unexpected failures, and flight software must compensate for such failures through reconfiguration or repair. Finally, spacecraft operations involve parallel activities between coupled subsystems: sensors (star trackers, sun sensors, gyros), actuators (thrusters, reaction wheels) and science instruments. These hardware/software subsystems operate as concurrent processes that must be co-ordinated to ensure meaningful interactions. New Millennium Program missions will demonstrate these new technologies. Each one of the missions already planned has clearly defined scientific objectives, although recent discussions have raised the issue of doing too much science and not enough technology. By using new technology to successfully accomplish these objectives, the New Millennium Program missions will demonstrate that the technology is not only reliable but also applicable to future NASA missions [Rayman 1998].

1.3.1 Deep Space 1 – Validating New Technology –

The first of the New Millennium Program missions, Deep Space 1 (DS1), has validated a dozen new technologies in flight. Deep Space 1 was launched on a Delta 7326 rocket on Saturday October 24, 1998 and has now completed the first leg of its mission with the flyby of comet Braille on July 29, 1999, Figure 1.4.

Figure 1.4 Artist impression of Deep Space 1 at comet Braille

An additional encounter with the short period comet Borrelly was performed in September 2001. One of the technologies to be validated is solar-electric propulsion: a Xenon ion engine coupled with solar concentrator arrays, which provides a power source for the ion engine [JPL 1998a]. Ion propulsion allows faster access to interesting regions of the solar system with a lower launch mass. Sensors evaluating the impact of ion propulsion on the spacecraft help determine the compatibility of the propulsion system with other spacecraft subsystems and science instruments [JPL 1998b]. More importantly, DS1 tested an artificial intelligence system designed to plan and execute spacecraft activities. The Remote Agent Experiment (RAX) was scheduled to act as an agent of the operations team on-board the spacecraft, formulating its own plans [JPL 1998c]. The Remote Agent devises its plan by combining mission goals, provided by the operations team, with its detailed knowledge of both the conditions of the spacecraft and how to control it. It then executes the plan, constantly monitoring its own progress. Should problems develop,

the Remote Agent is able to repair them, or work around them in most cases. The Remote Agent software uses model-based reasoning algorithms, constraint-based, goal-directed planning and execution algorithms, and a fail–operational fault-protection approach. Specifically RAX is made up of three components with each playing a significant, integral role in controlling the spacecraft. The Planner and Scheduler (PS) produces flexible plans, specifying the basic activities that must take place in order to accomplish the mission goals. Smart Executive (EXEC) carries out the planned activities while the Mode Identification and Recovery (MIR), also known as Livingstone, monitors the health of the spacecraft and attempts to correct any problems that occur. These three parts work together and communicate with each other to make sure that DS1 accomplishes the goals of the mission. EXEC requests a plan of action from PS. A plan for a given time period, based on the general mission goals and current state of the spacecraft is produced by PS. EXEC receives the plan from PS and fills in the details of the plan – determining which subsystem must be activated to complete the planned activities – and commands the spacecraft systems to take the necessary actions. MIR constantly monitors the state of the spacecraft, and in the case of failures, suggests recovery actions. EXEC executes the recovery action or requests a new plan from PS that will take into account the failure. All components of RAX are constantly communicating, using inter-process communication, with each other and with external components of the spacecraft. MIR receives information regarding the state of different components from monitors located throughout DS1. PS must receive information from planning experts in order to generate a plan: the navigation system reports to PS regarding the spacecraft's current attitude, and the attitude control system tells PS how long it will take to turn the spacecraft to a new

attitude. Finally EXEC sends commands to other pieces of the flight software which in turn control the spacecraft's systems or flight hardware.

May 1999 represented a milestone in the history of the development of spacecraft autonomy. In two separate experiments the Remote Agent was given control of Deep Space 1 and demonstrated numerous autonomy concepts ranging from the ability to respond to high level goals by generating and executing plans on-board, to robust plan execution and model-based fault protection. The Remote Agent Experiment was scheduled to be performed during a three week period starting May 10, 1999. An unexpected anomaly on board DS1, which led to spacecraft safing, delayed the start of the experiment and took time away from the preparation for the Braille asteroid encounter. In order not to jeopardize the encounter, the DS1 team decided to limit RAX to just one week of operation starting May 17, 1999, reclaiming the following week for encounter preparations. On Monday May 17, 1999, at 03:04 GMT, mission control received a telemetry packet confirming the beginning of the RAX on DS1. The first plan was generated correctly, but not after some unexpected circumstances created some apprehension. PS was generating the plan following a different search trajectory than what had been observed in ground testing with no apparent reason for this discrepancy. It was later found out that the spacecraft and the ground test-bed differed on the contents of the file containing asteroid goals, and PS was actually solving a slightly different problem than the one it had solved on the ground. In fact this unexpected circumstance allowed RAX to demonstrate that PS problem solving was robust to last minute changes in the planning goals.

The two day scenario continued smoothly and uneventfully with a simulated Miniature Integrated Camera and Spectrometer (MICAS) switch failure, the ensuing re-plan, and the start of Ion Propulsion System (IPS) thrusting. The following day

however it became apparent that RAX had not commanded the termination of the IPS thrusting as expected. The experiment was stopped shortly after, with an estimated 70% of the RAX validation objectives achieved. The cause of the problem was identified as a missing section in the plan execution code. This created a race condition between two EXEC threads. If the wrong thread won the race, a deadlock situation would occur, by which each thread would be waiting for an event from the other. This is what happened in flight, although this same situation never arose in more than a thousand ground platform simulations. Following the discovery of this problem, the DS1 team generated a 6 hour RAX scenario to demonstrate the remaining 30% of the RAX validation objectives. This new scenario was activated on Friday May 21, 1999, and everything ran smoothly until the time to activate the IPS arose. Unfortunately an unexpected problem in the supporting software failed to confirm an IPS state transition thus causing RA to correctly stop commanding the IPS start-up sequence. This discrepancy however did not cause any major problems, and RA was able to continue executing the rest of the scenario to achieve the rest of its validation objectives [Nayak et al. 2000].

Future work regarding the Remote Agent can be divided into three categories: fundamental improvements in the capabilities of its components, improvements in usability and upcoming applications. Several basic research areas are being pursued to improve future iterations of the Remote Agent. Contingent planning enables a planner to create a plan with branches that may be taken if any of a range of likely events occur, reducing the need to re-plan. Improving uncertainty handling will allow MIR to better track multiple ambiguous trajectories the system may be following and recommend actions that are safe and goal directed. New tools for graphically creating and debugging models are being developed to make Remote Agent and similar

technologies more capable, easier to use, and easier to test and validate. Remote Agent technology is also being successfully transferred beyond the original team, to other NASA missions [Bernard et al. 1999].

1.3.2 Deep Space 2 – Networked Science on the Martian Surface –

The Deep Space 2 (DS2) mission was launched on January 3, 1999 piggybacking on the Mars Polar Lander. DS2 consisted of two small probes designed to conduct experiments below the surface of Mars [JPL 1998d]. On December 3 1999, five minutes before entering Mars' upper atmosphere, the lander was to jettison the cruise stage, to which the DS2 probes were attached. The force of separation would initiate mechanical pyro devices, which in turn would separate the microprobes from the cruise stage, approximately 18 seconds later. Each DS2 entry system consisted of a 27 x 35 cm elliptical aeroshell containing the probes. Upon impact with the Martian surface, the aeroshell would shatter and the probe would separate into two parts. The forebody would penetrate as far as 1 meter below the surface, with the aftbody remaining on the surface to relay data back to Earth via the Mars Global surveyor spacecraft, which has been orbiting Mars since September 1997.

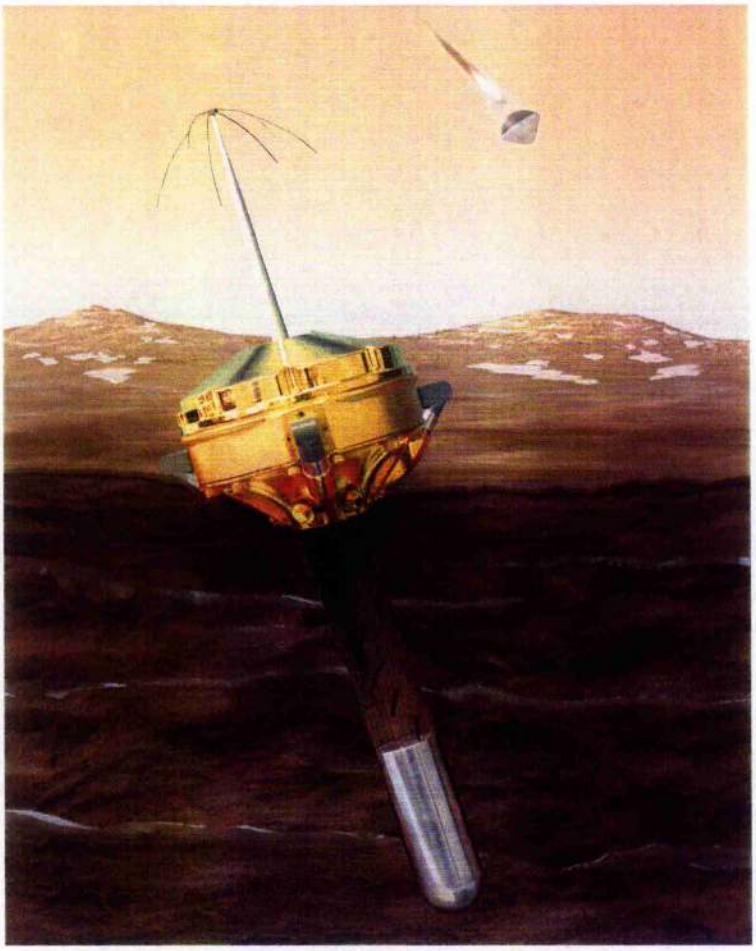

Figure 1.5 Deep Space 2 probing the Martian surface

Communications between the aftbody and the forebody would be ensured by a flexible cable. This mission targets several scientific and technological goals. The primary goal of using two probes was to demonstrate networked planetary missions. Following impact the probes would have started collecting data to validate new microelectronic and micromechanical technologies. Each probe would then transmit data to the orbiting Mars Global Surveyor using a radio in the UHF band at 7000 bits per second. Normally each probe would be in a low-power listening mode until receiving a signal from Mars Global Surveyor telling it to transmit data. The orbiter would switch back and forth between communicating with each of the DS2 probes for about two minutes apiece and then either transmit the data to Earth immediately, or

store the data temporarily and transmit it as soon as possible. Unfortunately since December 3, 1999, there has been no contact between Earth ground stations and either the Mars Polar Lander or the Deep Space 2 microprobes. Investigations are currently underway to try and understand the dynamics of the accident and provide explanations.

1.3.3 Deep Space 3 – Formation Flying Optical Interferometry –

Deep Space 3 (DS3) will consist of three formation-flying spacecraft designed to image remote objects in great detail. Since Galileo's first telescope mankind has tried to build bigger and better telescopes to help us see further out into the universe, in increasingly great detail. A major new opportunity came with our ability to put large telescopes into orbit, above the Earth's obscuring atmosphere. The Hubble Telescope, launched a decade ago, was the first large optical telescope in space, opening up stunning new possibilities for astronomical research. Instead of constantly increasing the size of space telescopes, making them heavier and more expensive, DS3 will validate a new concept for viewing the distant Universe. The telescopes will be placed on individual spacecraft, and arranged to form a constellation, giving us the resolution of a single, very large telescope, Figure 1.6. The spacecraft carrying the telescopes will have to fly in an incredibly precise formation: a formation that would provide the greatest possible resolution. The amount of detail visible to such a telescope will allow unprecedented detail of nearby stars and galaxies [JPL. 1998e].

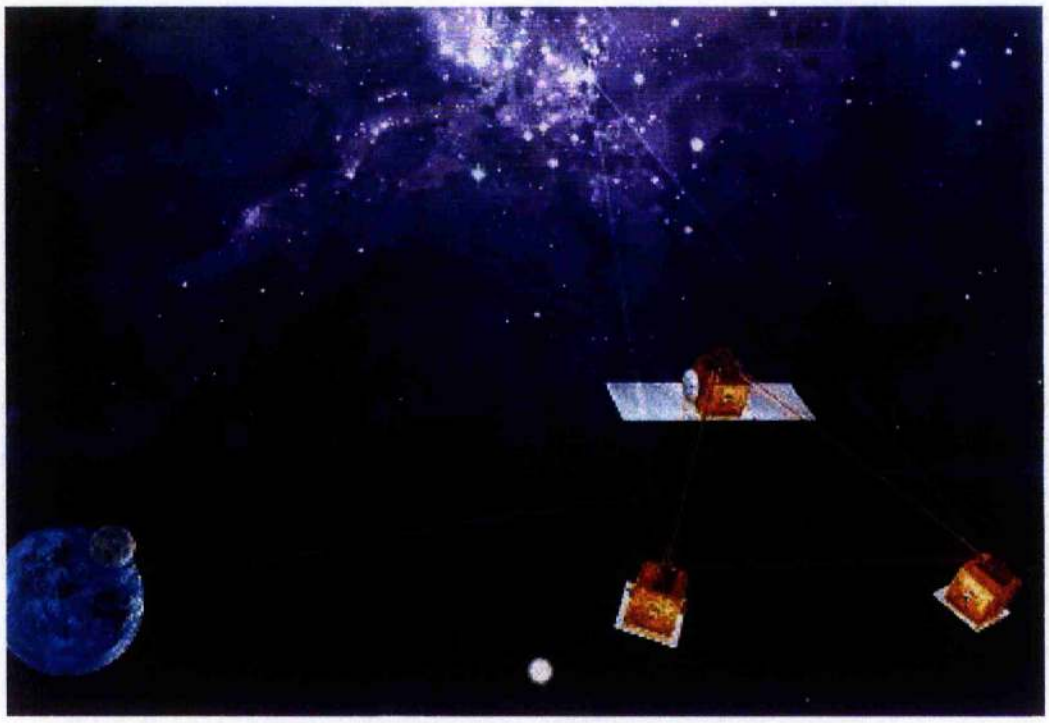

Figure 1.6 Deep Space 3 formation-flying

The technological obstacles for such a mission are high because of the demanding requirements of interferometry: the three spacecraft must be able to maintain their positions and orientation within ± 1cm and ± 1arcminute of each other [JPL 1998f]. The spacecraft will be separated across distances of order 1 km, and continuously turned and pointed at different stars, contracting and expanding the relative distances. These demanding conditions require high precision lasers and sensors to monitor millimetre-sized positional changes, miniature attitude control jets, and advanced autonomous control systems, to make the individual systems act as one. The scientific benefits are obvious, and the success of DS3 will make future interferometry missions (Space Interferometry Mission, Terrestrial Planet Finder and Terrestrial Planet Imager) more feasible and less expensive.

1.3.4 Deep Space 4 – Rendezvous With a Comet –

Deep Space 4 (DS4), also known as Champollion, was scheduled to launch in April 2003. It would have then rendezvoused with the comet Temple 1 and gone into orbit about the nucleus on April 2006. After four months of orbiting at 100 km, a lander would be deployed to soft-land on the comet's surface. A drill would then have been used to collect samples of the nucleus, which were to be analysed on-board with the resulting science data transmitted back to Earth. The possibility of returning the sample to Earth was scheduled for 2010 [Muirhead and Kerridge 1999]. Due to the small size, irregular shape and variable surface properties of small bodies, accurate position estimation is needed for safe and precise small body exploration. Because of the communication delay induced by the large distances between Earth and targeted small bodies, landing must be done autonomously using on-board sensors and algorithms.

Figure 1.7 Deep Space 4 lander on the cometary surface.

Current navigation technology does not provide the precision necessary to accurately land on a small body, so other positioning techniques had to be investigated. Computer vision offers a possible solution to the precise positioning problem; camera images can be automatically analysed to determine the position of the spacecraft with respect to a proximal body. A software tool was developed that enables autonomous position estimation near small bodies through on-board visual surface feature tracking and landmark recognition. Feature tracking and motion estimation are used to determine continuous updates to the spacecraft state vector. Visual landmark recognition and position estimation are used to estimate spacecraft position in a body-centred co-ordinate system. By combining continuous motion estimates with occasional position estimates, continuous body-centred position is obtained [Johnson and Matthies 1999]. Unfortunately this mission was cancelled in July 1999, due to budgetary constraints.

1.3.5 Space Technology 5 – Constellation Trailblazer –

This mission, planned for launch in 2003, will attempt to fly three miniature spacecraft in formation [JPL 2000a]. Space Technology 5 (ST5) will test methods for operating a constellation of spacecraft as a single system, Figure 1.8. Another eight new technologies will be validated in the harsh space environment near the boundary of Earth's protective magnetic field, known as the magnetosphere. ST5 will usher a new era of smart, miniature satellites, which will carry a range of spacecraft services including advanced guidance, navigation and control, attitude control, propulsion, high bandwidth and complex communication functions [JPL 2000b].

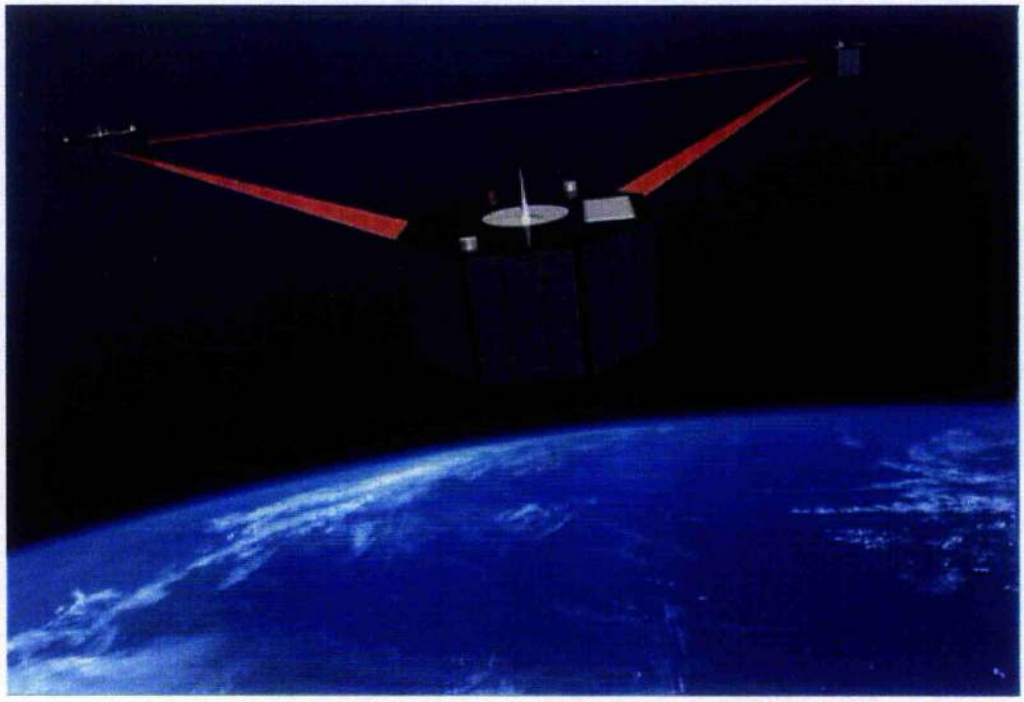

Figure 1.8 Space Technology 5 in orbit over the Earth

The scientific return will be concentrated on measuring the effects of solar activity on the Earth's magnetosphere. The goal is to achieve sufficient scientific understanding of solar activity and terrestrial magnetic storms to enable the forecasting of space weather and allow for its harmful effects on space and ground systems to be minimized [JPL 2000c]. Among the technologies that will be validated is the Formation Flying and Communications Instrument (FFCI). Currently under development at JPL, this is a miniature spacecraft communications system that provides the capability to communicate between spacecraft and determine the positions of the spacecraft relative to each other and the ground, using the Global Positioning System.

1.4 ESA HORIZON 2000

In 1983 it became clear that the European Space Agency (ESA) could no longer continue with its existing method of selecting projects without a long term prospective, and some form of commitment that would allow the scientific community to better prepare itself for the future [Bonnet 1995]. In June 1984, priorities had been established and the "Cornerstones" were approved in four domains: solar terrestrial physics, comet science, X-ray and submillimetre astronomy. In addition, the plan also included both small and medium size projects, but with no a priori exclusion of disciplines, so that a community not "served" by one of the scheduled missions could still find its place. In this way the programme had an element of flexibility and its contents could be adapted to the evolution of science, as well as to the opportunities offered by international cooperation. Along with the main missions, cheaper and faster missions, called Small Missions for Advanced Research in Technology (SMART) have recently been introduced. The purpose of these missions is to test new technological concepts to better prepare for future Cornerstones missions [ESA 1998].

1.4.1 SMART 1 – Lunar Observer –

The planetary objective selected for the SMART-1 mission is to orbit the Moon for a nominal period of six months and will mark the first time that Europe sends a spacecraft to the Moon, Figure 1.9. The project aims to have the spacecraft ready early in 2003 for launch as an Ariane-5 auxiliary payload, and designed to test new technologies for future missions including solar electric propulsion and on-board data handling.

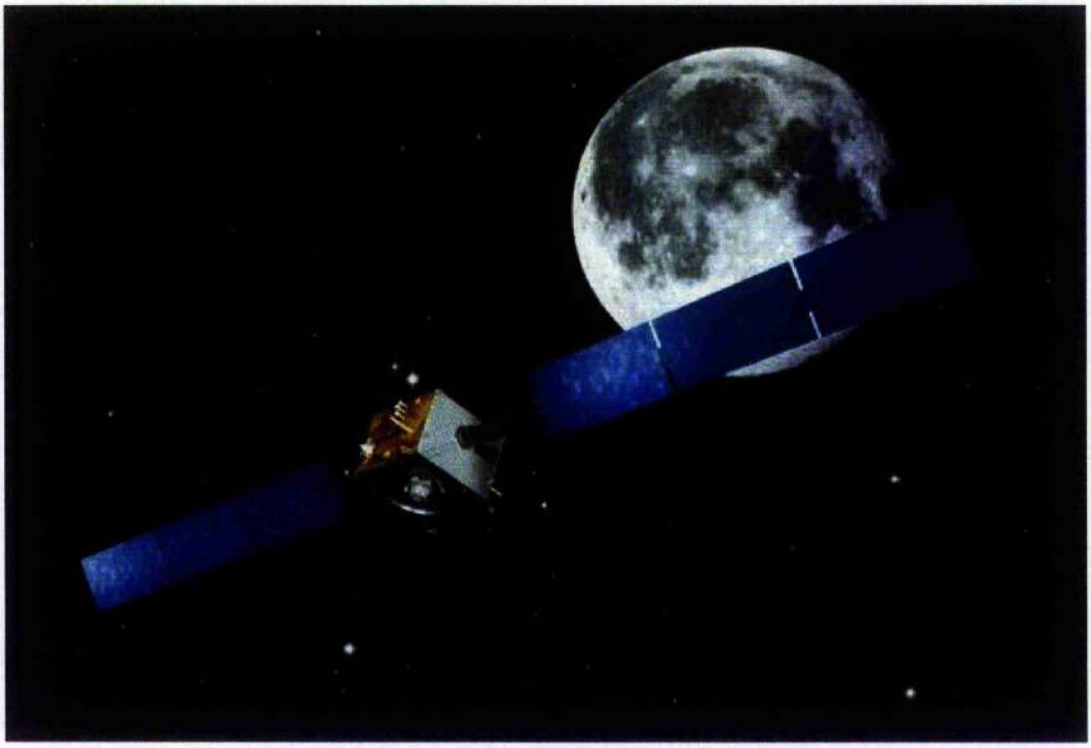

Figure 1.9 Smart 1 orbiting the Moon

It will take the spacecraft approximately 17 months to reach the moon and enter a polar lunar orbit of 1000 km perilune and 10,000 km apolune. For the following 6 months the spacecraft will carry out its scientific objectives, by returning data on the geology, morphology, topography and mineralogy of the Moon. Following in the steps of DS1, SMART 1 will be contributing to on-board autonomy with the On Board Autonomous Navigation (OBAN) experiment. The spacecraft will not be relying itself on OBAN for guidance and navigation, which will be managed from the ground station at the European Space Operations Centre (ESOC), but will function in open loop, obtaining all the data required for navigation. Instead of being processed on- board, this information will be sent back to be processed on Earth. The experiment will involve the spacecraft looking at certain celestial objects, taking images of them with the camera and relaying this together with information from the

attitude and control systems to the OBAN ground system, which will calculate the precise trajectory [ESA 2000].

1.4.2 Rosetta – Landing on a Comet –

The Rosetta mission is one of the cornerstone missions of the European Space Agency scientific programme. After launch in January, 2003 (the launch window opens January 15), Rosetta will fly out to Mars for a gravity assist in August 2005 and return for an Earth flyby on November 2005. A flyby of the main belt asteroid Mimistrobell will occur on July 2006, followed by a second gravity-assist Earth flyby on November 2007. Following another asteroid flyby (Rodari, April 2008) the spacecraft enters a heliocentric drift phase to intercept the comet at a point close enough to allow communication with the Earth. A rendezvous manoeuvre in November 2011 will lower the spacecraft velocity relative to that of Comet PJWirtanen to about 25 m/s and put it into the near comet drift phase, Figure 1.10.

Figure 1.10 Rosetta orbiting comet Wirtanen.

At the end of a ~90 day cometary observation phase, the relative velocity between Rosetta and Wirtanen will have been reduced to 2 m/s, at a distance of about 300 comet nucleus radii. At this point landmarks and radiometric measurements will be used to make a precise determination of spacecraft and comet relative positions and velocities and the rotation and gravity of the comet nucleus to fine-tune the approach. After global studies of the nucleus are completed, about five areas (500 x 500 m) will be selected for close observation at a distance down to 1 nucleus radius in August 2012. Using the information gathered from orbit, a landing site will be chosen for the Surface Science Package (SSP). The spacecraft will go into an eccentric orbit with a pericenter as low as 1 km over the landing site and an ejection mechanism will separate the SSP from the spacecraft. The lander will touch down on Wirtanen's surface at a relative velocity of less than 5 m/s and will transmit data from the surface to the spacecraft, which will relay it to Earth. The spacecraft will remain in orbit about the comet and make observations through perihelion on 10 July 2013 [Schwehm and Schulz 1999]. The role of autonomy in such a mission is obvious and multi-faceted. The spacecraft will have to contend with uncertainties in real-time due to the long time delay in communication with Earth. Rosetta will also have to select an appropriate landing site and descend to the cometary surface autonomously and safely, in a gravitational environment of which nothing is known at the moment [Bernard et al. 2002]

1.4.3 Beagle 2 – Exploring Mars –

Beagle 2 is the name given to the lander component of the ESA Mars Express mission. The main focus of Beagle 2 is to establish whether there is convincing evidence for past life on Mars, or to assess if conditions were ever suitable. The

eleven day launch window opens on June 1, 2003 with Mars Express arriving at Mars on December 26, 2003. The Beagle 2 lander will be released 5 days before this and coast for five days after release and enter the martian atmosphere. After initial deceleration in the martian atmosphere by an aeroshell, parachutes will be deployed and, about 1 km above the surface, large gas bags will inflate around the lander and protect it when it hard lands on the surface. After landing, the bags will deflate and the top of the lander will open. Beagle 2 is a flat cylindrical spacecraft (diameter of 65 cm and depth of 25 cm) and includes four deployable solar panels, Figure 1.11.

Figure 1.11 Beagle 2 on Martian surface.

At the heart of Beagle 2 is the on-board software that must execute all the activities of the lander. During the surface operations phase it is responsible for controlling all of the instruments and cameras together with the lander subsystems such as the robotic arm, communications and power. For most of the operations phase the lander will be out of contact with the Mars Express Orbiter and must autonomously perform the

experiments while maintaining the lander's safety. In addition, although it is only intended that the experiments will be performed sequentially, many other tasks must be performed continuously so that this is a naturally multi-tasking problem because the lander only has a single processor. During the operations phase the on-board software will be required to: ensure the safety of the lander by continuously monitoring and controlling the lander subsystems, deploy the instruments using the robotic arm, use the instruments to perform the experiments requested by the mission controllers, acquire images using the cameras, manage the communications sessions with the orbiter and execute telecommands and generate telemetry. In addition, this is a real-time system so there are many tasks, which could jeopardise the mission if they do not finish within a specified time or are out of sequence.

1.4.4 PROBA – Project for Onboard Autonomy –

This mission was initiated in February 1998 and is now in its final phase [Teston et al., 1997]. Proba was successfully launched on October 22nd 2001, and injected directly into its final polar sun-synchronous orbit at an altitude of 817 km, and 98.7° inclination, initially for a one year mission. The purpose of the mission is to demonstrate new on-board technologies and the opportunities and benefits of increased spacecraft autonomy. A high degree of spacecraft on-board autonomy, together with ground-station automation, considerably reduces the need for ground operations. Proba on-board automatic functions include: nominal operation and resource management computation and control of camera pointing and scanning from raw inputs from users (target latitude, longitude and altitude), payload operations scheduling and execution, data communications management. Proba ground-segment

automatic functions include: spacecraft pass operations, spacecraft performance evaluation, high-level user requests to spacecraft via Internet

Figure 1.12 Proba in flight

The main autonomy functions to be demonstrated by PROBA include the management of on-board resources, the planning scheduling and execution of scientific observations and the detection, identification and recovery from on-board failures [de Lafontaine et al., 1999]. Key to all these on-board autonomous functions is the Attitude and Control Navigation Systems (ACNS) software. The ACNS is responsible for acquiring and maintaining on-board knowledge of the attitude and orbit (the navigation function) for computing the reference trajectories required in various attitude manoeuvres (the guidance function) for executing the attitude control

commands (the control function) and for detecting and identifying on-board failures originating from, or observable by, the ACNS subsystem. During normal operations the attitude knowledge is acquired autonomously from the double-head star tracker. Each of the two optical heads can determine its three-axis inertial orientation starting from a "lost in space" attitude. Knowledge of the PROBA orbit is acquired autonomously via a GPS receiver which is a crucial component of the on-board autonomy demonstration. This will allow pointing of the spacecraft to any orbit-referenced attitude without the need of an Earth sensor. Pointing to geographical Earth references will either be to a fixed target, during ground station overfly or imager utilisation, or in a scanning motion over a 19 km user-selected target area.

1.5 NASDA & ISAS – Japanese Efforts –

Japan has been one of the most successful nations in the realm of terrestrial autonomy applications, and has a huge base of research and development, ranging from components to working systems, for manufacturing, construction and human service industries. From this base, Japan has looked to use autonomous technology in space applications, funding work since the mid-1980s. At first the efforts were primarily concentrated on space robotics, but have since moved on to encompass a wider range of applications. This work was initiated with the development of the Japanese Experimental Module (JEM), which is Japan's contribution to the International Space Station. Following this, the Japanese envision their own robotic space laboratory – Cosmo-Lab – and the slightly more visionary idea of an orbiting space hotel. To realize these scenarios NASDA has developed free-flying robots that

grab, dock and manipulate while in orbit. Also considered are multiple missions to the Moon and Mars with the aim of carrying out extensive surface explorations, using autonomous mobile robots.

1.5.1 Muses-C – To an Asteroid and Back –

The primary scientific objective of the Muses-C mission is to collect a surface sample of material from an asteroid and return the sample to Earth for analysis. The mission plan calls for a May 2003 launch with the arrival at the asteroid 1998 SF36 scheduled in the first half of 2006, Figure 1.13. Muses-C will initially survey the asteroid surface from a distance of about 20 km and then move close to the surface for a series of soft landings and collection of samples at three sites.

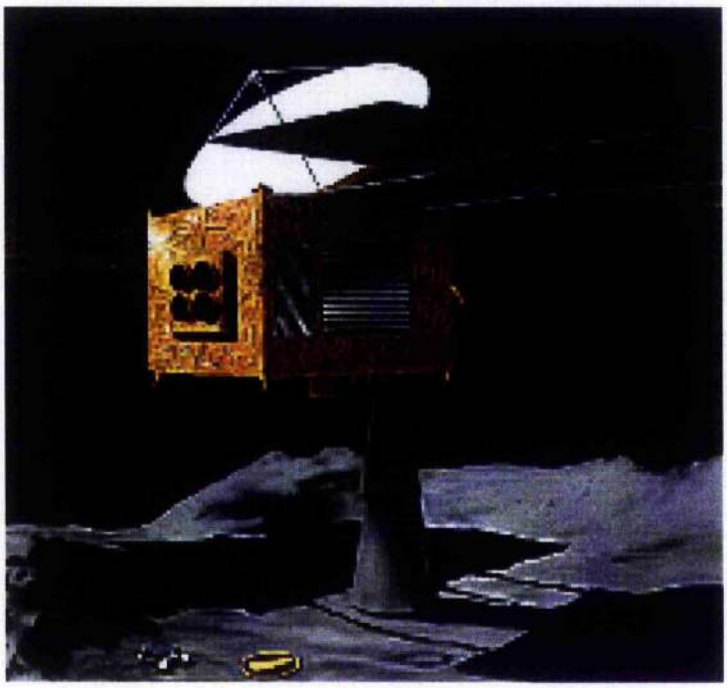

Figure 1.13 Muses-C probing the asteroid

On-board optical navigation will be employed extensively during this period since the long communication delay prohibits ground-based, real-time commanding [Kubota et al. 2000]. The mission also calls for the lander to deploy a small NASA rover onto the surface of the asteroid, however this project was recently cancelled. All operations at 1998 SF36 must take into account the extremely low gravity at the asteroid's surface. After a few months in close proximity to the asteroid, the spacecraft will fire its ion engines to begin its cruise back to Earth. The re-entry capsule will be detached from the main spacecraft and the capsule will coast on a ballistic trajectory, re-entering the Earth's atmosphere in June 2007, landing via parachute at a site yet to be determined.

The Muses-C spacecraft has a box-shaped main body 1.5 m along each side and 1.05 m high. The launch mass is 365 kg, including 64 kg of chemical propellant and 29 kg of xenon gas for its main ion engines. Two solar wings protrude from the side and a 1.5 m diameter high-gain parabolic antenna is mounted on top on a two-axis gimbal. The mission will be equipped with a camera, which will be used for imaging, visible-polarimetry studies and optical navigation near the asteroid, a laser ranging device (LIDAR), and a near-IR spectrometer. The lander will be equipped with a universal sample collection device which will gather 1 to 10 grams of surface samples taken from landings at 3 different locations. Prior to each sampling run, the spacecraft will drop a small target plate onto the surface from about 30 m altitude to use as a landmark to ensure the relative horizontal velocity between the spacecraft and asteroid surface is zero during the sampling.

The rover, or Small Science Vehicle (SSV), should have been dropped onto the surface of the asteroid by the Muses-C spacecraft [Jones et al. 2000]. The rover goals were to make texture, composition and morphology measurements of the

surface layer at scales smaller than 1 cm, investigations of lateral heterogeneity, investigation of vertical regolith structure and to measure constraints on the mechanical and thermal properties of the surface layer. The rover was scheduled to weigh about 1 kg and with capabilities of rolling, climbing, or hopping around on the surface of the asteroid. It was designed to run on solar power and projected to carry a multi-band imaging camera, a near-infrared point spectrometer, and an alpha/X-ray spectrometer (AXS).

1.5.2 Selene – Selenological and Engineering Explorer –

Japan's 30-year project to establish a lunar base is divided into three parts that will start with an unmanned probe and develop into a manned base. The first part of the project, known as the SELENE Project (SELenological and ENgineering Explorer), has already started, Figure 1.14.

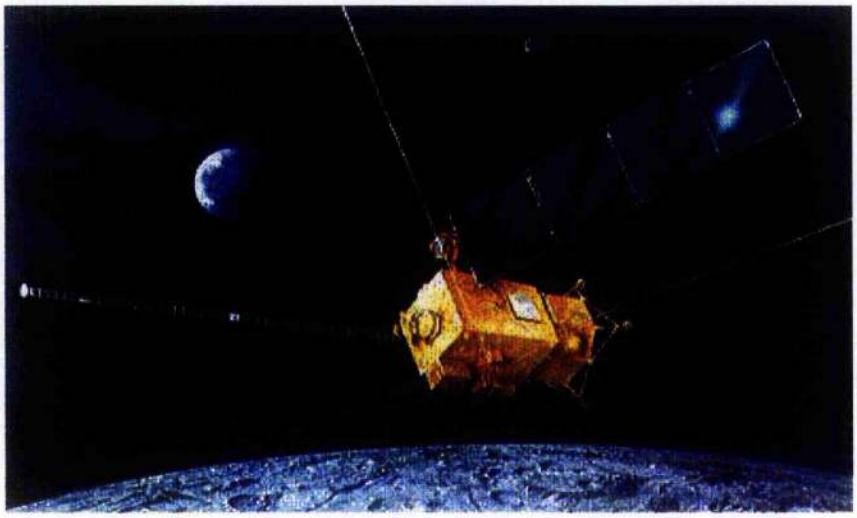

Figure 1.14 Selene orbiting the Moon

Japan plans to use the H-IIA rocket currently being developed to launch its own unmanned Moon probe around 2004. The plan calls for the collection and retrieval of

data to determine the origins and evolution of the Moon and development of technical abilities that will allow for a soft-landing on the Moon's surface. The lunar exploration stage of the SELENE Project involves an orbiter and a relay satellite. The orbiter consists of a mission module and a propulsion module. It will take five days after its launch to reach the relay satellite and enter its elliptical orbit. Then, as it gradually approaches the Moon's surface, it will separate from its relay satellite. At its furthest point in the lunar elliptical orbit, the apolune, the relay satellite will be 2,400 kilometres above the Moon's surface and will measure the gravitational field on the far side of the Moon, and also relay information between the satellite and the Earth. The satellite will take approximately one year and survey the entire Moon surface.

After leaving the lunar orbit at an altitude of 100 km, the propulsion module will reach perilune at a lunar altitude of 15 km. From perilune the module will start to descend via a minimum fuel path, using its main engine. About 4 km above the lunar surface it will stabilise its attitude to start a vertical landing. In the last descent phase it will reduce speed with decreasing acceleration and when 2 m above the surface will stop the descent engine, soft landing at a final speed of about 3 m/s [NASDA 1998]. The orbital correction manoeuvres together with the final soft-landing phase will be performed autonomously on-board and used as a technology demonstrator for future lunar missions.

1.6 MICRO AND NANOTECHNOLOGY

As seen in the previous subsections, the main objective of space agencies is to reduce the costs and delays associated with space-based services, by reducing

spacecraft lifecycle costs without reducing performance. Spacecraft manufacturing is currently a labour intensive task: few similar units are ever produced. Due to this fact, traditional cost reduction approaches such as new design, pre-fabrication and modularity will help reduce costs, but not to the levels required for space missions. One area where innovation is proceeding at a very fast pace is miniaturisation, as can be observed in consumer electronics. Miniaturisation may be achieved by applying micro and nanotechnologies. There are several advantages offered by micro/nanotechnologies. The resources required are reduced, high system reliability is made possible by incorporating several microsystems for redundancy, they can be produced in a batch process and small test facilities are suitable. These advantages are even more significant for the space sector, where each of the above points has a strong influence on costs.

Launch is one of the highest costs for space-based systems, and is directly related to mass. The payload and spacecraft bus are the two other major contributors to cost. The bus mass and cost are related to the payload mass, power requirements and volume. Any reductions in mass, volume and power requirements are therefore desirable and will have a significant effect on cost. Microsystems are considered an excellent means of obtaining these mass and cost reductions. They could also become the means to implement decentralisation, where a number of components could be used in place of a larger centralised one. This leads to cost reduction on space systems, not only at the payload and bus levels, but also in launchers and ground station facilities. The motivation behind the application of microsystems in space is therefore multiple: significant cost reductions, the possibility of enabling new functions and improving the performance of existing ones, better ways of achieving mission goals, the ability to accommodate data proliferation and increases in data

quality and shorter development times. All of these motivations amount to better performance per unit cost and mass. There are however some space specific limitations to microsystems which the space sector will have to devote resources to overcome if this technology is to become widespread and common. The two most critical limitations are the high costs of development and the high susceptibility to radiation. As for any other devices having a high degree of integration, such as microprocessors, costs will increase due the need to qualify them for space use. For example the risk of single event upsets, which are non destructive but disrupt operations, are problematic as devices shrink in size and packing becomes even more dense.

1.7 CURRENT APPROACHES TO AUTONOMY

As highlighted in the previous sections, future international deep space exploration provides unprecedented demands for autonomous spacecraft, rovers, aeroplanes and submarines. When considering the distances involved in deep space missions, and the ensuing communication delays, the need for autonomy becomes clear and obvious: Earth based mission controllers will be unable to communicate with and control distant spacecraft and non-human explorers to ensure timely precision and safety. The new generation of spacecraft and rovers must be smart, adaptable and self-reliant in harsh and unpredictable environments. Several different techniques are currently being investigated as possible methods for autonomy.

1.7.1 Expert and Knowledge-Based Systems

Simply described, expert systems are particular types of computer programs. They differ from most other computer programs in the following ways. Functionally, they can perform decision making or problem solving tasks within a well defined domain at performance levels almost comparable to those of humans. Expert systems primarily encode and manipulate symbolic knowledge rather than numerical data, mathematical equations or algorithms. The greater emphasis is on knowledge, rather than numerical computation. Expert systems arose out of the efforts to apply research in the field of artificial intelligence to practical issues. Artificial intelligence is primarily concerned with trying to model intelligence and human solving capabilities using computational techniques, the central concept being that computers could imitate human intelligence. The 1950s and 1960s were the period when artificial intelligence was primarily concerned with the development of computer programs that could perform tasks that were considered to require a high degree of intelligence, such as playing chess or theorem solving. The key development during this period was the idea of heuristics [Simon and Newell 1958], defined as guidelines for choosing among alternative actions and the creation of LISP (LISt Processing), a symbolic programming language [McCarthy 1962]. Broader aspects of intelligence began to be addressed in the early 1970s, with research being oriented towards model cognition, interpreting natural language, understanding narrative and ways to represent reason about diverse kinds of knowledge. During this period, artificial intelligence was applied toward solving practical real-word problems with the development of Dendral [Feigenbaum et al. 1971], Macsyma [Martin and Fateman 1971] and Strips [Fikes and Nilsson 1971]. The explosion of expert systems in the early 1980s was caused by the realization that computer programs could perform

useful tasks at expert level of performance, if they were endowed with large volumes of specialized knowledge, and were constrained to narrow but real domains. Researchers tried to reproduce human experts by capturing their empirical knowledge. Successful expert systems from this period were Mycin [Buchanan and Shortliffe 1976], Prospector [Duda et al. 1979] and R1 [McDermott 1982]. These successes led to the idea of an expert system that had the basic structure in which rules could be entered, and the matching capability to make deductions based upon these rules.

In a knowledge-based system, the amount of detail in which propositions have to be laid out for a computer to make use of them causes a problem in the management of the profusion of rules. One of the techniques employed to deal with the confusion of rules is to associate a number, called the certainty factor, with each assertion. This number would indicate how sure the system is about the truth. The certainty factor ranges from one – full belief – to minus one – disbelief. Anything in between would indicate a certain degree of doubt or ignorance. The system adopts the conclusion with the highest certainty factor at the end. Another technique is to link related ideas together in "frames", much in the same way the human mind can carry most ideas with a reasonable set of associations. A third approach has been to remove the limitation that an expert system cannot retract any inference drawn from its rules. Some inference engines do allow them to start again if a particular line of reasoning runs into a dead end. The predominant models of representation and reasoning are logic, rules and objects. Logic programming supports a declarative style of representation: knowledge about a domain is represented in the form of facts. The fact base can then be queried about the truth or falsehood of the statement to be tested. This method, also known as first-order predicate logic, though appealing has several

shortcomings. The syntax of assertions has to conform to a rigid framework of logic. These assertions have difficulty in dealing with time and neither do they possess the capability to retract conclusions that no longer hold true. Rule-based systems were first pioneered by applications like Mycin and R1, and are the most commonly used form of representation used in expert systems. Knowledge is represented as IF THEN rules, which are essentially association pairs. The system consists of three components: the rule base contains the knowledge expressed in IF THEN associations over variables, the working memory contains all facts which are true at any stage in the computational process, and the inference engine is the domain and knowledge-independent processing mechanism. The inference machine searches the rule base, matches variable values in the working memory to the preconditions and conclusions of rules in the rule base. When more than one rule is applicable in a situation, the inference engine uses conflict resolution to decide which one is used. The shortcomings of rule-based representation are that they are solely based on variable-value binding. There are other types of relationships essential to capturing knowledge about a domain that are outside the scope of a rule based representation. The use of meta-rules also obscures the actual problem solving strategy used by the system. Object-oriented representation addresses many of the shortcomings of rule-based representation. The structure used in object-oriented systems is an object with associated properties. One of the advantages of these systems is that they allow the representation of all declarative information about a process in a structured way. The disadvantage is that they generally have no built-in problem solving capabilities. The best systems use a hybrid structure, by coupling the object system with a rule base.

Expert systems have been used for many years with great success in various terrestrial fields, ranging from accountancy [Brown and Phillips 1991] to

meteorology [Takle 1990], and from medicine [Frenster 1989] to law [Walter 1988]. Despite these successes, expert systems have intrinsic disadvantages which would make their use in the space autonomy field problematic. The main problem is that knowledge based expert systems are not always able to cope successfully with unusual or rarely occurring situations; to account for all conceivable possibilities would make such a system extremely intensive computationally, while also never being absolutely sure of having covered all avenues. There is also the possibility that competing lines of action lead to a dead-end, virtually stalling the spacecraft, as recently witnessed during the Remote Agent Experiment on-board Deep Space 1. Coupled with the fact that expert systems are limited in their capabilities by their knowledge, makes them unlikely candidates to meet the stringent requirements of future space missions as, for example, the Europa hydrobot explorer, where there is a small knowledge base. The use of expert systems however can still prove very useful for ground station procedures during routine operations.

1.7.2 Fuzzy Logic

Fuzzy logic was devised in 1964 by Lofti Zadeh [Zadeh 1965]. The main idea behind fuzzy logic is that there are many cases where *true* and *false* or *on* and *off* fail to describe a given situation. These cases require a sliding scale where variables can be measured as *partly on* or *mostly true*. Traditional set theory is based on bivalent logic where a number or object is either a member of a set or it is not. With fuzzy logic, an object can be a member of multiple sets with a different degree of membership in each set. A degree of membership in a set is based on a scale from 0 to 1, with 1 being complete membership and 0 being no membership. In a control system, an output is calculated based on the amount of membership a given input

signal has in the configured fuzzy sets. Each combination of sets is configured to have a specified output, and the fuzzy control system calculates an output based on the weighted sum of the amount of membership in each set. Information flow through a fuzzy control system requires that the system inputs go through three major transformations before becoming system outputs. Figure 1.15 shows the three transformations known as fuzzification, fuzzy rule association and de-fuzzification.

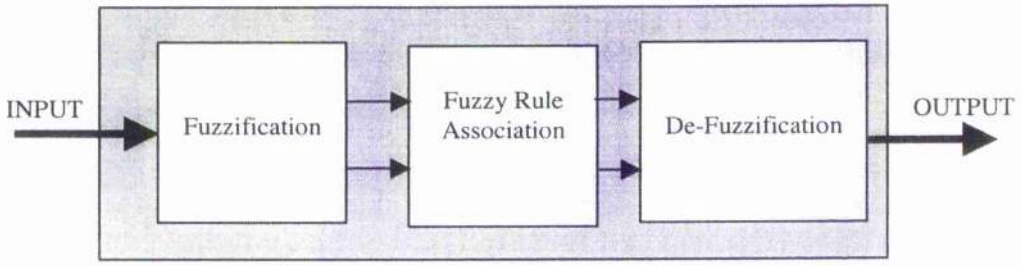

Figure 1.15 Fuzzy system block diagram.

Fuzzification is the process of decomposing a system input into one or more fuzzy sets. Each fuzzy set consists of three components: domain – the range of system input or output values over which the set is mapped, membership function – the curve which maps a system input or output value to a degree of membership value and degree of membership – and the value produced by the membership function. Many types of membership curves can be used; however, triangular shaped membership functions are the most common. Each fuzzy set spans a particular region of a system input or output value, and through the membership function produces a degree of membership value between 0 and 1. The result of the fuzzy set represents the degree to which a system input or output value is a member of that particular fuzzy set. Once the system inputs and outputs have been decomposed into their respective groups of

fuzzy sets, a set of rules associating these fuzzy sets must be defined to govern the system's behaviour. Each rule consists of a condition and an action, where the condition is a function of the input fuzzy sets and the action is a function of the output fuzzy sets as follows:

IF CONDITION **THEN** ACTION

where

CONDITION = f (Input Fuzzy sets)

ACTION = f (Output Fuzzy sets)

A fuzzy system usually requires more than one rule to completely describe all the necessary actions. In practice a set of rules, which comprise all combinations of all possible fuzzy sets for all system inputs, is necessary and can be denoted by an array called the Fuzzy Associative Memory (FAM). The inputs are evaluated using this matrix to determine which rules are true. Since a particular input may fall within more than one component of a fuzzy set, multiple rules may be true for any given set of inputs. Each cell in the matrix contains the control output change for the corresponding input combination. Whether the fuzzy system is performing control or modelling a process, the final result must be an exact – or "crisp" – value and not a fuzzy value. De-fuzzification is required to convert the fuzzy result into an exact value or number. The result of the fuzzy system is the combination of all of the results of all of the rules. For example, if the strength of the condition has a nonzero value, then the action is expected to contribute, at that strength, to the final output. Since several rules can "fire" at the same time, a weighted combination of each rule must be calculated to create a final output value.

Originally, the technique was devised as a means for solving problems in the soft sciences, particularly those that involved interactions between humans, or between humans and machines. It was when Yoshimura Terano [Terano et al. 1972] introduced fuzzy sets to Japan in 1972, that the full power of the method could be appreciated, leading to a host of commercial applications, almost entirely in the field of physical control. The current field of applications range from mass consumer applications [Terai 1991, Tobi and Hanafusa 1991, Klein 1996], to large-scale electro-mechanical processes [Yasunobu and Miyamoto 1985, Ujihara and Tsuji 1988, Spooner and Passino 1995].

Fuzzy logic has features that are particularly attractive in the light of the problems posed by spacecraft autonomy, allowing us to model different types of uncertainty and imprecision and build robust controllers starting from heuristic and qualitative models. However the current knowledge for such applications is still at a very early stage and different problems have to be solved before successfully validating such a technology. The formal analysis of a fuzzy behaviour is the object of intensive research. Some tools exist to prove stability given that a model of the system is available [Tanaka and Sugeno 1992]. However a new set of qualitative performance criteria are needed and formal tools that can tell when a fuzzy controller will, approximately, satisfy these criteria [Shin and Cui 1991]. Also, while fuzzy logic gives us a valuable tool for writing co-ordination strategies, it does not give a solution to the general problem of behaviour co-ordination. Currently there is no way to discriminate a situation where different commands proposed by different behaviours should be averaged, from one where they should be regarded as a conflict to be resolved in some way [Saffiotti 1997]. Before fuzzy logic can satisfy stringent

spacecraft autonomy requirements, progress towards stronger foundation theory and its semantics has to be made [Ruspini 1991, Höhle 1997, Bilgiç and Türksen 1998].

1.7.3 Neural Networks

The concept of neural networks in artificial intelligence evolved from the study of the human mind. In the human brain neurons are connected to sensory organs like the ears, nose, eyes, etc. These neurons are activated when a human is hearing, smelling, seeing, etc. The brain recognizes the experience based on the pattern of the neurons that are active and those that are not. Artificial neural networks simulate the same process within the computer in such a way that they can read sets of data and learn from them. McCulloch and Pitts [McCulloch and Pitts 1943] were the first to develop models of neural networks based on their understanding of neurology in the 1940s. The interaction between computer experts and neuroscientists continued establishing a multidisciplinary trend, which continues to the present day. Considerable interest and activity was stirred in 1958 when Rosenblatt designed and developed the Perceptron [Rosenblatt 1958, 1962]. This system could learn to connect or associate a given input to a random output unit. Another system was the ADALINE (ADAptive Linear Element) developed in 1960 by Widrow and Hoff at Stanford University [Widrow and Hoff 1960]. In 1969 a book by Minski and Papert [Minski and Papert 1969] generalised the limitations of single layer perceptrons to multi-layered systems, with the significant result of raising considerable prejudice against the research and consequent funding reductions. Although public interest and available funding were minimal, several researchers continued working to develop neuromorphically based computational methods for problems such as pattern recognition. During this period several paradigms were generated which modern

work continues to enhance. The progress of the works of Amari [Amari 1967], Werbos [Werbos 1975], Fukushima [Fukushima 1975], Grossberg [Grossberg 1976] and Klopf [Klopf 1982] were important to the re-emergence of interest in the neural network field.

The novel structure of the information processing system is the key element of neural networks: it is composed of a large number of highly interconnected processing elements that are analogous to neurons and are tied together with weighted connections that are analogous to synapses, as shown in Figure 1.16.

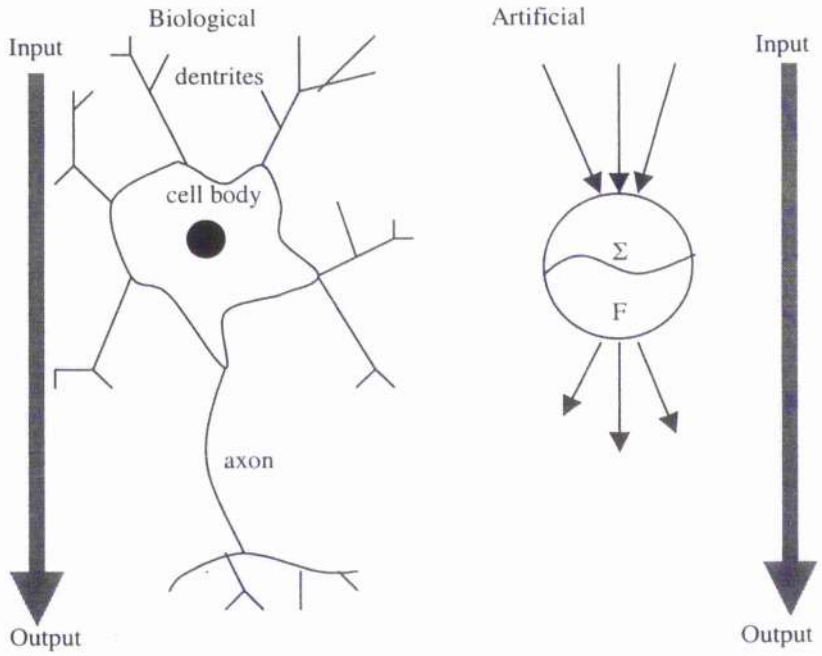

Figure 1.16 Biological and artificial neural networks. The cell receives and combines signals from other neurons through input paths called dendrites and when activated transmits a signal through a single path called axon.

The processing element of a neural network is an artificial neuron. In general each neuron has a set of n inputs x_j with $j \in [1...n]$. Each input is weighted before reaching the main body of the processing element by the connection strength or weight factor w_j. In addition, it has a bias term b_j and a threshold value Θ that has to

be reached or exceeded for the neuron to produce a signal. A nonlinearity function then acts on the produced signal giving an output, which becomes an input for other neurons. Artificial neurons process signals by first summing all the inputs reaching the neuron:

$$net_i = \sum_{j=0}^{n} w_{ij} x_j + b_j \qquad [1.1]$$

where net_i is the total input which reaches the artificial neuron, and second by firing if the summed input reaches or exceeds the threshold level

$$F(net_i) \geq \Theta \qquad [1.2]$$

The purpose of the nonlinearity function is to ensure that the neuron's response is damped as a result of large or small activating stimuli and thus is controllable. In the biological world, conditioning of a stimulus is done by sensory inputs. For example to perceive a sound as twice as loud, an actual tenfold increase of the sound must take place; hence the almost logarithmic response of the ear. The nonlinearity function used in neural networks however is not necessarily a close replica of the biological one; and is often used merely for mathematical convenience.

Currently neural networks are used in several fields for classification [Kathman 1993, Peltorana and Pfurtscheller 1996, Hyötniemi 1996], forecasting [Schöneberg 1990, Grudnitski and Osburn 1993, Azoff 1994, Gorr et al. 1994] and modelling [Miller and Sutton 1990, Harris and Stroud 1992, Horwitz and El-Sibaie 1995]. Despite the success of neural networks their use for spacecraft autonomy

would be problematic. The main problem lies in the fact that the performance of a neural net is entirely dependent on the training data used. If it is easy to obtain data for stock market predictions, medical outcomes or materials classification, it is not so for an environment of which little, if anything at all, is known. To account for all unknown parameters, conditions and situations would lead to validation problems. Neural networks also cannot handle the element of time very well, and this could prove to be a problem in deep space missions when the ground station may be available for communication for a limited period of time and even then with significant lag.

1.8 WORK OVERVIEW

This thesis aims to provide a method, which will allow the autonomous operation of single, and multiple spacecraft, using a behavioural algorithm. The previous sections have highlighted the need for increased spacecraft autonomy to meet the challenges and demands of future space missions, together with increased miniaturisation of components to reduce launch and operational costs. Different approaches to the problem of autonomy were investigated and, while generally successful, present problems in meeting the challenges of guaranteeing complete autonomy, while at the same time reducing the computational workload. In Chapter 2 we will consider the ethological theories and methods that have been used to provide successful motivational schemes for biological agents, animals, while in Chapter 3 we will see how these ideas can be transported into the realm of Artificial Intelligence and autonomous artificial agents. A rigorous mathematical foundation, based on

Pontryagin's Maximum Principle is then used to validate the behavioural algorithm that will allow the spacecraft to sequence its tasks to achieve mission goals. In Chapter 4 we will introduce an attitude control methodology generated by using potential functions. At first, Lyapunov's second method, upon which the control scheme is based, is presented. The potential function is described both in its attractive and repulsive components. The spacecraft attitude change is controlled through an attractive potential that forces the spacecraft to reach a target attitude (new position of equilibrium for the system) while through the repulsive potential we ensure that the spacecraft satisfies any pointing constraints that may be present. This attitude control method will be used to slew the spacecraft between the different objectives, as required by the behavioural algorithm introduced in Chapter 3. In Chapters 5, 6 and 7 the environment and spacecraft are modelled and simulations to ascertain the effectiveness and robustness of the behavioural algorithm are performed, both for a single and multiple spacecraft.

CHAPTER II

STATE SPACE APPROACH TO BEHAVIOURISM

2.1 PREFACE

In this chapter we will try and understand how optimal control theory and state space analysis are an appropriate framework for the multi-dimensional problems of artificial agent behaviour. It is within this framework that the ideas and theories are then expanded to be applied in the realm of Artificial Intelligence. An agent is defined here as any self-sufficient autonomous system, either biological or artificial. Although the motivation for the state space approach to behaviourism has come from biological systems, the application will ultimately be autonomous spacecraft.

2.2 INTRODUCTION

Traditionally, animal behaviour had been classified into functional categories, such as aggressive, feeding and parental behaviour. The assumptions were, not only that the activities within each category serve a common biological function, but also that they have causal factors in common. For example, the various aspects of feeding are said to serve the common function of food intake and are clearly driven by hunger. This led to the tendency of studying a motivational system in relative

isolation from others. In recent years however, interactions between motivational systems are taking on considerable importance.

On the basis of the generalised homeostatic (equilibrium) type of motivational system shown in Figure 2.1, McFarland distinguishes between primary and secondary aspects of motivation [McFarland, 1971].

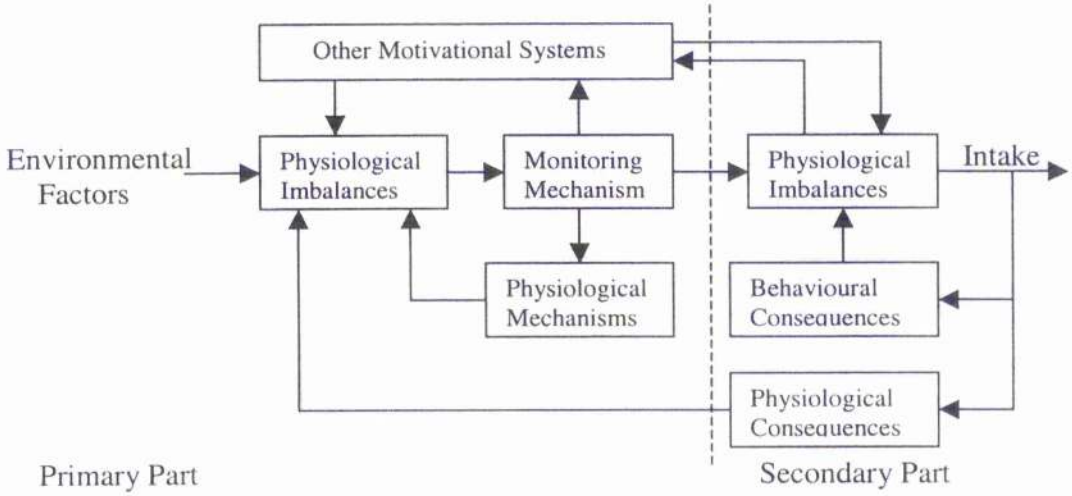

Figure 2.1 Homeostatic motivational system. (After McFarland 1971).

This motivational state system distinguishes between primary and secondary aspects of motivation reflecting the view that physiological imbalances happen both as a result of environmental factors, such as temperature, and as a result of influences from other motivational systems, such as the feeding system. These imbalances are monitored by the central nervous mechanism, which in turn actuates two types of corrective mechanism – physiological or behavioural, which act to conserve the commodity in imbalance, but are not always able to restore the balance. This is the prime function of the behavioural mechanism, the action of which results in intake of the required commodity. Such intake can have three types of effect: purely behavioural consequences, physiological consequences which act to restore the

balance, and it can influence other motivational systems – for example ingesting cold water can have thermoregulatory consequences. The primary part is always active, while the secondary part is active only when the animal is occupied in the appropriate type of behaviour. Interactions between motivational systems can exert their effects on either the primary or secondary parts. For example, we can distinguish between primary drinking, for which the causal factors relate to water imbalance, and secondary drinking, which may be a consequence of feeding or environmental changes [Fitzsimons 1968].

Within this system, three levels of interaction may be identified as shown in Figure 2.2. They are the primary level, the secondary level and the "final common path" level [McFarland and Sibly 1975].

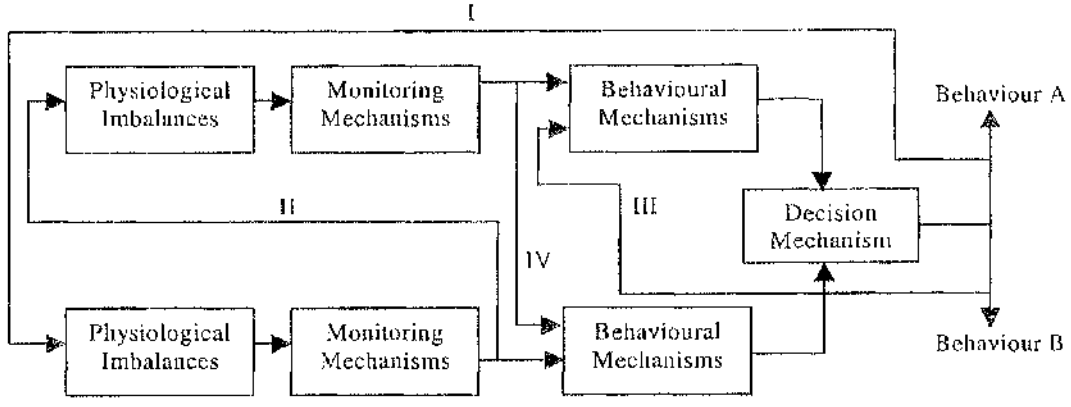

Figure 2.2 Interaction between motivational systems. (After McFarland et al. 1975).

At the primary level, influences may derive from the environment, but more commonly are a consequence of behaviour (I). Thus water balance may change due to feeding, as many foods have a high salt level which the body counters with water [McFarland, 1965]. The state of one system may change the physiological imbalances of another (II). Thus a high brain temperature induces sweating and consequent

changes in the water balance. Within the secondary level of interaction the results of one behaviour may influence the motivational state of another behaviour (III) [McFarland and Budgell, 1970]. There could also be a direct intervention of state variables in one system, which also affects the state variables in another system (IV). For example, the depressive effects of thirst on feeding are due to inhibition within the central nervous system [McFarland 1964, Oatley and Tonge 1969].

The problems arising here are that interactions become more complex when they are specified separately, thus making it difficult to have a clear picture of the control system in its entirety [Hinde 1959]. Extending this argument many ethologists proposed that drives, and motivational variables, should be expressed not as scalars but as vector quantities [Milsun 1966]. The consequences of feeding, not only reduces hunger but also alters different aspects of the animal's internal state, such as salt balance, fat levels, etc. It is therefore important to represent hunger for example, as a multidimensional vector. The interaction between behaviours discussed above and the vector approach to motivational variables will be the key to the state space approach to behaviourism, and its ultimate application to autonomous artificial agents.

2.3 BEHAVIOUR AND ITS CAUSAL FACTORS

McFarland and Sibly represent the animal's total motivational state in a causal factor space, hypothesising that the animal's behaviour is controlled by a set of causal factors [McFarland and Sibly 1975]. These causal factors result from the animal's perception of both environmental and internal stimuli. This can be represented in a

two dimensional space with one axis corresponding to the animal's internal variables and the other to environmental cues. For example the state of hunger might be represented in a two-dimensional space with one axis corresponding to the animal's degree of hunger, and the other to the strength of food cues -- the animal's estimate of the availability of food.

To formulate this model McFarland and Sibly had to make several assumptions. The first one is that an action is associated to one and only one behaviour. In other words, an action cannot happen at the same time as another one, and a behaviour is defined as a set of actions, which are mutually exclusive from other behaviours. The second assumption is that the state of the causal factors determines a unique action, and therefore behaviour will occur. In other words, a particular state of the causal factors will always lead to the same action although a certain action may be induced by more than one state of the causal factors. At any time the causal factors relevant to several actions might be present, but only one action can occur. Therefore, each action is a *candidate* to control the behaviour of the animal. There will always be a behaviour the animal cannot perform because of the lack of causal factors and other behaviours which display adequate causal factors, in competition among each other. The strength of one candidate over another is seen as a measure of the animal's tendency to perform the activity associated with that behaviour. This leads to the important point that the same tendency can be activated by different causal tendencies. Let us consider the feeding tendency of an animal represented by the degree of hunger and food cues as in Figure 2.3.

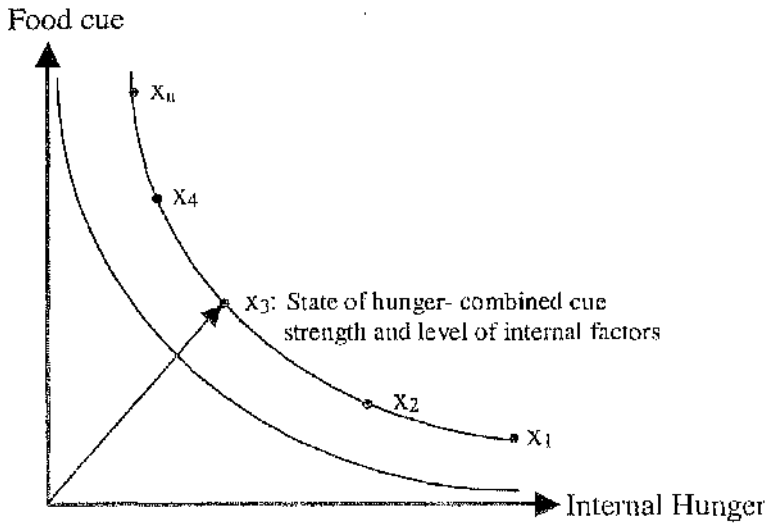

Figure 2.3 Two dimensional causal factor (cue-deficit) space for feeding. The feeding tendency follows a motivational isocline.

The line joining all the motivational states ($x_1 \ldots x_N$) yielding the same behavioural tendency is called a motivational isocline. A high hunger, but low food cue strength (x_1) gives the same feeding tendency as a high food cue strength but low hunger situation (x_N). This causal factor space (cue-deficit) is continually changing because of changes in the environment and the animal's own behaviour and internal state. These changes give rise to a trajectory in the causal factor space. As the trajectory moves across the motivational isoclines, there will be a change in the behavioural tendencies. If this shift causes some behavioural tendency to become larger than the previous largest tendency, a new behaviour will be observed. Therefore every trajectory in the causal factor space uniquely determines a sequence of behaviours. However, the characteristics of a trajectory are determined largely by the consequences of the behaviour, but the characteristics of the corresponding behaviour sequences are determined jointly by the path of trajectory and the shape of the isoclines which the trajectory crosses. The trajectories vary from occasion to occasion, but the isoclines remain the same. Each action initiated by a particular

combination of causal factors, is a candidate to control the behaviour of the animal. The situation is best summarized in Figure 2.4.

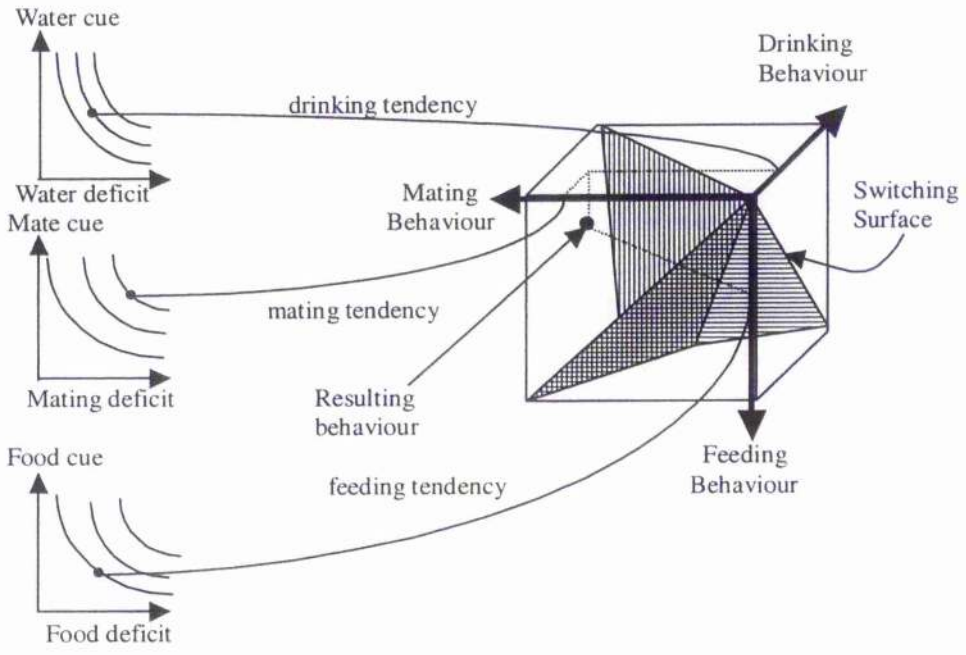

Figure 2.4 Scenario of an animal subject to three essential state variables: food, water and mating. The graphs on the left represent the cue-deficit or causal factor space in which the tendencies to perform behaviours are associated with each state variable are highlighted. On the right we have the candidate space, the space in which the tendencies are compared against the switching surface to determine which behaviour is to be performed. (After McFarland and Spier 1997).

In general a determined behaviour will be observed when the behavioural tendency for it is greater than the the tendencies of other behaviours. In Figure 2.4, the animal is subject to three different behavioural tendencies – eating, mating and drinking. When these tendencies are compared in the animal's state space, the animal will perform the behaviour that is associated with the highest tendency. As the animal performs a behaviour, the tendency for that behaviour decreases: for example, if hungry the animal will eat until satiated (restored to equilibrium) and the feeding tendency will be minimal. For particular values of feeding, mating and drinking, there will be a switching surface in the space which will trigger a change between

behaviours. For example after eating, the animal may suffer water imbalances, due to the presence of saline composites in the food and digestive processes. This leads to an increase in the drinking tendency which coupled with a reduction in the feeding tendency, may bring the animal to switch behaviour, from eating to drinking.

2.4 INTERNAL FACTORS IN MOTIVATION

Every activity performed affects the stability of the animal's internal environment through the use of energy and physiological mechanisms. The internal environment of an animal can be viewed as a system of interacting variables influenced by the animal's own behaviour. The state of any biological system can be characterised in terms of state variables of the system. The state of the internal environment can also be described in terms of a finite number of physiological state variables, each of which is represented in an axis of an N-dimensional space [Sibly and McFarland 1974]. Within this space there will be boundaries, determined by physiological constraints which cannot physically be reached, such as negative hormonal levels, and by lethal state variables values such as temperature extremes which would prove to be fatal. The origin of the physiological state is the optimal point on each axis: the value that is optimal in a biochemical or physiological sense. An example of a physiological space is presented in Figure 2.5

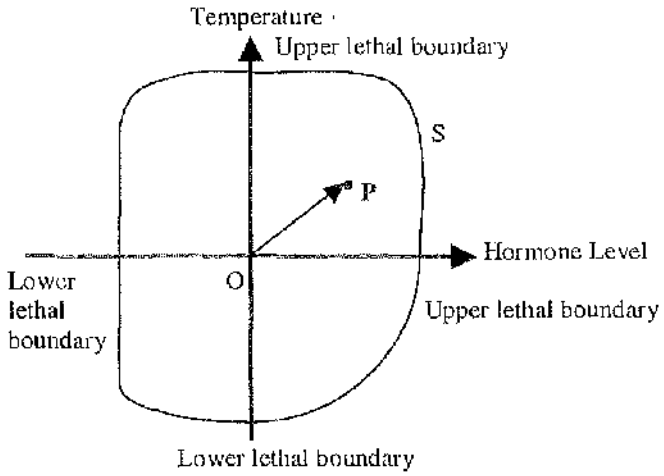

Figure 2.5 A possible two-dimensional state space with the origin *O* corresponding to optimal values for body temperature and hormone level. The current physiological state is identified by the vector **P**. The boundary line *S* separates the possible physiological states from the lethal region.

The physiological state of an animal is represented by the vector **P**. When **P** is pulled towards the lethal boundary *S*, through changes in external (temperature) and/or internal (hormone level) variables, physiological and acclimatisation mechanisms come into play.

The extent of the adaptation mechanisms is represented by the vector **a**. The adaptive vector may not necessarily directly oppose the displacement **d**, therefore there will be a resultant displacement **r**. The ways in which adaptive mechanisms oppose physiological state changes vary from short-term regulation to long-term acclimatisation. For example there is an obvious physiological displacement when a person is transported suddenly to high altitude. This is firstly counteracted by a short-term mechanism such as increased breathing rate. As time goes by the body increases the number of red blood cells circulating to account for the changed environmental conditions. Within the physiological space we can define a regulatory space in which the state is maintained by regulatory mechanisms. If extreme environmental conditions (high temperature, low salinity) are present, the regulatory mechanisms

may not be able to maintain the physiological state within the regulatory space, and a drift will occur as shown in Figure 2.6.

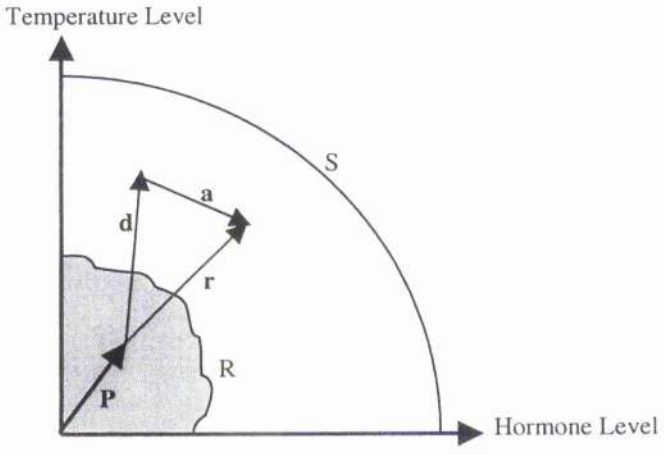

Figure 2.6 Regulatory space *R* within the physiological state space *S*. When the current physiological state **P** is displaced by a distance **d**, adaptive mechanisms act to an extent represented by **a**, so that the resulting displacement is **r**.

It is thus fundamental that the rate of drift be reduced to zero otherwise the physiological state will eventually be dragged towards the lethal boundary *S*. The physiological changes may be counteracted by different processes: behavioural, regulatory and acclimatisation. In the process of physiological adaptation these processes interact and combine to provide adaptation. Behavioural mechanisms can sometimes provide short-term relief. For example an animal or human in a hot climate may stay in the shade, thus reducing the cause of drift. Regulatory mechanisms provide another short-term adaptation: for example an increased breathing rate at high altitude. Acclimatisation, occurring in the longer term, alleviates the necessity for extreme behavioural or regulatory mechanisms. For example the individual may become acclimatised to the hot climate relaxing the behavioural measures, or increasing the number of circulating red blood cells, involved in high altitude acclimatisation. It is obvious from these examples that the

adaptation processes acts in parallel and their effects are additive, and at the same time the success of one mechanism reduces the necessity for another.

A change in physiological state is always involved in acclimatisation, and can be expressed by means of an acclimatisation vector **a** as shown in Figure 2.7.

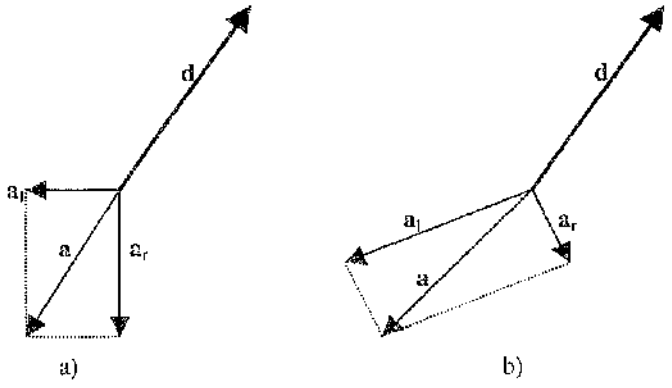

Figure 2.7 The drift is initially (a) opposed by a strong regulatory vector $\mathbf{a}_r$ combined with a weak acclimatisation vector $\mathbf{a}_l$. At a later stage (b) the contribution of acclimatisation is greater, reducing the regulatory effort.

The drift is in the short term opposed mainly by regulatory responses. As the organism becomes more used to the new conditions, the acclimatisation effect in the adaptation mechanisms may play a bigger role reducing the regulatory effort. The resultant adaptation **a** must, whatever the combination of mechanisms, be able to counteract the drift **d**, to maintain the stability. The adaptation vector **a**, is the sum of the mechanisms used to counteract the drift **d**, and is the sum of the regulation, behaviour and acclimatisation vectors, although these processes may not be sharply delineated from each other in reality. Physiological stability however, is dependent upon the efficiency of these processes.

2.5 EXTERNAL FACTORS IN MOTIVATION

Environmental changes may have a direct physiological impact on an animal, as discussed in this previous chapter, but also provide stimuli, which the animal evaluates perceptually. For example, an increase in environmental temperature is detected by peripheral thermoreceptors, and evaluated as a thermal cue, which induces a behavioural response [Benzinger 1969]. A number of assumptions have now to be made. Firstly, we must recognize that sensory capabilities are always limited, and no animal perceives every aspect of an environmental situation. This means that there will be particular environmental events, which have no role as cues, even though they affect the animal's state. For example certain types of radiation may alter the animal's physiological state, but are not detected by the animal's sensory apparatus [Rozin and Kalat 1971, McFarland 1973]. Secondly, certain aspects of the stimulus situation may have a uniquely powerful significance for an animal [Lack 1943]. The third assumption is that animals generally make the most of the available stimuli that they are able to detect. Little may be known of how the animal perceives the stimulus but it is somehow interpreted in accordance with the animal's interests and knowledge [Hailman 1977, Keeton 1974]. Finally, we assume that the evaluation of the environmental cues is, to some extent, quantitative, so that a stimulus may be said to be stronger, or more relevant, than what others are.

We can now treat the external causal factors in a manner analogous to that of internal factors as presented in Section 2.4. The effectiveness of an external stimulus, the cue strength, will have a number of dimensions, each generating different cue strengths. The various cue strengths are combined in a cue space, which has an

independent axis for each cue. A point in the cue space represents the cue state associated with a particular environment at a particular time.

Changes in the cue state can occur as a result of time cues. In addition to their influence upon the animal's internal state, endogenous clocks, circadian, lunar or circannual, can provide cues, which the animal can utilize in assessing the significance of external stimuli. Many animals are able to learn and adjust their behaviour on the basis of time [McFarland 1977]. For an animal to behave appropriately in the interactions with its environment, information about the environment must be incorporated in the mechanisms responsible for the behaviour.

2.6 OPTIMAL DECISION MAKING

The survival and reproductive success of an individual animal depends largely on the animal's use of resources such as food, territory, mates, etc. At any particular time an animal may have alternative courses of possible action so that a choice has to be made. Every activity will have associated costs and benefits in terms of the ultimate reproductive success or fitness of the animal [Wooton 1971]. Thus there are both benefits and costs associated with various activities. In general the costs and benefits are attached to both the behaviour of the animal and its internal state. Let us consider the situation of an animal in cold wet weather. The animal has a choice between standing up to feed and sitting down to shelter from the wind. There are costs and benefits associated with each behaviour. By standing the animal has a good field view and can easily look out for possible danger and it can also feed, but at the same time is much more exposed to the weather. By sitting the animal is able to save

energy, both by being less active and reducing heat loss in sheltering from the cold wind. On the other hand however, it is less well placed to spot possible predators and it cannot feed effectively. Clearly in assessing the relative merits of the two possible behaviours, the animal's state of hunger must be taken into account. If the animal is not hungry it can probably afford to sit down and wait for the storm to pass. If, however, it is in need of food, it may endanger its life by neglecting to feed because of the weather condition. Even for such a simple decision, the balance of costs and benefits is a delicate one. It is this interesting balancing of cost-benefit which brought ethologists to envisage a relationship between animal behaviour and economics [Darwin 1859, Fisher 1930, Hamilton 1963].

A general principle subscribed to by both economists and ethologists, is that in the process of decision making something is maximised. At the global level ethologists account for behaviour in terms of genes or fitness, whereas the economists introduce the more vaguely defined concept of value. At the individual level there is a more direct parallel between the concepts of cost and utility. A person obtains a certain amount of personal satisfaction or utility from leisure pursuits, which require a determined cost. However, for an animal building a nest, for example, the utility of nest material would generally be a decelerating function of the amount of nest material already obtained. In biological terms the cost of not having nest material decreases with the increasing amount of nest material as shown in Figure 2.8.

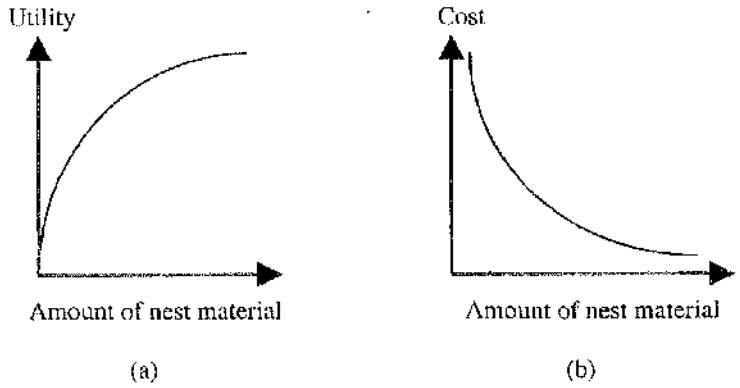

Figure 2.8 The decreasing utility of nest material (a) and its equivalent cost (b).

The implication is that a component of the risk to reproductive success is inversely related to the amount of nest material gathered. We can see therefore, that the concepts of cost and utility are the inverse of each other, and we can speak of an animal as maximising utility, or minimising cost.

It is a well established theory that the rational economic agent is a maximising agent, and the function that is maximised is generally called a utility function. Similarly, on the basis of decision theory, an animal can be considered an optimising machine, whose behaviour aims at maximizing an objective function as shown in Figure 2.9.

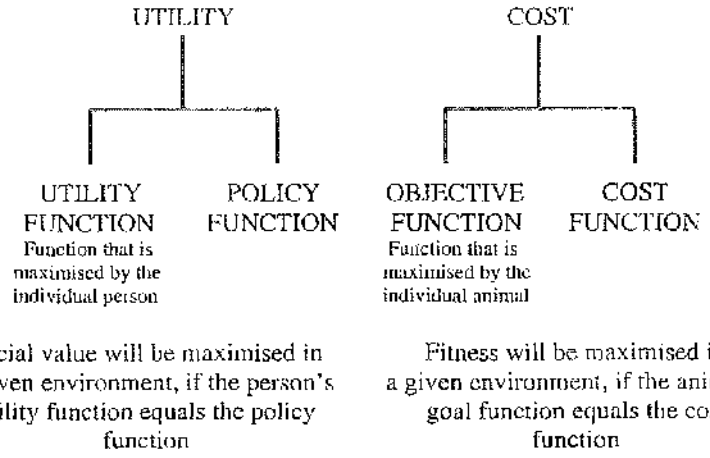

Figure 2.9 Parallel concepts between economics and ethology (After McFarland and Houston 1981).

Many biologists even take the view that the process of evolution is itself an optimising process [Oster and Wilson 1978, Maynard Smith 1978].

Alongside the objective function, which the animal actually maximizes, we have another function, called the cost function, which the animal should maximize if it were to perfectly adapt to the environment [McFarland 1977, McCleery 1978]. This function is a property of the environment rather than the animal. Only when the animal is perfectly adapted to its environment is the objective function identical to the cost function. In reality however, this will rarely be the case, because of genetic variations between individuals, competition, and evolution. In likening an animal to an economic consumer, we can regard energy as analogous to money. The animal can earn it by eating and drinking and spend it upon various activities. Over and above the basic continuous level of metabolic expenditure, the animal can save energy, by hoarding food or depositing fat, or can spend it upon various activities, such as mating, hunting, nesting. Much in the same way that humans, on top of basic daily expenditure (food, drink, etc.), can save money and use it on different activities such as holidays, sport, leisure, etc. When the price of an activity is high, the animal is subject to a tight budget constraint, and when the cost of an activity is reduced, the animal experiences an increase in income, and the budget constraint is relaxed.

There are three main stages in reaching an understanding of the decision-making process. Firstly a maximizing principle must be established; secondly there must be recognition that there will inevitably be some trade-off between various aspects of the problem; and thirdly a set of optimal criteria must be formulated. In the study of decision-making in animals, maximizing principles are seen in terms of cost. The trade-off is between activities that are mutually exclusive in the sense that they cannot be performed simultaneously, and the optimality criteria are embodied either

in a set of decision rules or in some kind of objective function. Let us consider the strength of feeding behaviour, as a result from a trade-off between internal hunger and strength of food cues. The same feeding tendency can result from different combinations of these variables. The line joining all points of equal candidature strength is called the motivational isocline (see Section 2.3), as the animal has to compare its feeding tendency against tendencies for other types of behaviour (see Figure 2.4). An animal in which the feeding tendency is too dominant over other aspects of behaviour or is too easily overruled is at a disadvantage compared to other animals. Therefore we would expect the optimality criteria (shape of the isoclines) for feeding to be designed by natural selection in accordance with the animal's ecological circumstances. For example where food availability is erratic, more emphasis should be given to cue strength, while the emphasis attached to hunger should be related to the animal's physiological tolerance [McFarland 1976]. Because there is a trade-off in terms of natural selection, which can be expressed in terms of a cost function (see Figure 2.9), there must also be a trade-off that is embodied within the decision making mechanisms of each individual animal. These trade-offs and optimality criteria will be explored within the next chapter.

2.7 RELEVANCE TO ARTIFICIAL AUTONOMOUS SYSTEMS

When trying to construct an artificial autonomous agent a critical issue has to be resolved. The problem is the ability to carry on lifelong adaptation in an open world environment. Open worlds are those for which no fixed boundary conditions can be guaranteed. They are characterized by chaotic dynamics and non-stationary processes, leading to significant difficulties in precise mathematical formulations,

which could be used to design strictly rational agents. The states of such worlds are difficult, if not impossible to predict, especially for longer time scales. This is the nature of the "real world" in which biological agents must compete for critical resources to survive and reproduce. That biological agents succeed in doing so attests to the efficacy of adaptation and learning. The real world into which artificial agents are expected to operate is not just dynamic it is also non-stationary, constantly changing. This means that patterns of association change over time in indeterminate ways. Typical machine learning systems have been monotonic with respect to the gain in knowledge, treating the world as a closed system. So long as the agent is exposed to environments that are indeed closed, even if highly stochastic, such a scheme can work reasonably well. In large part this pursuit was motivated by a simple motivation: closed worlds are subject to tractable mathematical analysis. One can offer proofs that a given algorithm produces a claimed result. These systems are aimed at stationary targets. The problem has been that when these same systems are aimed at different targets from the real world they fail to produce the promised results.

Natural environments are not closed worlds. Environmental interactions that took place in a prior time period on the periphery of the agent's immediate environment can alter relationships that the agent has already learned. The agent's knowledge is thus rendered less useful and certainly sub-optimal. Adding to the complexity of real worlds, the time scales of these indeterminate changes are themselves indeterminate. Anything from catastrophe to subtle, long-term changes can ensue depending on the dynamics of the interaction and the spatial scale involved. An earthquake, resulting from eons of pressure build-up in the tectonic plates, can alter the landscape in an instant. Changes in solar radiation due to sun spot

activity will cause colder or warmer seasons over many years. Animals, our best examples of autonomous agents in real world environments, need to adapt to a wide range of changing conditions to survive in the real world.

Autonomy means being able to make independent decisions while the agent is deployed on a mission. We can envision some missions extending over significant periods of time during which there would be no opportunity for re-training the agent. Under such circumstances the agent must be capable of learning continuously as the environment changes, and that is why the study of animal behaviour is extremely useful, and indeed vital, in the field of artificial autonomous agent research.

CHAPTER III

FROM ETHOLOGY TO ROBOTICS

3.1 PREFACE

In this chapter the ethological theories and methods presented in Chapter 2 will be applied to artificial agents. It will be shown how the state space and cue-deficit methods can be translated from biological systems and modified to a robotic model in general, and to a spacecraft model in particular. The concept of cost function is given a rigorous mathematical foundation and used to determine optimal behaviour with Pontraygin's Maximum Principle.

3.2 INTRODUCTION

Traditionally, Artificial Intelligence (AI) has, until recently, been focusing on higher order cognitive activities such as expert problem solving. The inspiration for Artificial Intelligence theories has mainly come from logic and the cognitive sciences, particularly psychology and linguistics as discussed in Chapter 1. In the last decade however, some research has been directed towards embodied intelligence and made strong alliances with biology and ethology. This has been characterised by bottom-up AI [Brooks 1986], the animat approach [Wilson 1991], behaviour-based

AI [Steels 1990] or animal robotics [McFarland 1992] as discussed in Chapter 2. The phenomena of interest are those traditionally covered by ethology and ecology, for animals, or psychology and sociology in the case of humans. The behaviour of a single or group of agents is analysed concentrating on what makes behaviour intelligent and adaptive, and how it may emerge. Behaviour is defined as a regularity observed in the interaction between the characteristics and processes of an agent, and the characteristics and processes of the environment. Behaviour can be considered intelligent if it maximises preservation of the agent in its environment. The main emphasis is not on the physical basis of behaviour, as in the case of neural networks, but on the principles that can be formulated at the behavioural level. For example explaining the formation of paths in ant society, with no reference to how they are neurologically implemented [Werner 2001].

The scientific community traditionally builds models in terms of a set of equations which link different observational variables to hypothesised theoretical variables. Advances in both the computational and mechanical fields, have brought to the fore two additional types of models : computational models, and artificial models. Computational models consist of a process-oriented description in terms of algorithms and data. When the algorithm is executed, modifying the data over time, different phenomena can be observed by observing the changes in the data structure. Artificial models on the other hand consist of a physical device whose behaviour can be compared to natural phenomena in similar circumstances. Clearly, computational and artificial models must be distinguished. For example it is possible to build a computational model of the flight mechanisms of a bird, by simulating the air flow around the bird, the aerodynamics of the body and wings, the pressure differential caused by the wings movements, etc. While surely a valuable tool, such a model

would clearly be incapable of physically flying through the air. In contrast a model could be built in terms of physical components – body, wings, etc. – but could only be considered useful if it could perform real flying. Another fundamental ingredient is a strong biological orientation, which shows up in the way intelligence is defined. The "classical" AI approach defines intelligence in terms of knowledge: a system is intelligent if it maximally applies the knowledge that it has [Newell 1982]. The behaviour oriented approach defines intelligence in terms of observed behaviour and self-preservation, or in the case of an agent, autonomy [McFarland and Bosser 1992]. It is based on the idea that the essence of biological systems is their capacity to continuously preserve and adapt themselves. The drive towards self-preservation applies to all organisms from the most simple, such as genes or cells, to the more complex, such as societies or species. An analogy with cells, which are the smallest biological autonomous agents can strengthen this case, as shown in Figure 3.1.

Cell	Behaviour System
Biochemical Processes	Transformation Processes
Biochemical Structures	Electrical signals and States
Genes	Behaviour Programs
Incoming Material	Energy Transduced by Sensors
Outgoing Material	Energy Transduced by Actuators
Adaptation to Cell Environment	Adaptation to External Environment

Figure 3.1 Comparison between cells and behaviour systems.

A cell consists of a group of biochemical structures, and processes, which are guided by genes, and take place when chemicals pass through the cell membrane in either

direction. A behaviour system similarly consists of a set of dynamic and static structures, which include physical components, such as sensors and body parts and networks through which electrical signals are propagated. The system is guided by a behaviour program, which acts on inputs coming from the outside which modify the internal state. Like a cell, a behaviour system is continuously active and adapting to environmental changes.

3.3 IMPORTANT ASPECTS OF BEHAVIOUR BASED AGENTS

Traditional robotics relies, much like classic AI, on exact models as well as symbolic and centralised control schemes. Behaviour based agents on the other hand, try to achieve control through simultaneous operations of simple processes, called behaviours. So behaviours stand in contrast to the classic notion of action where a single command activates an effect over a fixed period of time, with clear, well defined moments in time where the action begins and ends. Therefore, behaviours do not rely on complex world models but on close, continuous couplings between sensor outputs and actuator activation. Behaviour based agents present many characteristics and properties, which makes their use particularly promising for space missions.

The word autonomy is derived from the Greek words *αυτο* (self) and *νομοσ* (law, rule). So an autonomous agent is a self-governed system, independent from direct and continuous human supervision and maintenance. Autonomous agents face two major problems. Firstly they have to be capable of dealing with unforeseen circumstances, and secondly they have to be capable of some resource management, particularly with respect to energy. Obviously both capabilities can be extremely

useful for many applications. One important area is obviously space exploration (see Chapter 1), but also on Earth there are many areas where humans cannot or should not have access, and where direct control of robots is difficult if not impossible [Kirchner and Hertzberg 1997].

Unlike classical robots, which are based on precise mechanics, as they rely heavily on exact models, behaviour based agents are more like natural devices. There is no need for high demands on part assembly and maintenance, and they can therefore be produced more cheaply [Fujita and Kageyama 1997]. While valid for Earth based agents this is not always the case in space missions, where often, new technological advances in hardware miniaturisation may lead to cost increases. There is however the possibility of using off-the-shelf mechanical or electromechanical components, which have been repeatedly space validated. Partially as a consequence of their mechanical imprecision, behaviour oriented agents cannot rely on precise complex world models. Instead they have to be controlled with simple rules. As a positive side effect, their need for computational resources is small. For example, instead of intensive calculations of inverse kinematics for articulated robots, simple couplings between sensor outputs and motor activation are used. Therefore, less processing power is needed. For mobile robots, instead of detailed maps, simple beacons and sensors are used to navigate the robot. Therefore, less memory is needed.

Learning and adapting, defined as the ability of the agent to change and improve its performance through experiences, can help in coping with surprises due to its mechanical imprecisions, with unexpected situations in the environment, new tasks, and so on. Last but not least, behaviour oriented robots are not seen as isolated devices, but as part of an environment. The environmental cues have to be exploited for stable operation of the agent.

3.4 THE BASIC CYCLE

Self-sufficient agents have, just like animals or people, to decide how to allocate scarce resources among a variety of alternative uses. If the agent has to be not only self-sufficient, but also economically viable, then there are two basic resources that must be provided by the agent's environment. These are energy E, which the agent must be able to obtain in some way, and work W, which can be generated by performing useful tasks. When considering a single self-sufficient agent, it is evident that it should perform a basic cycle of activities to maintain its viability. The agent goes through a cycle of: work – find fuel – refuel. When working the agent gains W and loses E. At some point the agent breaks off work and goes to find fuel. This also leads to a reduction in E, but what happens to W? Since W represents the utility of the agent's work, from the point of view of a user there are three basic possibilities outlined in Figure 3.2

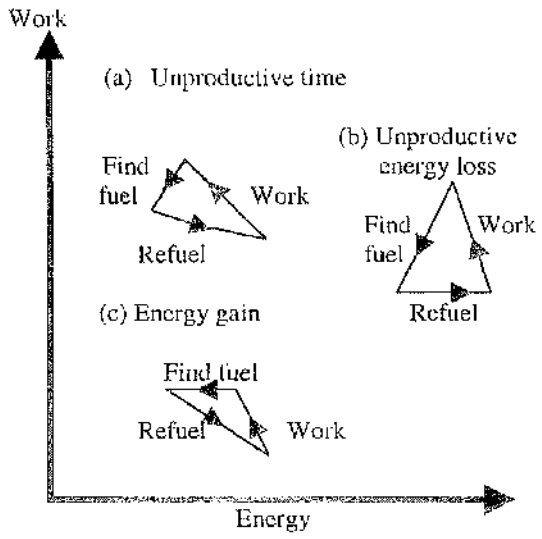

Figure 3.2 Three different types of basic cycle represented in the Energy-Work plane. In (a) W declines throughout all unproductive time: when the agent is not working. In (b) W declines only when there is unproductive energy loss: when the agent is looking for a fuel source. In (c) W declines when the agent is refuelling: the agent is effectively paying for its fuel with W.

If the user is mainly interested in an agent that spends as much time as possible doing useful work, irrespective of energy expenditure, then there will be no utility gain from the time spent not working as shown in Figure 3.2 (a). If the user is concerned about energy expenditure on activities that are not productive, then W will decline during that period of the basic cycle, as shown in Figure 3.2 (b). If on the other hand the user is concerned to minimise energy expenditure in general, then it makes sense for the agent to pay for its fuel. In Figure 3.2 (c) W is earned during work, and spent during refuel.

The basic cycle however defined, will always consists of: work – find fuel – recharge. A certain amount of time of the cycle is devoted to work, some to finding the fuel, and some to recharging. The portion of cycle spent not recharging is called the active time, during which energy is spent by the agent either by working or by searching for fuel. This energy must be recoverable during recharging. Some of the active time is spent working and some is spent in finding the fuel. Clearly the agent must not spend too much time and energy working, or it may be unable to find the fuel before it runs out. The agent must decide when to stop working and start looking for fuel, if it does this too early, it will not be working to maximal efficiency, if it leaves it too late it may run out of fuel. Similar arguments apply to the decision to stop recharging and start working. We can now imagine an optimal cycle, in which the agent switches from one activity to another at the optimal point. Optimality approaches provide a useful design guide since they provide methods to determine the upper bound to the performance of an agent, where the concept of self-sufficiency provides the lower bound.

3.5 THE AGENT AS A STATE SPACE

The state space model for agents was proposed by Sibly and McFarland [Sibly and McFarland 1974, McFarland and Sibly 1975] and further developed by McFarland and Houston [McFarland and Houston 1981]. Within this framework the agent is characterised as possessing a minimal set of internal variables that can completely describe its state. In such a description of a biological system we could possibly identify hunger, thirst, temperature, hormone level, etc, as essential physiological state variables (see Figure 2.6). For a robot we could identify energy, oil level, task achievement, etc. The first to develop this model for a spacecraft was Gillies et al. who identified three state variables as being essential: energy, measured through battery level, internal temperature and memory level [Gillies et al. 1999]. These variables sit within an Euclidean vector space with the states as its orthogonal axes as shown in Figure 3.3.

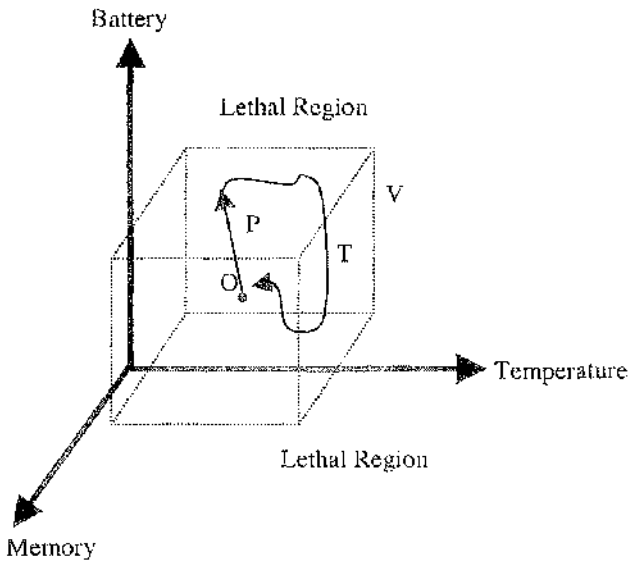

Figure 3.3 An example of a possible three dimensional state space with origin *O*. The current state is indicated by the vector P. The boundary volume *V* separates the possible state values from the lethal limits. *T* is a possible trajectory the satellite could take to return to the homeostatic equilibrium point *O*.

Within this space there will be regions that the satellite can physically never encounter, for instance negative memory or negative battery level, and regions, that should the satellite cross into, it would cease to function, such as below the lower or above the upper possible operating temperatures. The boundaries that separate the regions that are fatal to the satellite from those that are not are called lethal limits. The task of the spacecraft within such a model is therefore to maintain the homeostasis (equilibrium) of its state variables under the perturbation of its own behaviour, and the environment's impact on its resources. For example during eclipse the satellite must activate the heater to stay above the lower lethal temperature, while also draining the battery. In the robotics literature each axis is associated with a specific task the agent has to perform [Blumberg 1994, Steels 1994, Spier and McFarland 1996, and McFarland and Spier 1997]. However this is not the case for the spacecraft model. The temperature axis bounds the operational limits for the different subsystems, but is not directly part of the action selection algorithm.

The spacecraft will be able to perform useful work W, to sustain its viability, by either obtaining images through a payload camera, or gathering data through some appropriate payload instrument, and then storing the data on a hardware device, or downloading, by means of a transmitter, the recorded data to an Earth ground station. Both activities do however require a certain amount of energy E, to be consumed, draining the battery level. To replenish its energy source the spacecraft must point its solar array towards the Sun, thus recharging the depleted battery. We can see therefore that the spacecraft is subjected to three different types of behaviour: target pointing, Earth pointing, and Sun pointing. The temperature seems to bear no importance within the state space since it is not directly related to any particular behaviour. However it has to be noted that temperature plays a fundamental role in

space mission design. All hardware devices work within well-defined temperature limits. It is therefore vital for the mission's success that the internal temperature is kept within a predefined range to ensure that all subsystems function properly. The spacecraft is therefore equipped with a heater, which automatically switches on when the temperature reaches a certain lower limit; clearly this requires a certain amount of energy. The temperature therefore is not linked directly to a behaviour, but indirectly affects the spacecraft's behaviour selection.

3.6 THE OPTIMALITY CRITERION

It was discussed in Chapter 2 that an animal could use behavioural means to regulate its physiological state: for example drinking or moving towards a shaded area in hot weather. Under favourable conditions an animal may be able to do all it would 'like' to do, but when resources are scarce it may have to make a decision about what to do and what to leave undone. In order to predict how an animal should allocate its time and energy under such circumstances, we must know the costs associated with various deviations from the 'ideal' state. It was also shown in Chapter 2 that an animal's state could be represented in an n-dimensional space. The state can be thought of as a specification of the value of n variables, where n is large enough to characterise the animal. The model incorporates a very simple relationship between behaviour and state. It is assumed that when the animal is performing activity u_i, the rate of change of the state x_i ($i = 1$-n) is given by:

$$\dot{x}_i = -r_i = -c_i u_i \qquad [3.1]$$

This means that activity u_i, has consequences only along axis x_i. The value of r_i in this model represents the 'return' the animal gets from performing activity u_i mediated through a constant parameter c_i which links the sensitivity of a variable in relation to an activity.

It seems reasonable to assume that the risk of death, or failure in the case of an artificial agent, must increase steeply the nearer a state variable is to its lethal boundary. For example it is obviously dangerous to allow hunger to approach lethal levels if a future food supply is not guaranteed. Let us therefore consider a physiological variable $\tilde{z}$ which takes values between two lethal boundaries $\tilde{z}_0 = 0$ and $\tilde{z}_1 = L$. Let us assume that when the animal is not performing the behaviour relevant to this state variable, the variable moves either to the right or to the left, with a probability of half. If M is the expected number of moves required for $\tilde{z}$ reaching either $\tilde{z}_0$ or $\tilde{z}_1$, then M is given by the following equation [Feller, 1957]:

$$M(\tilde{z}) = \tilde{z}(L - \tilde{z}) \qquad [3.2]$$

so that $M = 0$ if $\tilde{z} = 0$ or $\tilde{z} = L$. By the symmetry of the model, M must be at a maximum when $\tilde{z}$ is equidistant from $\tilde{z}_0$ and $\tilde{z}_1$, or when $\tilde{z} = L/2$. This suggests introducing a new variable $z = \tilde{z} + L/2$, which gives us the displacement from the optimal state. Equation 3.2 therefore becomes:

$$M(z) = \left(z + \frac{1}{2}L\right)\left(L - z - \frac{1}{2}L\right) = \frac{1}{4}L^2 - z^2 \qquad [3.3]$$

so that M, gives some indication of how safe it is to be at point z. As $L^2/4$ is a constant, this suggests a cost function of the form:

$$C(z) \propto z^2 \qquad [3.4]$$

Although this encourages the view that the cost function is proportional to z^2 – i.e. the cost function is quadratic – it is not a proof of its validity. The choice of a quadratic function has been made for mathematical simplicity, although clearly any convex function may be used [Sibly and McFarland, 1976].

When more than one state is being considered, some assessment of the total cost $C(\mathbf{z})$ must be made. If $C(\mathbf{z})$ can be represented as the sum of the cost associated with each z_i in $\mathbf{z}$ (i = 1-3), then $C(\mathbf{z})$ is said to be separable. This means that the risk associated with the value of one variable is independent of the values of the other variables. For example, if the probability of death from heat stress were unaltered by the nutritional condition of the animal. This is not to say that foraging does not influence the probability of survival, but that the effect of body temperature on survival is independent of nutritional condition. So the cost $C(\mathbf{z})$ of being in state $\mathbf{z}$ is a weighted sum of the squares of the displacements that constitute $\mathbf{z}$. For example if $\mathbf{z} = [z_1, z_2, z_3]$ then:

$$C(z) = \frac{z_1^2}{Q_1} + \frac{z_2^2}{Q_2} + \frac{z_3^2}{Q_3} \qquad [3.5]$$

where the weighting parameters Q_i (i = 1-3) are referred to as the resilience of the variable z_i (i = 1-3) [Houston and McFarland 1980]. The optimality criterion then

amounts to requiring the animal to spend its time in such a way that the displacements from the homoestatic position results in the smallest possible cost.

To complete the specification of the optimisation problem we then have to resort to Equation 3.1 to link the animal's behaviour to consequences for its state. If during some time span the duration of time spent performing activity u_i is d_i then the total consequence of such a behaviour for axis x_i will be $d_i r_i$. In other words if x_i began at a value $x_i(0)$, its value at the end of the time span considered $x_i(T)$ will be given by $x_i(T) = x_i(0) - d_i r_i$. Therefore at the end of the time span considered the state of the agent will have resulted in a deficit for that axis. As will be seen d_i plays a fundamental role in the action selection algorithm

3.7 STATIC OPTIMISATION

We have just shown how an agent's state (or a spacecraft's state) could be represented in an n-dimensional space. The state can be thought of as a specification of the value of n variables, where n is large enough to characterise the agent – or the spacecraft in our case – for our purposes. Control laws for each of these variables now have to be computed with a dynamic optimisation method. The method chosen is Pontryagin's maximum principle, which is a fundamental method in the field of dynamic optimal control. As it has to be considered with its static optimisation counterpart, Lagrange Multiplier theory, we will first introduce this to understand more easily what lies beneath Pontryagin's maximum principle.

The optimality criterion in the case of a static optimisation is based upon the minimisation of a cost function. The use of the word 'cost' is due to the fact that these optimisation methods were first used in the field of economics. However, the term

suits well to the idea that each action involves a cost regarding one or several resources of the system. There is a cost associated with being in each particular physiological state, this cost being related to the survival of the system. When more than one state variable is being considered, as it will be the case here, the total cost $C(\mathbf{x})$ can be represented as the sum of the cost associated with each state variable x_i as discussed earlier. The total cost function in the more general case will therefore have the following form:

$$C(\mathbf{x}) = \sum_{i=1}^{n} a_i x_i^2 \qquad [3.7]$$

where the coefficients a_i are constants depending on the weighting of the importance of each state variable in the cost function. These are just the inverse of the resilience, defined in section 3.6.

The purpose of the optimisation will thus be to minimise this function, under a constraint linked to the way the system, which is being investigated, is working. Given the problem of maximising some function $C(\mathbf{x})$ subject to the constraint $N(\mathbf{x}) = 0$, the optimal solution can be found by constructing the function $L(\mathbf{x},\lambda)$ defined as:

$$L(\mathbf{x},\lambda) = C(\mathbf{x}) - \lambda N(\mathbf{x}) \qquad [3.8]$$

where λ is the Lagrange multiplier. To better understand what lies beneath the Lagrange multiplier, let us assume that there are two state variables, x_1 and x_2 and that the cost is given by some function $C(x_1, x_2)$ and the constraint to be some function $N(x_1, x_2) = 0$. The optimal solution is found by finding the isocline of lowest cost

compatible with the constraint and can be denoted by $(\bar{x}_1, \bar{x}_2)$. This point is characterised by the fact that the cost isocline is tangent to the constraint curve and so their slope must be equal. The common slope for cost function and constraint is given by:

$$\frac{dC}{d\bar{x}_1}\frac{d\bar{x}_2}{dC} = \frac{dN}{d\bar{x}_1}\frac{d\bar{x}_2}{dN} \qquad [3.9]$$

which means that:

$$\frac{dC}{d\bar{x}_1}\frac{d\bar{x}_1}{dN} = \frac{dC}{d\bar{x}_2}\frac{d\bar{x}_2}{dN} \qquad [3.10]$$

If we let λ be the value of both sides of Equation 3.10 we can rearrange to write:

$$\frac{\mathrm{dC}}{\mathrm{d}\bar{x}_i} - \lambda\frac{\mathrm{dN}}{\mathrm{d}\bar{x}_i} = 0 \qquad [3.11]$$

We can now define a new function $L(x_1, x_2) = C(x_1, x_2) - \lambda N(x_1, x_2)$ such that at the optimal solution $\mathrm{d}L/\mathrm{d}x_i$ is zero (i = 1,2). The implication is that the problem of minimising C subject to the constraint N has been replaced by the unconstrained minimisation of L.

Let us try and illustrate the use of Lagrange Multipliers with the following example in which we want to minimise the function $C(x, y) = x^2 + y^2$ subject to the constraint $N(x, y) = (1 + x)^2 + y = 0$. We can define a new function $L(x, y) = C(x, y) - \lambda N(x, y)$ and then minimise it with respect to the state variables x and y so that:

$$\frac{dL}{dx} = 2x - 2\lambda(1+x) = 0 \qquad [3.12a]$$

$$\frac{dL}{dy} = 2y - \lambda = 0 \qquad [3.12b]$$

Therefore we find that:

$$x = \frac{\lambda}{1-\lambda} \qquad [3.13a]$$

$$y = \frac{1}{2}\lambda \qquad [3.13b]$$

and so substituting the values of the Lagrange multiplier into the constraint equation we obtain a third order polynomial:

$$\lambda^3 - 2\lambda^2 + \lambda + 2 = 0 \qquad [3.14]$$

The only real root of this equation is: $\lambda = -0.698$ and as a consequence we can now find the following constrained solution: $x = -0.411$ and $y = -0.349$. Following this illustration of static optimisation, the problem of dynamic optimisation will now be considered.

3.8 DYNAMIC OPTIMISATION

In the previous section we introduced the concept of static optimisation in which time does not enter directly into the problem. In this section we will consider dynamic problems, in which any action taken at any given time has consequences, which are evaluated over some period of time into the future. In this case the problem is to look at the cost associated with different paths through some state space. The optimal solution will be the one along which the total accumulated cost is least. Finding this total cost involves the mathematical operation of integration.

The optimal control problem can now be defined. We have an objective function $C(\mathbf{x}, \mathbf{u}, t)$ dependent on the state variable $\mathbf{x}$, and the behavioural control $\mathbf{u}$. The aim is to move the system, to a specified state or for a specified amount of time, such that the integral of the objective function is minimised. A technique that is applicable in such cases was developed by Pontryagin in the 1950s [Pontraygin 1962].

3.8.1 Pontryagin's Maximum Principle

The dynamic problem of finding the path of least cost appears to be very similar to the static problem solved in the previous section by the introduction of the Lagrange multiplier method. In fact Pontryagin approached the optimal control problem by defining a state function called the Pontryagin (also known as Hamiltonian) function denoted by H. Pontryagin's maximum's principle states that the problem of finding the path of least cost is equivalent to the more direct problem of instantaneously maximising the function H – the principle can also be considered as an instantaneous minimisation.

A new sort of constraint is however introduced by the method itself, similar to the static optimisation method introduced previously. In the static case, one way to solve the problem was to introduce a function λ, known as the Lagrange multiplier, which can be seen as the cost of the constraint. This formalisation merely takes into account that two state variables x_1 and x_2 cannot be varied independently. In a similar way, the dynamic problem of optimal control must represent the fact that the state variable $\mathbf{x}$ and the control variable $\mathbf{u}$ that constitutes the instantaneous cost function cannot be varied independently. The reason for the dependence is the fact that $\mathbf{u}$ controls $\mathbf{x}$, the nature of this control being given by the system equation – Equation 3.1.

In the dynamic case λ becomes a function of time but still plays the same role as in the static case. Here λ represents the change in total future cost along the optimal trajectory that results from a small change in state and is called the costate vector. It is, in effect, a set of Lagrange multipliers, introduced to satisfy the system equation constraint.

Pontryagin's function can therefore be thought of as the gradient of the cost functional, that is to say H indicates how cost varies with a chosen control at any given position of time. Let us now sum up the principle: In order to minimise the total cost $\int_{t=0}^{T} C(\mathbf{x},\mathbf{u},t)dt$, the control law $\mathbf{u}$ must be chosen in such a way as to instantaneously maximise the Pontryagin function:

$$H = \lambda^{\mathrm{T}} f(\boldsymbol{x},\boldsymbol{u},t) - C(\boldsymbol{x},\boldsymbol{u},t) \qquad [3.15]$$

where $C(\mathbf{x}, \mathbf{u}, t)$ is the objective function giving the total cost, $f(\mathbf{x}, \mathbf{u}, t)$ represents the system equation and λ^T is the matrix transpose of the costate vector λ. The rate of change of both the state and costate vectors are then given by the following equations [Dixit, 1976]:

$$\dot{x} = \frac{\partial H}{\partial \lambda} \qquad [3.16]$$

$$\dot{\lambda} = -\frac{\partial H}{\partial x} \qquad [3.17]$$

To show how Pontryagin's principle works, let us consider the case of how an animal feeds. We assume that the animal's goal is to maximise its rate of energy intake. If an animal starts with a given energy deficit that it must diminish, the dynamic optimisation involves looking for a trajectory from the initial deficit along which the total value of the objective function is minimised.

We therefore chose a quadratic cost function:

$$C = ax^2 + u^2 \qquad [3.18]$$

and therefore have to minimise the integral of the cost function under the system equation constraint $\dot{x} = -cu$. We can define the Pontryagin's function H as follows:

$$H(x,u) = -\lambda cu - ax^2 - u^2 \qquad [3.19]$$

Since we have to find the optimal control u that minimise H, we now have to differentiate H with respect to u and equate the result to zero to obtain:

$$u = -\frac{\lambda c}{2} \qquad [3.20]$$

Moreover, by definition of the rate of change of state and costate vectors we find from Equations 3.16 and 3.17 that:

$$\dot{x} = \frac{\lambda c^2}{2} \qquad [3.21]$$

$$\dot{\lambda} = 2ax \qquad [3.22]$$

Differentiating Equation 3.21 and substituting into the result the value of $\dot{\lambda}$ from Equation 3.22 we obtain the following differential equation of the second order

$$\ddot{x} = \frac{c^2}{2}\dot{\lambda} = c^2 ax \qquad [3.23]$$

As the state of the system cannot diverge, the optimal trajectory for the food deficit is given by the solution of Equation 3.23 as:

$$x(t) = x_0 e^{-cat} \qquad [3.24]$$

which implies that the control (the behaviour of the animal) should have a trajectory of the form:

$$u(t) = ax(t) \qquad [3.25]$$

$$u(t) = ax_0 e^{-cat} \qquad [3.26]$$

Equations 3.25 and 3.26 are equivalent forms of the control law for the problem. The first is expressed as a function of the state variable, while the second as a function of time. The exponential decrease in the rate of behaviour can be explained intuitively. When x is large, it is worthwhile to feed as soon as possible to reduce x, since a change in food deficit reduces the cost substantially. When x is small, however the cost of a high rate of behaviour would not be offset by a reduction in x, so u declines as x is reduced. The optimal behaviour results in the exponential decline in the control function u expressed by Equation 3.26.

3.9 AVAILABILITY AND ACCESSIBILITY

Two parameters, the availability r and the accessibility k model the resources in the environment. This duality may seem arbitrary, and r and k should be united into one single variable. However, these two parameters provide a powerful way with which to consider the environment. The availability is associated with the density of the resource in the environment. Such a density can be manifested in many ways. For instance, water could be in small units but uniformly distributed over a large area, much like dew, or food could be in large units but at a low density, like insect prey. Both alternatives could yield the same global density of resource in the environment.

The accessibility is associated with the ease with which an agent can obtain the resource through its own behaviour. For example, consider the scenario of an agent trying to find food underneath a carpet of leaves in a garden. A bird may peck

at individual leaves, lifting them up, to inspect for nuts beneath; such behaviour involves great effort but does not yield many nuts. Consequently this behaviour would have a low accessibility. A mobile robot may be fitted with a vacuum attachment, which sucks up the leaves and nuts, spitting out the leaves and catching the nuts; such behaviour would have a high accessibility.

Applying these definitions to the spacecraft problem allows us to assess the environmental resources at hand for the spacecraft. The availability and accessibility will be associated with the different behaviours the spacecraft is capable of performing. Charging the battery, recording and transmitting data, will therefore all have an assigned accessibility and availability. The spacecraft is equipped with sensors – Sun sensor, and GPS – that determine the availability r_i of any resource ($i = 1 - n$). For example when the satellite detects, via its Sun sensor, that it is in sunlight $r_{sun} = 1$, while we will have $r_{sun} = 0$ if the satellite is in the eclipsed arc of its orbit. The ground station availability will be $0 < r_{ground\ station} < 1$ when the satellite detects through a global positioning system or up-link signal, that the ground station is present, otherwise $r_{ground\ station} = 0$. Similarly if the satellite is in sight of the target area $0 < r_{target} < 1$ and $r_{target} = 0$ if not. The rate at which the satellite can perform a certain task is modelled by the accessibility k_i ($i = 1 - n$) and is associated with the ease with which the spacecraft can obtain a resource through its behaviour. For example the rate k_{sun} at which the satellite can charge the battery by pointing towards the Sun is the maximum array power output. If the solar array is damaged then k_{sun} is lowered: for example if 50% of the array fails at $t = t_{failure}$, then $k_{sun}(t_{failure}) = 0.5k_{sun}(t_{launch})$. Similarly we will have $k_{ground\ station}$, and k_{target} which are defined by hardware constraints before launch and determined by the maximum data rates for acquiring and down-linking data. Should the satellite suffer an antenna, transmitter or payload

instrument failure, these parameters would be lowered accordingly. Importantly it will be found that explicit failure detection is not required and that the satellite will resequence its actions to compensate for failure modes. This is one of the key benefits of the algorithm which will be presented.

3.10 OPTIMAL BEHAVIOUR

We now have all the tools to determine the optimal behaviour the agent will perform at any given time. The solution obtained from Pontryagin's Maximum Principle (the optimal behaviour) depends on the conditions constraining the animal's or the agent's behaviour [Sibly and McFarland 1976]. There are four important constraints that need to be considered:

1. The impossibility of performing behaviour at a negative rate implies that $u_i(t) \geq 0$.
2. Behaviours are rate limited, so that the agent cannot work faster than some limiting rate defined by the accessibility k_i, therefore $u_i \leq k_i$.
3. The rate of performing a behaviour is defined by $\dot{x}_i = -r_i u_i$, for availability r_i where $\dot{x}_i$ is the rate of change of the state x_i $(i = 1\text{-}n)$.
4. The agent can perform only one behaviour at a time. For example, for an animal, the act of feeding limits the amount of time available for other activities. In the case of a spacecraft, if it is pointing towards the Sun for battery charging it cannot downlink to the ground station or activate the payload.

This last point is worth looking at more closely. If a proportion s, of the animal's time is allocated to feeding, then a proportion $(1 - s)$ is available for drinking. This,

assumes that drinking and feeding are the only two behaviours that the animal performs. If feeding occurs at a maximum rate, then the rate of feeding at that stage is sk_1. In general, considering condition 2 we can say that $u_1 \leq sk_1$ and $u_2 \leq (1 - s)k_2$, which can be expressed, taking into account condition 1 as:

$$0 \leq \frac{u_1}{k_1} + \frac{u_2}{k_2} \leq 1 \qquad [3.27]$$

We now have all the tools to help us determine what the optimal behaviour at any given time. Let us consider a quadratic cost function with two state variables x_1 and x_2: $C = x_1^2 + x_2^2 + u_1^2 + u_2^2$, subject to the constraint introduced with condition 3. Following the formulation of Pontryagin's Maximum Principle we can define the new function to be maximised as:

$$H = \lambda_1 \dot{x}_1 + \lambda_2 \dot{x}_2 - x_1^2 - x_2^2 - u_1^2 - u_2^2 \qquad [3.28]$$

If constraint 3 holds, then $\dot{x}_i = -r_i u_i$ and Equation 3.28 can be expressed as:

$$H = -\left[\left(u_1 + \frac{\lambda_1 r_1}{2}\right)^2 + \left(u_2 + \frac{\lambda_2 r_2}{2}\right)^2 - \left(\frac{\lambda_1 r_1}{2}\right)^2 - \left(\frac{\lambda_1 r_1}{2}\right)^2\right] - x_1^2 - x_2^2 \qquad [3.29]$$

The optimal behaviour therefore requires the controls u_i to maximise H subject to the constraints 1-4 introduced previously. The solution to this is most easily found geometrically in a space with axes $u_1 + \lambda_1 r_1/2$, $u_2 + \lambda_2 r_2/2$ in which lines of equal H

appear as segments of circles. The origin is the point of highest H, which decreases as the diameter of the circles increases, as shown in Figure 3.4.

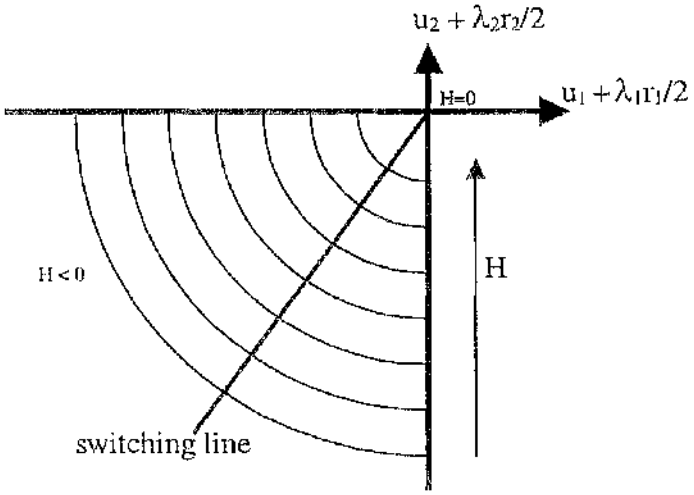

Figure 3.4 Lines of equal H, which increases the closer it is to the origin. The switching line separates the two possible behaviours (adapted from Sibly and McFarland, 1976).

The optimal control strategy is to set $u_1 = k_1$ and $u_2 = 0$ if the current state of the agent is to the left of the switching line and $u_1 = 0$ and $u_2 = k_2$ if the current state is to the right. This switching line is the two dimensional equivalent of the switching surface introduced in Chapter 2. Therefore we will have the two following situations:

Perform behaviour 1 at rate k_1 if $\lambda_1 r_1 k_1 > \lambda_2 r_2 k_2$

Perform behaviour 2 at rate k_2 if $\lambda_2 r_2 k_2 > \lambda_1 r_1 k_1$

Thus the optimal trajectory heads towards the switching line - where $\lambda_1 r_1 k_1 = \lambda_2 r_2 k_2$ – and then follows it to the origin. Moreover if we look at how we defined the Pontryagin function, Equation 3.28, and how the costate vector λ is defined, Equation

3.17, we can introduce a new parameter called deficit which is defined as [Elgerd, 1967]:

$$d_i = \frac{\partial C}{\partial x_i} \qquad [3.30]$$

and therefore if we consider the two competing behaviours as eating and drinking we will have:

Eat at rate k_1 if $d_1 r_1 k_1 > d_2 r_2 k_2$

Drink at rate k_2 if $d_2 r_2 k_2 > d_1 r_1 k_1$

This solution combines the agent's state with the parameters that describe the environment. The interesting property to note is that the structure of the rule does not change depending on the type of cost function chosen. The cost function acts simply as a scaling factor to the state variables. We can therefore say that the optimal behaviour is to perform an activity at the maximum rate at which it is available and a choice made between behaviours. Therefore, the choice between feeding and drinking should be made according to whether the product of deficit × availability × accessibility is greater for food or water. Several examples of this motivational behaviour have been studied in the animal kingdom [Bolles 1967, Schoener 1971, Krebs 1973, Sibly 1975, McCleery 1977]. This switching rule now forms the basis for the spacecraft action selection algorithm.

3.11 SATELLITE ACTION SELECTION ALGORITHM

We can now apply what we have introduced previously to the case of an autonomous agent, and in particular to the case of an autonomous satellite. For a spacecraft possessing the three essential state variables discussed earlier: battery charge, memory level and internal temperature, the cost function has been determined to have the following expression [Gillies et al. 1998].

$$C = b^2 + t^2 + m^2 \qquad [3.31]$$

Where b represents the battery charge deficit, t represents the data transmission deficit and m represents the data recording deficit. A deficit is defined as being the magnitude of the difference between some current state variable and its nominal equilibrium value. The deficits have the following expression:

$$b = \frac{b_{max} - b_c}{b_{max} - b_{min}} \qquad [3.32a]$$

$$m = \frac{m_{max} - m_c}{m_{max}} \qquad [3.32b]$$

$$t = \frac{m_c}{m_{max}} \qquad [3.32c]$$

where the subscript c identifies the current value of a state variable and the subscripts *max* and *min*, identify the upper and lower lethal values for the state variable. It can be noted how the deficit for the battery charge increases as the value of the current battery charge decreases. Similarly the deficit for recording data is greatest when the

current available memory space, identified by m_c, is zero, and decreases as the storage device fills with recorded data. Opposite is the behaviour of the transmission deficit t, which is highest when the memory is full, and decreases as data is down-linked to the ground station freeing up storage space. Essentially, the state variable deficits determine how far away from the origin that state variable is. Finally, it must be noted that a quadratic cost function has the desirable property that the cost of possessing any particular deficit increases more rapidly, than linearly, the further away from the homeostatic equilibrium point the spacecraft's variable lies. This is important because the closer the spacecraft is to a lethal limit, the more likely it is that it will suffer a failure and cease to operate. The system equations, which link the rate of change of a state variable with a behaviour for the satellite are:

$$\dot{b} = -r_{\text{sun}}u_{\text{s}} \qquad [3.33a]$$

$$\dot{t} = -r_{\text{transmit}}u_{\text{t}} \qquad [3.33b]$$

$$\dot{m} = -r_{\text{record}}u_{\text{r}} \qquad [3.33c]$$

with the constraint on the behaviours given by:

$$0 \leq \frac{u_{\text{s}}}{k_{\text{sun}}} + \frac{u_{\text{t}}}{k_{\text{transmit}}} + \frac{u_{\text{r}}}{k_{\text{record}}} \leq 1 \qquad [3.34]$$

To ensure its survival, the spacecraft must never drain its battery below the lower lethal limit. The satellite energy deficit b, is the measure of how much the batteries have discharged. Pointing the solar panels towards the Sun and charging the battery reduces this deficit. The spacecraft must also produce useful work, by

recording data from its payload and transmitting it back to Earth. The payload will be associated with a work deficit composed of a recording deficit m, and a transmitting to Earth ground station deficit t. By storing data, the spacecraft may reduce the recording deficit, while downloading data back to Earth will reduce the transmission deficit. It has been shown earlier that the behaviour to be performed by the spacecraft is the one associated with the highest drk product. In this formulation the deficits from the state variables combine with stimuli from the environment to determine a behavioural sequence. The stimuli are considered to be a cue to resources that will have consequences for the agent's state variables.

The decision to perform a particular behaviour is made by calculating the tendencies to perform all the various activities the spacecraft may exhibit and choosing the behaviour that possesses the highest tendency as explained in section 3.10. Empirical evidence that this occurs in animals has been discussed at length [Barends et al. 1955, Sibly 1975, Houston and McFarland 1976]. In addition, the cost function model predicts that such a multiplicative combination rule, when applied to the deficit and cue, should generate optimal behaviour sequencing. We can therefore finally summarise the problem of optimal control for the spacecraft as: behaviour $\Rightarrow$ Max[deficit×availability×accessibility].

$$\text{Max}[b \cdot r_{\text{sun}} \cdot k_{\text{sun}}] \Rightarrow \text{Charge the battery} \qquad [3.35a]$$

$$\text{Max}[m \cdot r_{\text{target}} \cdot k_{\text{target}}] \Rightarrow \text{Record data} \qquad [3.35b]$$

$$\text{Max}[t \cdot r_{\text{ground station}} \cdot k_{\text{ground station}}] \Rightarrow \text{Transmit to Earth ground station} \qquad [3.35c]$$

The satellite selects the optimal behaviour by computing the various deficits, taking environmental cues to assess availability and accessibility of the resources and

finally calculating the *drk* product associated with each behaviour. The optimal behaviour at any time is therefore the one which yields the highest of the above products. This algorithm also shows a degree of opportunism, because it considers environmental factors together with internal deficits. For example even if the battery deficit is low and the work deficit is high, the satellite may still opt to charge the batteries if sunlight is available and cues for doing work – visibility of ground station or target area – are low. Such opportunism is one of the major benefits of this algorithm and it is difficult, if not impossible, to code into conventional artificial intelligence engines. Another significant advantage of such a method is that the spacecraft measures environmental parameters (such as the presence of sunlight or ground station) and internal parameters (such as battery charge and memory level) so that complex models of the environment are not required to select the appropriate behaviour. Also, it is not necessary to have complex models of the spacecraft and its internal subsystems. If we consider the battery charge as an example, the model used for it is not directly relevant to the performance of the action selection algorithm; the algorithm uses the direct measure of battery charge rather than a model of the battery. Therefore, we can expect that the modelling of more complex and numerous spacecraft subsystems will not change the qualitative behaviour of the algorithm. This method however may easily incorporate additional tasks which will either form part of the action selection process, or which can be scheduled at a particular time by setting the *drk* product to equal unity at a fixed time. Adding extra tasks is straightforward; each new behaviour will be given a deficit, availability and accessibility. The resulting behaviour will always be the one with the highest *drk* product.

CHAPTER IV

POTENTIAL FUNCTIONS

4.1 PREFACE

In this chapter we introduce an attitude control methodology generated using Lyapunov's Second Method. This control method has the desirable properties of guaranteeing smooth convergence to the desired final attitude, not being software intensive and being fully autonomous. It will be used to slew the spacecraft between different objectives – Sun, ground station, and target area – as required by the action selection algorithm.

4.2 INTRODUCTION

A spacecraft attitude control system aims to adapt and stabilise the attitude of the spacecraft with regard to its present state and the tasks it has to perform [Chobotov 1991]. In general, it consists of four major functional sections: sensing, logic, actuation and vehicle dynamics as shown in Figure 4.1. In the case of an autonomous control system, these four elements work in a closed-loop. The sensing function determines the satellite attitude, the logic programs the signals to be sent in the correct sequence to the torque producing elements (momentum wheels, gas jets,

etc.), which in turn rotate the spacecraft about its centre of mass. The resulting motion is then monitored by the spacecraft sensors, thus closing the loop.

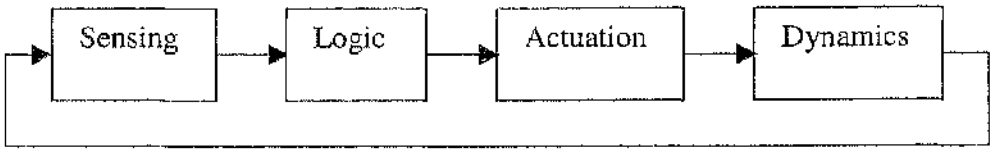

Figure 4.1 Structure of a spacecraft attitude control system

Currently many spacecraft missions have the requirement of performing large angle slew manoeuvres. Open-loop schemes have been proposed [Vadali and Junkins 1983], which do not require feedback measurements, avoiding the possibility of closed-loop instability. However these methods are sensitive to spacecraft parameter uncertainties and disturbances. Also, these manoeuvres are often constrained because of payload safety considerations. These constraints arise from either not directing sensitive instrumentation towards bright sky regions, or avoiding blinding of attitude sensors. Also, three-axis stabilized satellites must perform large angle slew manoeuvres to safe pointing modes in the case of system failures.

The planning of constrained manoeuvres can be time consuming, particularly for missions with frequent payload re-targeting. Conventional approaches to on-board autonomy have centred on artificial intelligence or expert systems [Olszweski 1990] to allow real time on-board navigation and control. However these methods necessitate the implementation of significant on-board software, increasing the loads on limited flight computers. Similarly, approaches using neural networks [Carrara and Rios Nieto 1999], although successful, are difficult to explicitly validate. Potential function methods have been used as a basis for computationally efficient

autonomous guidance and control systems. Applications range from terminal descent to a planetary surface to constrained proximity manoeuvring for space station rendezvous to on-orbit assembly [McInnes 1993, Roger and McInnes 2000, McQuade and McInnes 1997].

In feedback control the attitude of the spacecraft must be known at all times. For large angle manoeuvres the orientation can be represented by a cosine matrix, Euler angles, or quaternions. We will presents the stability and control analysis of large angle feedback manoeuvres for a spacecraft using Euler angles for ease of illustration. The method is based firstly on defining a scalar potential function which meets the conditions of Lyapunov's theorem. This function is defined to have a global minimum at the desired final attitude and later includes regions of high potential which represent pointing constraints. Once the state space has been mapped onto an appropriate potential function, the controls are then chosen such that the derivative of the potential function is rendered negative definite. This then assures that the spacecraft converges to the desired terminal state without violating the desired pointing constraints.

4.3 LYAPUNOV'S SECOND METHOD

Aleksandr Mikhailovich Lyapunov (1857-1911) first proposed a novel method for determining the stability properties of non-linear systems at the end of the 19th century [Lyapunov 1892]. Despite being extensively used by other Russian mathematicians and engineers, the method did not achieve popularity in the West until Kalman and Bertram applied it to a wide range of control problems [Kalman and

Bertram 1960]. Since then, Lyapunov's second method has been widely applied to stability problems for both terrestrial and spacecraft control problems [Grantham and Chingcuanco 1984, Rimon and Koditchek 1992].

The aim of Lyapunov's second method is to guarantee the stability of a set of differential equations which describe a dynamical system. In physical terms, this has been described as:

"*If the rate of change of $dE(\mathbf{x})/dt$ of the energy $E(\mathbf{x})$ of an isolated physical system is negative for every possible state $\mathbf{x}$, except for a single equilibrium state $\mathbf{x}_e$, then the energy will continually decrease until it finally assumes its minimum value $E(\mathbf{x}_e)$.*"

This intuitively corresponds to the definition of all stability problems. If a stable system is perturbed from its equilibrium state, it will always return to it. In mathematical terms this can be expressed as:

"*A dynamical system is stable (in the sense that it returns to equilibrium after any perturbation) if and only if there exists a Lyapunov function, a scalar function $V(x)$ of the state with the following properties*":

$$V(x) > 0 \text{ and } \dot{V}(x) < 0 \qquad \text{for } \mathbf{x} \neq \mathbf{x}_e \qquad [4.1a]$$

$$V(x) = 0 \text{ and } \dot{V}(x) = 0 \qquad \text{for } \mathbf{x} = \mathbf{x}_e \qquad [4.1b]$$

where $\mathbf{x}_e$ is the equilibrium state of the dynamical system. If these conditions are satisfied, it is possible to guarantee that the origin of the state space is a point of asymptotic global attraction and that all the trajectories inside the space, regardless of

the initial conditions converge to this point.

An extended form of the Lyapunov function, the called potential function, will be used in the following analysis. This function can be defined analytically and will be used to force the state vector of the dynamical system to converge to the desired goal. The mechanism which drives the convergence is based upon the rate of change of the potential function. If the rate of change of the potential $\dot{V}(\mathbf{x})$ is negative definite the state vector will converge to the goal point, which is the global minimum of the potential function. If $\dot{V}(\mathbf{x})$ is positive however, we will see the state vector diverging from the goal point. In this case, to render $\dot{V}(\mathbf{x})$ once again negative, some form of control is required. It is therefore possible to derive a control methodology which forces the convergence to the desired goal of the dynamical system. Defining a potential function based on some state vector $\mathbf{x}$ so that:

$$V = f(x) \tag{4.2}$$

and differentiating this potential function with respect to time yields:

$$\dot{V} = \nabla f \cdot \dot{x} \tag{4.3a}$$

where

$$\nabla f = \frac{\partial f}{\partial x} \tag{4.3b}$$

Therefore, since $\dot{\mathbf{x}}$ is a function of the control variable, by analytically determining

the potential derivative $\dot{V}(\mathbf{x})$, it is possible to calculate the control inputs, which are required to render $\dot{V}(\mathbf{x})$ negative, and so ensure the convergence of the dynamical system to the desired goal point. In the following sections, we will introduce two different control methods. The first is a continuous control method, the second is a discrete control method. The continuous method forces the rate of change of potential to be continuously negative by implementing a continuous control action. The discrete method differs in that the control is only implemented when the rate of change of the potential is zero or positive.

4.4 ATTITUDE DYNAMICS AND KINEMATICS

The majority of space-based systems require the use of accurate pointing, either as part of an antenna or payload mechanism or indeed a complete structure such as the Hubble Space Telescope. The control mechanism for modifying the attitude of the spacecraft may be momentum wheels, magneto-torquers, gas jets, etc.

Consider a rigid body having a set of body fixed axes, rotating about its centre of mass with angular velocity ω. The origin of the set of axes is chosen to be at the centre-of-mass of the body. The angular velocity vector has components ω_1, ω_2 and ω_3 along the x, y and z body axes respectively. Therefore if $\mathbf{i}$, $\mathbf{j}$ and $\mathbf{k}$ are the unit vectors in the x, y and z direction we have:

$$\omega = \omega_1\mathbf{i} + \omega_2\mathbf{j} + \omega_3\mathbf{k} \qquad [4.4]$$

Now, the angular momentum vector $\mathbf{h}$ of the body can be expressed as the matrix

product of the inertia tensor **I** and the angular velocity ω such that:

$$\mathbf{h} = \begin{bmatrix} I_{11} & I_{12} & I_{13} \\ I_{21} & I_{22} & I_{23} \\ I_{31} & I_{32} & I_{33} \end{bmatrix} \begin{bmatrix} \omega_1 \\ \omega_2 \\ \omega_3 \end{bmatrix} = \mathbf{I} \cdot \omega \qquad [4.5]$$

where I_{ii} (i = 1-3) is the moment of inertia of the body around the i-th axis, while I_{ij} (i, j = 1-3) is the product of inertia around the i-th and j-th axis. It is known that the external moment, **M** is equal to the rate of change of angular momentum with respect to a fixed axes system [Likins et al. 1983]. However, with reference to the body fixed axis system, this becomes:

$$\mathbf{M} = \dot{\mathbf{h}} + \omega \times \mathbf{h} \qquad [4.6]$$

In component form, Equations 4.5 and 4.6 lead to:

$$M_1 = \dot{\omega}_1 I_{11} + (\omega_1\omega_3 - \dot{\omega}_2) I_{12} - (\dot{\omega}_3 + \omega_1\omega_2) I_{13} + (\omega_3^2 - \omega_2^2) I_{23} + \omega_2\omega_3 (I_{33} - I_{22}) \qquad [4.7a]$$

$$M_2 = \dot{\omega}_2 I_{22} + (\omega_1\omega_2 - \dot{\omega}_3) I_{23} - (\dot{\omega}_1 + \omega_2\omega_3) I_{12} + (\omega_1^2 - \omega_3^2) I_{13} + \omega_1\omega_3 (I_{11} - I_{33}) \qquad [4.7b]$$

$$M_3 = \dot{\omega}_3 I_{33} + (\omega_2\omega_3 - \dot{\omega}_1) I_{13} - (\dot{\omega}_2 + \omega_3\omega_1) I_{23} + (\omega_2^2 - \omega_1^2) I_{12} + \omega_1\omega_2 (I_{22} - I_{11}) \qquad [4.7c]$$

which are Euler's equation of motion for a rigid body rotating about its centre-of-mass. As they stand Equations 4.7 are difficult to manipulate. Considerable simplification can be made by allowing the body fixed axes to coincide with the principal axes of inertia, thus defining the products of inertia to be zero and reducing the system of equations to:

$$M_1 = \dot{\omega}_1 I_{11} + \omega_2 \omega_3 (I_{33} - I_{22}) \quad [4.8a]$$

$$M_2 = \dot{\omega}_2 I_{22} + \omega_1 \omega_3 (I_{11} - I_{33}) \quad [4.8b]$$

$$M_3 = \dot{\omega}_3 I_{33} + \omega_1 \omega_2 (I_{22} - I_{11}) \quad [4.8c]$$

When defining the orientation of a body with respect to a fixed reference frame, a series of pure rotations is used which results in an orthogonal transformation. The associated rotations uniquely determine the orientation of the body. The sequence of rotations from inertial frame (X,Y,Z) with unit vectors (**I**, **J**, **K**) to body frame (x,y,z) with unit vectors (**i**, **j**, **k**), used here, is illustrated in Figure 4.2 and can be listed as:

a) Rotation about the Z-axis through angle θ_1.

b) Rotation about the x'-axis through θ_2.

c) Rotation about the z'-axis through θ_3 to produce x, y and z axes.

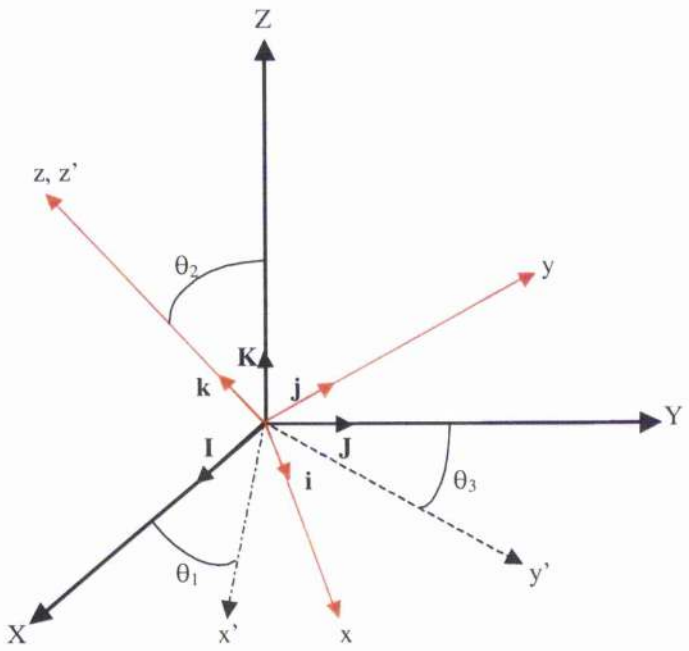

Figure 4.2 Rotational sequence used to defined Euler's angles and unit vectors.

where each rotation is characterized as an orthogonal transformation. It is possible to link the Euler angles to the body rates ω_1, ω_2 and ω_3 through the following kinematic relation:

$$\dot{\theta}_i = \sum_{j=1}^{3} G_{ij}\omega_j \qquad [4.9]$$

where G_{ij} is the transformation matrix:

$$G_{ij} = \begin{bmatrix} \sin\theta_3 \sec\theta_2 & \cos\theta_3 \sec\theta_2 & 0 \\ \cos\theta_3 & -\sin\theta_3 & 0 \\ -\sin\theta_3 \cot\theta_2 & -\cos\theta_3 \cot\theta_2 & 1 \end{bmatrix} \qquad [4.10]$$

We can then obviously express the body rates in terms of the rotational rates by using an inverse transformation to obtain:

$$\omega_1 = \dot{\theta}_1 \sin\theta_2 \sin\theta_3 + \dot{\theta}_2 \cos\theta_3 \qquad [4.11a]$$

$$\omega_2 = \dot{\theta}_1 \sin\theta_2 \cos\theta_3 - \dot{\theta}_2 \sin\theta_3 \qquad [4.11b]$$

$$\omega_3 = \dot{\theta}_1 \cos\theta_2 + \dot{\theta}_3 \qquad [4.11c]$$

These transformations will be used later following the definition of the potential function.

4.5 CONTINUOUS CONTROL

The required solution for the problem is to bring the spacecraft to rest at some desired attitude. The terms which must be controlled therefore are the Euler angles – θ_1, θ_2 and θ_3 – and the body rates – ω_1, ω_2 and ω_3. The potential function will now be defined to have the following form:

$$V = V_{\text{Euler}} + V_{\text{Body Rates}} \qquad [4.12]$$

The components of the potential function due to the Euler angles will take the form of a quadratic polynomial function:

$$V_{\text{Euler}} = \frac{1}{2}\sum_{i=1}^{3} \alpha_i \left(\theta_i - \tilde{\theta}_i\right)^2 \qquad [4.13]$$

where $\tilde{\theta}_i$ is the goal attitude and α_i is a shaping parameter. The potential function component due to the body rates will have a simpler form with the goal corresponding to null body rates:

$$V_{\text{Body Rates}} = \frac{1}{2}\sum_{i=1}^{3} I_i\, \omega_i^2 \qquad [4.14]$$

The global potential, being the sum of the Euler and body rate components will

therefore take the form:

$$V = \frac{1}{2}\sum_{i=1}^{3} I_i\,\omega_i^2 + \frac{1}{2}\sum_{i=1}^{3}\alpha_i\left(\theta_i - \tilde{\theta}_i\right)^2 \qquad [4.15]$$

To satisfy Lyapunov's theorem, the rate of change of the potential $\dot{V}$ must be rendered negative definite. Therefore differentiating the potential leads to:

$$\dot{V} = \sum_{i=1}^{3} I_i\omega_i\dot{\omega}_i + \sum_{i=1}^{3}\alpha_i\left(\theta_i - \tilde{\theta}_i\right)\dot{\theta}_i \qquad [4.16]$$

Rearranging and substituting Equations 4.8 and 4.9 into the rate of change of the potential and simplifying, leads to the following equation:

$$\dot{V} = \sum_{i=1}^{3}\omega_i M_i + \sum_{i=1}^{3}\alpha_i\left(\theta_i - \tilde{\theta}_i\right)\sum_{j=1}^{3} G_{ij}\omega_i \qquad [4.17]$$

which will be used to generate the control laws. A possible control torque which will render $\dot{V}$ negative definite may be expressed by:

$$M_i = -k_i\omega_i - \alpha_i\sum_{j=1}^{3} G_{ij}^T\left(\theta_j - \tilde{\theta}_j\right) \qquad [4.18]$$

where k_i (i = 1-3)is a positive definite shaping parameter. When the control torque is substituted into Equation 4.17 the potential derivative then takes the form:

$$\dot{V} = -\sum_{i=1}^{3} k_i \omega_i^2 \qquad [4.19]$$

so that the control laws which will rotate the spacecraft to the desired goal attitude are available in analytical form. We will now consider a case study to evaluate the performance of the controller.

For illustration we will define a spacecraft as a solid cube with a length of 20 cm, and we assume a mass of 25 kg. The moments of inertia are then easily calculated from:

$$I_1 = I_2 = I_3 = \frac{2}{3} m l^2 = 0.7 \text{ kgm}^2 \qquad [4.20]$$

where m is the mass of the spacecraft and l is its side length. Furthermore we will now define the initial conditions for the body rates and Euler angles as:

$$\omega_1 = \omega_2 = \omega_3 = 0$$
$$[\theta_1, \theta_2, \theta_3] = [0, 1, \pi] \qquad [4.21]$$

and the final goal conditions for the body rates and Euler angles as:

$$\omega_1 = \omega_2 = \omega_3 = 0$$

$$\left[\tilde{\theta}_1, \tilde{\theta}_2, \tilde{\theta}_3\right] = [0, 0, 0] \qquad [4.22]$$

Equations 4.8 and 4.9 form a system of six differential equations which fully characterise the rotation of the body. Together with the initial conditions we can numerically integrate the equations using a Runge-Kutta method. The control torques are implemented as expressed by Equation 4.18 with k_i = 10 (i = 1-3) and α_i = 1 (i = 1-3). The results are shown in Figures 4.3-4.6. In Figure 4.3 we can see the behaviour of the Euler angles, which represent the attitude of the body. We can clearly see that the control algorithm slowly damps the three angles to the desired goal attitude. The body rates are shown in Figure 4.4. Once again we can see that the three angular velocities are driven to the desired goal values identified by the body at rest. In Figure 4.5 we can see how the magnitude of the torques decay as the body approaches the goal attitude, thus allowing for smooth convergence. In Figure 4.6 we see that the potential is reduced to zero, while the rate of change of the potential remains clearly negative definite, thus complying with Lyapunov's theorem and guaranteeing convergence. We can also note a strong coupling about each body axis. As axis 2 and 3 are controlled, there is a clear displacement of axis 1 as a consequence. The potential function control algorithm, however, brings the body to rest at the desired goal attitude. We have therefore demonstrated that the potential function method can successfully control a complex non-linear dynamical system by continuously controlling the rate of change of the potential.

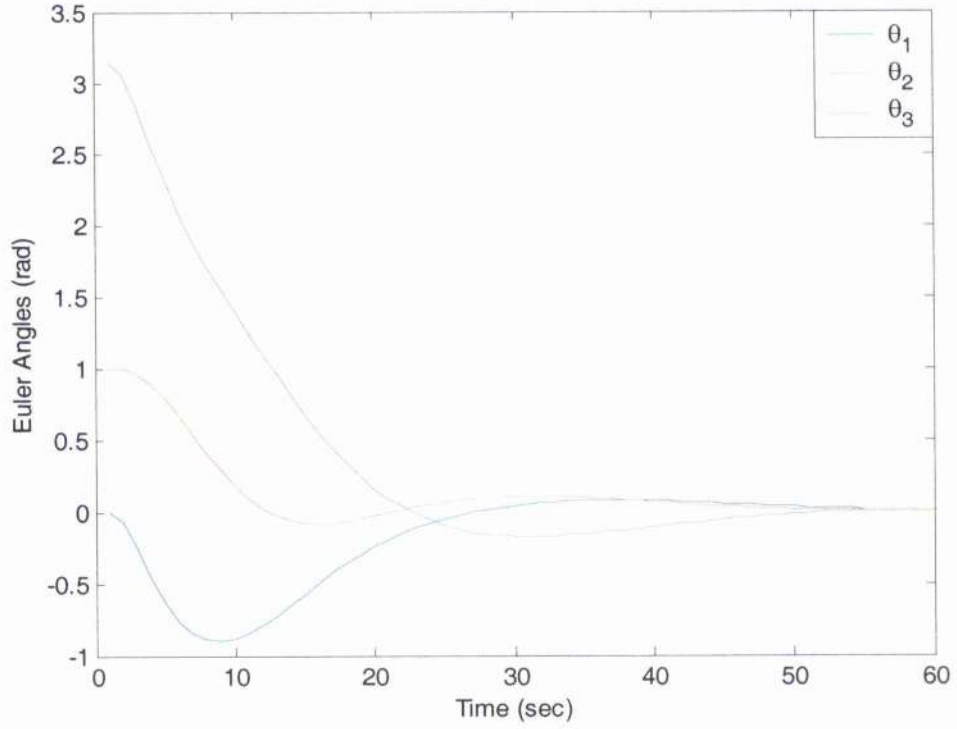

Figure 4.3 Continuous control: Euler angles

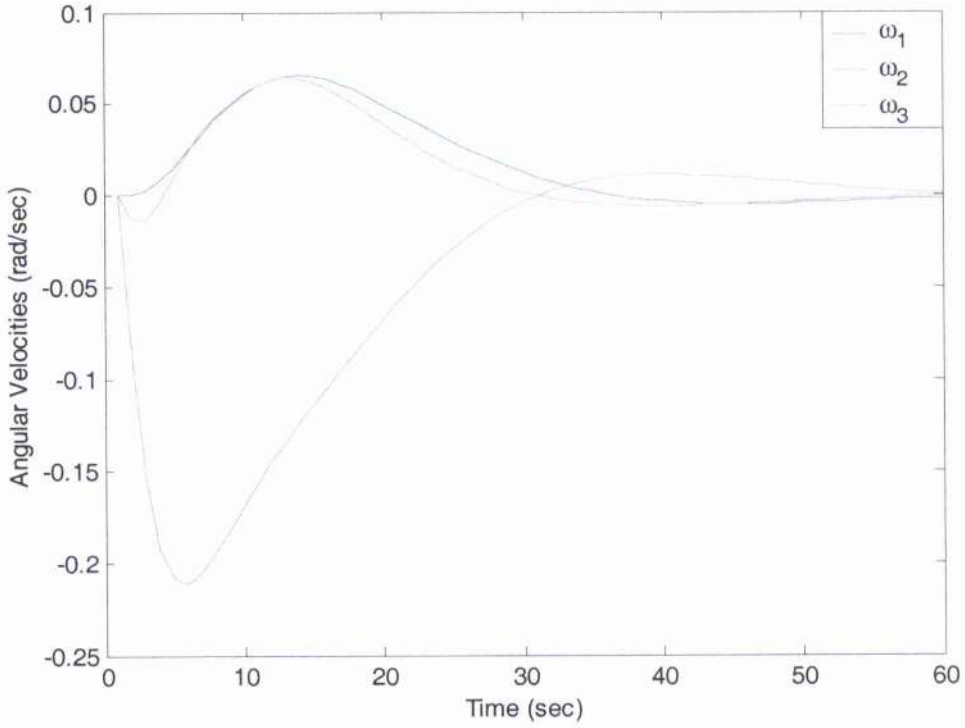

Figure 4.4 Continuous control: body rates

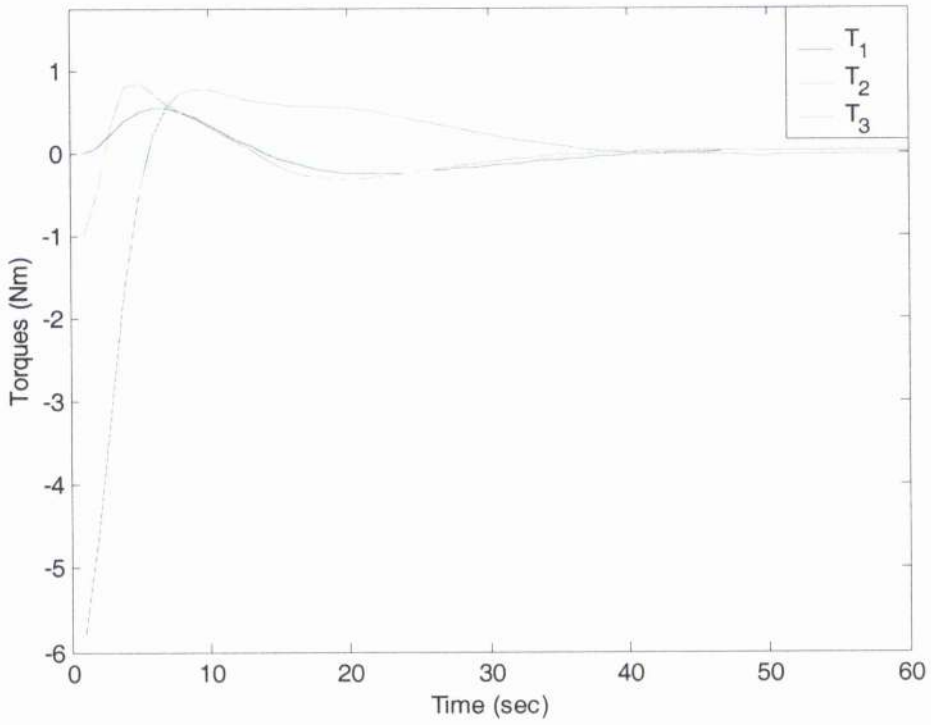

Figure 4.5 Continuous control: control torques

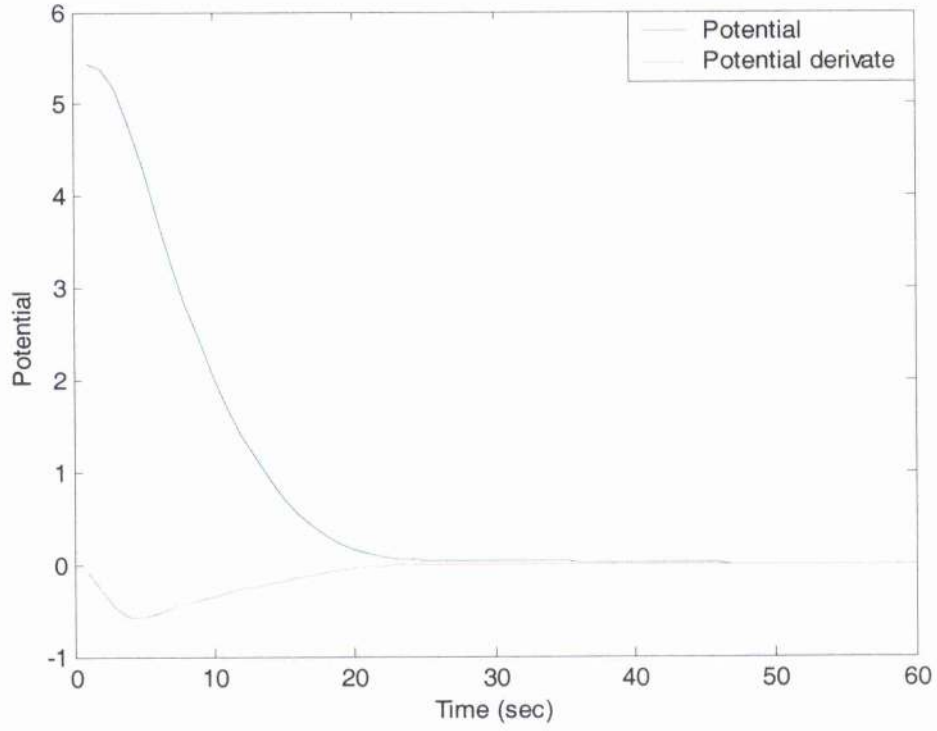

Figure 4.6 Continuous control: potential function

4.6 DISCRETE CONTROL

We will now have to introduce a new potential function, which complies with the conditions required by Lyapunov's Second Method [Radice and McInnes, 2000]. Only when the rate of change of the potential is positive, will control action be taken so as to render the rate of change negative once again, thus ensuring convergence to the goal attitude. We will now consider the current attitude of the satellite by means of a vector $\mathbf{n}_s$ assumed to be directed along the axis of the payload. We also have the goal attitude identified by the vector $\mathbf{n}_f$ such that:

$$\mathbf{n}_s = (\sin\theta_1\sin\theta_3 + \cos\theta_1\sin\theta_2\cos\theta_3)\mathbb{I} + (\sin\theta_1\cos\theta_3 + \cos\theta_1\sin\theta_2\sin\theta_3)\mathbb{J} + \cos\theta_1\cos\theta_2\mathbb{K} \qquad [4.23]$$

$$\mathbf{n}_f = \cos\alpha_f\cos\varepsilon_f\,\mathbb{I} + \sin\alpha_f\cos\varepsilon_f\,\mathbb{J} + \sin\varepsilon_f\,\mathbb{K} \qquad [4.24]$$

where $\mathbb{I}$, $\mathbb{J}$ and $\mathbb{K}$ are the unit vectors along the inertial frame of reference axes, and where α_f and ε_f are the azimuth and elevation angles of the goal attitude, as shown in Figure 4.7.

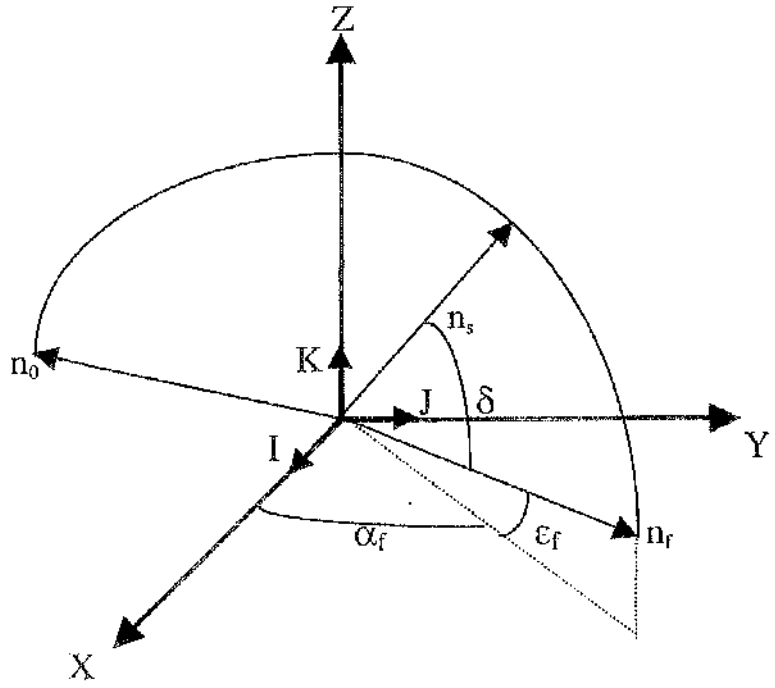

Figure 4.7. Schematic large angle slew

We can then obtain the slew angle δ from the scalar product between these two vectors:

$$\delta = \arccos\left(\boldsymbol{n}_s \cdot \boldsymbol{n}_f\right) \qquad [4.25]$$

which then allows us to define the potential function as a quadratic function of the slew angle δ, given by:

$$V = \frac{1}{2}\delta^2 \qquad [4.26]$$

The time derivative of the potential function is given by:

$$\dot{V} = \delta\,\dot{\delta} \qquad [4.27]$$

where $\dot{\delta}$ can be calculated analytically from Equation 4.25. When this function is negative the attitude motion is propagated in open-loop. If it assumes a positive value, control action is activated as previously discussed. The method now consists of finding the change in slew rate necessary to render the rate of change of the potential negative definite again. This can be achieved by calculating the necessary change in slew rate as:

$$\Delta\dot{\theta} = \dot{\theta}_r - \dot{\theta}_c \qquad [4.28]$$

where $\dot{\theta}_c$ is the current attitude rate of the satellite with respect to the goal, while $\dot{\theta}_r$ is the slew rate that has to be implemented to render the potential derivative negative definite with the vector $\theta = (\theta_1, \theta_2, \theta_3)$. Since the torque levels are finite, the body angular accelerations are finite, meaning that the change in slew rate to ensure that the rate of change of the potential is negative cannot be achieved instantaneously, leaving the possibility that the rate of change of the potential is positive, while $\Delta\dot{\theta}$ is being reduced to zero. To avoid this problem a threshold parameter $\beta > 0$ can be introduced. The control will therefore be activated when the potential derivative surpasses this fixed threshold: $\dot{V} > -\beta$. The required rate is now defined as:

$$\dot{\theta}_r = -\Omega\mathbf{n} \qquad [4.29]$$

with $\mathbf{n}$ being the unit vector down the gradient of the potential function, defined as:

$$\mathbf{n} = \frac{\nabla V}{\|\nabla V\|} \qquad [4.30]$$

and Ω is some shaping function. A particular function which slows the attitude slew as the satellite approaches the goal point is given by:

$$\Omega = \Omega_0\left(1 - exp(-\lambda\delta^2)\right) \qquad [4.31]$$

where λ and Ω_0 are free parameters which influence the weight that Ω has as a shaping function. Ω_0 is the mean angular velocity, and the higher the value the quicker the satellite will slew to the desired goal point. λ is linked to the angular deceleration of the satellite approaching the target. The values of the two shaping parameters affect the time and fuel consumption of the slew manoeuvre.

The body rates are linked to the rotational angles by Equation 4.11. Knowing the value of $\dot{\theta}_i$ we can therefore obtain the required body rates ω_r. Since the current body rates ω_c are known by means of the satellite sensors we can find the necessary change in body rates as:

$$\Delta\omega = \omega_r - \omega_c \qquad [4.32]$$

Through Euler's simplified equations of motion, Equation 4.8, we can now determine the thruster pulse width Δt_i (i = 1-3) for each axis as:

$$\Delta t_1 = \Delta \omega_1 \frac{I_1}{M_1} \qquad [4.33a]$$

$$\Delta t_2 = \Delta \omega_2 \frac{I_2}{M_2} \qquad [4.33b]$$

$$\Delta t_3 = \Delta \omega_3 \frac{I_3}{M_3} \qquad [4.33c]$$

The activation of the thrusters will therefore render the potential derivative negative once again. The process is then repeated again when the rate of change of the potential surpasses the activation threshold; $\dot{V} > -\beta$. The thrusters are assumed to produce a constant thrust of 1 N. To avoid excessive control activity, they are activated only if the required pulse width is longer than 0.01 sec. To fine tune the manoeuvre in the proximity of the target the pulse width can be decreased. The resulting attitude motion consists of a series of open-loop arcs connected by a set of discrete control events.

To initially validate this control method, a simple analysis is carried out. The spacecraft is forced to move from some initial attitude, to a desired final attitude. After having demonstrated the success of a single point-to-point transfer, the method will be expanded so that the spacecraft has to move between several target attitudes before reaching the final attitude. The spacecraft again is characterized by the following moments of inertia: $I_1 = I_2 = I_3 = 2.7$ kgm^2, as defined in section 4.5. The free parameters used to model the shaping function are the following: $\lambda = 100$ and $\Omega_0 = 0.01$. The initial conditions are set as $\omega_1 = \omega_2 = \omega_3 = 0.01$ with the final conditions requiring the spacecraft to be at rest. Results from such a simulation are shown in Figures 4.8-4.11.

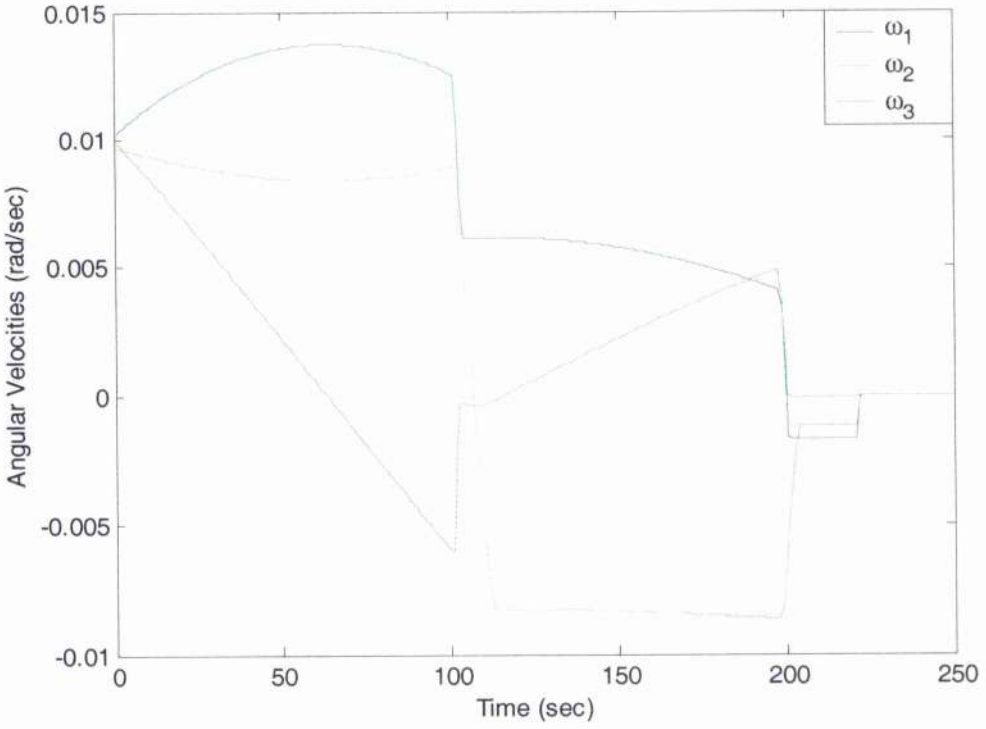

Figure 4.8 Discrete control: body rates

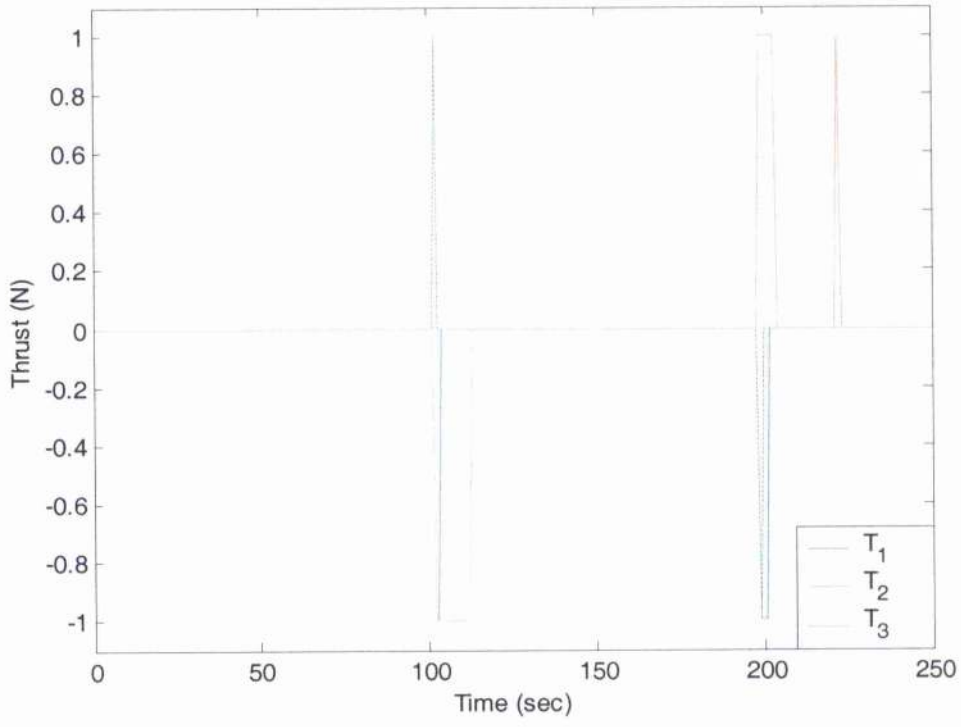

Figure 4.9 Discrete control: control thrusts

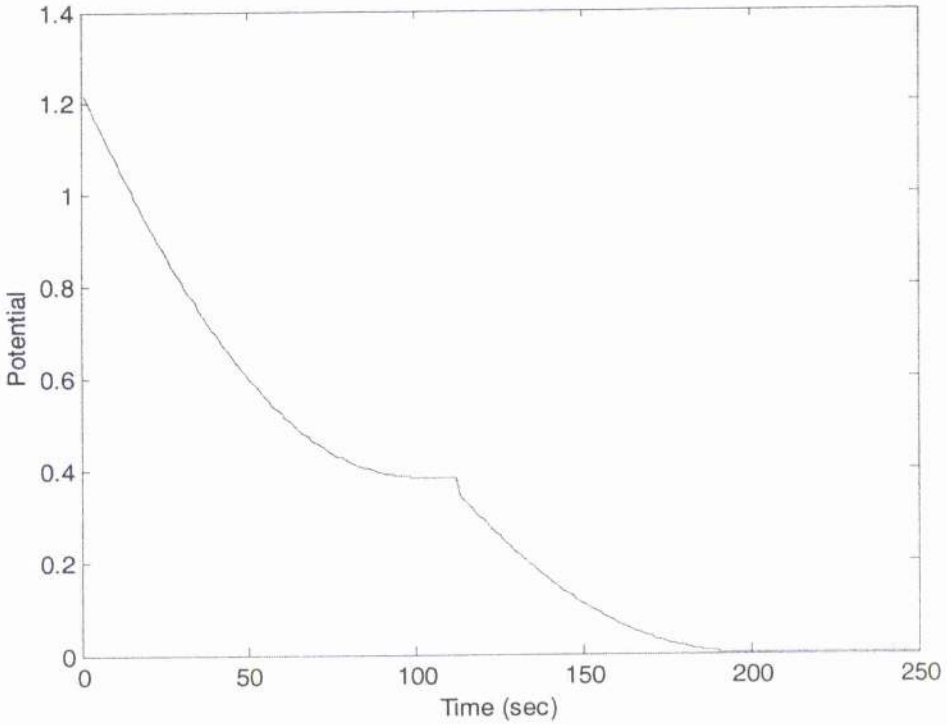

Figure 4.10 Discrete control: potential

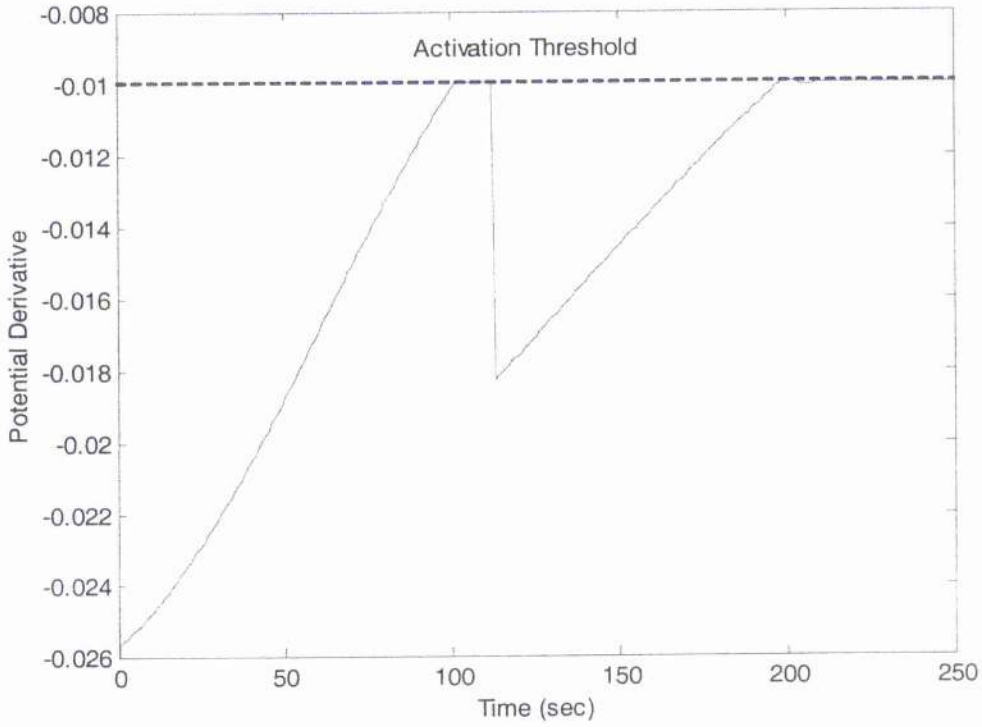

Figure 4.11 Discrete control: potential derivative

It can be seen, from Figures 4.8-4.11 that the angular velocity tends to zero as the satellite reaches the final attitude; since the shaping function Ω has the property of slowing the attitude slew as the satellite approaches the goal point. The potential function decreases monotonically as predicted by Lyapunov's theorem. The thrusters are activated once, in correspondence to the moment when the potential derivative assumes a $\dot{V} > -\beta$ value, with $\beta = 0.01$.

Having shown the effectiveness of the method we now extend the analysis so that the satellite will be slewed between a number of target attitudes and so we will have to define the potential in a different form. The potential function is used, as before, to generate a path between the various targets. Each target point will be defined as a local minimum for the potential. Once a desired attitude is reached, the potential will assume a new form to take into account that a goal point has been reached. Firstly the satellite is driven by the potential towards the nearest goal point, which is a local minimum for the potential function. Once the i-th target is reached, a switching parameter L_i is changed from 1 to 0 to remove that local minimum. The satellite then progresses to the next nearest goal point, again a local minimum for the potential function, where once again the corresponding value of L_i is switched from 1 to 0. The procedure is then re-iterated until the satellite reaches the final goal point, which will now be the global minimum of the potential. A potential function which can satisfy these requirements, will be defined as a sequence of polynomials for N targets using:

$$V = \frac{1}{2}\sum_{i=1}^{N} L_i \delta_i^2 \qquad [4.34]$$

with δ_i being the angle between the current satellite vector $\mathbf{n}_s$ and the i-th goal attitude and L_i is the switching parameter. The intermediate attitudes are local minima for the potential, with the final attitude being the global minimum. This method is not suitable for optimal path planning, however it does guarantee that all targets are visited only once. Results for a simulation in which the spacecraft is required to reach four intermediate goal attitudes before the final attitude are shown in Figures 4.12-4.13. The spacecraft is considered to have an initial angular velocity of 0.01 rad/sec around each axis. The goal attitudes are identified by the following pairs of values of azimuth and elevation: $(\alpha_1, \varepsilon_1) = (-\pi/2, 0)$; $(\alpha_2, \varepsilon_2) = (0, 0)$; $(\alpha_3, \varepsilon_3) = (0, \pi/2)$; $(\alpha_4, \varepsilon_4) = (\pi/2, 0)$; $(\alpha_5, \varepsilon_5) = (\pi, 0)$. Figures 4.12a and 4.12b show the behaviour of the potential as the spacecraft moves between the desired target attitudes, while the thrusters pulses are shown in Figure 4.13. The following considerations can be made. As the spacecraft reaches a target the switching parameter L_i in the potential function changes from the value one to zero. The potential will therefore assume a new form with the following local minimum becoming the new target. The intermediate attitudes are local minima for the potential, with the final attitude being the global minimum. Again, this method is not suitable for true optimal path planning, however it does guarantee that all targets are visited, and visited only once.

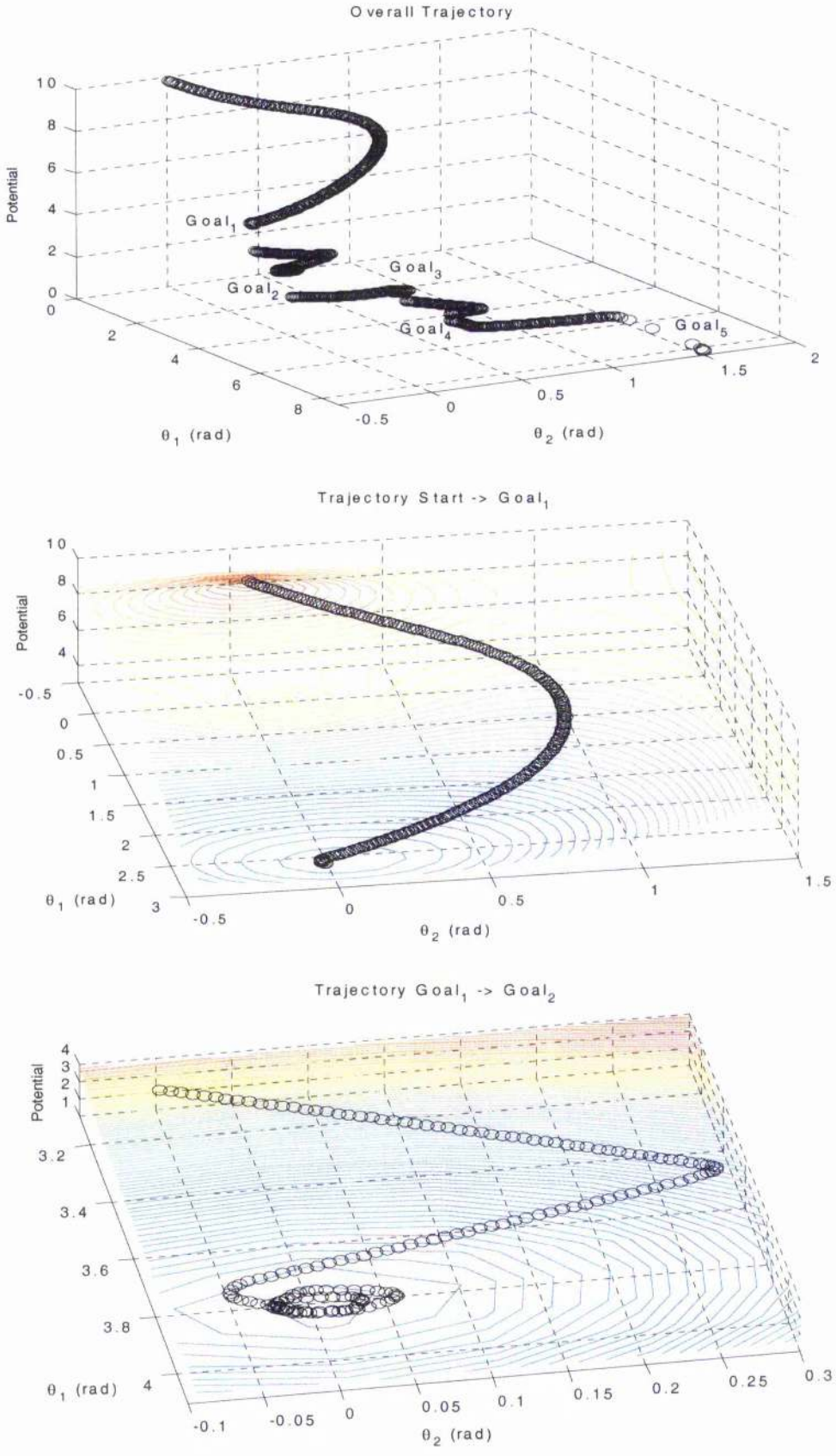

Figure 4.12a Multiple target transfer

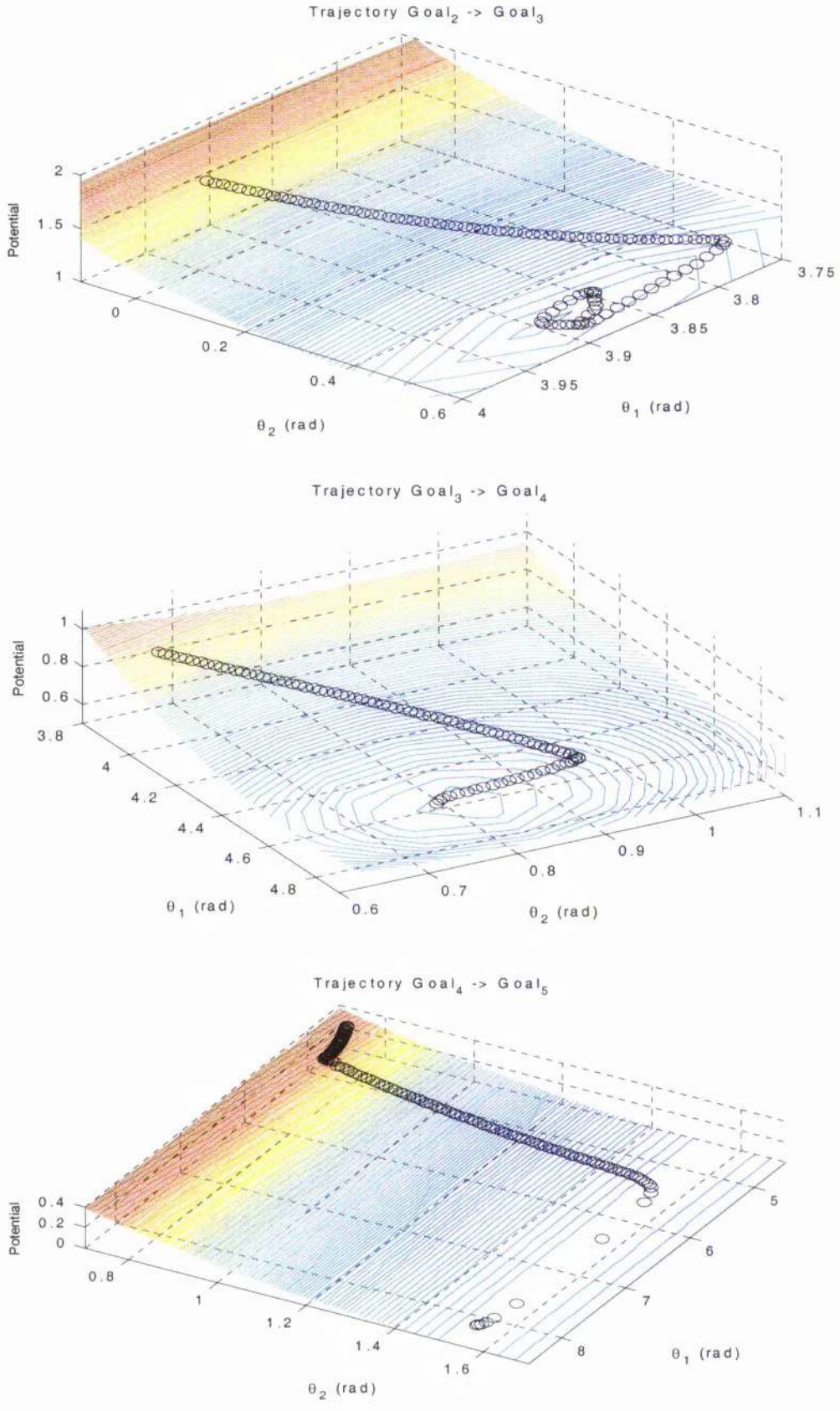

Figure 4.12b Multiple target transfer

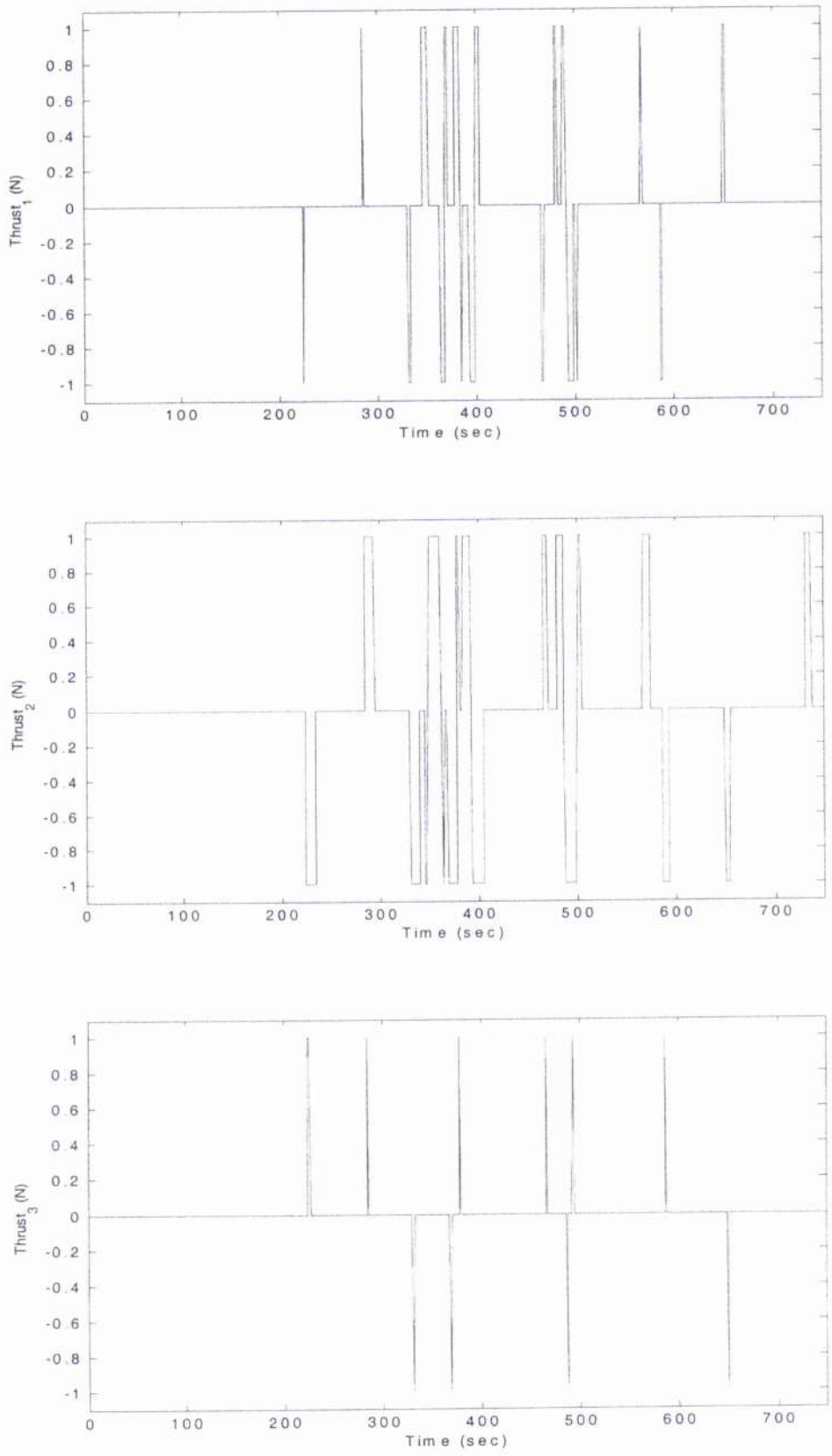

Figure 4.13 Thruster pulses for multiple target transfer

4.7 POINTING CONSTRAINTS

For any system using potential functions, active constraint enforcement may be implemented to constrain the separation of the satellite payload axis and any pointing constraints which may be present. Such constraints, for a sensitive payload, may represent for example pointing towards the Sun, or other bright sky regions. A constraint may be identified within the potential field by placing a large potential around this direction, therefore preventing the satellite from pointing the payload towards the constraint. This large repulsive field is defined using a polynomial function of the form:

$$V_o = \frac{1}{2}\frac{1}{(\delta_o - \delta_c)^2} \qquad [4.35]$$

where δ_o is the angle between the spacecraft's current vector $\mathbf{n}_s$ and the vector $\mathbf{n}_o$ which identifies the pointing constraint given as:

$$\mathbf{n}_o = \cos\alpha_o \cos\varepsilon_o \mathbb{I} + \sin\alpha_o \cos\varepsilon_o \mathbb{J} + \sin\varepsilon_o \mathbb{K} \qquad [4.36]$$

The parameter δ_c determines the form of the potential, by determining the size of the constraint's angular radius, while α_o and ε_o are the azimuth and elevation of the constraint as shown in Figure 4.13.

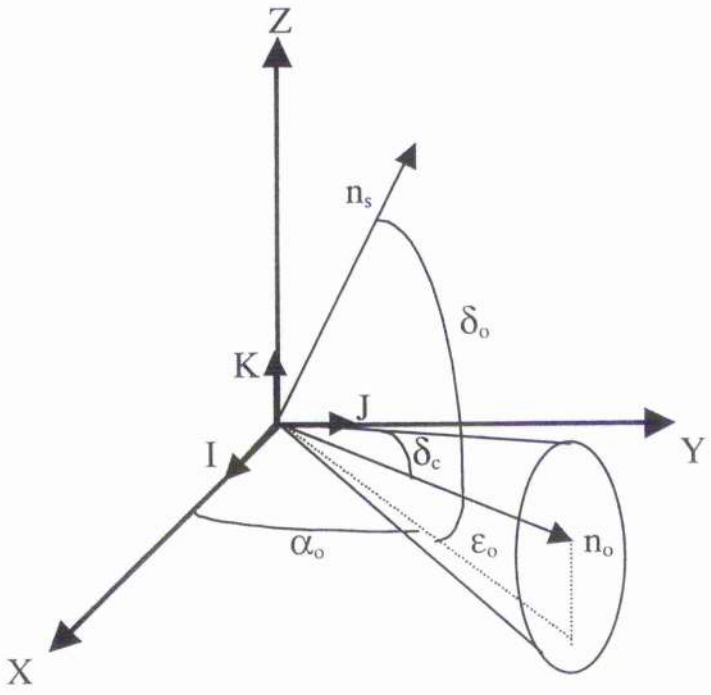

Figure 4.14 Schematic large angle slew with pointing constraint

When the angular distance between the satellite and the pointing constraint decreases, the repulsive component of the potential increases. This increase modifies the rate of change of the potential. The controls are therefore activated and the satellite is slewed away from the constraint. The path is therefore shaped in such a way, so as to avoid the pointing constraint. The repulsive component of the potential will therefore have the following form:

$$V_{\text{repulsive}} = \frac{1}{2(\delta_o - \delta_c)^2} \qquad [4.37]$$

Let us now consider the case of two pointing constraints which have different orientations; one along the *X*-axis, and one along the *Z*-axis. It can be seen that the projection of the constraint in the θ_1-θ_2 plane is different in the two cases. This is due

to the fact that the projection varies depending on where the constraint is in reference to the *X-Y* plane. The projection of the constraint is circular, if positioned vertically above the *X-Y* plane. As the position of the constraint is changed, its projection on the *X-Y* plane changes. At first it assumes an elliptical form and then it will eventually become a strip in the θ_1-θ_2 plane, as shown in Figure 4.15.

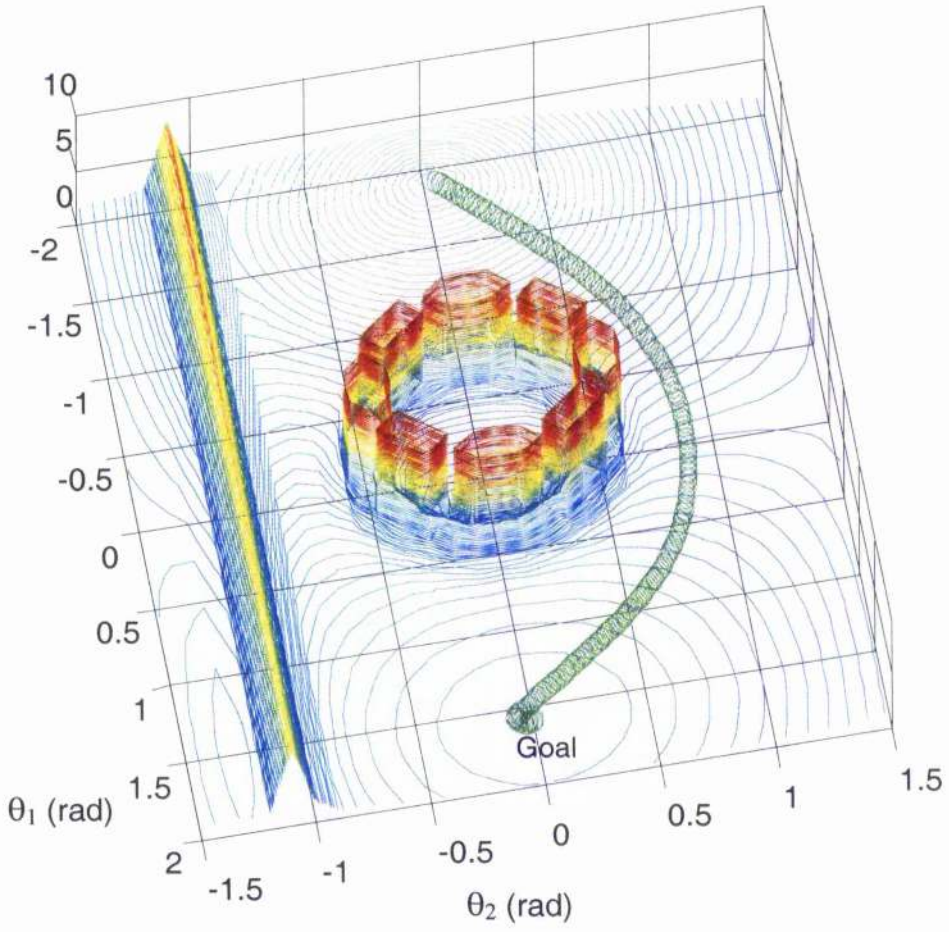

Figure 4.15 Obstacle avoidance slew

4.8 GLOBAL POTENTIAL

In the more general case we will have to deal with multiple targets (N) and multiple obstacles (M) [Radice and McInnes 2001]. Therefore the global potential which will be used to control the spacecraft will comprise an attractive component, which guides the spacecraft towards the desired attitudes, and a repulsive component which guarantees that the spacecraft avoids those regions which could prove damaging for the payload or sensors:

$$V_{\text{global}} = V_{\text{attractive}} + V_{\text{repulsive}} = \frac{1}{2}\sum_{i=1}^{N} L_i \delta_i^{\,2} + \frac{1}{2}\sum_{j=1}^{M} \frac{1}{\left(\delta_{jo} - \delta_{jc}\right)^2} \qquad [4.38]$$

The form of the potential is now such that we can guarantee that the satellite will avoid any pointing constraints due to the repulsive component. The presence of an attractive component guarantees that the satellite will also reach the desired goal location. For the potential defined in Equation 4.38 the possibility of a local minimum occurs. However, this local minimum is usually an unstable saddle point and so is not problematic. A range of methods exists to deal with true local minima [Zelek 1994]. With the potential expressed in the above form, we ensure that the spacecraft will visit all N targets, due to the attractive component and avoid all the M pointing constraints because of the repulsive component. It can also be appreciated that as the distance to the obstacle decreases, the repulsive potential increases until such a point that the global potential is dominated by that component. This causes the potential derivative to become positive, thus activating the necessary control actions and slewing the satellite away from the pointing constraint. The path to the goal attitude is

therefore shaped to avoid the obstacle cone while moving towards the next target.

We can now see how the control algorithm performs, with the spacecraft initially at rest, and having to reach one intermediate attitude before the final goal, while at the same time avoiding two pointing constraints. The desired attitudes are identified by: $(\alpha_1, \varepsilon_1) = (0, \pi/2)$ and $(\alpha_2, \varepsilon_2) = (-\pi/2, 0)$, while the obstacles are identified by $(\alpha_{o1}\ \varepsilon_{o1}) = (-\pi/4, -\pi/4)$ and $(\alpha_{o2}, \varepsilon_{o2}) = (5\pi/4, \pi/4)$. In Figures 4.15-4.16 we can see the results of such a simulation. In Figure 4.15 we can see the overall and partial trajectory in the potential field. It can be seen that the two obstacles have an elliptical shape in the θ_1-θ_2 plane, because of their 45° elevation in the X-Y plane. Once again as the first target is reached the parameter L_1 associated with it is switched to zero, and therefore the potential assumes a new form with the second target becoming the new minimum. We can also note the periodicity of the potential field; this is because the potential is defined as a function of trigonometric functions and therefore 2π symmetric. We can see that the thrusters are activated immediately to slew the spacecraft towards the intermediate target attitude. After approximately 450 seconds this goal is reached and the spacecraft rests for 20 seconds before firing the thrusters again to reach the final target attitude. It is thus shown that the spacecraft is successfully guided to the two target points while steering away from the two pointing constraints.

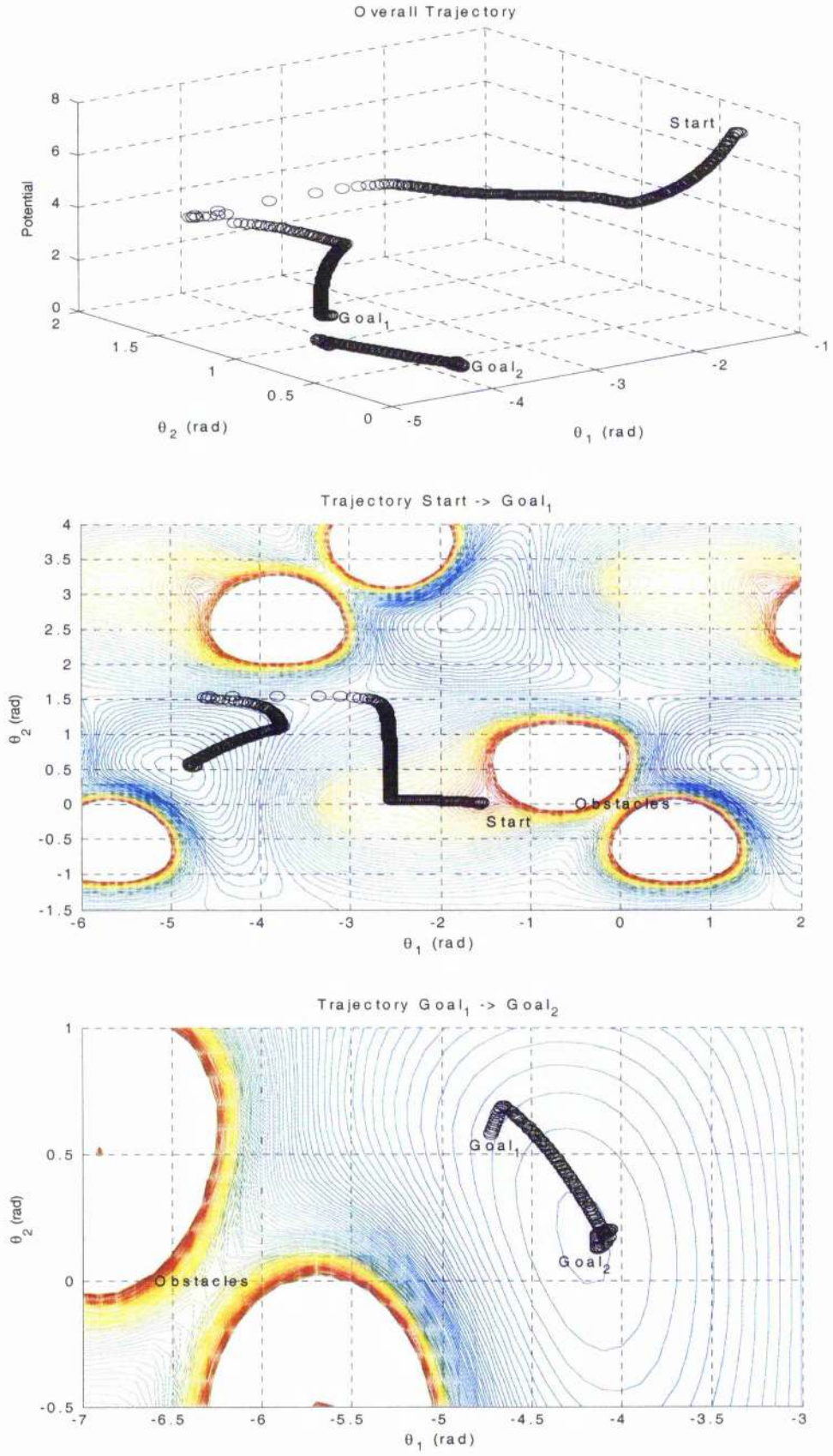

Figure 4.16 Multiple target transfer with obstacle avoidance

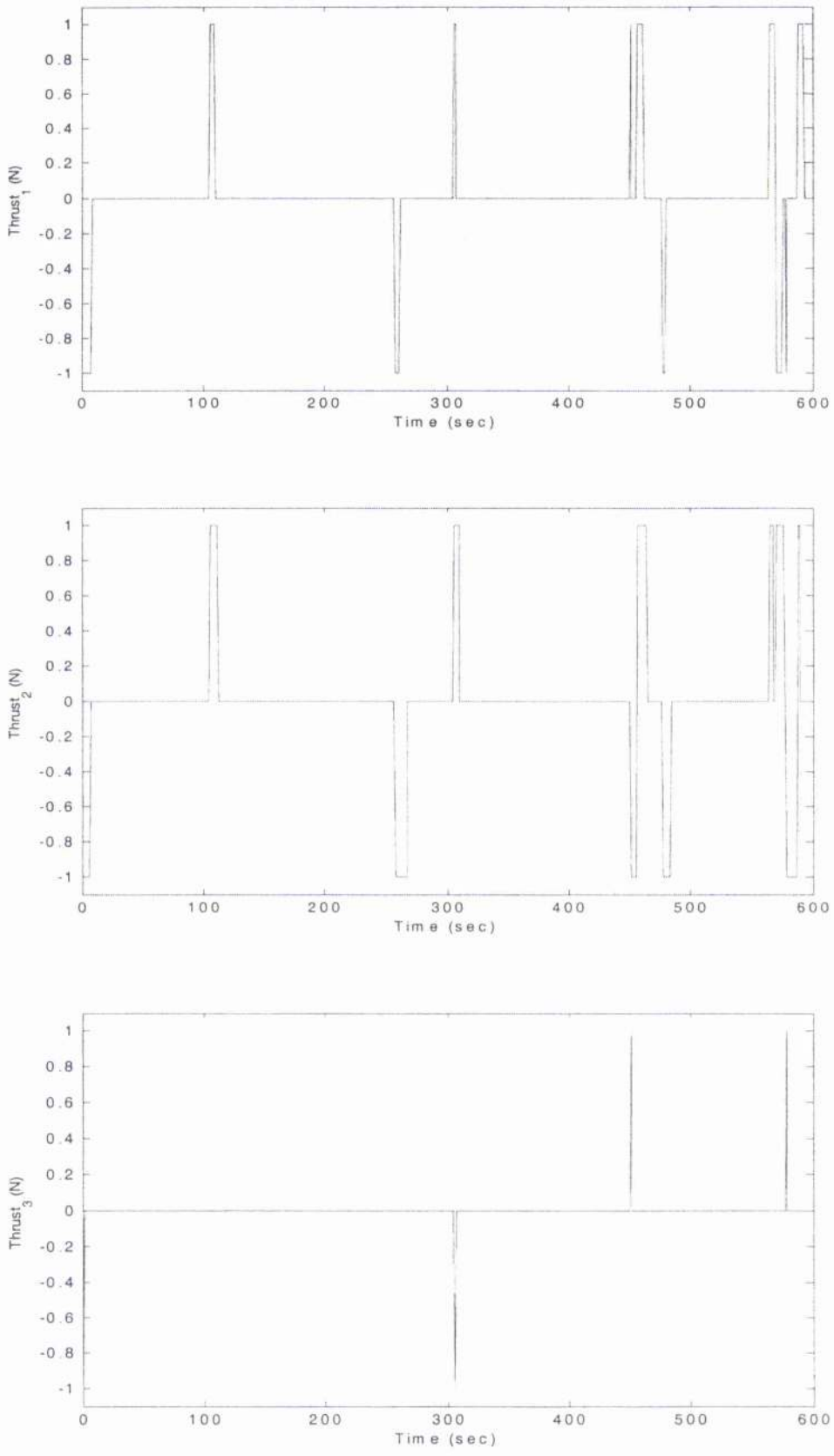

Figure 4.17 Thruster pulses for multiple target transfer with obstacle avoidance

4.9 CONCLUSIONS

An analytic method has been presented to control constrained large angle slew manoeuvres. This method can provide the basis for a computationally efficient autonomous guidance and control system. The method hinges on defining a potential function, in principle in accordance with Lyapunov's theorem. The control algorithm presented here meets the criteria defined for spacecraft control. Two different methodologies were presented, the discrete and continuous method, and both proved to be satisfactory. The potential function control method will then be used to slew the spacecraft between targets as demanded by the action selection algorithm introduced in Chapter 3.

CHAPTER V

ORBITAL AND SPACECRAFT MODEL

5.1 PREFACE

We will now examine how the spacecraft and orbital models are constructed using Simulink. The mathematical and geometrical considerations of the two-body problem and the formulation of Kepler's equation, will be investigated and the different subsystems that comprise the spacecraft will be presented. It will also be shown how the action selection algorithm, presented in Chapter 3, and the attitude control, presented in Chapter 4 are integrated within the spacecraft model.

5.2 TWO BODY PROBLEM

For all practical situations involving spacecraft, one of the masses in the two-body problem is much greater then the other. The force of attraction is always directed to a fixed point in inertial space with magnitude solely a function of distance between the field point and the centre of attraction. The basic equation of motion for the two body problem is [Roy 1982]:

$$\ddot{\mathbf{r}} + \frac{\mu}{r^3}\mathbf{r} = 0 \qquad [5.1]$$

Where $\mu = G(M + m)$ is the gravitational parameter of the problem with G being Newton's gravitational constant. If $M >> m$ it becomes evident that the much smaller body of mass m, has no influence on the motion of the much larger body of mass M, which can be seen as an inertial body as far as the small body is concerned. If we consider Figure 5.1, since the motion is in a plane, we can introduce the polar coordinates r and θ.

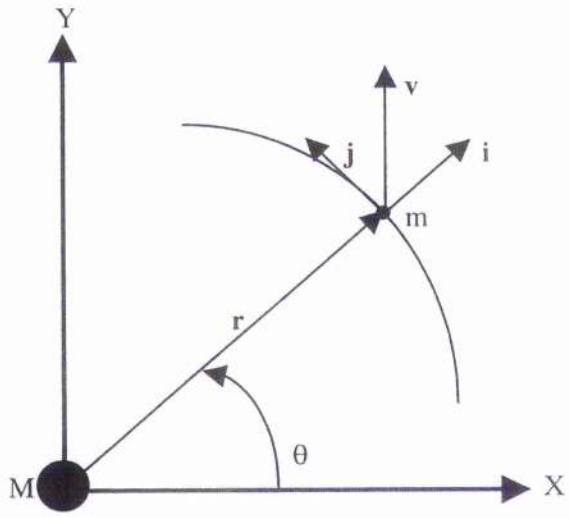

Figure 5.1 Radial and tangential components of the velocity.

The vectors **i** and **j** are unit vectors in the directions of respectively **r** and the normal to **r**. In this notation the components of the acceleration acting on m along and perpendicular to the radius vector are found to be [Roy 1982]:

$$\ddot{\mathbf{r}} = \left(\ddot{r} - r\dot{\theta}^2\right)\mathbf{i} + \left(2\dot{r}\dot{\theta} + r\ddot{\theta}\right)\mathbf{j} \qquad [5.2]$$

and so substituting into Equation 5.1 we obtain:

$$\left(\ddot{r} - r\dot{\theta}^2\right)\mathbf{i} + \left(2\dot{r}\dot{\theta} + r\ddot{\theta}\right)\mathbf{j} + \frac{\mu}{r^2}\mathbf{i} = 0 \qquad [5.3]$$

Therefore equating the coefficients of the Equation 5.3 gives us:

$$\ddot{r} - r\dot{\theta}^2 = -\frac{\mu}{r^2} \qquad [5.4a]$$

$$\frac{1}{r}\frac{\mathrm{d}}{\mathrm{dt}}\left(r^2\dot{\theta}\right) = 0 \qquad [5.4b]$$

The integration of Equation 5.4b provides the angular momentum integral $r^2\dot{\theta} = h$. We now make use of the substitution $u = 1/r$, and eliminating time in Equation 5.4a leads to:

$$\frac{\mathrm{d}^2u}{\mathrm{d}\theta^2} + u = \frac{\mu}{h^2} \qquad [5.5]$$

the general solution of which is:

$$u = \frac{\mu}{h^2} + A\cos\left(\theta - \theta_0\right) \qquad [5.6]$$

where A and θ_0 are the two integration constants. If we now reintroduce r, Equation 5.6 becomes:

$$r = \frac{\frac{h^2}{\mu}}{1 + \frac{Ah^2}{\mu}\cos(\theta - \theta_0)} \qquad [5.7]$$

which can be rewritten as:

$$r = \frac{p}{1 + e\cos\theta} \qquad [5.8]$$

where p and e are geometrical constants of the orbits, respectively the semi-latus rectum and eccentricity. Equation 5.8 is the equation of a conic section: the general orbit equation from which different families of orbits are generated – circular, elliptic, parabolic and hyperbolic.

5.3 TIME AND KEPLERIAN ORBITS

The location of a body in any orbit can be described either in terms of its angular deviation from the major axis, or by the time elapsed from its passage through perigee. The true anomaly θ is defined as the angle between the major axis pointing to the perigee and the radius vector from the prime focus F to the moving body. To define the eccentric anomaly we draw an auxiliary circle with radius a, centred at the centre of the major axis. The eccentric anomaly ψ is then defined as in Figure 5.2

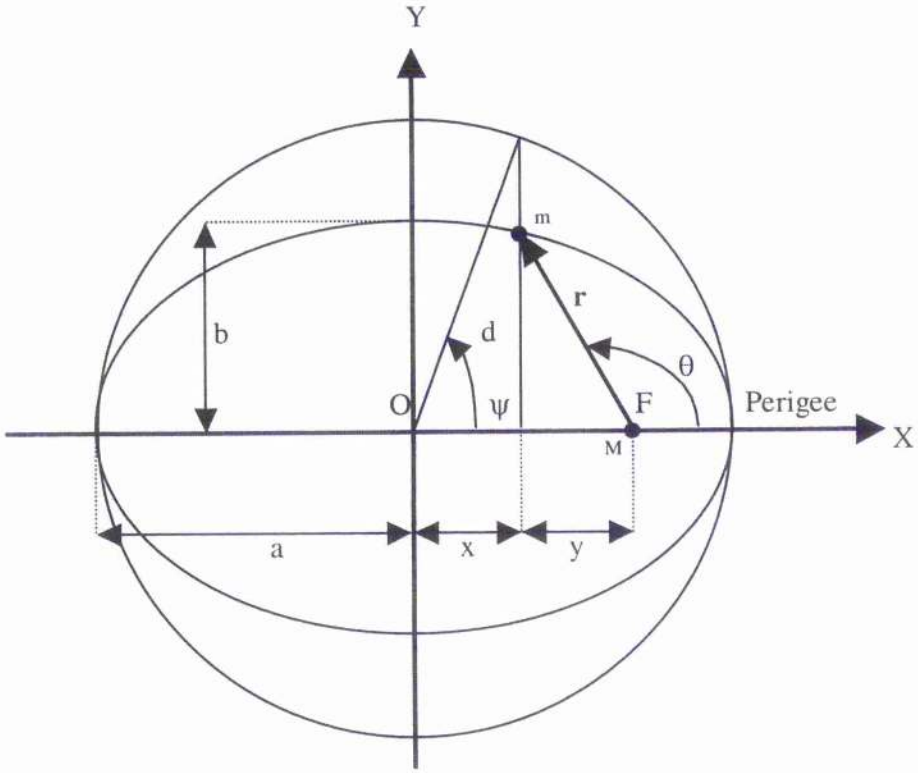

Figure 5.2 Geometry for finding the relationship between θ and ψ.

We can now find some important relationships between the true and eccentric anomalies. Referring to Figure 5.2 we find that: $x + y = c = ae$, also $x = a\cos\psi$ and $y = r\cos(\pi - \theta) = -r\cos\theta$, hence $x + y = a\cos\psi - r\cos\theta = ae$.

Using the geometrical relationships evinced from Figure 5.2 we can rewrite Equation 5.8 as:

$$a\cos\psi = ae + \frac{a\left(1-e^2\right)\cos\theta}{1+e\cos\theta} = \frac{ae + a\cos\theta}{1+e\cos\theta} \qquad [5.9]$$

and

$$\cos\psi = \frac{e+\cos\theta}{1+e\cos\theta} \quad ; \quad \sin\psi = \frac{\sin\theta\sqrt{1-e^2}}{1+e\cos\theta} \qquad [5.10]$$

$$\cos\theta = \frac{\cos\psi - e}{1-e\cos\psi} \quad ; \quad \sin\theta = \frac{\sin\psi\sqrt{1-e^2}}{1-e\cos\psi} \qquad [5.11]$$

Also, it can be shown that [Roy 1982]:

$$\tan\left(\frac{\theta}{2}\right) = \sqrt{\frac{1+e}{1-e}}\tan\left(\frac{\psi}{2}\right) \qquad [5.12]$$

It can now be shown that it is possible to express the true anomaly θ in series as a function of the eccentric anomaly ψ and the eccentricity e:

$$\theta = \psi + \left(e + \frac{e^3}{4}\right)\sin\psi + \frac{1}{4}e^2\sin 2\psi + \frac{1}{12}e^3\sin 3\psi + \sigma\left(e^4\right) \qquad [5.13]$$

We can now introduce a new parameter called mean anomaly M, defined as the angle swept by a radius vector rotating with mean angular velocity n, with $n = \sqrt{\mu / a^3}$, in the interval of time $(t - \tau)$ where τ is defined as the time of perigee passage. Geometrical considerations allow us to express the mean anomaly as a function of the eccentric anomaly ψ:

$$M = \psi - e\sin\psi \qquad [5.14]$$

Lagrange developed a solution to Equation 5.14 in the form of a trigonometric series:

$$\psi = M + \sum_{k=1}^{\infty} \frac{1}{k} J_k \, k \, e \sin(kM) \qquad [5.15]$$

where J_k is a Bessel function of the first kind of order k. We can now combine Equations 5.13 and 5.15 to obtain the equation of the centre, which expresses the true anomaly θ as a function of the mean anomaly M:

$$\theta = M + \left(2e + \frac{e^3}{4}\right)\sin M + \frac{5}{4}e^2 \sin 2M + \frac{13}{12}e^3 \sin 3M + \sigma\left(e^4\right) \qquad [5.16]$$

Thus when e and M are given, the true anomaly can be found directly by using Equation 5.16. As $M = n(t - \tau)$ we will be able to express θ as a function of time for small values of the eccentricity. This formulation is used in the simulation of the orbital model which will be introduced in the next section.

5.4 ORBITAL MODEL

For an Earth orbiting spacecraft, it is common use to define an inertial frame of reference with the centre-of-mass of the Earth as its origin. For practical purposes this system of reference can be accepted as being inertial, despite the Earth moving around the Sun. The Z-axis is the axis of rotation of the Earth. The X-Y plane of this system of coordinates is taken as being the equatorial plane of the Earth, which is perpendicular to the Earth's rotation axis. The X-axis coincides with the line formed

by the intersection of the Earth's equatorial plane and the ecliptic plane, which is the plane of the Earth's orbit around the Sun. The third axis *Y*-completes a right-handed orthogonal system. Having defined the geometric coordinate system we need to introduce an additional three parameters to position an orbit in space. In Figure 5.3 the orbital plane is inclined with respect to the *X*-*Y* plane by an angle *i*, the inclination of the orbit.

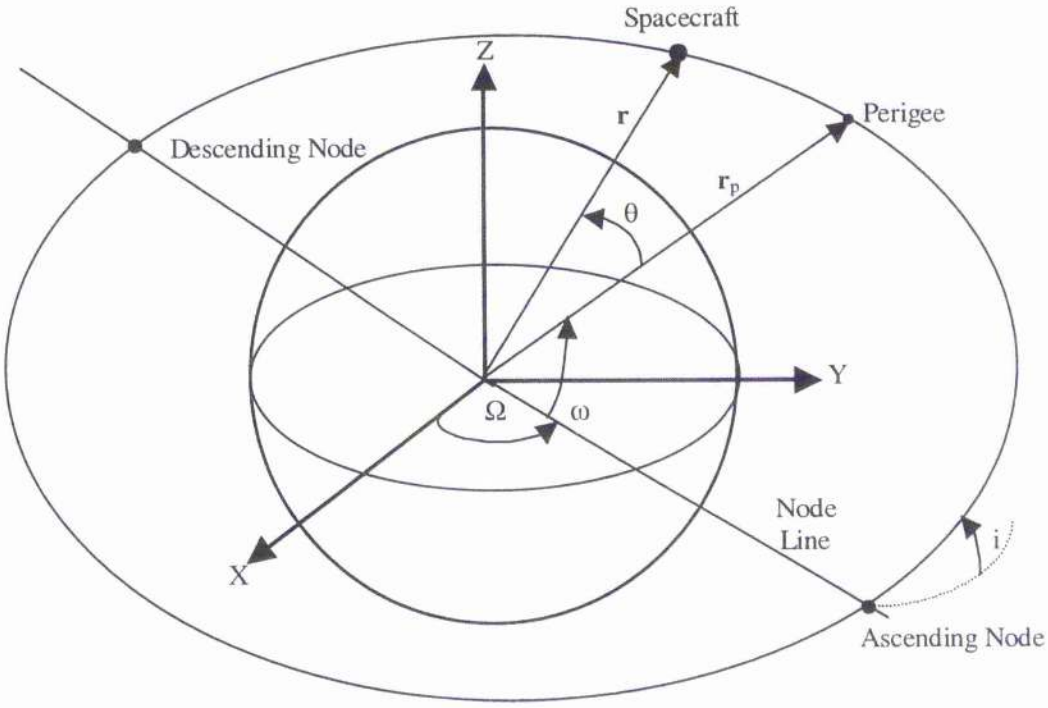

Figure 5.3 Parameters that define the location of orbits in space

The orbital plane and the equatorial plane intersect at the nodal line. The angle in the equatorial plane that separates the node line from the *X*-axis is called the right ascension of the ascending node Ω. In the orbital plane, $\mathbf{r}$ is the radius vector to the moving body; $\mathbf{r_p}$ is the radius vector to the perigee of the orbit. The angle between $\mathbf{r_p}$ and the node line is ω, the argument of the perigee. These three parameters together with the eccentricity *e* the semi-major axis *a* and the true anomaly θ, complete a

system that suffices to define a location in space of a body moving in any Keplerian orbit. A Simulink model was created using the previous analysis. The user can define five key parameters which uniquely characterise an orbit in space. The output is the projection of the radius vector r, along the three inertial axes, as a function of time. In Figure 5.4 we can see the blocks of the Simulink model used to represent the orbital dynamics of the problem.

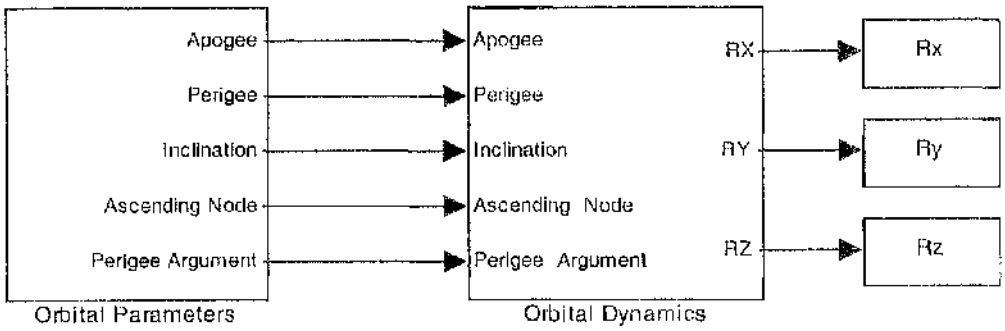

Figure 5.4 Simulink model of orbital dynamics.

Looking at the orbital dynamics model in more detail, in Figure 5.5, we can see that we use Equation 5.16 to obtain the true anomaly. Knowing the true anomaly allows us to calculate the orbital radius ||r|| using Equation 5.8. The projection of the orbital radius ||r||, along the inertial axes can be determined using the following equations:

$$R_x = r\left[\cos\Omega\cos(\omega+\theta) - \cos i\sin\Omega\sin(\omega+\theta)\right]\mathbb{I} \qquad [5.17a]$$

$$R_y = r\left[\sin\Omega\cos(\omega+\theta) + \cos i\cos\Omega\sin(\omega+\theta)\right]\mathbb{J} \qquad [5.17b]$$

$$R_x = r\left[\sin i\sin(\omega+\theta)\right]\mathbb{K} \qquad [5.17c]$$

where $\mathbb{I}$, $\mathbb{J}$ and $\mathbb{K}$ are the unit vectors along the X, Y and Z axis respectively. In Figure 5.5 we can see a detailed picture of the orbital dynamics model.

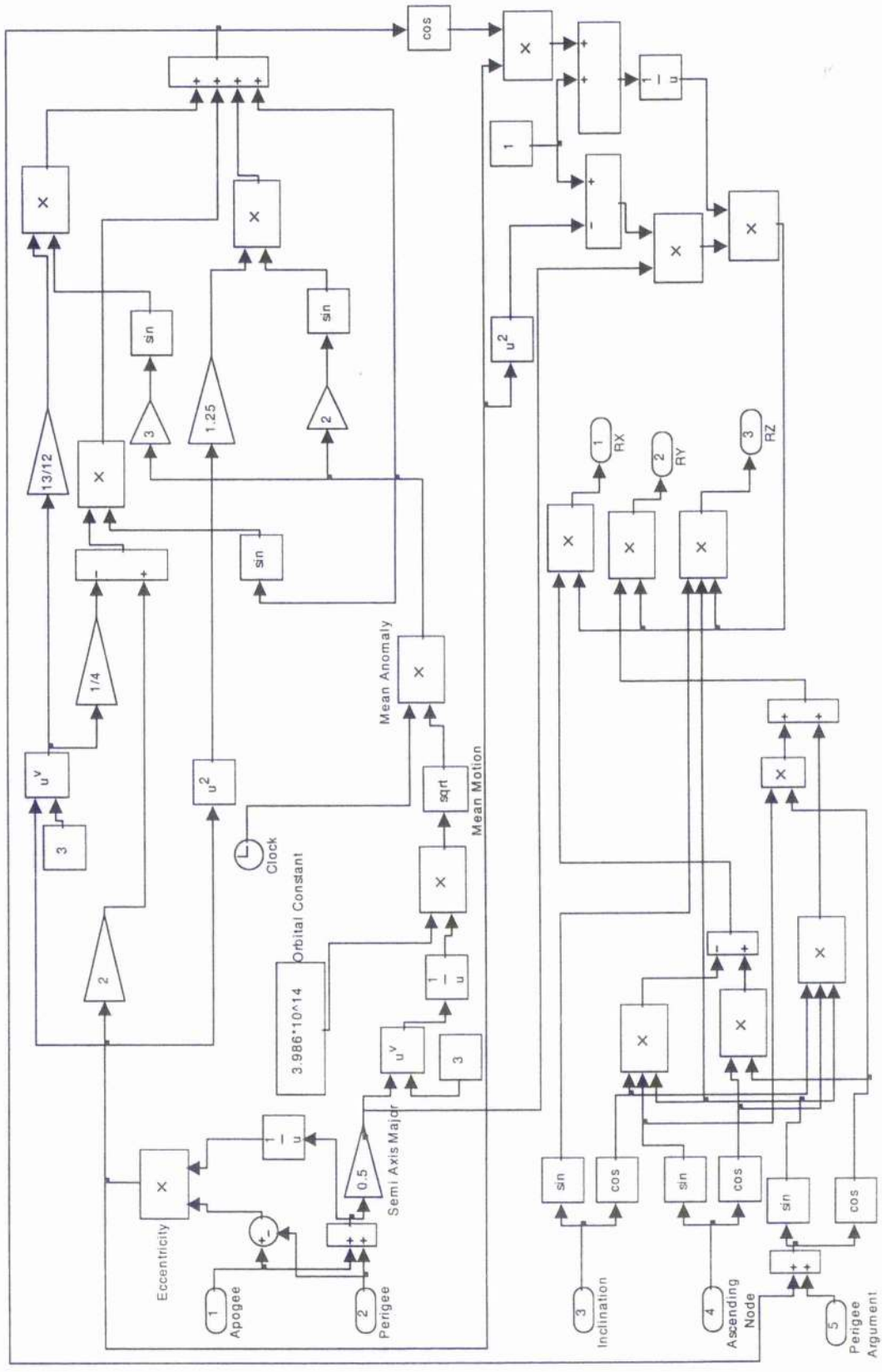

Figure 5.5 Detailed model of orbital dynamics

In Figure 5.6 we present behaviour of the position vector components (R_x, R_y, R_z) in the case of a 1000x10000 km orbit with an inclination of 86°. This orbit has a period of 3 hours, 34 minutes and 38 seconds. We can see that the orbital radii have a periodic pattern, with the recurrence being given by the orbital period.

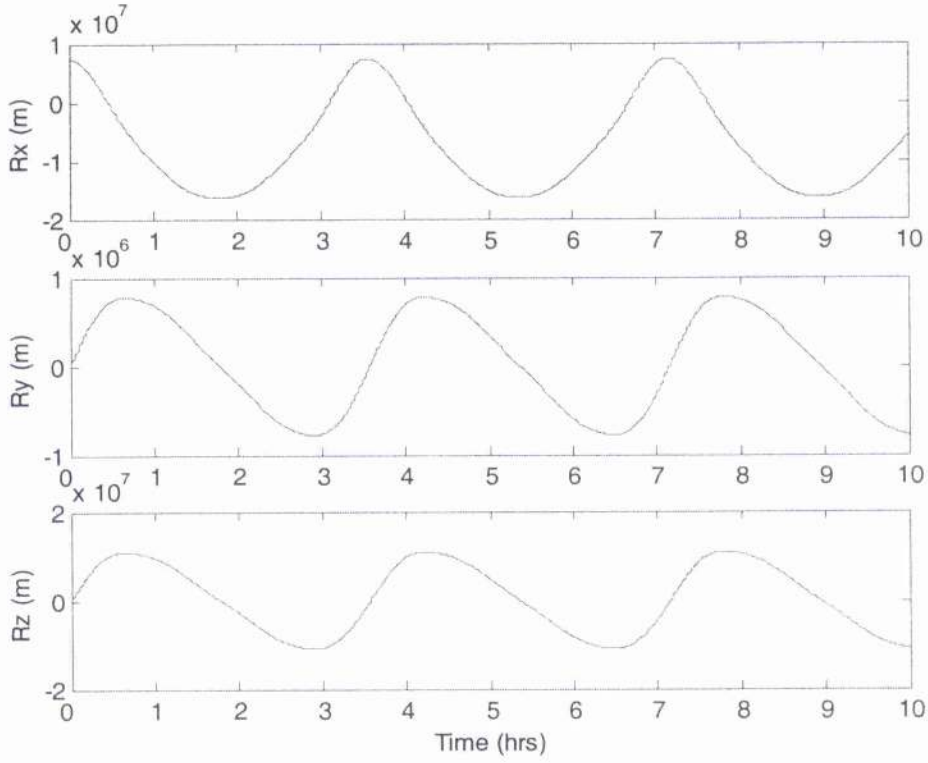

Figure 5.6 Orbital radii for a 1000x10000 Earth orbit.

This orbital model will be used to generate state information for the different orbits required for the case studies in Chapter 6 and 7.

5.5 ECLIPSE MODEL

During each orbit the spacecraft may be in Sun eclipse. This means that the orbit the spacecraft is following takes the satellite into the shadow cone of the Earth and therefore is not in direct sunlight. This affects the temperature of the spacecraft, which will if necessary have to switch a heater on, which in turn affects the electrical power subsystem as energy is consumed to activate the heater. In Figure 5.7 we can see the Simulink model used.

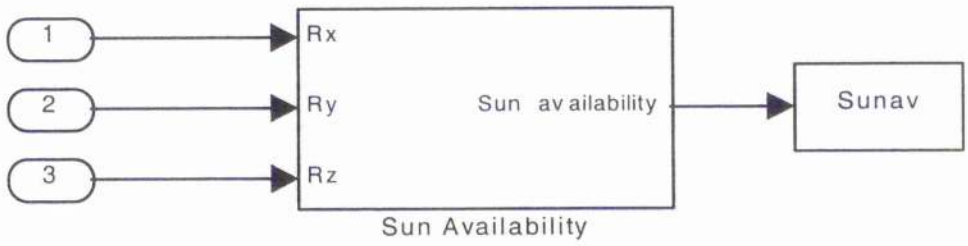

Figure 5.7 Simulink model of eclipse

The sun availability algorithm takes the input (the projection of the spacecraft position vector along the inertial axes) from the orbital dynamics model introduced previously. It returns 1 if the spacecraft is in sunlight, and 0 if it is in eclipse. To explain this in more detail we can look at Figure 5.8. The Sun is considered to be aligned along the X-axis, therefore the spacecraft will be in sunlight if $R_x \geq 0$. If on the other hand $R_x < 0$, the satellite will be in sunlight if the following condition is satisfied: $\sqrt{R_y^2 + R_z^2} > R_{\text{Earth}}$. Should the two conditions not be met, the spacecraft will be in eclipse.

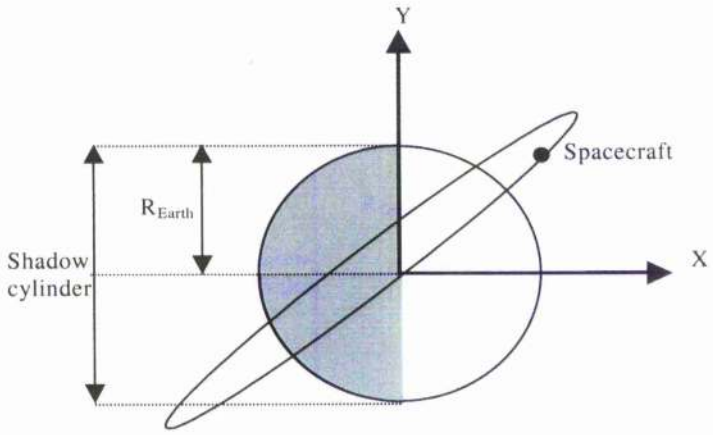

Figure 5.8 Geometrical configuration for eclipse condition

In Figure 5.9 we can see the different Sun availability between a 200 km orbit and a 1200 km orbit. As expected, the lower altitude orbit has a lower sun availability period compared to the higher altitude orbit. However having a shorter orbital period and therefore viewing the Sun more often offsets this to some extent.

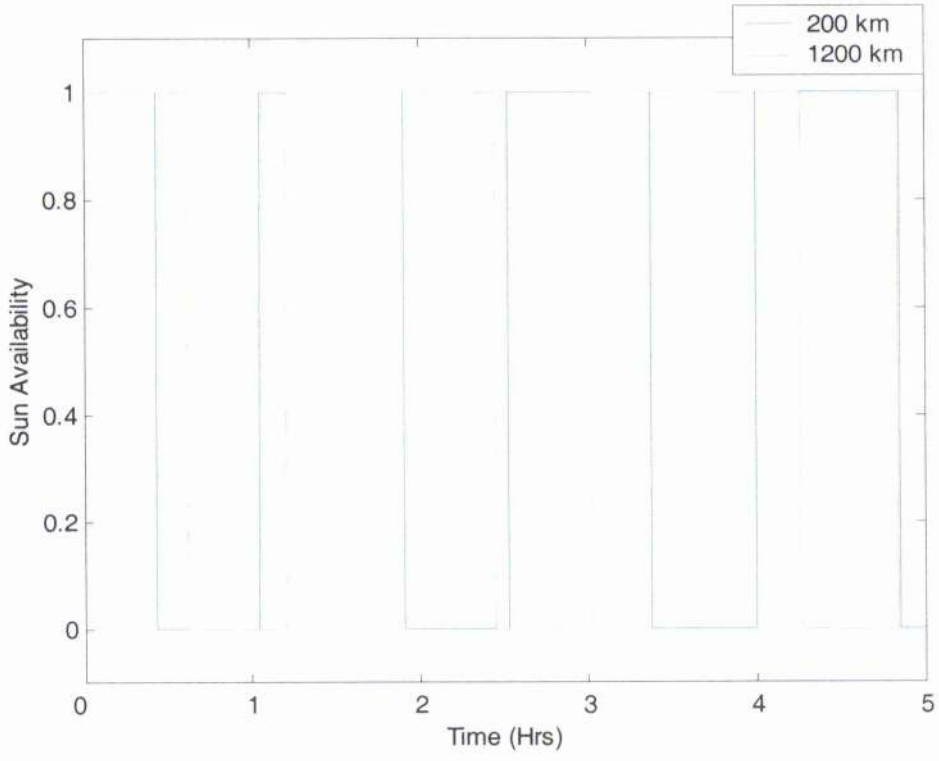

Figure 5.9 Sun availability for two different orbits

5.6 SPACECRAFT MODEL

The satellite is considered to have three rotational degrees of freedom, which can be controlled by reaction wheels. The electrical power system consists of a solar array, battery and several electrical loads. The payload is a camera that records at a steady data rate when active, solid state memory and a radio transmitter to down-link data to the ground station. The individual subsystems are coupled together: for example. switching the transmitter on drains the battery and reduces the amount of stored data. The satellite is controlled by switching the camera, the transmitter and an internal heater on or off, and commanding an attitude control subsystem to track one of the three objectives – Sun, payload target and Earth ground station – by activating the reaction wheels. To provide pointing constraints, the solar panel is located on a different face of the 20 cm cube shaped micro-satellite to the camera and antenna, as shown in Figure 5.10. In Appendix I the procedure to determine an estimated sizing of the spacecraft is explained.

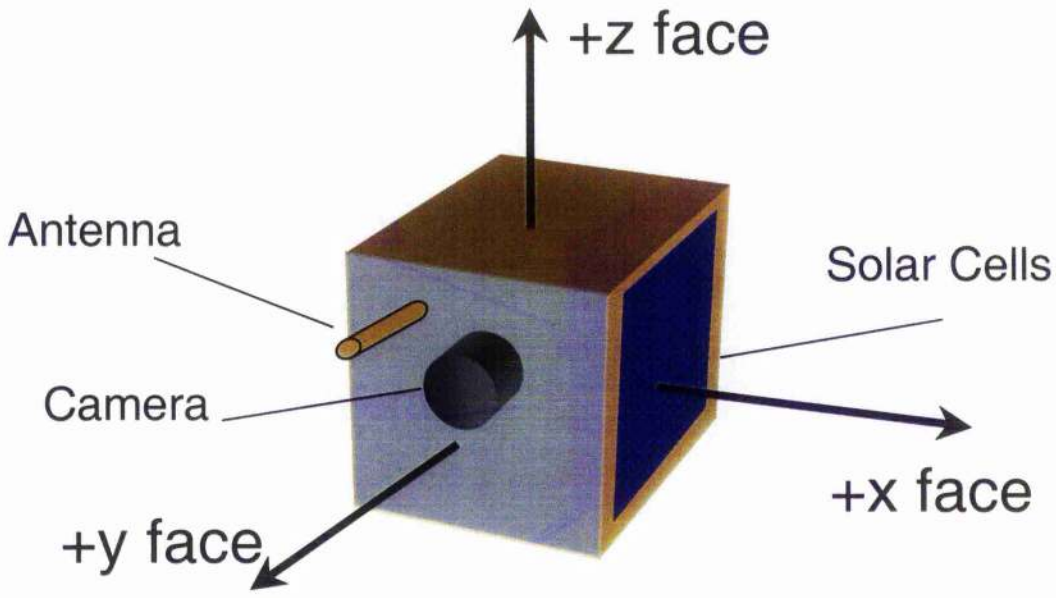

Figure 5.10 Satellite model

The internal heater may be switched on or off independently of what other task the spacecraft may be performing; the heater automatically turns on when the temperature drops below a certain fixed threshold value of 240 K and is not commanded by an action selection algorithm. The choice of the threshold value is linked to the performance of the on-board sensors and actuators which have well defined temperature ranges in which to operate. Activating the heater however drains the battery, and therefore indirectly influences the action selection. In Figure 5.11 we can appreciate how the action selection algorithm is implemented within the satellite model.

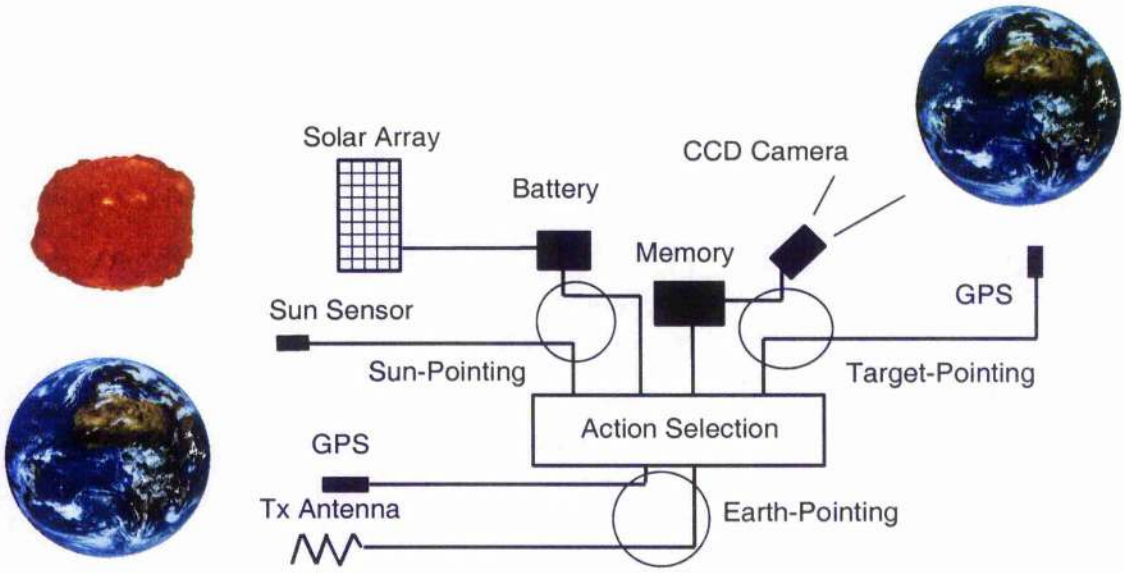

Figure 5.11 Action selection model

The satellite can perform three different tasks. It can charge its battery by pointing the solar panel towards the Sun, detected by the Sun sensor, it can record data by activating the camera and it can download data to Earth ground station through the transmitter when the GPS determines that the target or ground station are present. The spacecraft selects the optimum behaviour at any time by evaluating the

deficits of the state variables, assessing the availability and accessibility of the environmental resources and finally computing the *drk* product as discussed in Chapter 3. To avoid oscillating between behaviours with similar *drk* products, the spacecraft switches between different behaviours when the difference between two *drk* products surpasses a fixed threshold.

5.6.1 Subsystems

Individual spacecraft can be very different from one another and might display widely different design approaches in solving the same or similar mission architecture problems. More recent spacecraft, thanks to improvements in various technological fields, often have a smaller volume and are less massive than their predecessors, yet there are common functions carried out by different spacecraft regardless of size. Not all types of spacecraft, though, present the same subsystem typology. The satellite model used here can be considered as a generic orbiter type spacecraft and the following subsystems comprising the spacecraft will be presented and discussed, motivating the choices and assumptions made: payload, data handling, attitude control, telecommunications, electrical power, and thermal control.

5.6.1.1 Payload

Spacecraft designers often consider the most important component of the spacecraft to be the payload. Although all subsystems must work equally well to guarantee success, it is the payload that fulfils and justifies the space mission requirements. All the engineering subsystems and components serve a single purpose: to deliver science or other instruments to their destination and enable them to carry

out their observations and experiments, and return data from the instruments. There are many different kinds of scientific instruments although they all fall into one of the two following categories: direct sensing and remote sensing. Direct sensing instruments interact with physical phenomena in their immediate vicinity while registering their characteristics. Examples of such instruments are a heavy ion counter, dust detector and magnetometer. These instruments measure properties such as mass, speed, direction and do not attempt to form any image of the source. Remote sensing instruments on the other hand, form some kind of image or characterisation of the source of the phenomena. They record characteristics of the objects at a distance and sometimes form an image by gathering, focusing and recording light. Examples of this are altimeters, which use radar pulses to determine variations in the height of the terrain being overflown, or traditional optical imaging.

The science instrument present on the generic satellite considered here is a camera. An imaging instrument uses optics such as lenses or mirrors to project an image onto a detector plane where it is converted into digital data. Light falling on a well is absorbed by a photoconductive substrate, such as silicon, and releases a quantity of electrons proportional to the intensity of the light. The CCD detects and stores accumulated electrical charge representing the light level on each well. These charges are then read out for conversion to digital data. In Figure 5.12 we can see the Simulink model of the payload. The payload is activated when the spacecraft is flying over the target and the *drk* product associated with the 'record' behaviour is the highest of the three. In output the payload produces a data rate of 5000 bits per second, which is stored within the solid state memory, and a power consumption of 0.09 Watts which affects the battery charge [Lu 2001].

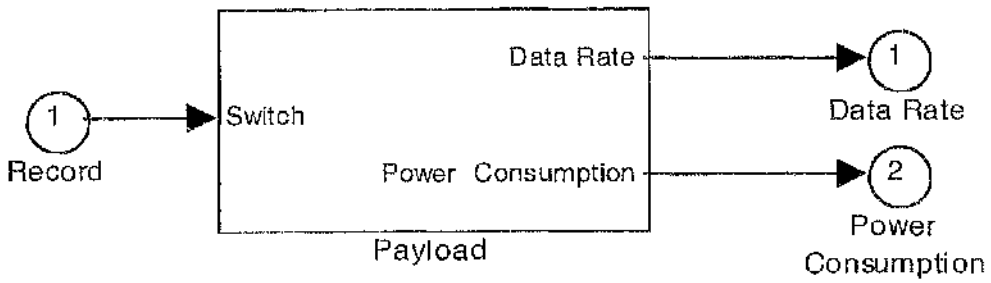

Figure 5.12 Payload model

5.6.1.2 Data Handling

There is usually one computer identified as the spacecraft central computer, responsible for overall management of the satellite's activities. This unit is often referred to as command and data subsystem. It maintains timing, interprets commands from Earth, collects, processes and formats the telemetry data to be returned to Earth, and manages high-level fault protection and safing routines. Because of the way the spacecraft is modelled (antenna on a single face), not only will it not always be in contact with the ground station, but also when the spacecraft is not Earth pointing. There is therefore a requirement for a data storage device such as tape or solid-state recorder. The storage device can be commanded to transmit stored data when a downlink is available, and then to overwrite the old data with new. The choice was to opt for a model of a solid state recorder. Unlike the tape recorder, the solid state recorder has no reels, tape and no moving parts to wear out and limit lifetime. Data is digitally stored in memory chips until it can be played back to Earth ground station. Not having moving parts means that the solid state recorder cannot fall victim to failures, such as a break in the tape or a mechanical defect. It also doesn't need any pressurised sealing to protect the tape and the delicately lubricated moving parts from

the hazards of space vacuum. In Figure 5.13 we can see the Simulink block for the data handling device.

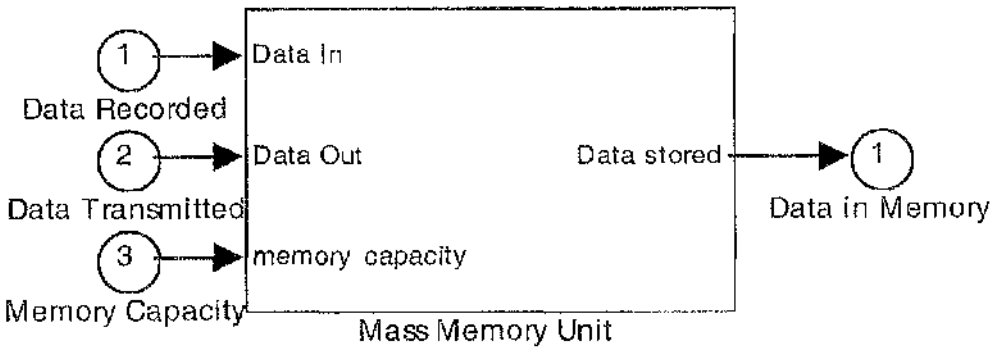

Figure 5.13 Data handling model

The mass memory takes in input the data recorded by the payload, the data sent back to the ground station by the transmitter, and the memory capacity. In output it produces the amount of data which is currently stored on-board the spacecraft. The maximum amount of data that can be stored on board is 5,000,000 bits [NASA 2002].

5.6.1.3 Attitude Control

A spacecraft's attitude must be stabilised and controlled so that it may accurately point the antenna to Earth, direct the solar panel towards the Sun or accomplish precise pointing for collection of data by directing the on-board camera towards the desired targets. There are three ways of controlling a spacecraft: passive, spin and three axes. Passive control methods use the fact that an elongated object in a gravity field aligns its longitudinal axis through the Earth's centre. To achieve stabilisation the satellite uses electrically powered reaction wheels. These wheels are mounted in three orthogonal axes on the spacecraft. They provide a means to trade angular momentum back and forth between the spacecraft and wheels. To rotate the

spacecraft in one direction, the proper wheel must be spun up in the opposite direction. To rotate the spacecraft back, the wheel is slowed down. The satellite is also assumed to be equipped with sensors, which determine the attitude with respect to a defined reference frame.

To generate the maximum amount of power, a solar array needs to be facing the Sun, perpendicular to the incident sunlight, as flux through the surface is greatest when the flow direction is normal to that surface. The Sun sensor is a device that can determine the location of the Sun. The horizon sensor is an infrared device that uses the contrast between the cold of deep space and the heat of Earth's horizon as reference. The spacecraft therefore has to perform the double task of first assessing its attitude with respect to the Sun, ground station and target area, and then slew towards the environmental resource it needs: the Sun to charge the battery, the ground station to download data, and the target area to record data. In Figure 5.14 we can see the geometric configuration of the first problem: determining the relative orientation of spacecraft and environmental resources.

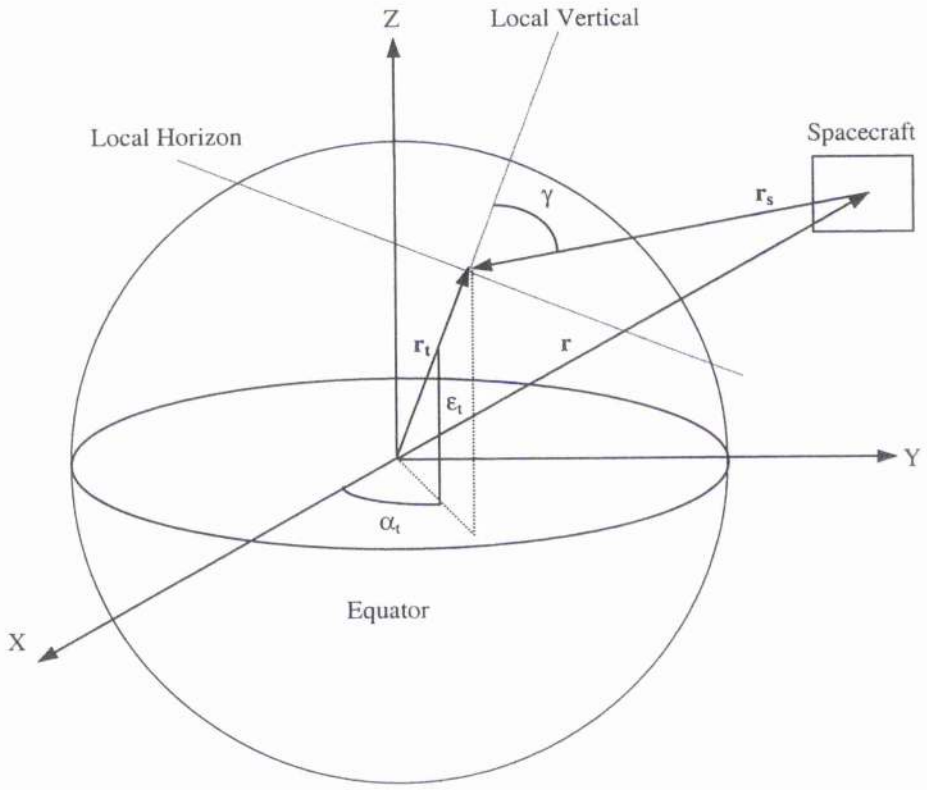

Figure 5.15 Definition of parameters for line of sight

The availability of the target or the ground station is defined by the angle γ, which is the angle between the local vertical and the spacecraft and is defined as:

$$\gamma = \arccos\left(-\frac{\mathbf{r}_t \cdot \mathbf{r}_s}{\|\mathbf{r}_t\| \|\mathbf{r}_s\|} \right) \qquad [5.18]$$

where

$$\mathbf{r}_t = \cos\alpha_t \cos\varepsilon_t \mathbf{I} + \sin\alpha_t \cos\varepsilon_t \mathbf{J} + \sin\varepsilon_t \mathbf{K} \qquad [5.19]$$

where α_t and ε_t are the azimuth and elevation angles of the target. The azimuth angle is a function of time as: $\alpha_t = \alpha_{t0} + \omega_E(t - t_0)$ with ω_E is the angular velocity of the

Earth and defined as $\omega_E = 2\pi/T_E$ where T_E is the Earth rotational period. The satellite vector $\mathbf{r}_s$ is defined as:

$$\mathbf{r}_s = \frac{\mathbf{r}_t - \mathbf{r}}{\|\mathbf{r}_t - \mathbf{r}\|} \qquad [5.20]$$

It can be seen that the angle γ will vary between $-\pi/2$ and $\pi/2$. Accordingly, the availability will be maximum when the spacecraft is directly above the local vertical. As the spacecraft moves away from the local vertical the availability will decrease its value until it reaches the local horizon plane. At that point the availability will become zero, and the spacecraft will not be able to view the target or ground station. In Figure 5.15 we can see the Simulink model for the resource availability.

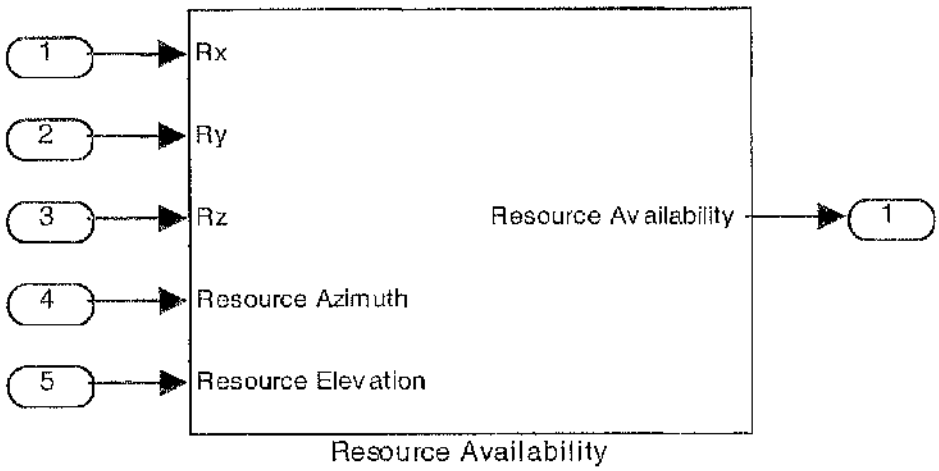

Figure 5.15 Resource availability model.

The azimuth and elevation of the target and the ground station can be defined by the user and uniquely identify the desired location. The availability module also receives

the three position vector projections (R_x, R_y and R_z) from the orbital dynamics model as inputs, and produces the resource availability in output.

In Figures 5.16-5.18 we can see how the availability varies, depending on the spacecraft orbit and on the location on the Earth of the target. In Figure 5.16 we have two equatorial circular orbits of varying altitude with the resource located at 0° latitude on the Equator. We can see that as the resource and spacecraft orbit lie on the same plane, the satellite will always fly directly above the resource and therefore the availability will be maximum. The lower altitude orbit, having a smaller orbital period will fly over the resource more often, 3 times more in just over one day, but for less viewing time than the higher altitude orbit.

In Figures 5.17-5.18 we see what happens in the case of two polar circular orbits with the target located first on the Artic Polar Circle, at 66.5° and then located on the Tropic of Capricorn at −22.5°. We can see that in these two cases the viewing pattern is far more irregular than the previous case. The spacecraft does not, in the time interval examined, fly directly over the resource and therefore the availability never reaches the value of 1. Also, as the resource rotates with the Earth, the availability has a different value from one fly over to the next. Moreover, it appears as if in this case, not only is the higher altitude orbit beneficial as the time spent flying over the resource is longer, but that the higher orbit has more viewing opportunities than the lower orbit. This is clearly because the spacecraft in the higher orbit has a larger view area of the Earth's surface.

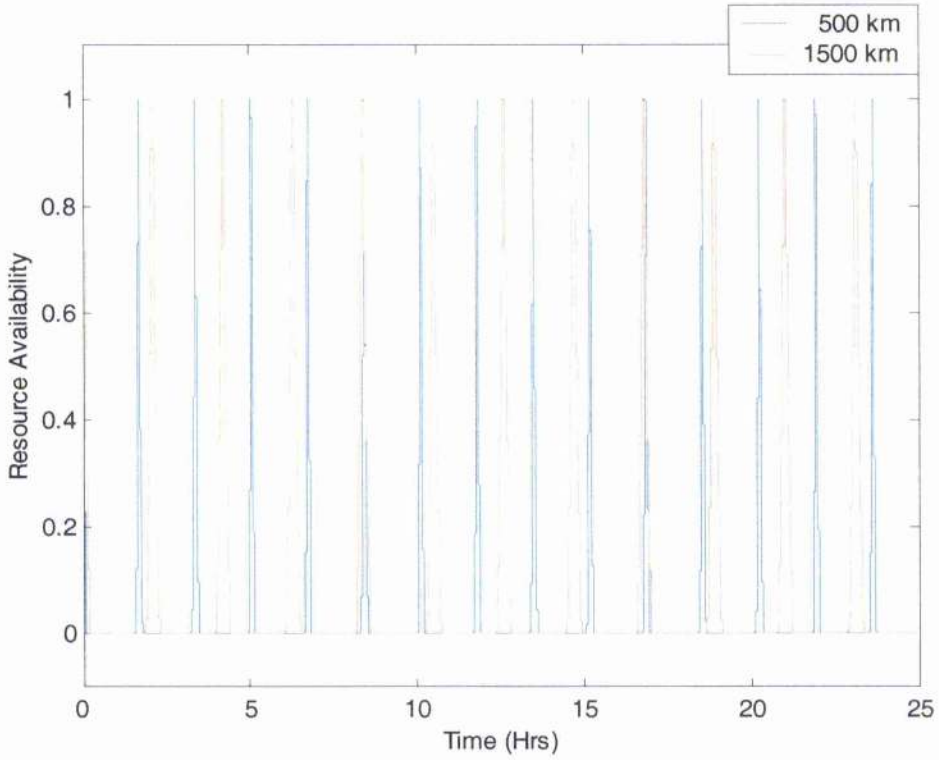

Figure 5.16 Resource availability for two equatorial orbits with target located on Equator

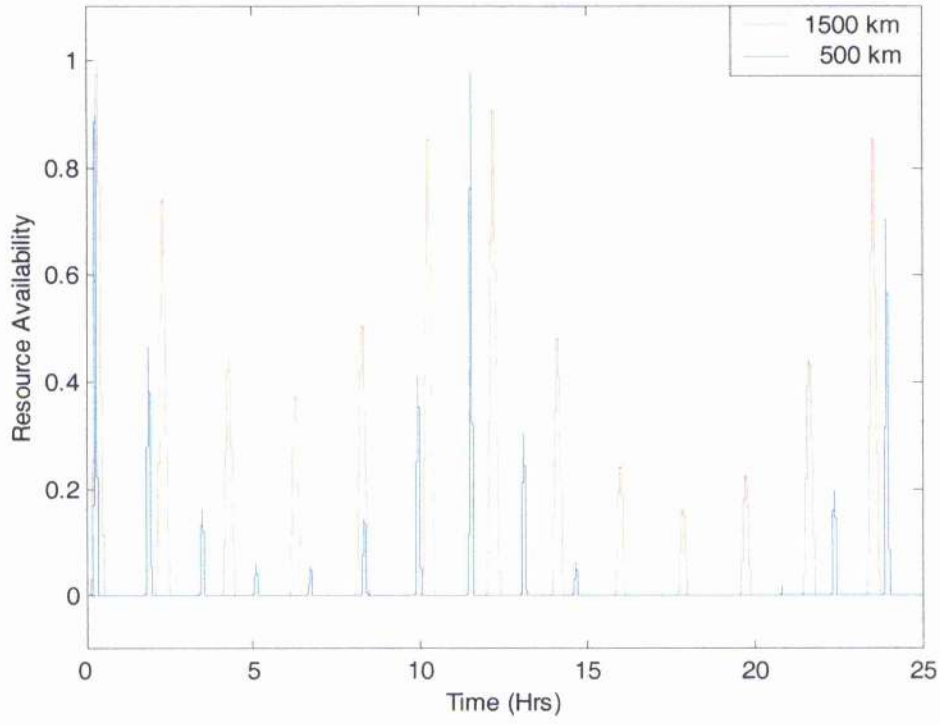

Figure 5.17 Resource availability for two polar orbits with target located on Artic Polar Circle

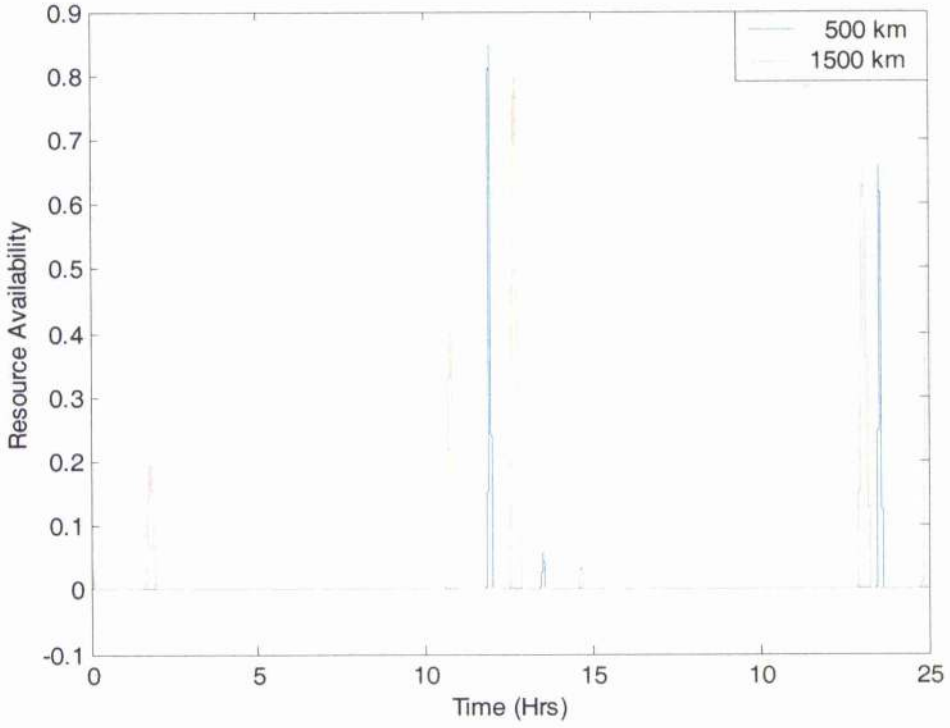

Figure 5.18 Resource availability for two polar orbits with resource located on Tropic of Capricorn

Having explained how the spacecraft determines the resource location, we must now solve the problem of slewing the spacecraft between the different resources. Once the spacecraft has selected which behaviour to perform, it must slew towards the desired attitude to point the transmitter towards the ground station, the camera towards the target or the solar array towards the Sun. The geometric configuration is illustrated in Figure 5.19

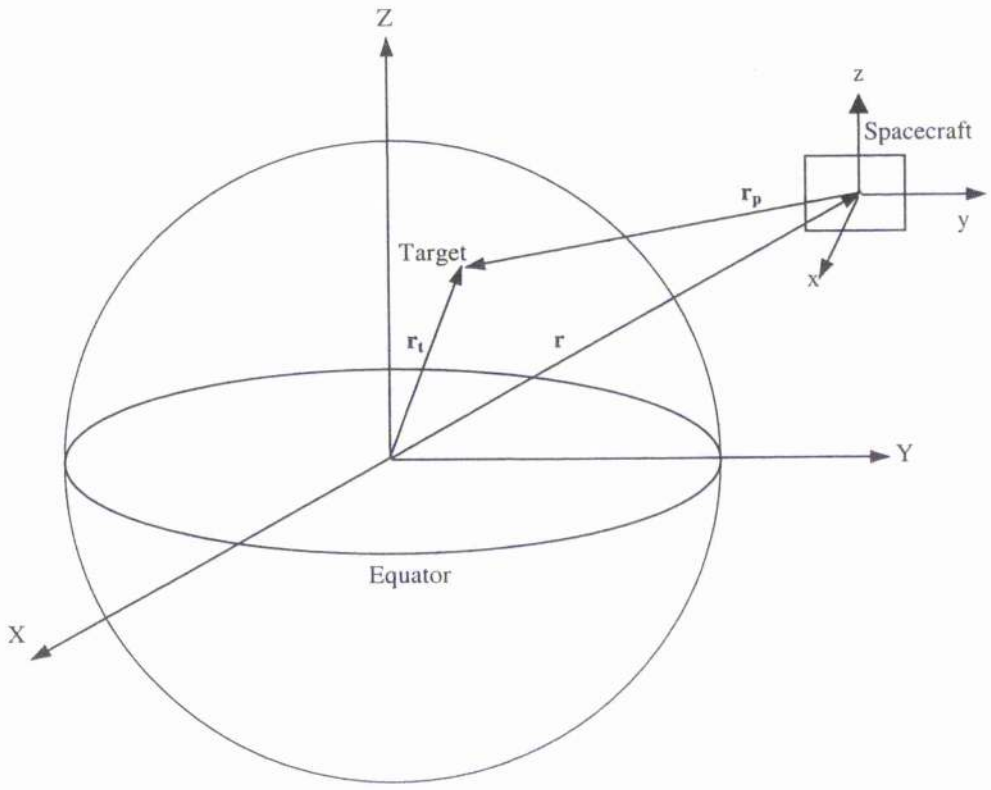

Figure 5.19 Definition of parameters for target pointing

The spacecraft must orient itself such that the correct instrument is directed towards the appropriate resource to be able to carry out the required task. The direction along which the spacecraft must direct its payload is given by:

$$\mathbf{r}_p^{\text{inertial}} = \frac{\mathbf{r}_t - \mathbf{r}}{\|\mathbf{r}_t - \mathbf{r}\|} \qquad [5.21]$$

where $\mathbf{r}$ is obtained from the orbital dynamics block and $\mathbf{r}_t$ is defined by the user as explained previously. The spacecraft has a camera and an antenna placed on the face normal to the y body axis, identified by:

$$\mathbf{r}_p^{\text{body}} = \mathbf{j} \qquad [5.22]$$

where $\mathbf{j}$ is the unit vector along the y-axis of the body frame of reference. Now the $\mathbf{r}_p$ vector must be transformed into one common frame of reference. This is done by using the transformation matrix $\mathbf{R}$ obtained through the 3-1-3 Euler angle sequence and explained in Chapter 4.

$$\mathbf{r}_p^{\text{inertial}} = \mathbf{R}^{\mathbf{T}}\,\mathbf{r}_p^{\text{body}} \qquad [5.23]$$

This then yields three equations with the three unknowns being the desired Euler angles.

$$\mathbf{r}_p = \left(\cos\theta_1\cos\theta_3 - \sin\theta_1\cos\theta_2\sin\theta_3\right)\mathbf{I} + \left(\sin\theta_1\cos\theta_3 - \cos\theta_1\cos\theta_2\sin\theta_3\right)\mathbf{J} + \sin\theta_2\sin\theta_3\mathbf{K}$$

[5.24]

However, because θ_2 is the rotation angle along the camera and antenna axis its value is not required, therefore we can arbitrarily set its value to $\pi/2$. This also has the positive effect of avoiding any possibility of a singularity during the solution of Euler's equations. In Figure 5.20 we can see the Simulink block used.

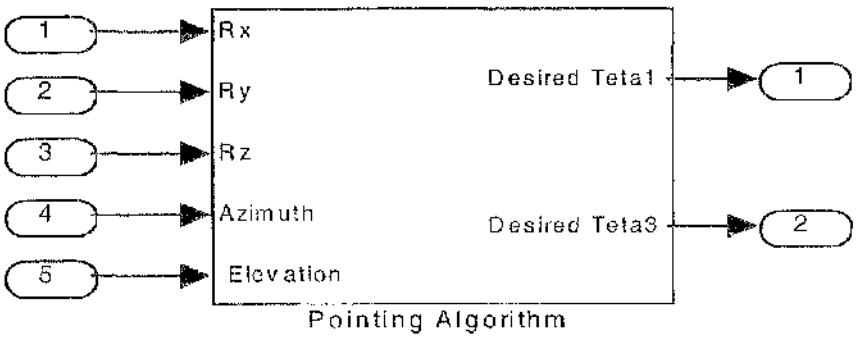

Figure 5.20 Target pointing model

The block receives the azimuth and elevation of the target or the ground station, together with the projection of the position vector along the inertial frame of reference. The output is the required Euler angles the spacecraft has to slew towards through so as to point towards the target or ground station.

To slew the spacecraft we use the potential function control method introduced in Chapter 4. In Figure 5.21 we can see the top level Simulink model of the attitude control algorithm.

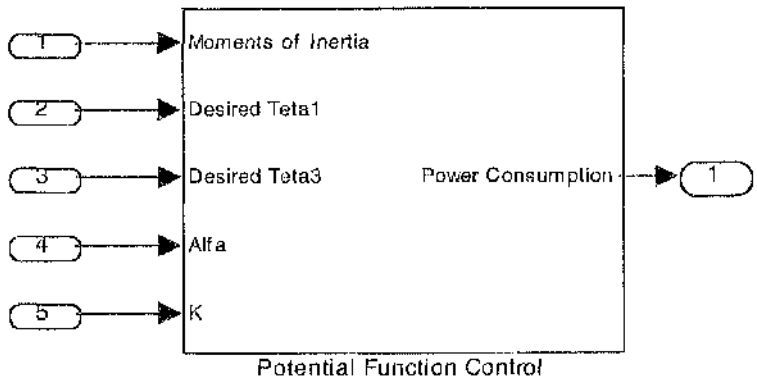

Figure 5.21 Top level attitude control algorithm model

The user defines the inertia moments I_i (i = 1-3) of the spacecraft, while the pointing algorithm introduced previously feeds the desired attitude angles to the attitude control algorithm. The parameters α_i and k_i (i = 1-3) are chosen by the user and influence the slewing rate and slewing time as explained in Chapter 4. The demand on the power subsystem, when the potential function control is active, is 1.5 Watts [Wertz 1992]. In Figure 5.22 we can see the bottom level Simulink model of the control algorithm.

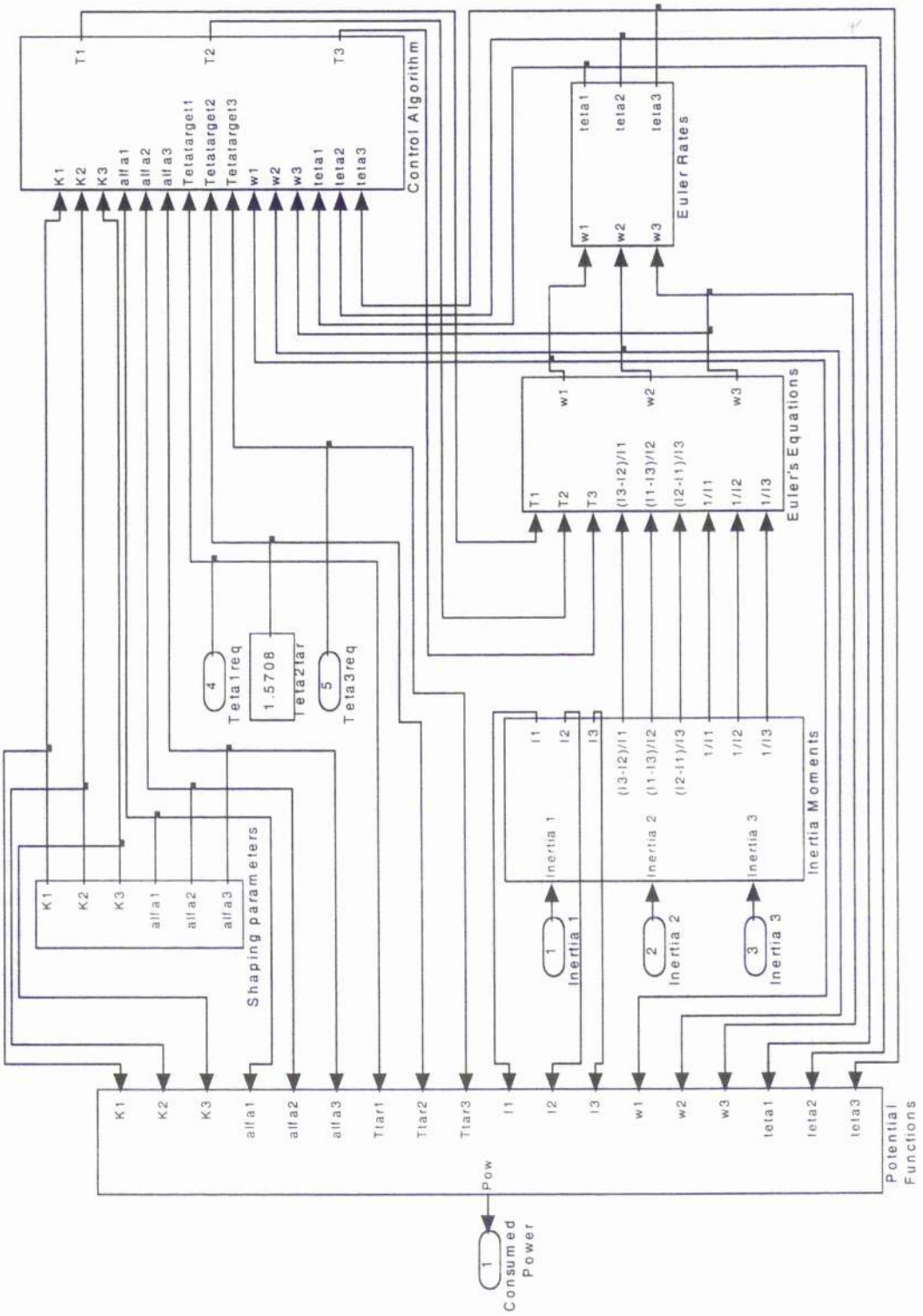

Figure 5.22 Bottom level attitude control algorithm model

We can now see that the desired attitude angles are fed into the potential function control algorithm, together with the shaping parameters α_i and k_i. The control algorithm, Equation 4.18, produces as outputs the torques necessary to slew the spacecraft to the desired orientation. The value of the torques are linked into Euler's equation, Equation 4.8, together with the moments of inertia for the spacecraft. In turn, this provides the angular velocities, which are then, through Equation 4.11, used to generate the current attitude angles, thus closing the control loop.

5.6.1.4 Telecommunications

The communications subsystem is the interface between the spacecraft and Earth, or other satellites. The transmitter and receiver must be in view of each other, using frequencies high enough, above 100 MHz, to easily penetrate the Earth's ionosphere. Since the satellite is designed for a near Earth orbit, there is no need to equip it with a high gain antenna and a powerful transmitter, which would result in a useless weight and power increase. The transmitter, when active, downloads to the ground station 10000 bits of data per second, and requires 2.88 Watts to operate [Winton et al. 1996]. In Figure 5.23 we can see the Simulink model of the transmitter.

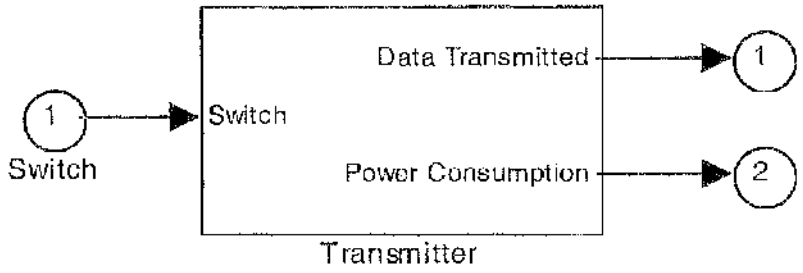

Figure 5.23 Transmitter model

The transmitter is switched on when the spacecraft is flying over the ground station and the *drk* product associated with the 'transmit' behaviour is the highest of the three. In output, the transmitter block produces a data rate, which affects the solid state memory, and a power consumption which affects the battery charge.

5.6.1.5 Electrical Power

The main function of the electrical power subsystem is to provide, store, distribute and control the electrical power on board the spacecraft. On a spacecraft, electrical power is required to power the computers, radio transmitters and receivers, motors, valves, data storage devices, instruments, sensors and other devices. We assume the use of a 20 x 20 cm solar array composed of silicon cells, which have an energy conversion efficiency of approximately 15% [Wertz 1992]. The Simulink model of the solar array is shown in Figure 5.24

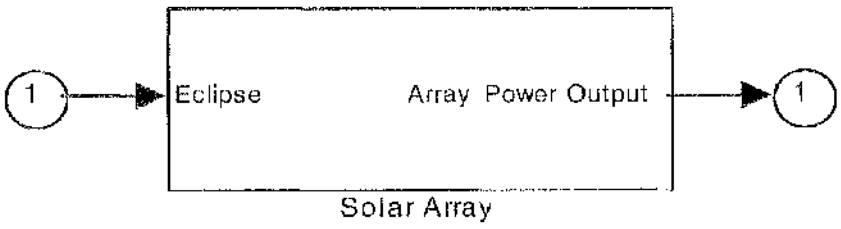

Figure 5.24 Solar panel model

The solar panel produces a constant power output of 8 Watts when in direct sunlight, while there is obviously no power output if the spacecraft is in eclipse.

Energy storage is an integral part of the spacecraft's electrical power subsystem. Any spacecraft that uses photovoltaic cells as a power source requires a system to store energy for peak power demands and eclipse periods. Energy storage typically occurs in a battery, which receives a charge from the main bus when the

solar panels are in the sunlight, and a discharge into the bus to maintain its voltage whenever the solar panels are shadowed by the planet, or off Sun-pointing during spacecraft manoeuvres. A battery can convert chemical energy into electrical energy during discharge and electrical energy into chemical energy during charge. The Simulink model of the battery is shown in Figure 5.25.

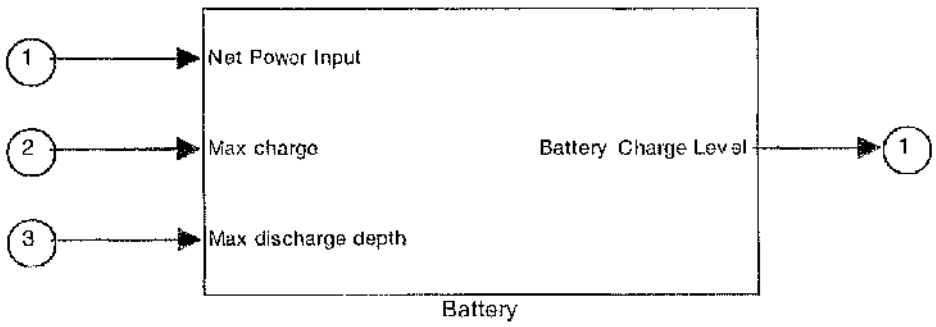

Figure 5.25 Battery model

The battery model receives the net power input from the different subsystems which require energy such as payload and transmitter, as well as the upper and lower lethal limits. The battery is considered to have a capacity of 24 KJ and an efficiency in converting the power coming from the solar array of 0.3. The minimum charge to guarantee the spacecraft's survival is 8 KJ. In output, the block produces the current battery charge level [Wertz 1992].

Integrating the solar array model and the battery model, we obtain the electrical power model shown in Figure 5.26

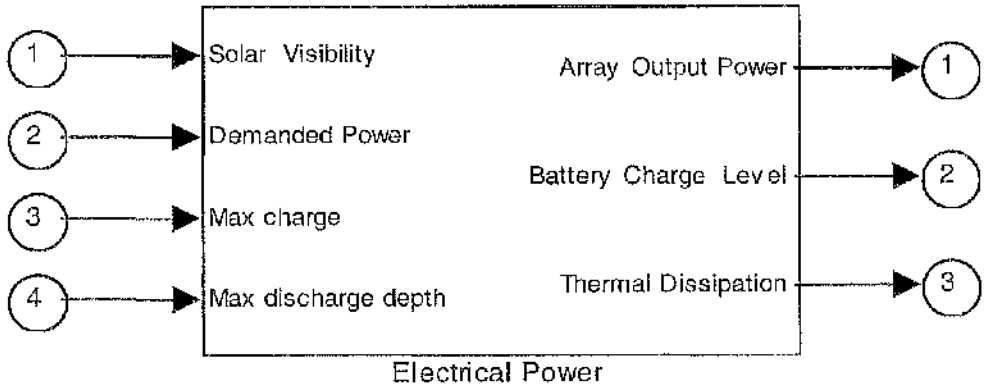

Figure 5.26 Electrical power model

The electrical power subsystem provides the battery charge, which affects the action selection algorithm, as well as producing a thermal dissipation term, which influences the thermal subsystem discussed below.

5.6.1.6 Thermal Control

The thermal control subsystem tries to maintain all the elements of the spacecraft system within their temperature limits during all the mission phases. A satellite orbiting Earth will be subjected to different heat fluxes: Solar, Earth reflected (albedo) and Earth emitted energy. The thermal control system affects, and is affected, by almost all other spacecraft systems. For example, the power subsystem interacts strongly with the thermal control subsystem since the latter must account for all dissipated electrical energy and radiate this energy to space. The spacecraft is assumed to be equipped with an electric heater and a temperature sensor. When the internal temperature reaches a fixed threshold the heater is automatically switched on to ensure that the temperature is raised to the desired level. In Figure 5.27 the temperature control model is shown.

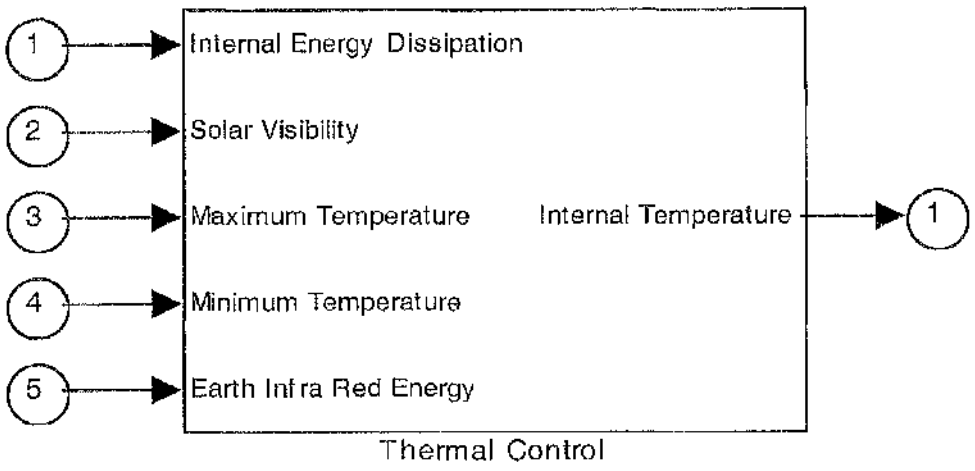

Figure 5.27 Thermal control model

The thermal control model receives as inputs, the energy dissipated by other on-board subsystems, the Sun availability, the upper and lower lethal temperatures and the Earth infrared emitted energy. The maximum temperature is chosen to be 350 K while the minimum is 220 K [Wertz 1992]. Within this range the components in the different subsystems will operate normally, while outwith this range the spacecraft will cease to function. The output of the block is the current internal temperature level. When the temperature reaches the threshold value of 240 K the heater is activated to ensure that the spacecraft temperature is kept above the minimum lethal value. The heating subsystem is shown in Figure 5.28.

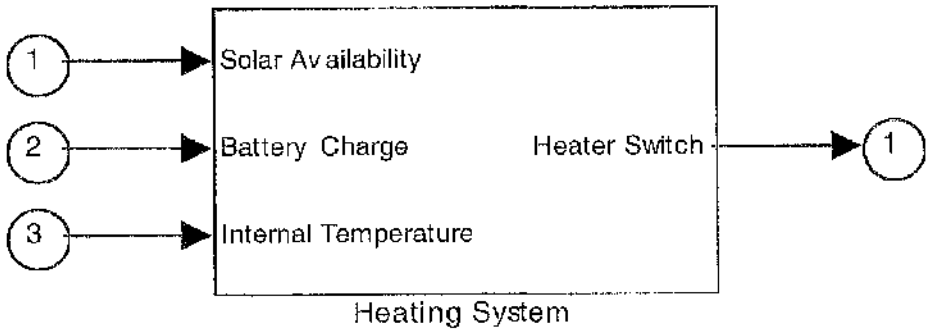

Figure 5.28 Heating subsystem model

The value of the internal temperature is used together with Sun visibility and the battery charge to activate the heating subsystem. The output is a command, which switches the heater on or off as required, as shown in Figure 5.29.

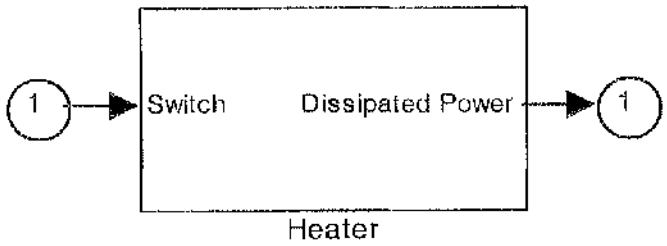

Figure 5.29 Heater model

The heater requires 10 Watts to operate, and has the task of maintaining the internal temperature above a lethal threshold value while at the same time it consumes electrical power [Wertz 1992].

5.6.1.7 Task Sequencing Algorithm

We will now show how the action selection algorithm introduced in Chapter 3 is modelled within the spacecraft. In Figure 5.30 we can see the top level of the task sequencing Simulink model.

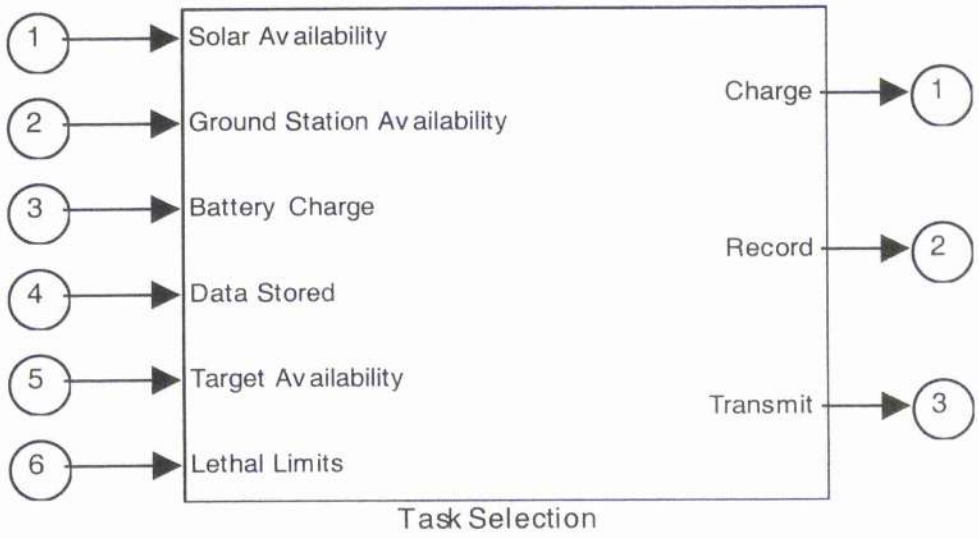

Figure 5.30 Top level task sequencing model

The inputs are the availabilities for the different resources: the solar availability arrives from the eclipse model, while the target and ground station availabilities arrive from the resource availability models. The lethal limits for the state variables, together with the values of the battery charge and the amount of data stored are used to calculate the deficits. The outputs are the three behaviours which the spacecraft can perform: charging the battery, recording data and downloading data. In Figure 5.31 we can see the details of the action selection algorithm.

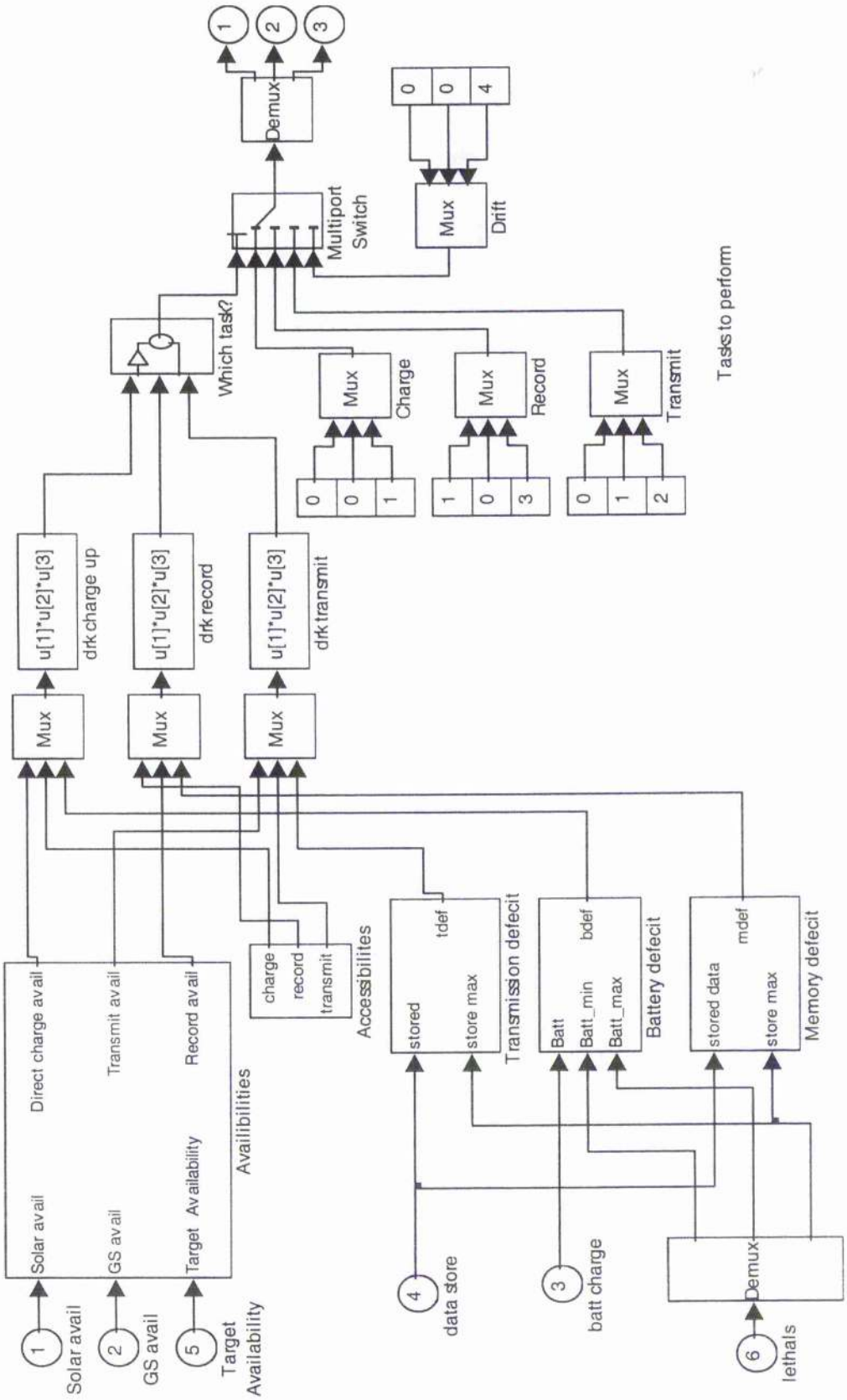

Figure 5.31 Detailed task sequencing model

The deficits are calculated as explained in section 3.12, while the accessibilities are fixed by hardware constraints and have the following values: $k_{charge} = 1$, $k_{record} = 1$ and $k_{transmit} = 1$. The values of the deficits, availabilities and accessibilities are then multiplied to obtain the *drk* product associated with each behaviour. The values are then passed through the Simulink model, which determines which task has to be performed and shown in Figure 5.32.

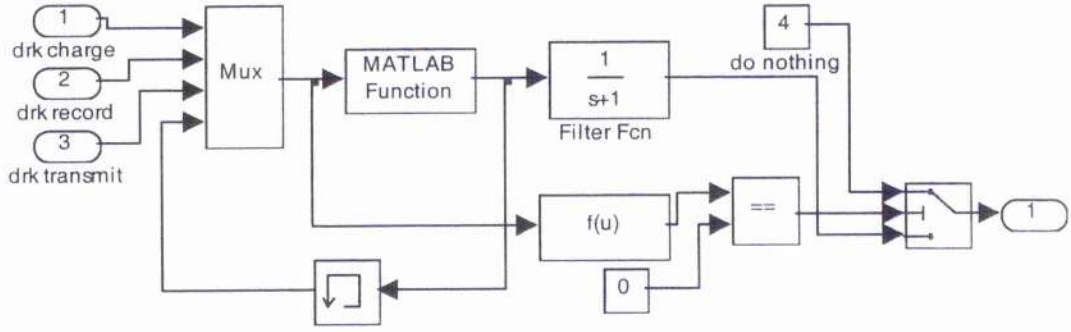

Figure 5.32 Task selection model

This block decides which *drk* product is the highest and hence what task should be performed. A filter is added so that the spacecraft does not oscillate between tasks with similar *drk* products. To perform a new behaviour, the *drk* associated with it has to surpass the *drk* product associated with the behaviour the spacecraft is currently performing by 0.1. Also, should the *drk* products be all larger than 0.9 or all zero, the spacecraft will not perform any task, and simply drift along its orbit.

5.7 COMPLETE MODEL

Having introduced the individual subsystems and components that make up the model, we can now appreciate the complete system, shown in Figure 5.32. We can see that there are two main blocks in the model. The first one is the action selection block, in which the algorithms introduced in Chapter 3 are put into action. In this block the deficits, availabilities and accessibilities of the environmental resources are computed to determine which task the spacecraft has to perform. The second major block is the orbital dynamics and spacecraft model. Here the spacecraft moves along its orbit and assesses the availabilities of the resources. As the task coming from the action selection block is linked in here, the spacecraft will change its attitude, using the potential function attitude control, and, according to the task being performed, there will be variations in the state variables as the satellite will charge the battery, record, or download data. The new values of the environmental availabilities and state variable deficits are then passed to the action selection algorithm thus closing the entire global loop.

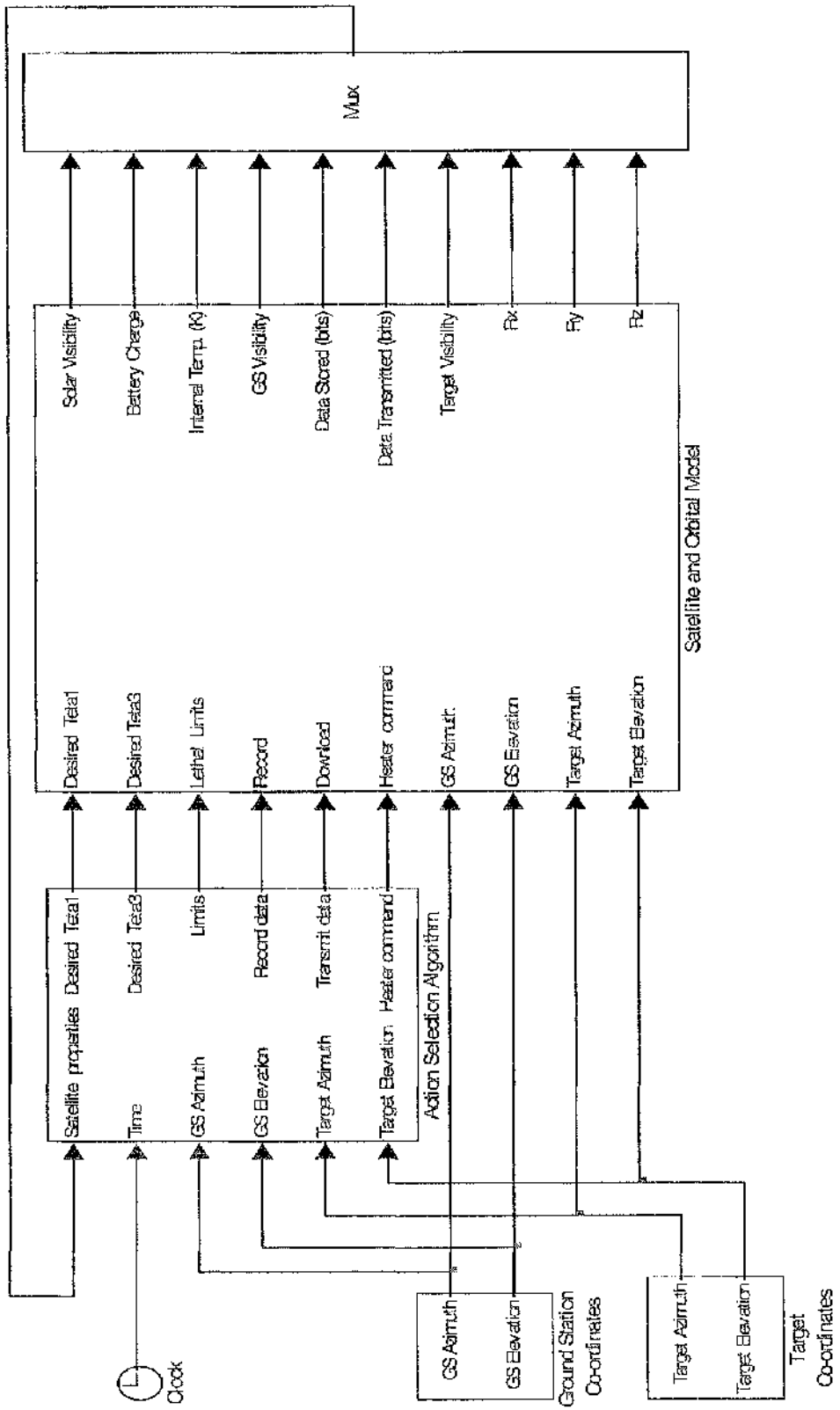

Figure 5.33 Complete Simulink model

CHAPTER VI

SINGLE SPACECRAFT

6.1 PREFACE

In this chapter we will evaluate the performance of the attitude control algorithm, based on Lyapunov's Second Method introduced in Chapter 4, and the behavioural sequencing algorithm introduced in Chapter 3, within the spacecraft and environmental models introduced in Chapter 5.

6.2 CASE STUDIES

As explained in the previous chapter, the satellite will operate in different orbits and is considered to have three rotational degrees of freedom that can be controlled by reaction wheels. The electrical power system consists of a solar array, battery and several electrical loads. The payload is a camera that records at a constant rate when active and a radio transmitter to broadcast data to the ground station. The individual subsystems are coupled together: switching the transmitter on drains the battery and reduces the amount of stored data. The spacecraft is controlled by switching the camera, the transmitter and an internal heater on or off, and commanding the attitude control subsystem to track one of the three targets, Sun, Earth ground station and Earth target, by activating the reaction wheels. The

spacecraft has an internal heater which may be switched on or off independently of what other task the spacecraft may be performing; the heater is automatically activated when the temperature drops below a certain threshold value fixed at 240 K and is not commanded by an action selection algorithm. The heater however drains the battery, and therefore indirectly influences the action selection process. The spacecraft selects the optimum behaviour at any time by evaluating the deficits of the state variables, battery and memory level, assessing the availability and accessibility of the environmental resources, Earth ground station, Sun and Earth target, and finally computing the *drk* product. The spacecraft will switch between different behaviours when the difference between two *drk* products surpasses a fixed threshold. To test the performance of the model we will consider two different types of low Earth orbits: a polar orbit and an equatorial orbit.

6.2.1 Polar Orbit

The spacecraft is at first inserted into a polar low Earth orbit. Low altitude polar orbits are widely used for Earth observation since each day the Earth rotates below the spacecraft, so that the entire surface can be covered over a repeat cycle. Polar orbiters are used for mainly used for Earth-monitoring and weather observations. In Tables 6.1-6.3 we can see the simulation parameters used to select the orbit, the target and ground station location and model the spacecraft. The simulation runs for just over 100 orbits, which equates to over 6 mission days. In Figures 6.1-6.12 we can see the results of the simulation.

Parameter	Value
Semi major axis (km)	6788.14
Eccentricity	0
Inclination (deg)	86
Right ascension (deg)	0
Argument of perigee	0
Orbital period (sec)	5677

Table 6.1 Orbital parameters

Parameter	Value
Ground station latitude (deg)	40
Ground station longitude (deg)	0
Target latitude (deg)	57
Target longitude (deg)	180

Table 6.2 Ground station and target parameters

Parameter	Value
Maximum battery charge (KJ)	24
Minimum battery charge (KJ)	8
Initial battery charge (KJ)	16
Maximum temperature (K)	350
Minimum temperature (K)	220
Initial temperature (K)	300
Maximum data storage (Mbits)	5
Minimum data storage (Mbits)	0
Initial data storage (Mbits)	0
Battery charge accessibility	1
Recording accessibility	1
Transmission accessibility	1
Moment of Inertia (Kgm^2)	60

Table 6.3 Spacecraft parameters

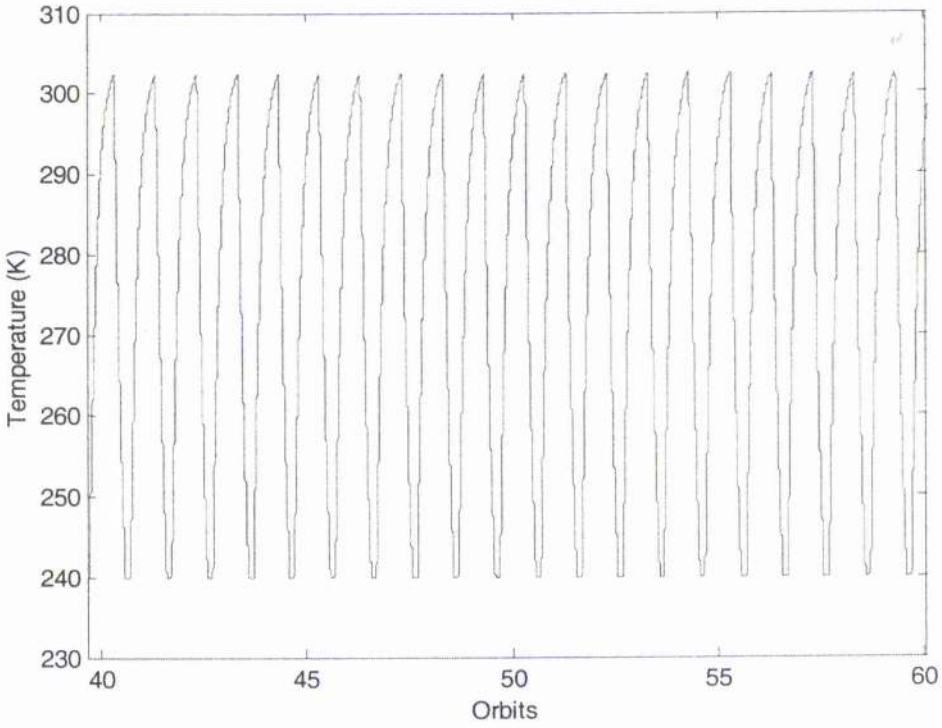

Figure 6.1 Internal temperature

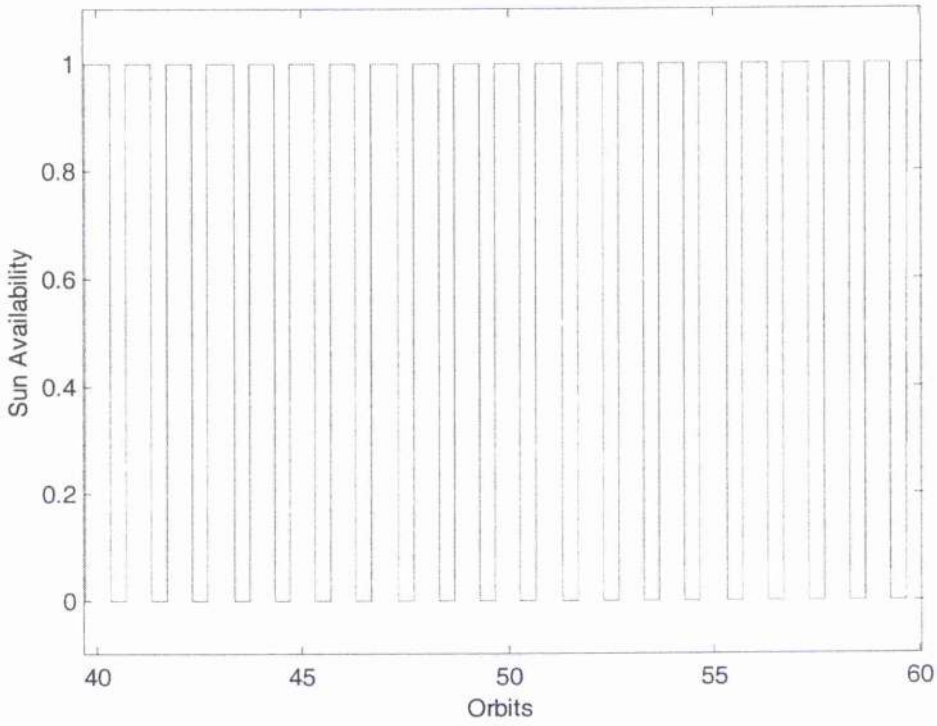

Figure 6.2 Sun availability

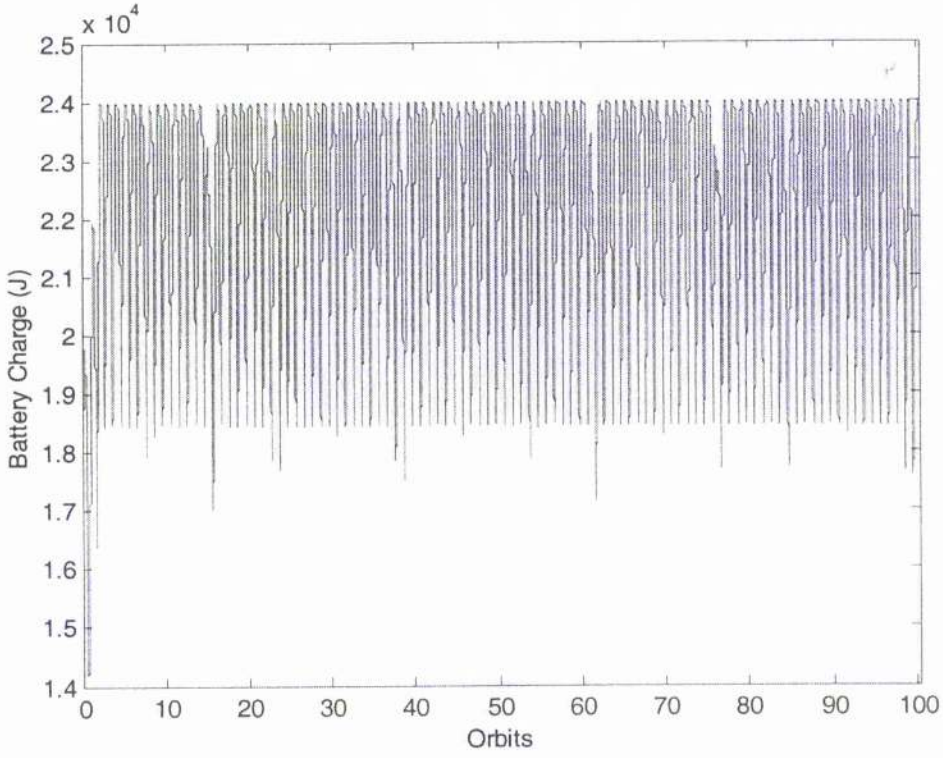

Figure 6.3 Battery charge

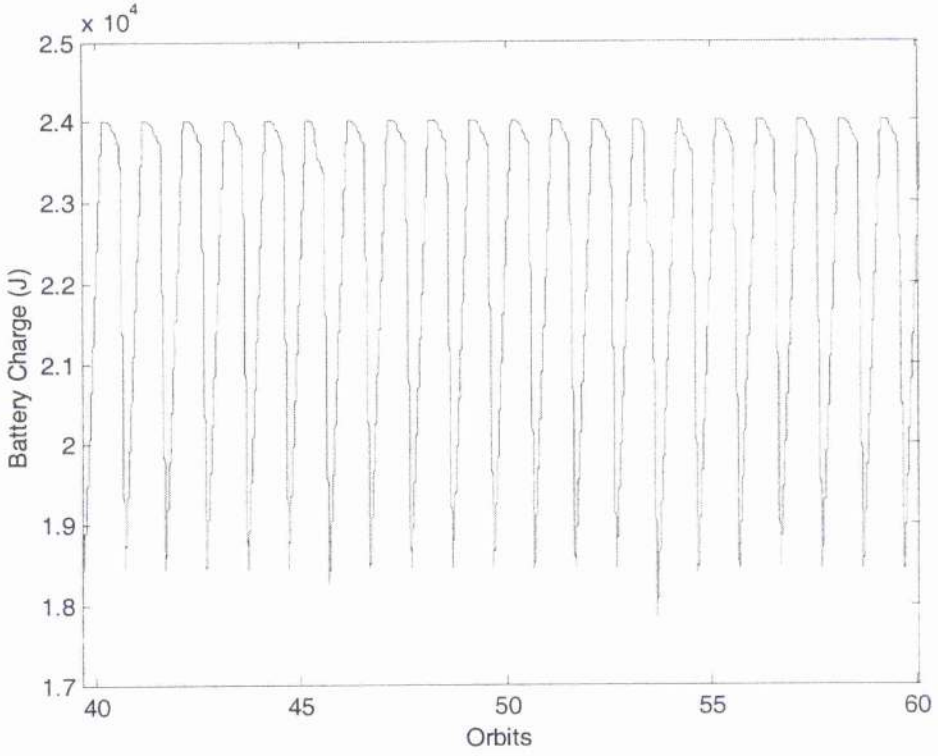

Figure 6.4 Battery charge close up

As we can see from the Figures 6.1-6.4, the battery charge, internal temperature and Sun availability are strongly coupled. When the spacecraft is in eclipse we can see that the temperature rapidly decreases as the Earth eclipses the spacecraft as evidenced by Figures 6.1 and 6.2. In Figure 6.4 we can see different slopes as the battery charge level decreases. This is due at first to the transmitter or payload being active; when either is operational there is a demand on the battery for their activation. After that, there is a period during which the transmitter or payload is not active and the discharge in the battery level proceeds at a lower rate. When the heater is then turned on to maintain the internal temperature, above the minimum lethal level of 220 K, the battery is discharged at an increased rate. When the spacecraft exits the eclipse, the temperature increases as the satellite experiences the solar heating. The battery charge also increases as the spacecraft slews and points the solar panel towards the Sun.

In Figures 6.5-6.8 we can see how the spacecraft handles the data management by recording data when flying above the target, and by transmitting data when in view of the ground station, depending on the resource availability and accessibility. It can be noted that as the spacecraft downloads data, there is obviously a decrease in the amount of data stored on-board. What is more interesting to highlight however, is the behaviour of the spacecraft with respect to the availability of the target and ground station. As was explained in Chapter 5, the resource availability varies with each orbital pass, depending on where the spacecraft is, with respect to the target or ground station. We can actually see that the spacecraft has several orbits without flying over either one or the other. The non-periodic nature of the ground station availability and target availability is due to the fact that the orbital period of the spacecraft in a 500km circular orbit is 94.62 minutes, and therefore not

repeatable during the 24 hour rotation period of the Earth. There are then two interesting differences that we can highlight when looking at the stored data and the target availability. When the availability of the resource is high the spacecraft records a significant amount of data. However when the availability of the target area is low the spacecraft may opt not to image, as highlighted by the amount of data stored in the memory remaining constant. This is because the spacecraft may have more pressing needs; i.e. charging the battery or downloading recorded data, or because recording data during a low availability flyby is not an efficient activity from an energetic point of view. Looking at the data transmitted and the ground station availability allows us to make similar considerations. We can see how, when the ground station has a good availability the spacecraft transmits significant data. On the other hand, when the ground station availability is poor there is little data transmitted back to Earth. Finally, we can see how storing of data starts immediately. This is because at the beginning of the mission scenario the deficit for the 'recording' behaviour is maximum. On the other hand, transmission of on-board data to the ground station starts after approximately 8 orbits, since the deficit for this behaviour is at first zero and then increases, as data is gradually stored in the memory.

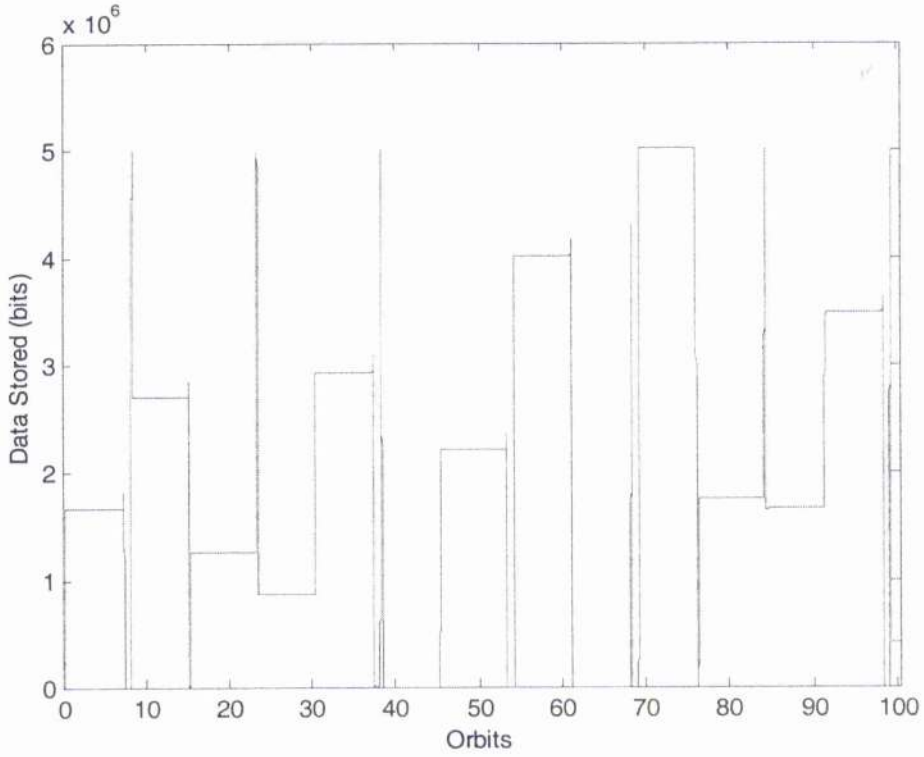

Figure 6.5 Data stored

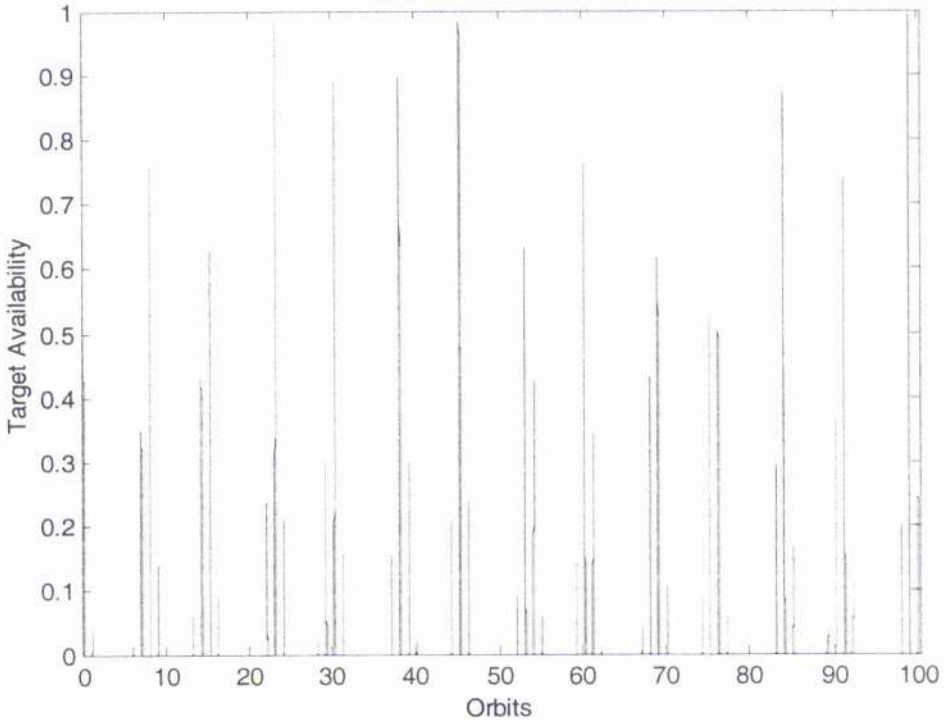

Figure 6.6 Target availability

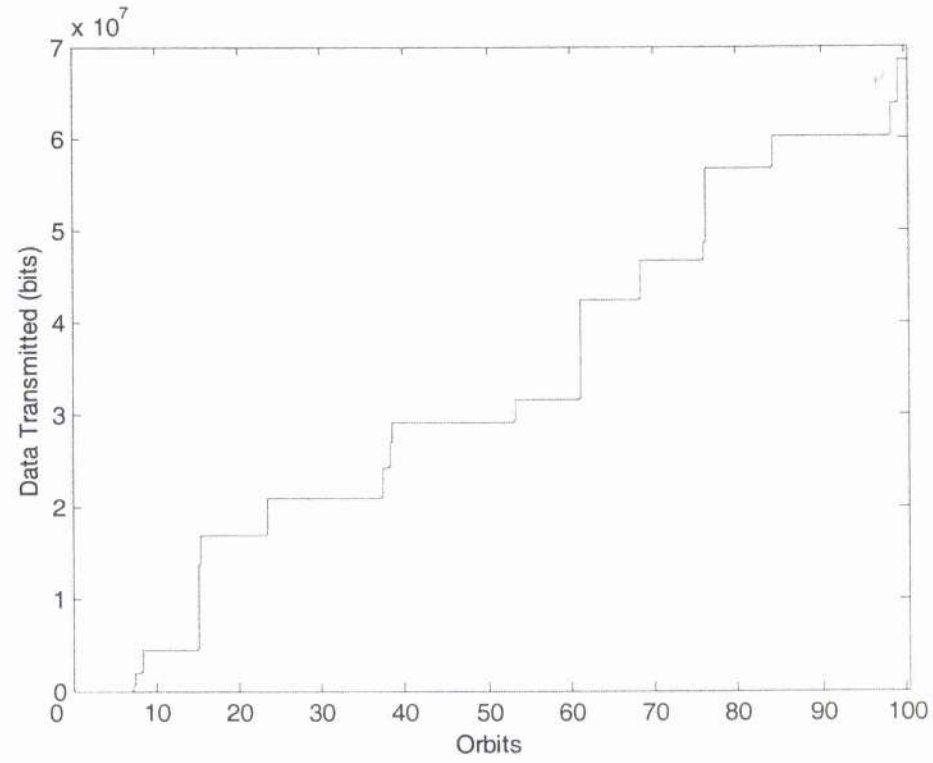

Figure 6.7 Data transmitted

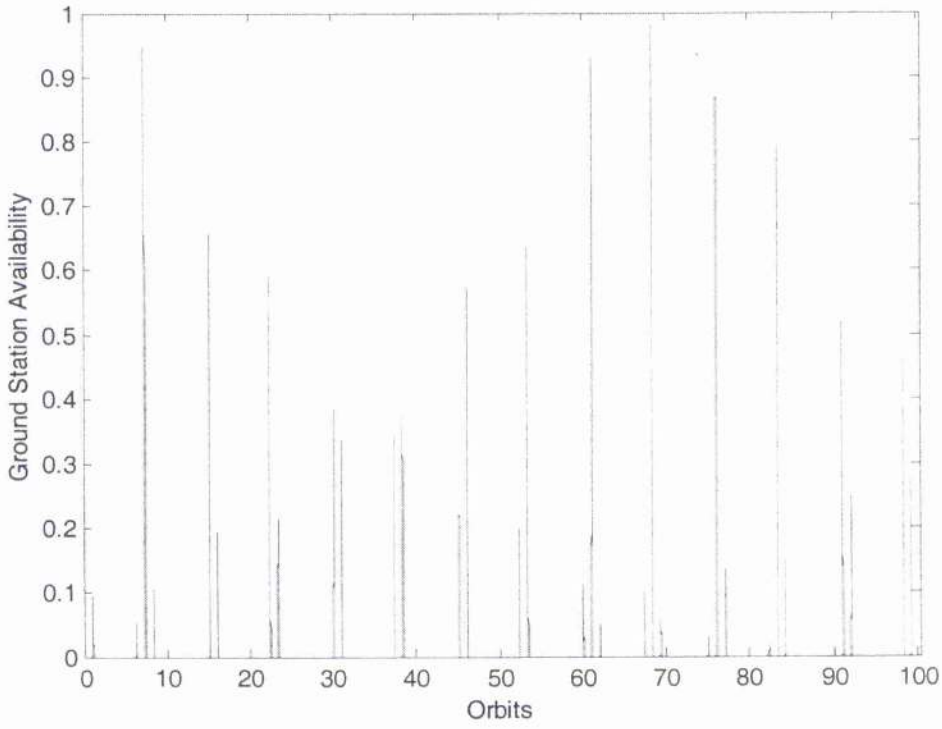

Figure 6.8 Ground station availability

It is also interesting to look at the behaviour of the spacecraft's state variables, battery charge, memory level and internal temperature, during the mission. This is shown in Figures 6.9-6.12, where the state variables are first viewed in a three-dimensional state space and then projected in a two-dimensional state plane to facilitate the interpretation of the data. The values of the state variables are normalised between one and zero. We can see that the spacecraft settles down to a limit cycle after an initial transient of a few orbits, due to the difference between the initial conditions and the nominal operating conditions. We can then see how the two most critical state variables, battery charge and internal temperature, both stay well within the lethal limits during the mission and never once is the spacecraft put into a situation which could lead to a permanent failure. Looking in detail at each state variable we can see that the temperature oscillates between normalised values of 0.4 and 0.8; it never surpasses 0.8, as that is the value at which the heater is turned on to maintain the temperature above the lethal level. The battery charge oscillates between normalised values of 0 and 0.4, which signifies that the spacecraft is always close to, or at, full charge. The memory state on the other hand ranges from normalised values 0 to 1 as data is recorded and downloaded, filling the memory to completion and then emptying it in full.

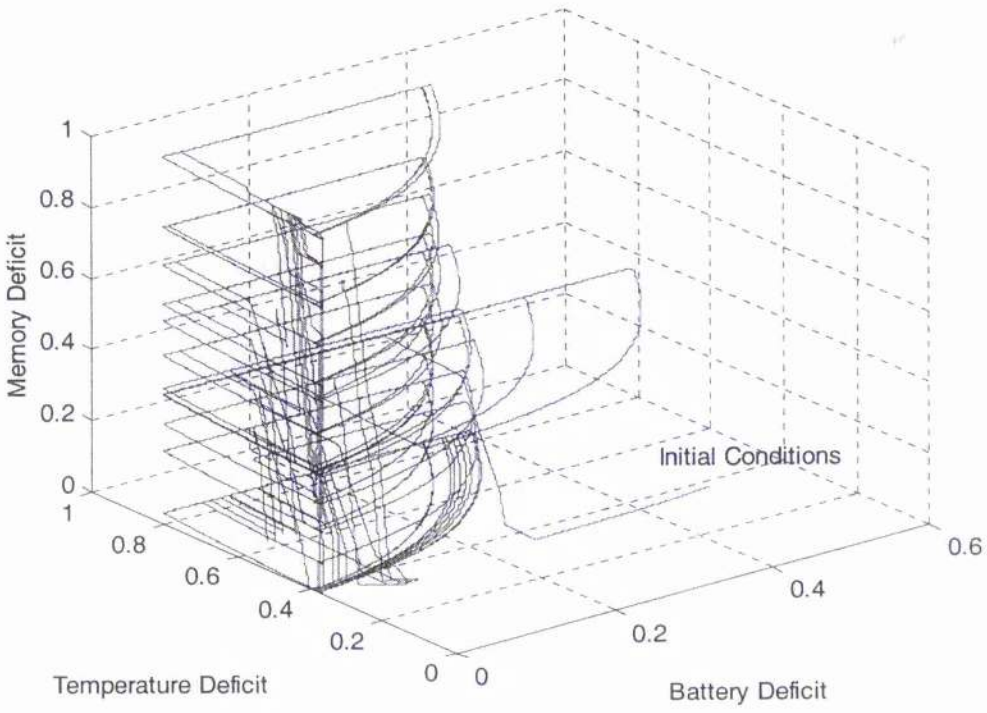

Figure 6.9 State variables within state space (normalised variables)

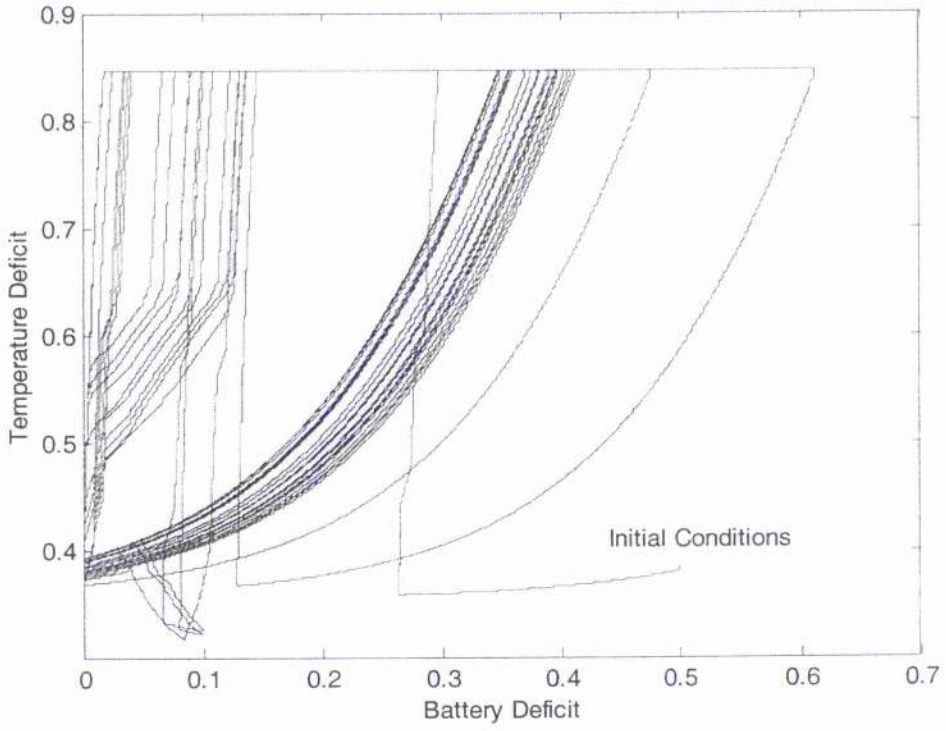

Figure 6.10 Battery and temperature deficits in state space (normalised variables)

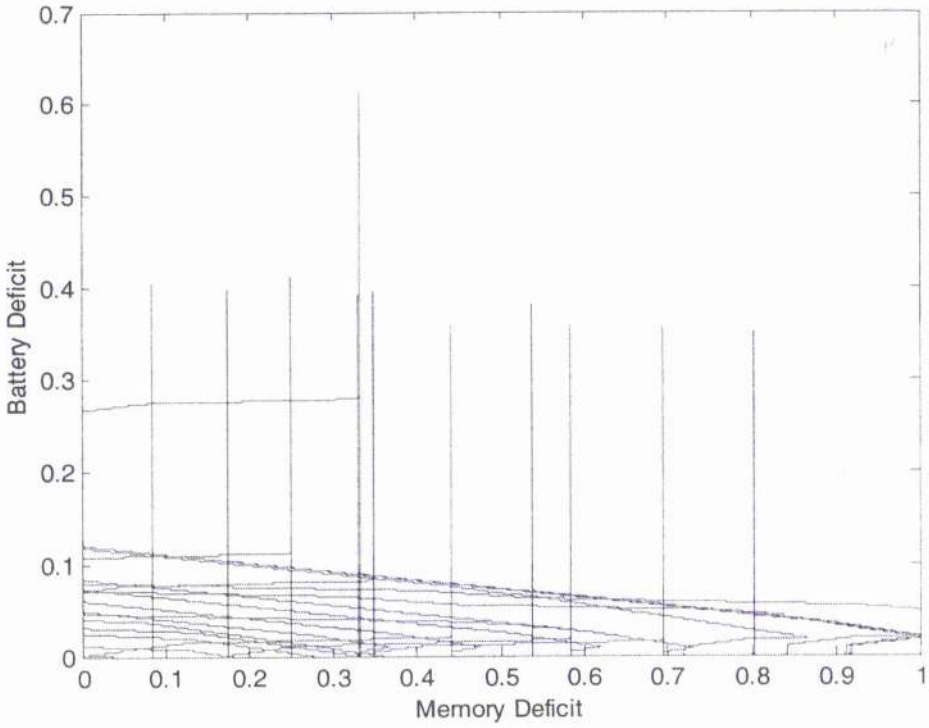

Figure 6.11 Memory and battery deficits in state space (normalised variables)

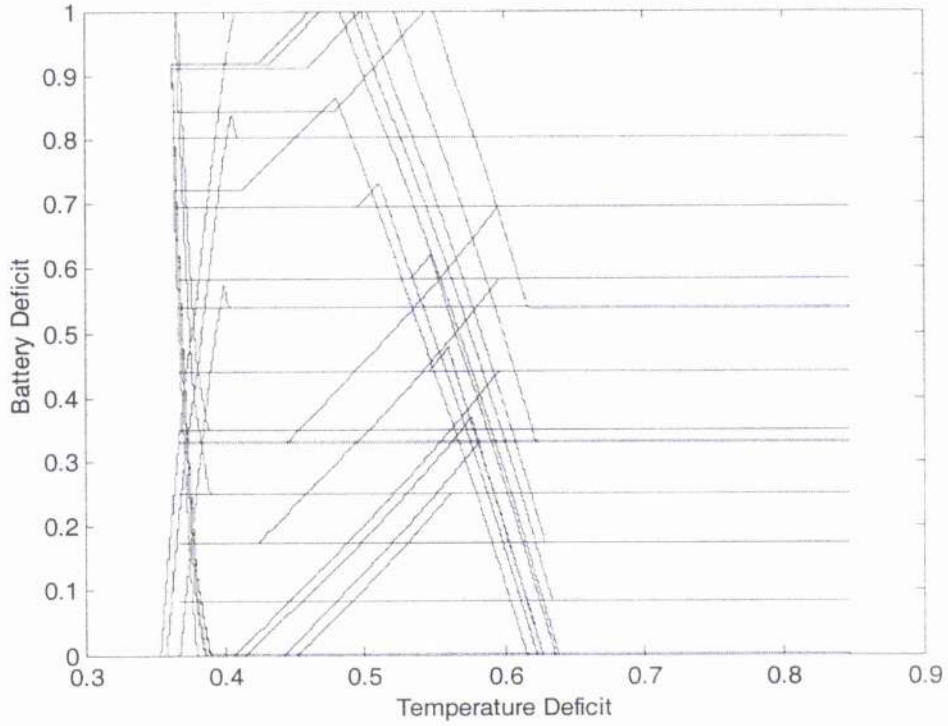

Figure 6.12 Temperature and memory deficits in state space (normalised variables)

6.2.2 Equatorial Orbit

Tropical countries around the equatorial belt are at a disadvantage from the point of view of polar satellites because of short and infrequent pass times. In these highly inclined orbits, each LEO satellite appears above the horizon for only 10 to 15 minutes per pass on the average. On the equator there may be at most 2 or 3 good passes on any one day. In the regions around the equator, a re-visit time of 16 days for remote sensing applications is not uncommon. In Tables 6.4-6.6 we can see the parameters used for the orbit, the target, ground station and the spacecraft. The simulation runs for just over 100 orbits, which equates to over 6 mission days. In Figures 6.13-6.24 we can see the results of the simulation.

Parameter	Value
Semi major axis (km)	6788.14
Eccentricity	0
Inclination (deg)	0
Right ascension (deg)	0
Argument of perigee	0
Orbital period (sec)	5677

Table 6.4 Orbital Parameters

Parameter	Value
Ground station latitude (deg)	0
Ground station longitude (deg)	0
Target latitude (deg)	0
Target longitude (deg)	180

Table 6.5 Ground station and target parameters

Parameter	Value
Maximum battery charge (KJ)	24
Minimum battery charge (KJ)	8
Initial battery charge (KJ)	16
Maximum temperature (K)	350
Minimum temperature (K)	220
Initial temperature (K)	300
Maximum data storage (Mbits)	5
Minimum data storage (Mbits)	0
Initial data storage	0
Battery charge accessibility	1
Recording accessibility	1
Transmission accessibility	1
Moment of Inertia (Kgm^2)	60

Table 6.6 Spacecraft parameters

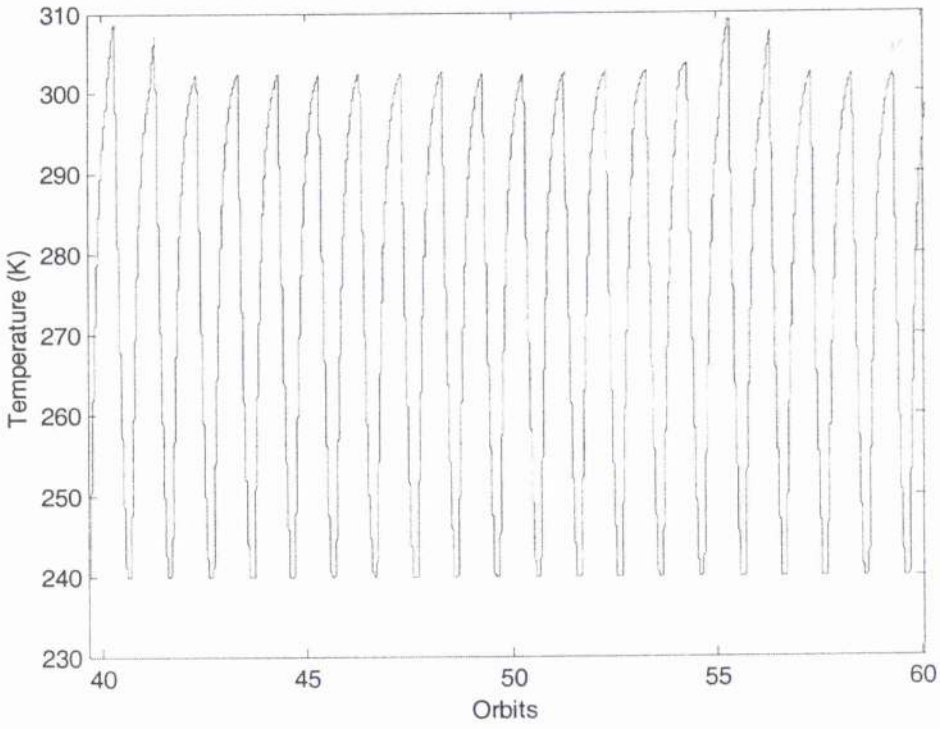

Figure 6.13 Internal temperature

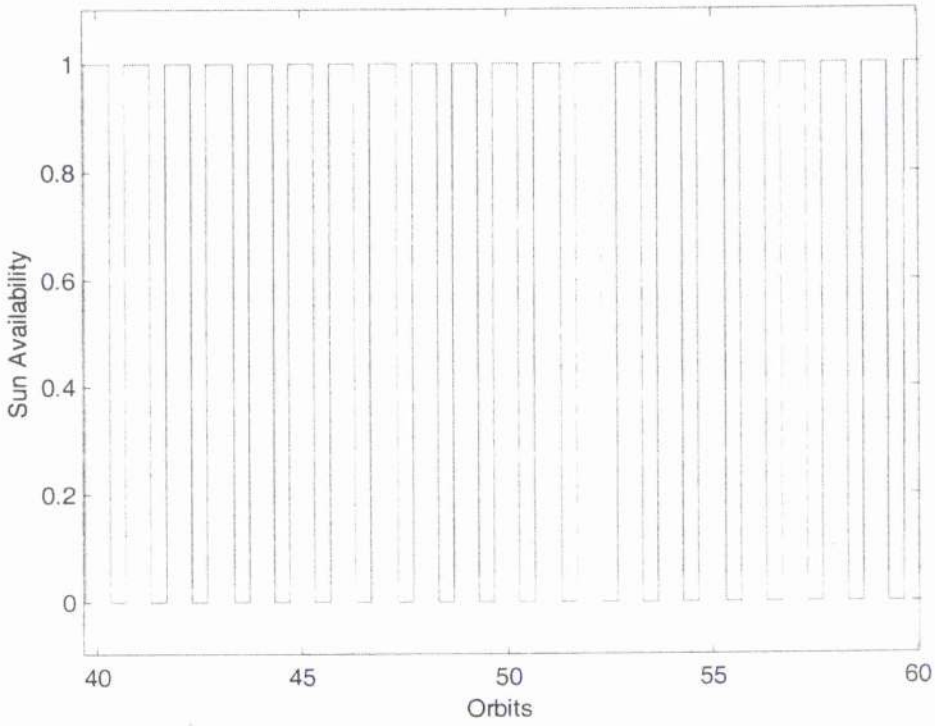

Figure 6.14 Sun availability

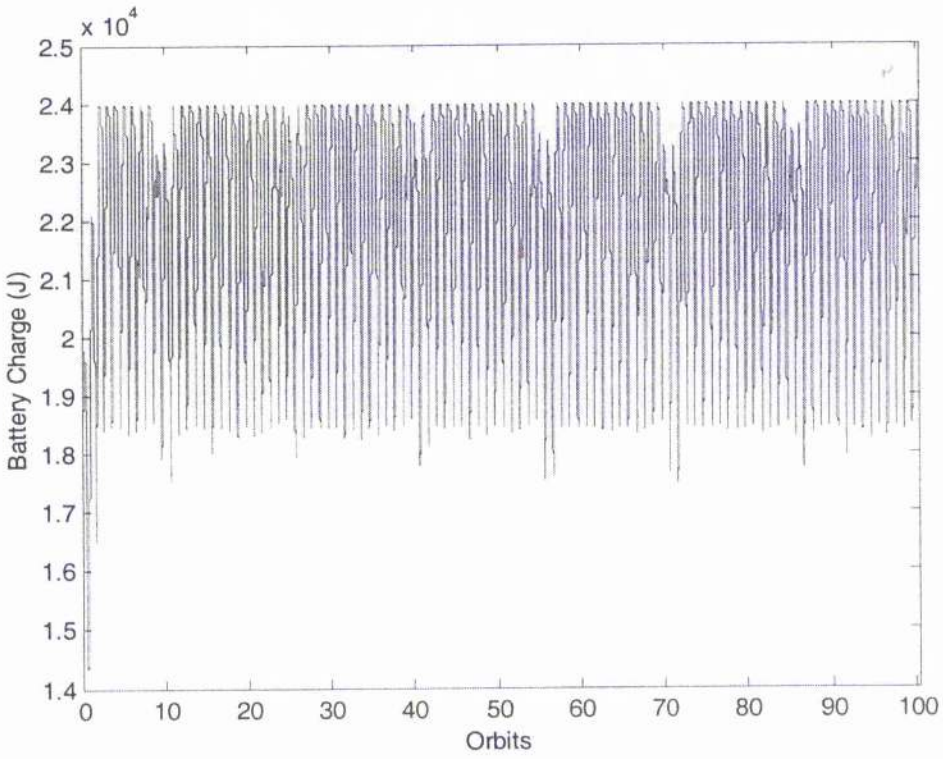

Figure 6.15 Battery charge

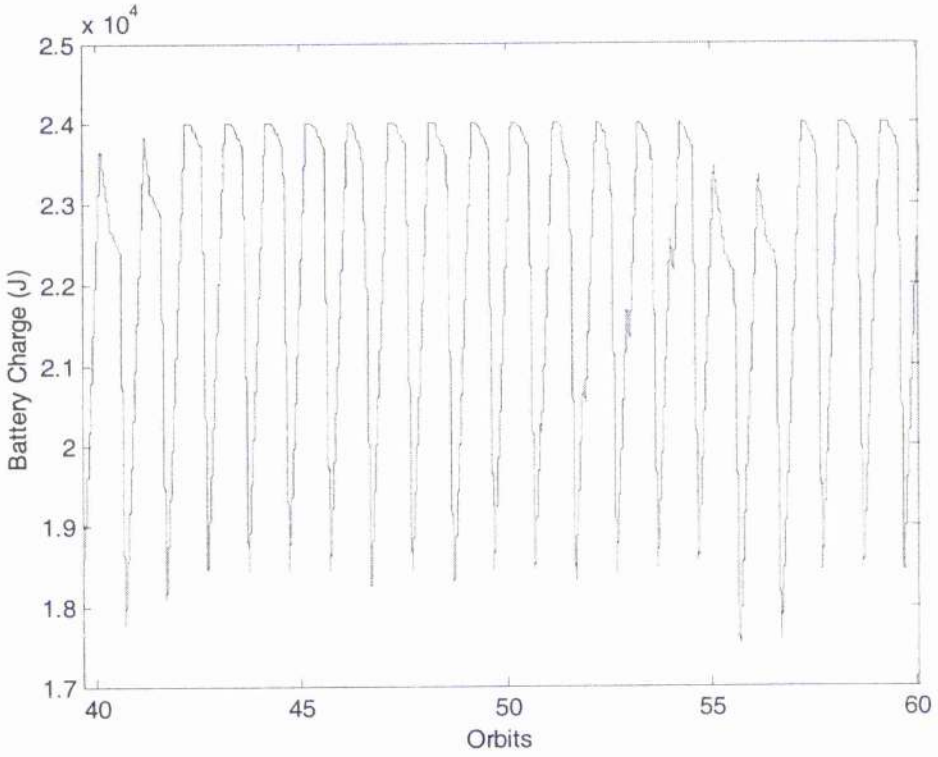

Figure 6.16 Battery charge close-up

The considerations made for the polar orbit case could be easily repeated for the equatorial orbit, when looking at the internal temperature and battery charge. Once again it is easy to see how the Sun availability strongly affects both the internal temperature and the battery charge. It is worth noting however, how there is an approximately 15 orbit cycle during which the battery charge reaches a slightly lower value than average. This happens in connection with a slightly higher value than average for the temperature, once again highlighting the coupling between the two state variables. The explanation of this phenomenon can be the following: every 15 orbits the spacecraft reaches the threshold temperature of 240 °K in an earlier portion of the eclipse than usual. Therefore the heater is activated sooner and as a consequence the battery has a higher discharge rate.

It is more interesting however to note the differences in the two cases with regards to the data management. The difference is apparent by comparing the evolution of the data stored (Fig 6.5 and 6.17) and the data transmitted (Fig 6.7 and 6.19) in the polar orbit case, and in the equatorial orbit case. We can see that in the equatorial case the data handling appears to have a far more regular pattern. This can be easily understood and explained by comparing the target (Fig 6.6 and 6.18) and ground station (Fig 6.8 and Fig 6.20) availabilities in the two cases.

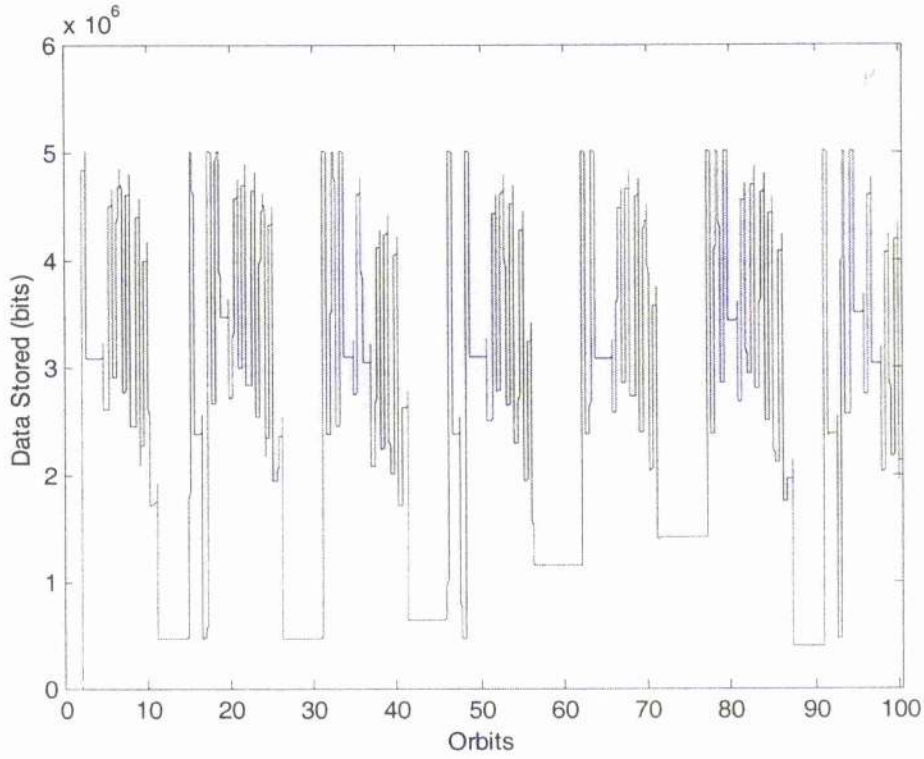

Figure 6.17 Data stored

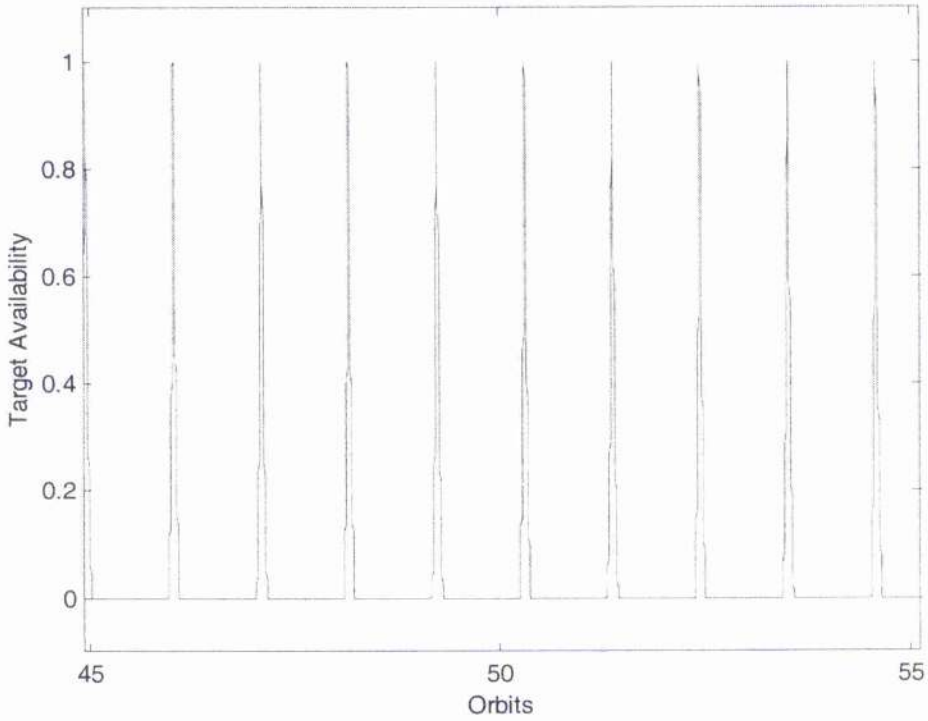

Figure 6.18 Target availability

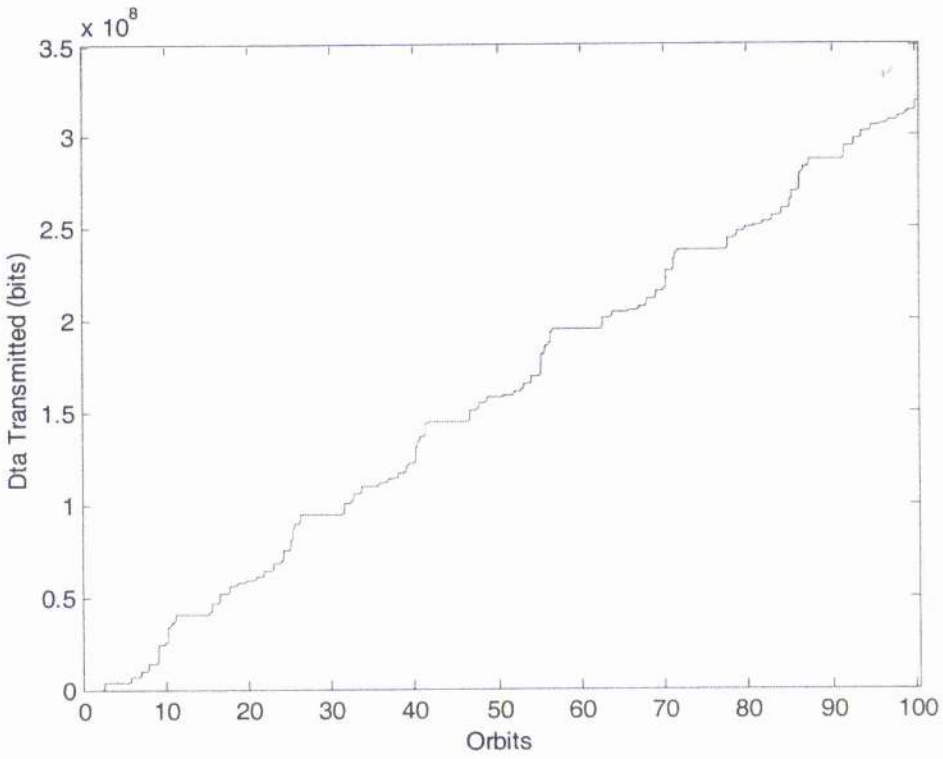

Figure 6.19 Data transmitted

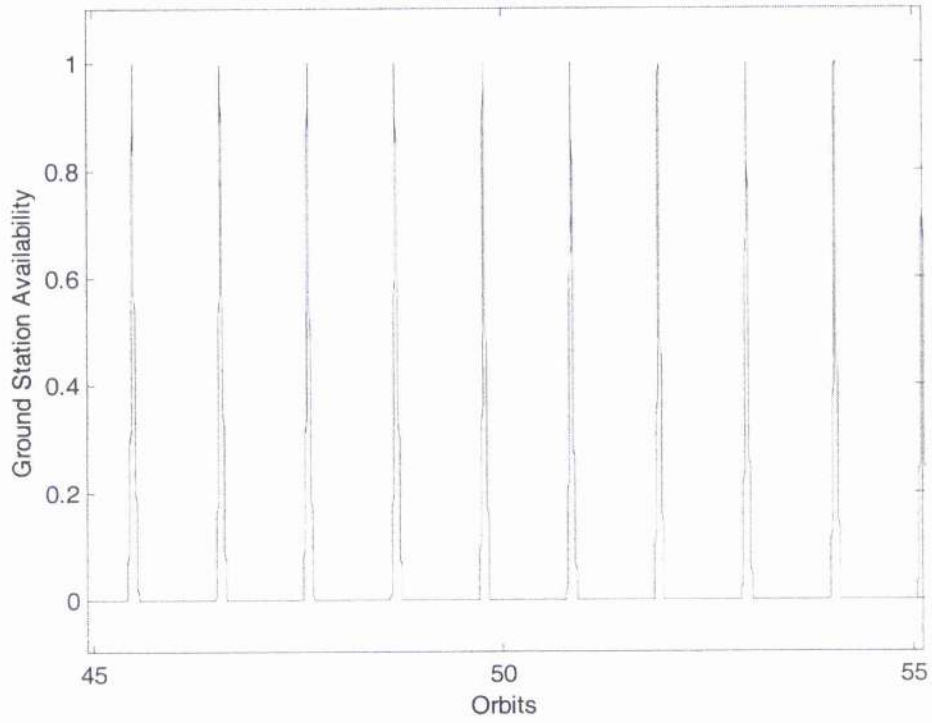

Figure 6.20 Ground station availability

In the equatorial orbit the spacecraft has a regular viewing pattern of both the target and the ground station, due to the characteristics of the orbit, and the location of the environmental resources. The satellite orbits over the target and ground station every orbit and the availability of the resource is always maximum, as the fly over is vertical. On the other hand for the polar orbit, the spacecraft does not view the target and ground station during each orbit period, due to their location with respect to the satellite orbit. The resource availability is also always less than maximum, as the spacecraft never flies directly over them. This means that not does only the spacecraft in equatorial orbit have more opportunities of recording and downloading data, but that the *drk* products associated with these behaviours are generally higher due to the higher environmental cues than for a polar orbit. Also, the longer time spent in view of the target or ground station means that the spacecraft can record or download more data. Finally, it can be seen that because of what has just been explained, the spacecraft in equatorial orbit transmits more data to the ground station than when in polar orbit; in fact one order of magnitude more.

Once again it is interesting to look at the behaviour of the spacecraft's state variables, battery charge, memory level and internal temperature, during this mission. This is shown in Figures 6.21-6.24 where the state variables are first viewed in a three-dimensional state space and then projected in a two-dimensional state plane to facilitate the interpretation of the data. Again we can see that the spacecraft settles down to a limit cycle after an initial transient of a few orbits, due to the difference between the initial conditions and the nominal operating conditions. We can see how the two most critical state variables, battery charge and internal temperature, stay both well within the lethal limits during the mission and, again, never once is the spacecraft put into a situation which could lead to a permanent failure.

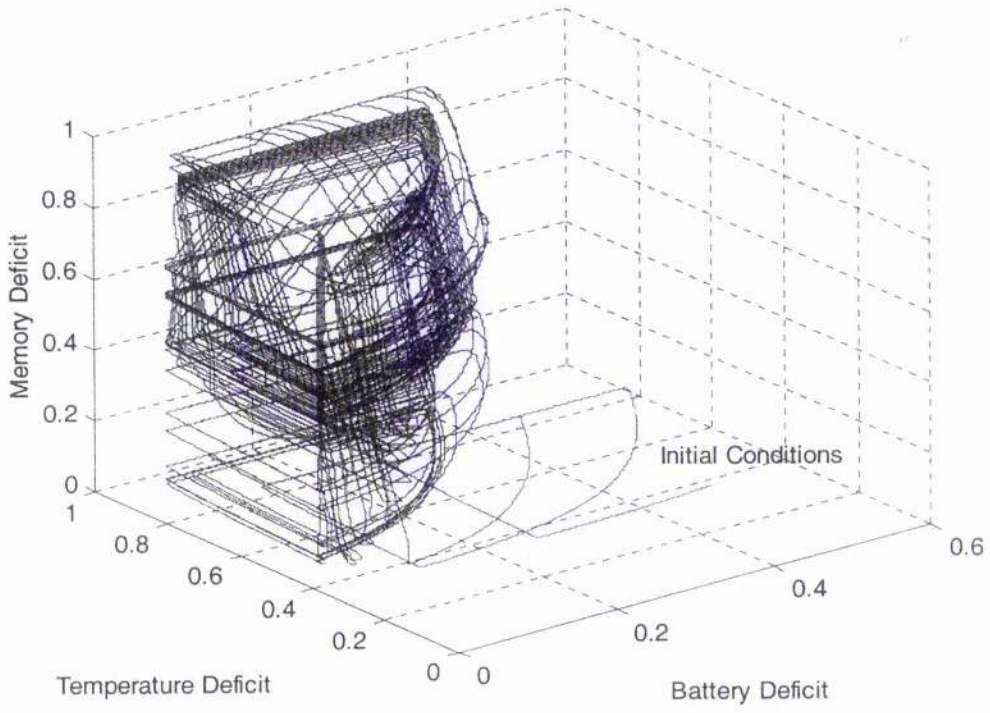

Figure 6.21 State variables deficits within state space (normalised variables)

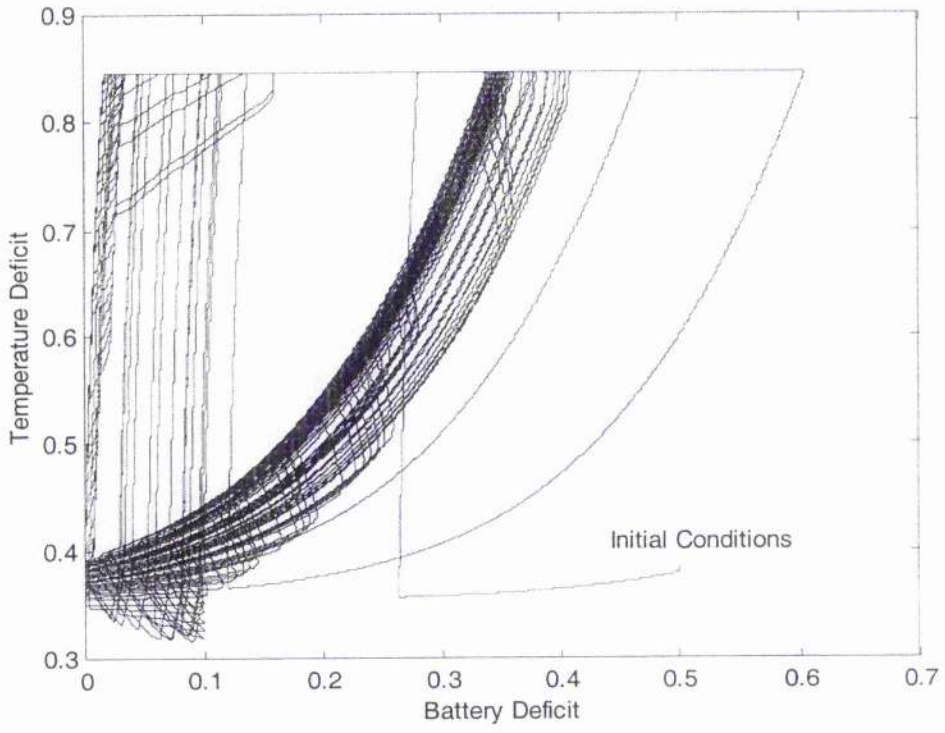

Figure 6.22 Battery and temperature deficits in state space (normalised variables)

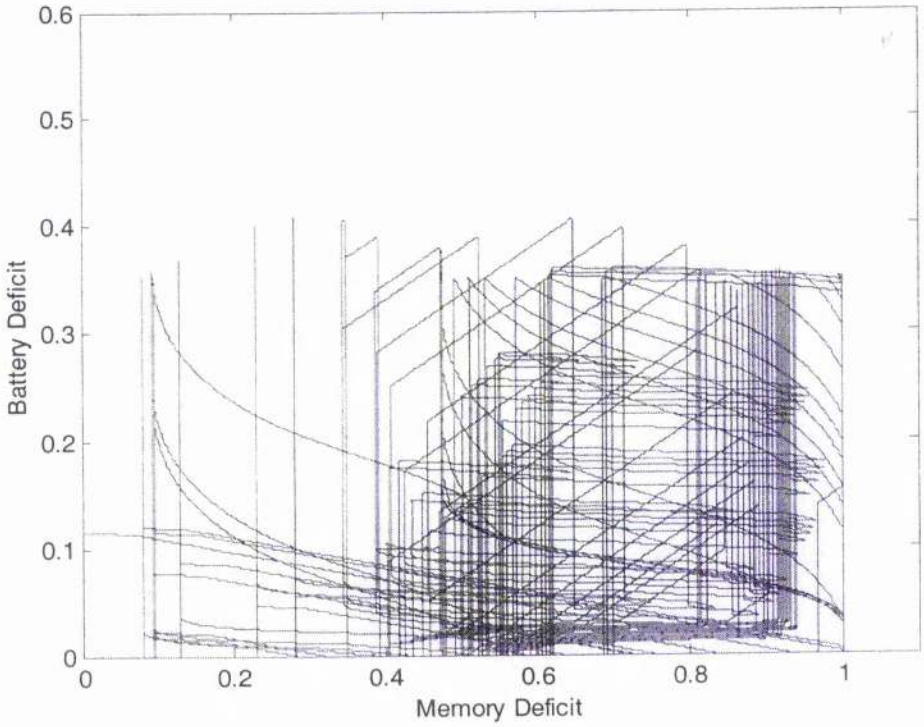

Figure 6.23 Memory and battery deficits in state space (normalised variables)

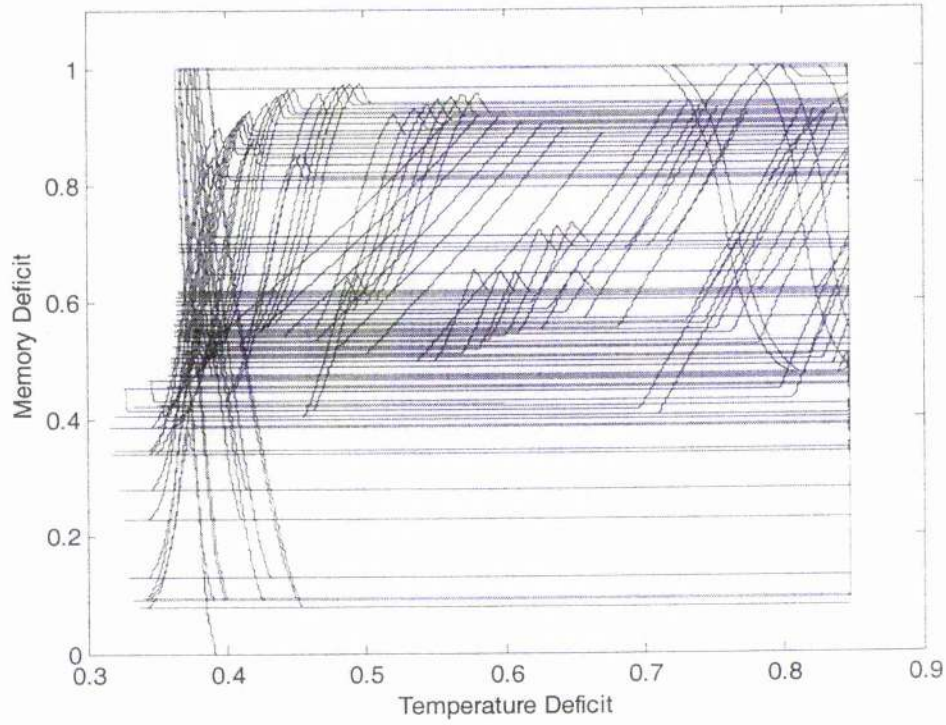

Figure 6.24 Temperature and memory deficits in state space (normalised variables)

6.3 OPPORTUNISM

As was shown in the previous section, the action selection algorithm manages the spacecraft tasks readily. It is in displaying opportunism however, that this algorithm has an advantage over a traditional controller, which simply selects tasks based on the most pressing need. In Figures 6.25-6.27 we can compare the deficits of the state variables with the spacecraft's cue-deficit products and behaviour. It can easily be seen that there are several instances in which the spacecraft does not select the behaviour associated with the highest deficit. This is because the action selection algorithm decides what to do, based not only on the deficit of the state variable, but also on the environmental cues associated with that particular behaviour. For example, if the spacecraft has a high transmit deficit and a lower charge deficit, it may still opt to charge the battery if sunlight is available and the visibility of the ground station is low. This is clearly an opportunistic behaviour. It should also be noted, in Figure 6.25, how the transmission deficit and the recording deficit are strictly coupled. Following the definition of the two deficits in Chapter 3, we can see that the evolution of one mirrors the other: as the recording deficit decreases, the transmission deficit increases by the same amount. As can be seen clearly from Figure 6.26, the *drk* products associated with the different behaviours depend from the environmental cues, and will be greater than zero only when a resource is present. In Figure 6.27 we can see how the spacecraft alternates between behaviours as it moves along its orbit. There are several points during the mission simulation in which none of the environmental resources – Sun, target and ground station – are present and therefore the spacecraft simply drifts without performing any behaviour.

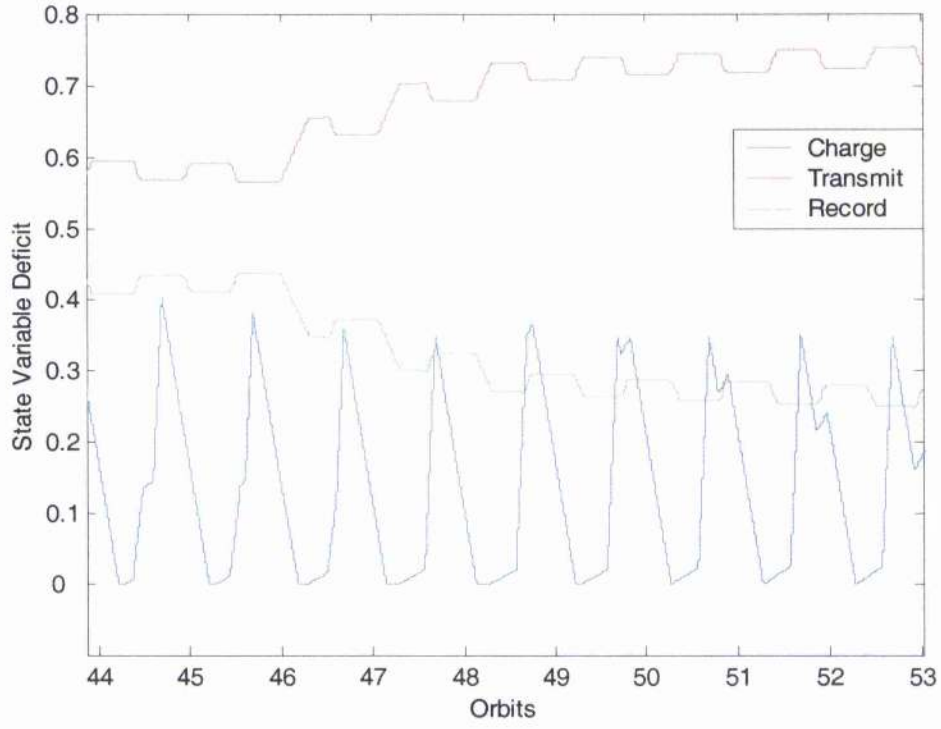

Figure 6.25 State variable deficits

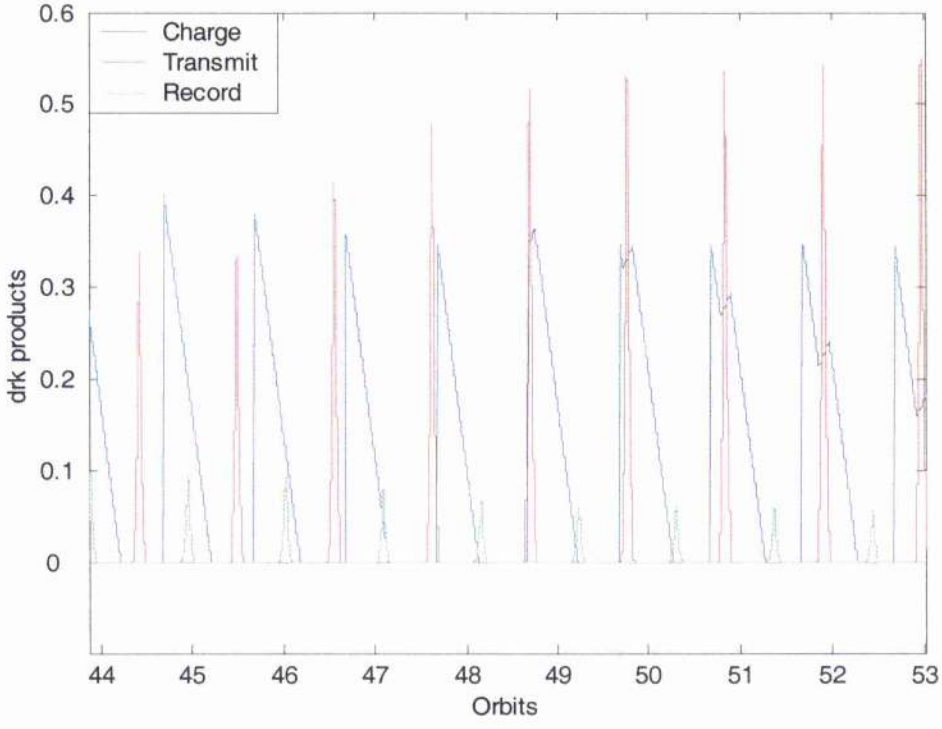

Figure 6.26 Behaviour *drk* products

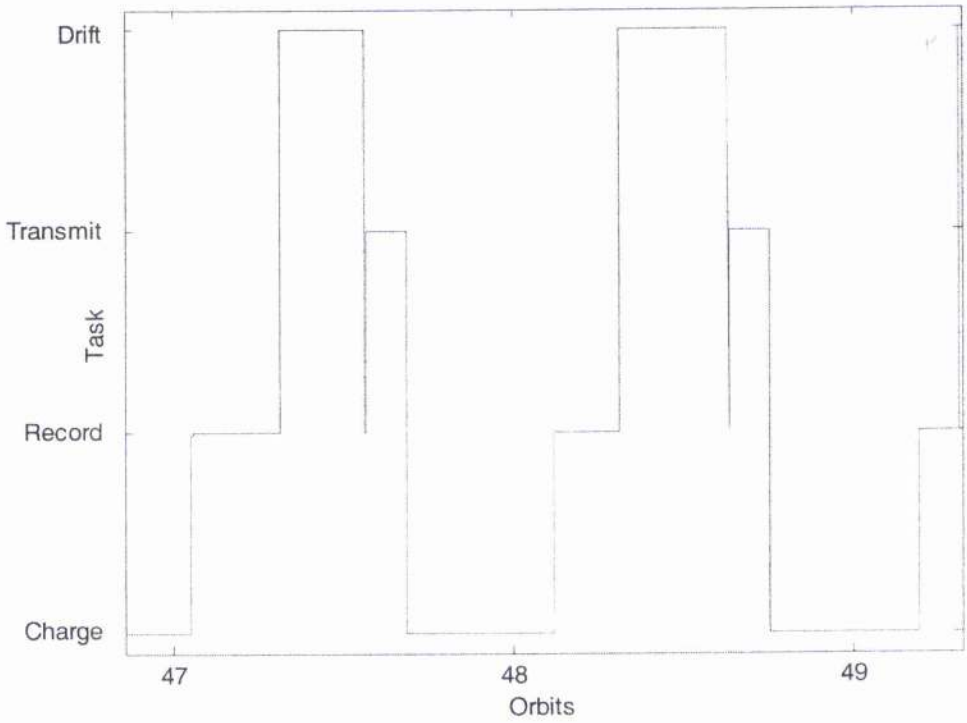

Figure 6.27 Spacecraft tasks

6.4 ATTITUDE CONTROL ALGORITHM

We will now evaluate the performance of the attitude control algorithm introduced in Chapter 4. As was explained in Chapter 5, once the spacecraft has determined where the environmental resource associated to a particular behaviour is, it has then to perform a slew to reach it. A potential field is generated as a function of the desired attitude angles necessary for the slew manoeuvre. Torques are then generated to slew the spacecraft to the desired orientation. We perform the analysis of the attitude control algorithm in the case of the equatorial case. The orbital, environmental and spacecraft parameters are listed in Tables 6.4-6.6. In the case of an equatorial orbiter, θ_1 will be the more solicited attitude angle as it relates to the East-

West orientation of the spacecraft. In the case of a polar orbit θ_3 will be the more solicited attitude angle as it is related to the North-South orientation of the spacecraft. As explained previously, the spacecraft has to rapidly change attitude to track the ground station, the target and the Sun. The required attitude orientation for ground station and target tracking are given by the pointing algorithm introduced in Chapter 5. To track the Sun the required attitude angles are $\theta_1 = \theta_3 = 0°$ since the Sun is assumed to be fixed along the X inertial axis. In Figures 6.28 and 6.29 we can see the results for such a simulation. In Figure 6.28 we see how the control algorithm forces θ_1 to follow the desired attitude necessary for target tracking. As the spacecraft flies over the target the spacecraft maintains its pointing towards it. Once the target is out of view, the control algorithm changes the spacecraft attitude to track the Sun. In Figure 6.29 we see how the control algorithm forces θ_1 to follow the desired attitude necessary for ground station tracking. As the spacecraft flies over the ground station the spacecraft maintains its pointing towards it. Once the ground station is out of view, the control algorithm changes the spacecraft attitude to track the Sun. It can easily be seen therefore, how the control algorithm, introduced in Chapter 4, guides the spacecraft to successfully follow the desired orientation to track the Sun, target and ground station.

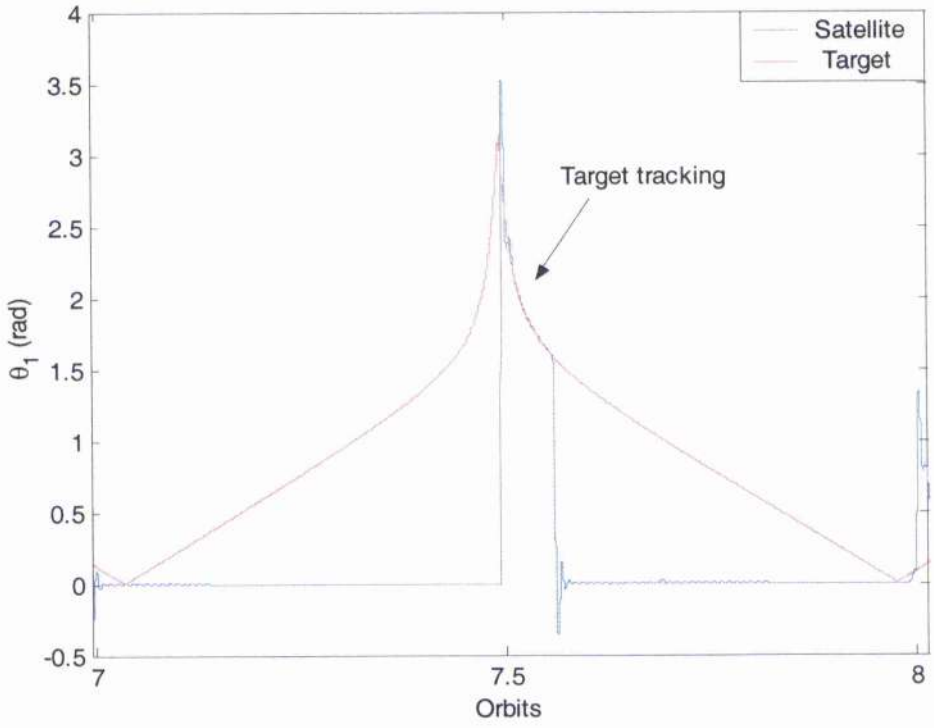

Figure 6.28 Evolution of the pitch angle (target tracking)

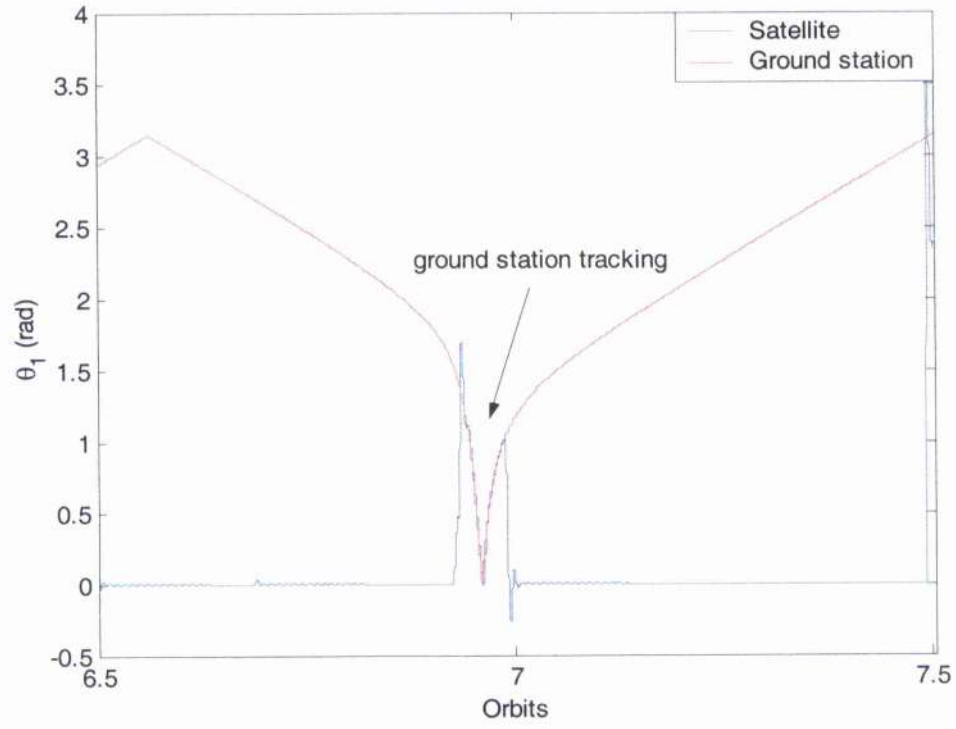

Figure 6.29 Evolution of the pitch angle (ground station tracking)

In Figures 6.30 and 6.31 we can see the evolution of the angular velocity and the control torques for the spacecraft. When the spacecraft has to slew between different targets, the control algorithm commands the torques that have to be applied to reach the desired attitude by following Equation 4.18. As the reaction wheels produce the required torques, the spacecraft at rest, increases its angular velocity. When the final attitude is reached the spacecraft is set back at rest, until another target slew has to be performed. In Figures 6.32 and 6.33 we can see how the potential and potential derivative vary during the spacecraft mission. As a new target has to be reached and a potential field generated, the control algorithm forces the spacecraft towards the desired attitude. As the spacecraft is moving towards the goal attitude, the potential decreases until it reaches zero when the desired attitude has been attained. Finally it should be noted that the potential derivative is always negative, thus satisfying the conditions laid down by Lyapunov's Second Method.

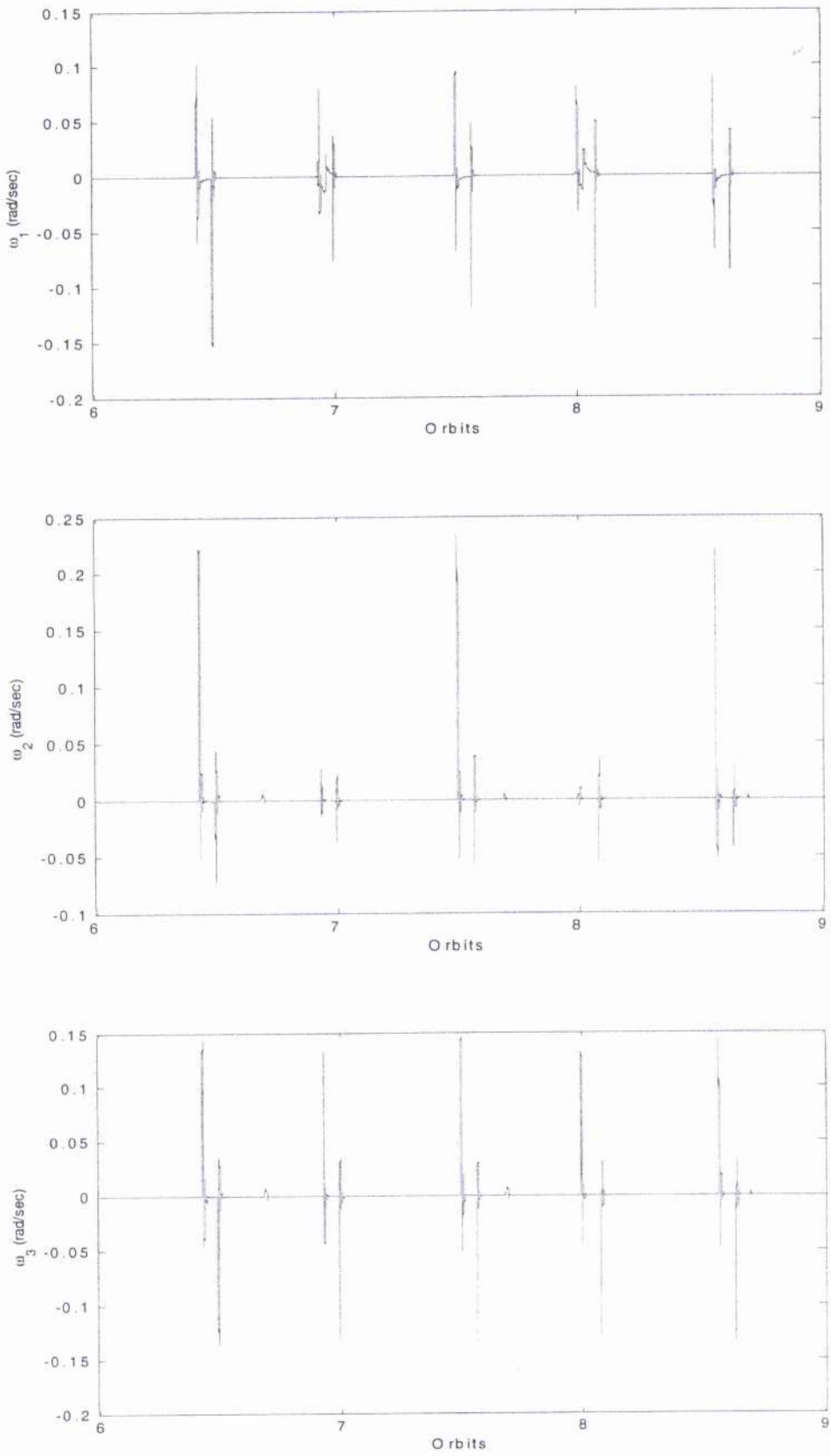

Figure 6.30 Evolution of spacecraft angular velocity components

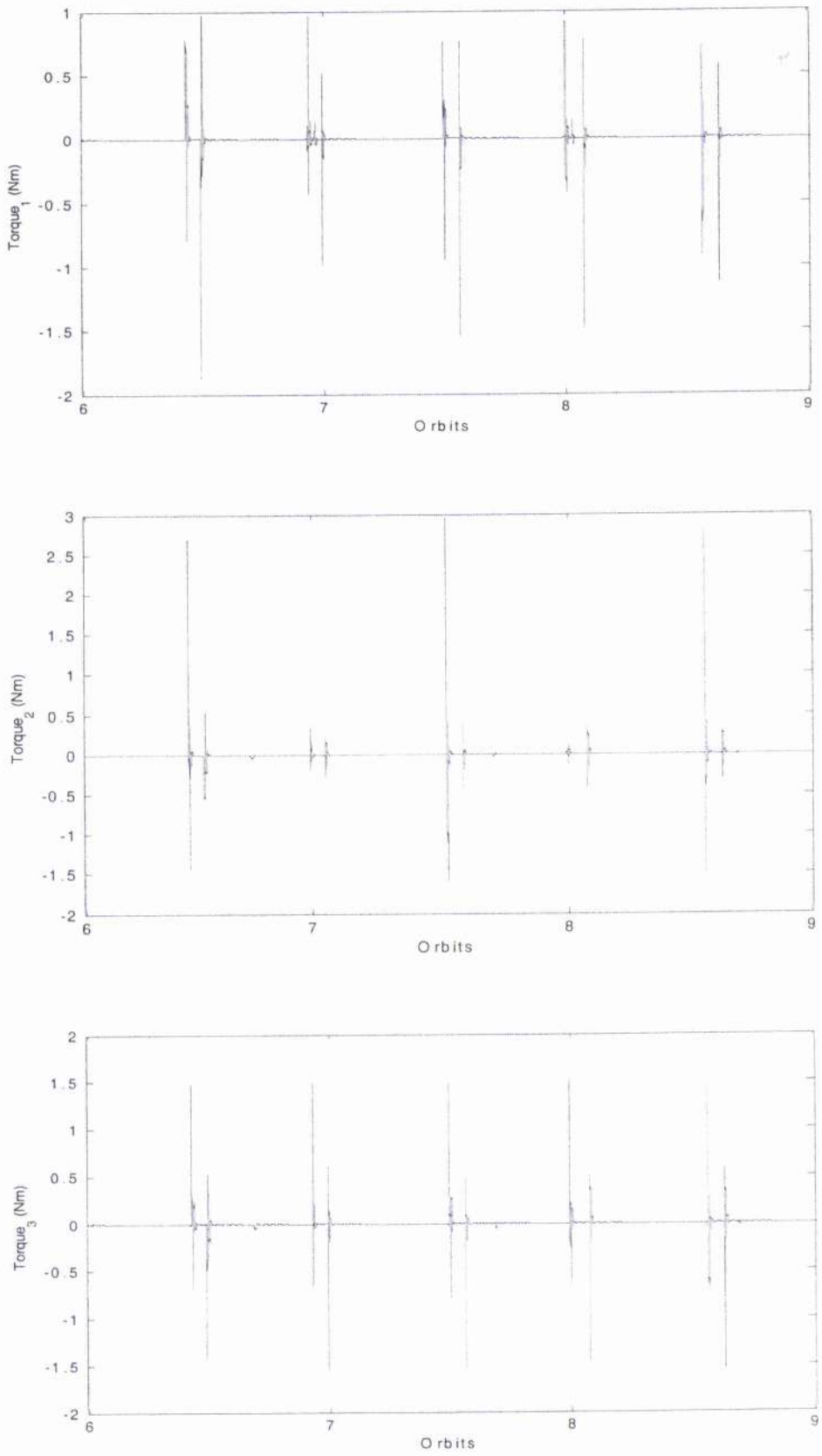

Figure 6.31 Evolution of spacecraft control torques

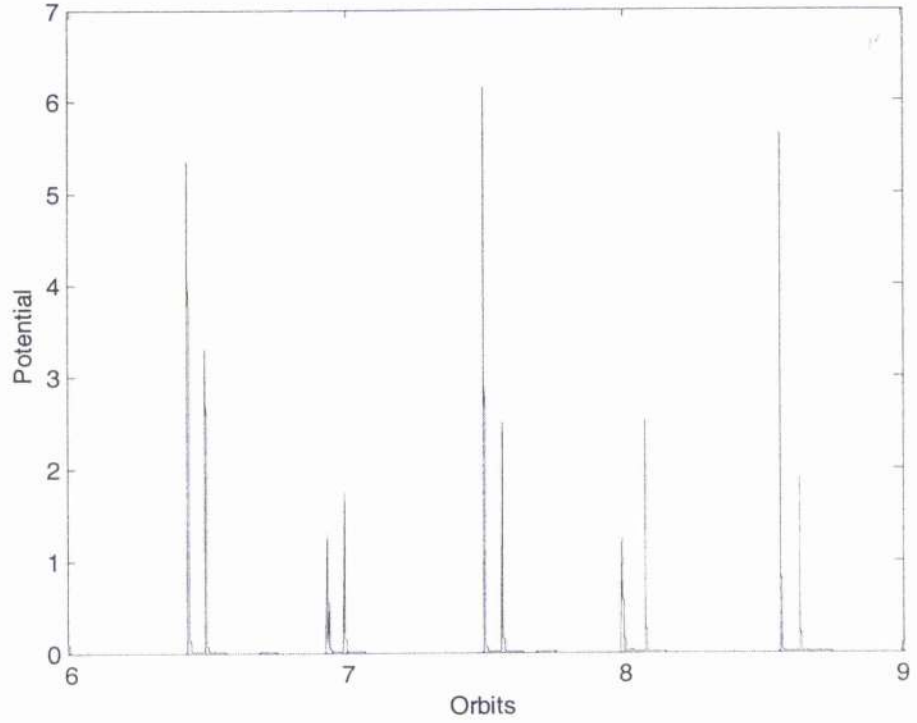

Figure 6.32 Evolution of potential

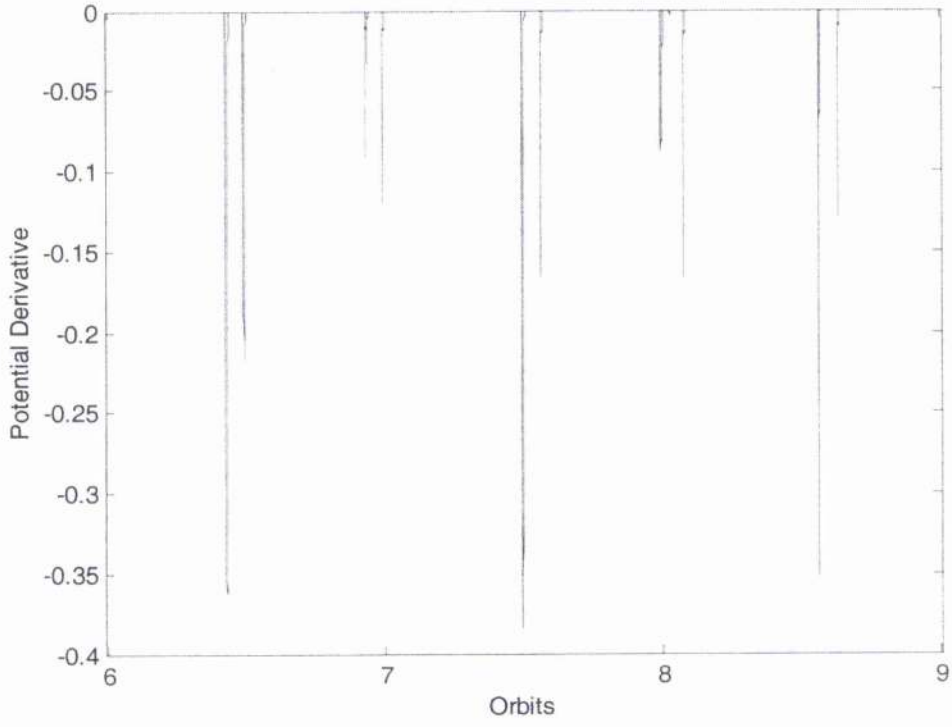

Figure 6.33 Evolution of potential derivative

6.5 ENERGY MANAGEMENT

It is interesting to note how the spacecraft manages its internal energy available through the battery, and the external energy available through the Sun and solar array during its mission, shown in Figure 6.34. The spacecraft has a steady load of 0.2 Watts, which is used to power all the on-board sensors, subsystems and central processing unit (CPU) that have to always be operational. As the spacecraft alternates between behaviours, such as recording or downloading data, the consumed power increases as either the camera or the transmitter are active. There is also a power demand from the attitude control subsystem as the spacecraft has to activate the reaction wheels to slew between targets. It is interesting to note that, as expected, the highest power consumption occurs when the spacecraft is in eclipse. During this phase of the orbit the temperature decreases to the lower temperature threshold value, which then activates the heater. The heater is therefore turned on to maintain the internal temperature above the lower lethal value and the power consumption increases greatly, reaching 10 Watts. As the spacecraft moves out of eclipse, and returns to sunlight, the internal temperature increases, the heater is switched off and the consumed power drastically decreases. During the sunlit portion of the orbit the solar panels produce a steady power of 8 Watts, which is used to power the spacecraft and recharge the battery, drained during the eclipse.

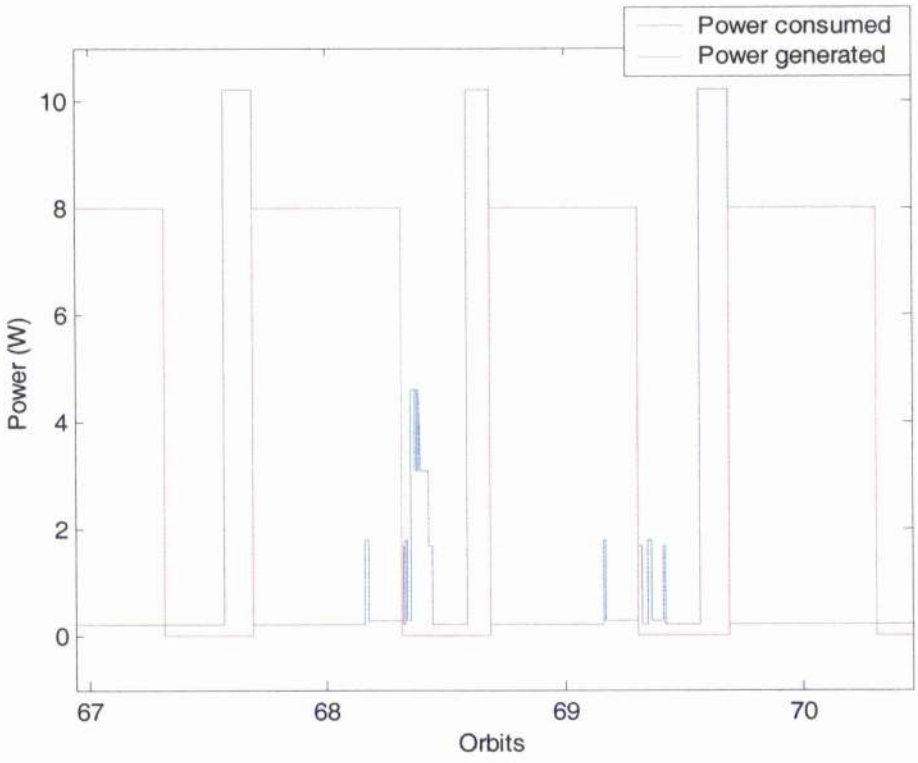

Figure 6.34 Energy management

6.6 HARDWARE FAILURES

To test the robustness of the action selection algorithm, the spacecraft is subjected to non-critical hardware failures. The failure of the solar array, the transmitter and the payload are investigated. It will be shown that the spacecraft successfully reschedules its tasks to account for the degraded performance of the solar panel, transmitter or payload. A failure of the Sun sensor or global positioning system (GPS) would be far more critical as the spacecraft would not receive any cues as to the presence of the environmental resources. If such a failure would occur the spacecraft would not be able to continue its operation autonomously.

6.6.1 Solar Panel Failure

Results for a simulation where 50% of the solar panel fails during a mission are shown in Figure 6.35. The array fails after 30 of the 70 orbit mission simulation. This failure means that the accessibility associated with the charging behaviour is reduced from 1 to 0.5. This decrease will obviously influence the action selection algorithm in the form of the *drk* product associated with the charging behaviour. A partial damage to the solar panel also implies a reduction in the amount of power that the solar array can produce, decreasing from 8 Watts to 4 Watts. The battery charge settles into a periodic pattern after a few orbits, and the spacecraft starts recording data, and after approximately 4 orbits, downloading data. Following the solar array failure, after an initial transient due to the new operational conditions, the battery charge settles down to another periodic pattern, which has a slightly lower average charge, but nonetheless ensures the spacecraft's survivability. It can be seen that this failure does not compromise the mission as the spacecraft continues recording and downloading data. In fact, we can see that there is not a big difference when comparing the data handling before and after the solar array failure. It is therefore shown that the spacecraft successfully reschedules its tasks to account for the reduced capabilities of the solar panel.

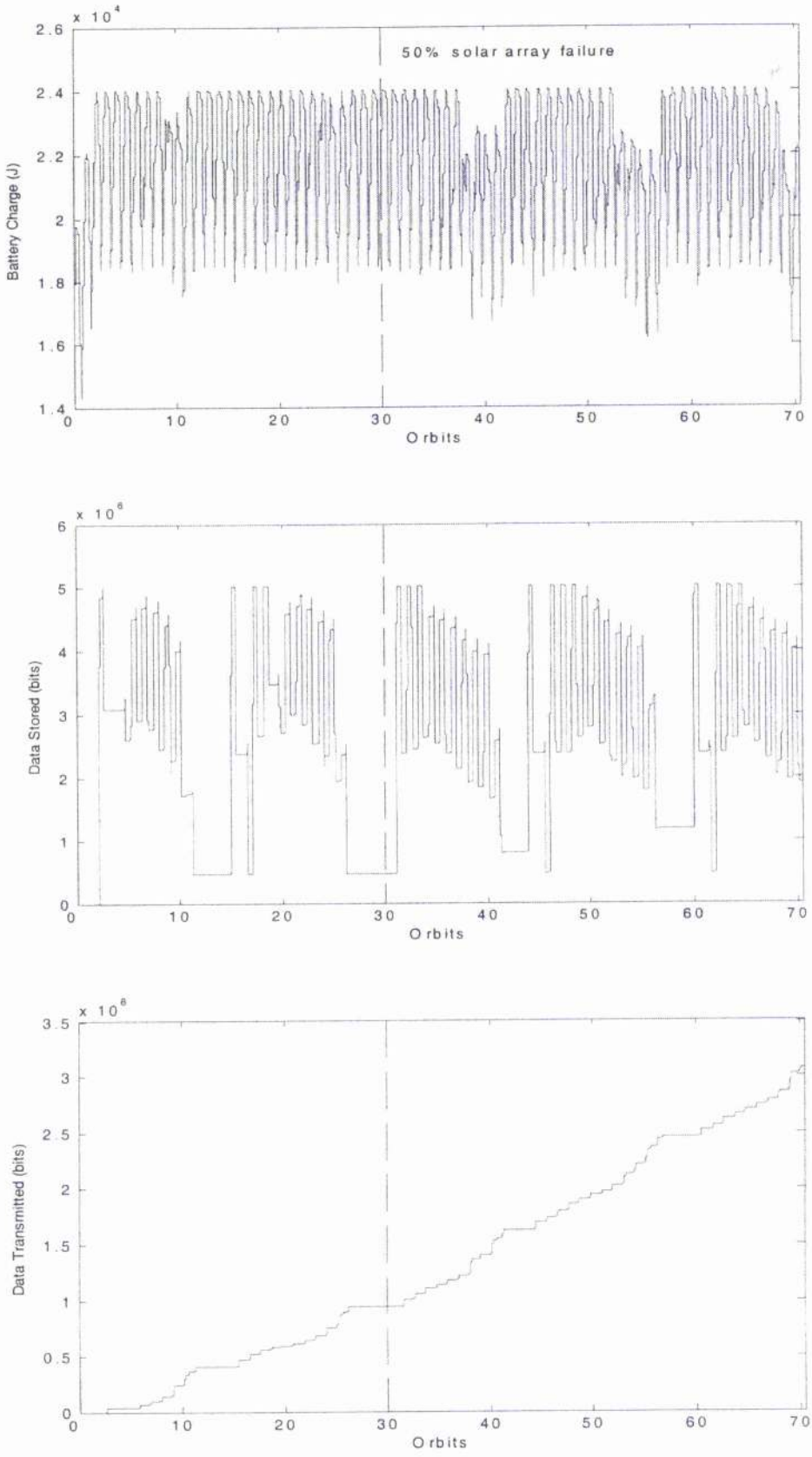

Figure 6.35 Spacecraft performance during partial solar panel failure

6.6.2 Payload Failure

Results for a simulation where 50% of the payload capacity fails during a mission are shown in Figure 6.36. The payload fails after 30 of the 70 orbit mission simulation. This failure means that the accessibility associated with the recording behaviour is reduced from 1 to 0.5. This decrease will obviously influence the action selection algorithm in the form of the *drk* product associated with the recording behaviour. A partial damage to the payload camera also implies a reduction in the amount of data that is recorded, decreasing from 5000 bits to 2500 bits. It can be seen that the amount of data stored increases far less rapidly after the payload failure as the reduced accessibility affects the *drk* product associated with this behaviour. As was shown in the section 6.3, the recording deficit is coupled with the transmission deficit, therefore a reduced payload activity implies a reduced transmitter activity. This is because, if data is stored at a low rate, due to a payload failure, the transmission deficit will grow slowly. It can be seen that less data is stored after the failure and as a consequence less data is transmitted back to the ground station. Nevertheless the spacecraft successfully reschedules its tasks to account for the reduced capabilities of the payload.

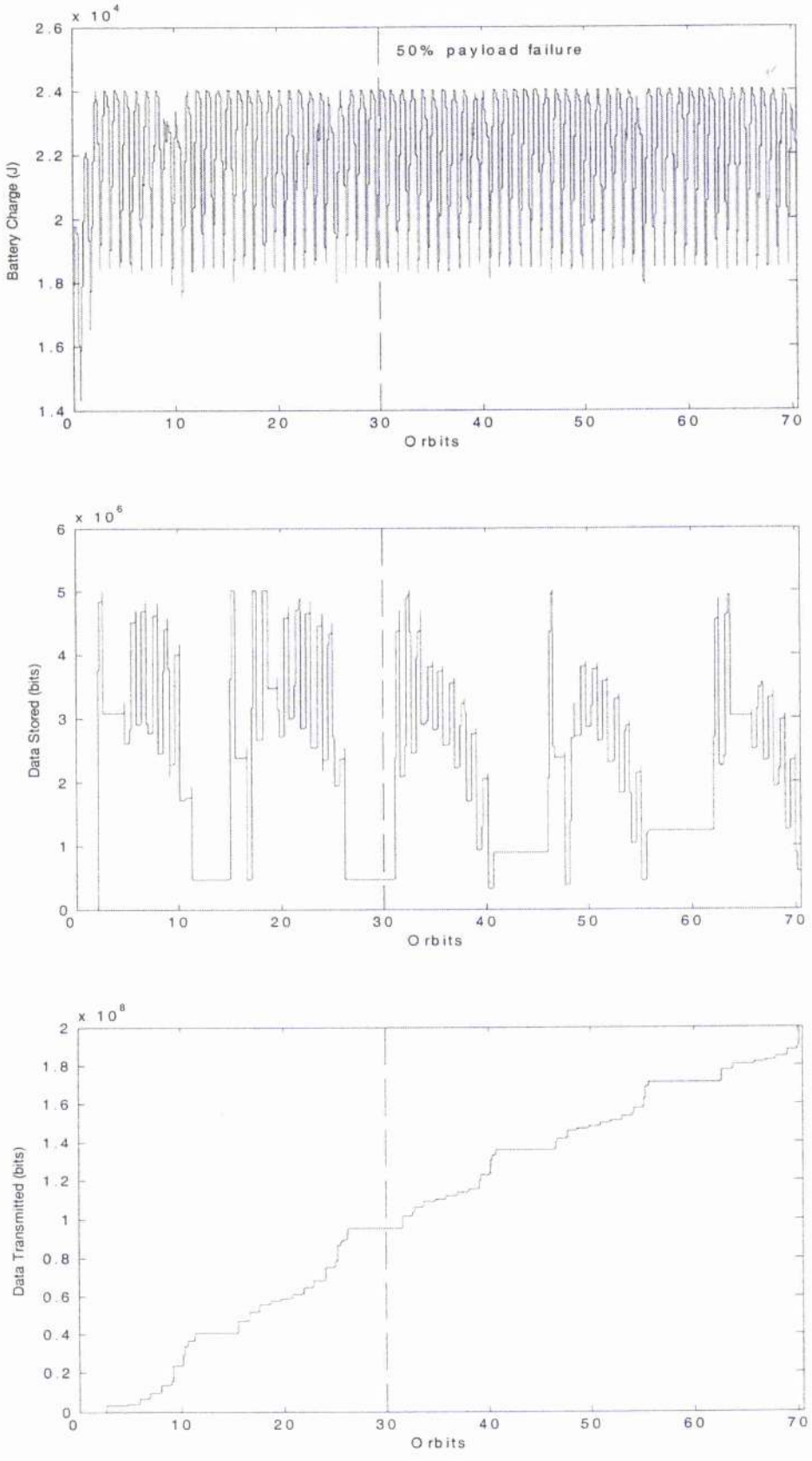

Figure 6.36 Spacecraft performance during partial payload failure

6.6.3 Transmitter Failure

Results for a simulation where 50% of the transmitter capacity fails during a mission are shown in Figure 6.37. The transmitter fails after 30 of the 70 orbit mission simulation. This failure means that the accessibility associated with the transmitting behaviour is reduced from 1 to 0.5. This decrease will obviously influence the action selection algorithm in the form of the *drk* product associated with the transmitting behaviour. A partial damage to the transmitter also implies a reduction in the amount of data that is downloaded to the ground station, decreasing from 10,000 bits to 5000 bits. Once again we can see the coupling that exists between the recording and transmitting behaviours. As less data is downloaded to the ground station because of the reduced transmitter capabilities, the memory storage decreases less rapidly than before the failure. This means that the deficit associated with the recording behaviour decreases more slowly than before, and therefore to account for this, less data can be acquired and stored. It is shown however that once again the spacecraft successfully reschedules its tasks to account for the reduced capabilities of the transmitter.

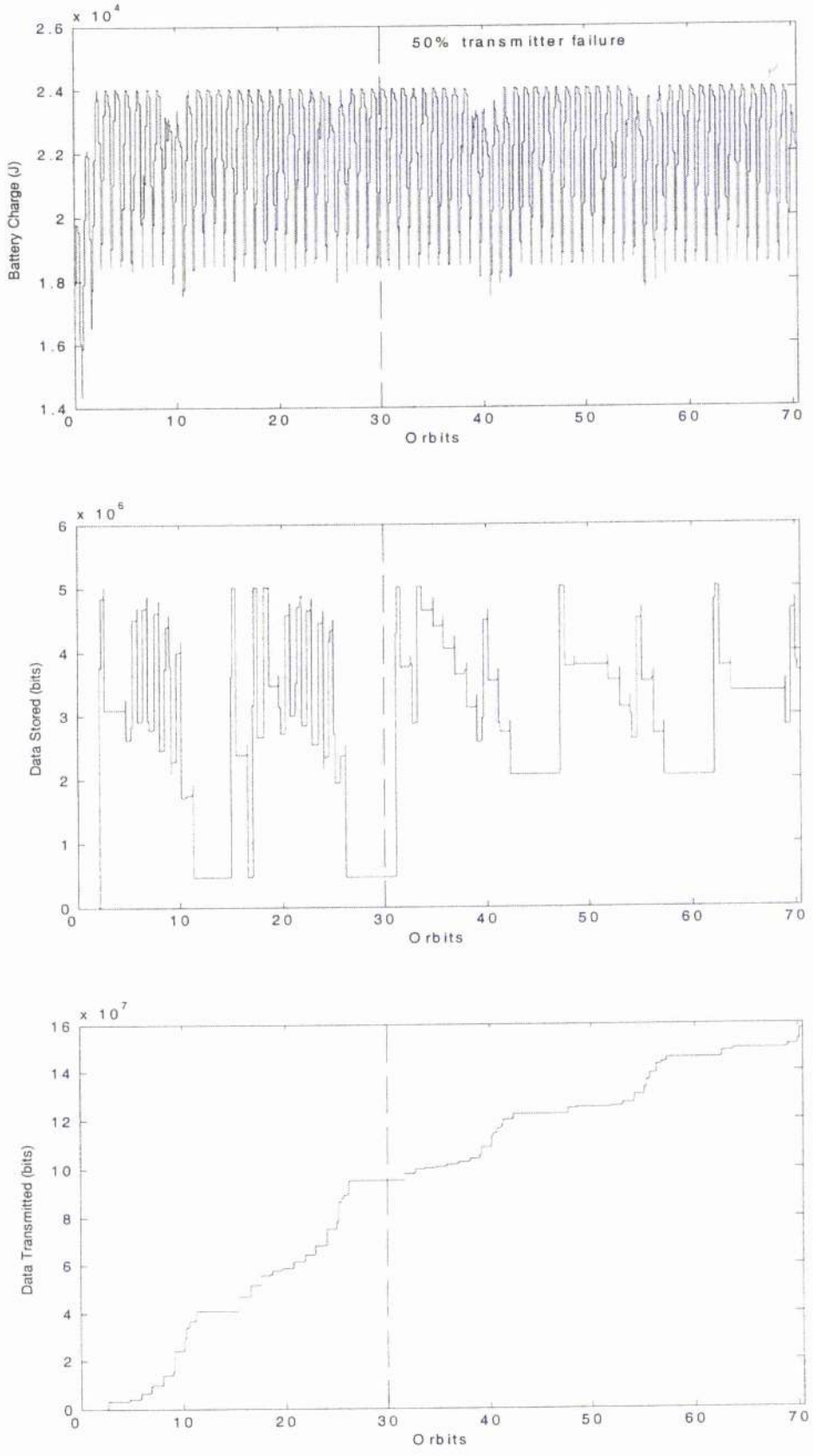

Figure 6.37 Spacecraft performance during transmitter failure

6.7 COST FUNCTION ANALYSIS

As was explained in Chapter 3, the choice of a particular cost function has the potential for modifying the overall performance of the artificial autonomous agent. This is due to the relationship between the cost function and the deficit of a resource. The deficit is defined as the partial derivative of the cost function with respect to that particular resource, as shown in Equation 3.30. Our aim is now to understand if the satellite exhibits different overall performances depending on the type of cost function associated to its state space [Radice et al. 2000]. We will now choose four quadratic cost functions to determine which one provides the best performance. The best spacecraft performance is defined here as the amount of data received by the ground station while not placing itself in an irrecoverable position. We will compare a normal quadratic cost function with other cost functions that emphasize either the energy aspect or the work aspect of the spacecraft. As we explained in Chapter 3, work is defined as data handling, either recording or transmitting information, while energy is defined as battery charging. The cost functions are defined as:

$$\begin{aligned} C_1 &= b^2 + m^2 + t^2 \\ C_2 &= \alpha b^2 + m^2 + t^2 \\ C_3 &= b^2 + \beta_1 (m^2 + t^2) \\ C_4 &= b^2 + \beta_2 (m^2 + t^2) \end{aligned} \qquad [6.1]$$

where α, β_1 and β_2 are scaling factors inserted in the cost function equation to increase the weight of energy and work respectively. The values chosen for the scaling factors are the following: $\alpha = \beta_1 = 10$ and $\beta_2 = 50$. In Figure 6.38 we can see the result of a 70 orbit simulation. The spacecraft, environmental and orbital

parameters are listed in Tables 6.4-6.6. It can easily be seen that the cost function C_2, which emphasises energy acquisition provides the worst spacecraft performance. This is because almost any time the spacecraft is in sunlight, it will slew towards the Sun and charge the battery, even if target or ground station may be present for data recording or download. The quadratic cost function C_1, provides a good performance averaging the battery charging with data handling, reaching a spacecraft performance one order of magnitude greater than C_2. It is however with the work cost functions, C_3 and C_4, that we obtain the best spacecraft performances. In this case the spacecraft will, almost always, record and transmit data when flying over the target or ground station. Almost twice the volume of data is transmitted with a work cost function than with the normal cost function.

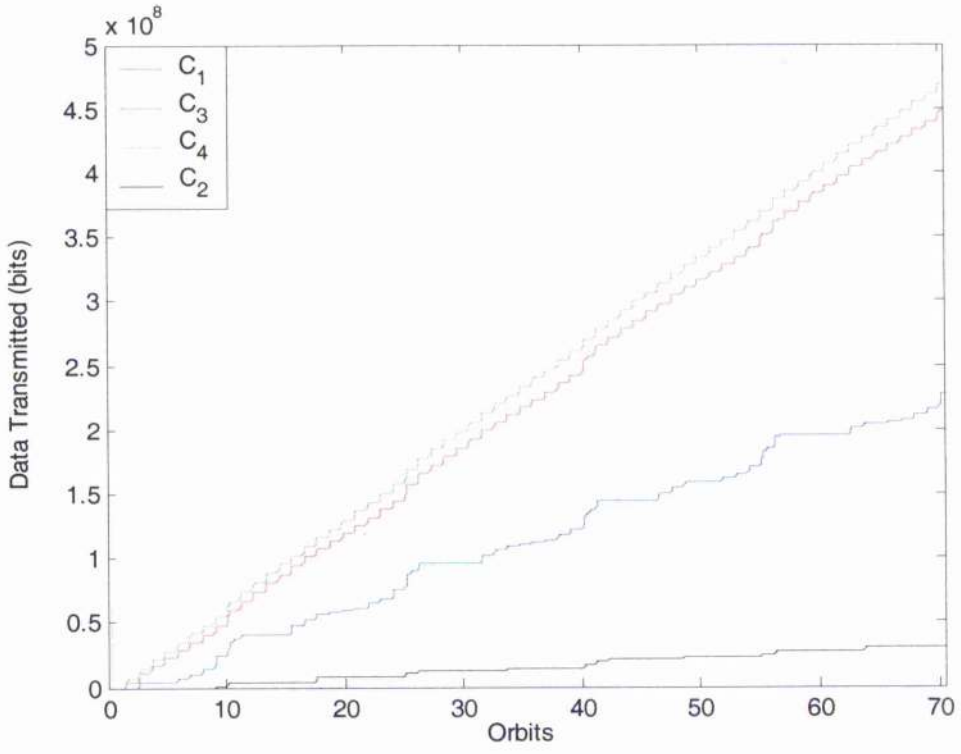

Figure 6.38 Cost function comparison

6.8 CONCLUSIONS

An innovative and appealing method for spacecraft task selection, introduced in Chapters 3, 4 and 5, has been here tested to assess its performance. It was shown that the action selection algorithm successfully sequences tasks to achieve both, mission goals and spacecraft survival. The differences in performance between a spacecraft in a polar orbit and an equatorial orbit were investigated. It was also shown that this particular behavioural algorithm displays a degree of opportunism that is difficult, if not impossible, to code into traditional controllers. The performance of the attitude control algorithm was assessed and found to be good as the spacecraft is slewed between objectives to track the target, ground station or Sun. To test the robustness of the action selection algorithm, the spacecraft was subjected to non-critical hardware failures. It was shown that the spacecraft successfully reschedules its tasks to account for the degraded performances of the solar array, payload or transmitter. Finally an investigation of how the choice of the cost function affects the spacecraft performance was carried out, and an optimum work-based cost function explored.

CHAPTER VII

CLUSTERED SPACECRAFT

7.1 PREFACE

In this chapter we will be considering a cooperating spacecraft constellation. We will at first try and understand why there is cooperation in biological systems and then identify the conditions under which autonomous agents may benefit from cooperation. This will be then used to extend the concept of a single spacecraft introduced in Chapter 6 to a cluster of cooperating spacecraft.

7.2 INTRODUCTION

The fact that a highly autonomous agent, capable of functioning in a changing environment has still to be created has led artificial intelligence researchers to propose the organization of several simpler robots into collections of cooperating populations [Jung 1995]. It has been hypothesised that systems of multiple autonomous agents should prove more efficient and more fault tolerant due to their number, more cost effective due to their individual relative simplicity and more flexible in their working configurations due to their redundancy, than a single more complex agent [Taipale and Shigeoki 1992]. The concept of cooperation has been the

subject of countless philosophical ponderings. Cooperative behaviour, in one form or another, has been investigated by many brilliant individuals in the fields of economics, anthropology, psychology, evolutionary biology and more recently robotics. It is however important to understand that 'cooperation' is a word, something which helps define a human concept. In this case, the concept refers to a category of human, animal and also artificial agent behaviour. It does not follow that this behaviour is necessarily beneficial to the people, animals or artificial agents involved. As we shall see later, animal and human cooperative behaviour is a conglomerate of various behavioural tendencies selected for different reasons. However, since the design of cooperative autonomous agents is in a different context, we would like to understand why humans and animals cooperate so that we can determine if the same principles and benefits apply to autonomous artificial agents.

7.3 COOPERATION IN BIOLOGICAL SYSTEMS

The theory of biological evolution is based on the concept of survival of the fittest [Darwin 1859]. Darwin's theory of natural selection implies that individuals behave in a completely selfish manner to increase their own fitness, yet cooperation is common between members of the same species and even members of different species. Therefore, the question of why do biological organisms cooperate arises. Darwin resolved this paradox by outlining inclusive fitness theory more than 100 years before Hamilton [Hamilton 1963]. He recognised that, if natural selection operated at colony or group level, then many features of the individuals, including their cooperative behaviour and altruistic tendencies were readily understandable.

The emotions that have evolved to support cooperation between mates, siblings and other kin, have, thus far, a genetic basis. These do not explain why humans and animals are altruistic towards and cooperate with individuals with whom they are unrelated. The process by which altruistic relationships arise between unrelated individuals is called reciprocal altruism [Trivers 1971]. There are, however, a number of prerequisites to be met before an evolutionary stable strategy will arise. The cost of an altruistic act must be low in relation to the received benefit. Individuals must be able to recognise each other as individuals and be capable of keeping track of their history in previous dealings, including detecting cheaters. In addition, stable groups are required for the same individuals to encounter each other repeatedly in situations that present opportunities for altruistic acts. When these prerequisites are met, individuals can cooperate following the tit-for-tat strategy [Axelrod 1984].

Primate societies, including humans, are based on a dominance hierarchy. The individuals who are at the top of the hierarchy are commanding the greatest resources, such as access to females, power over other individuals, food and protection. With the advent of language, one of the most important resources became information. Two individuals can profit by forming a relationship based on reciprocal altruism, an alliance or friendship. This provides the opportunity to barter these resources, and information, for mutual benefit. The strength of the alliance, or the willingness to cooperate, is based on the amount of trust between the individuals involved. The type of relationship requires that individuals can uniquely identify each other and remember past dealings.

7.3.1 Cellular Cooperation

Cooperation between simple organisms on Earth is almost as old as life. Biologists have long understood that bacteria live in colonies, but only recently has it become evident that most bacteria communicate using a number of sophisticated chemical signals and engage in altruistic behaviour [Kaiser and Losic 1993]. The chemical signals only have a meaning when interpreted in the behavioural context. The resulting cooperative behaviour is an emergent consequence of the behaviour policy indirectly genetically encoded in each individual. Multi-cellular organisms, such as insect and animals, are also a common example of cellular cooperation. In this case however, the cells cooperate not just by taking on specialised behaviour in particular circumstances, but also by having evolved differentiated forms. The key issue is that communicated signals have no intrinsic meaning; they have a meaning when interpreted. Therefore a signal may have two possible meanings, one according to the 'speaker' and one according to the 'listener', and they may not be the same. Only when the signal is interpreted correctly, will there be efficient cooperation.

7.3.2 Social Insects Societies

The idea of the social insect colony as a superorganism can be dated back to the end of the 19th century [Weismann 1893]. Of the social insect societies the most thoroughly studied are those of ants, bees, termites and wasps [Wilson 1971, Wilson 1975, Crespi and Choe 1997]. Much of what has been learned has been applied to robotics [Srinivasan et al., 1997]. Ants display a large array of cooperative behaviours, only some of which will be described. Just like bacteria, ants use

interaction with the environment to implement cooperative foraging. Upon describing a new food source, a worker ant leaves a pheromone trail during its return to the nest [Pasteels et al., 1987]. Recruited ants will follow this trail to the food source with some variation while laying their own pheromones down. Any variations that result in a shorter trail to the food will be reinforced at a slightly faster rate, as the time back and forth is less. Therefore, it has been shown that a near optimal shortest patch is quickly established as an emergent consequence of simple trail following with random variation.

7.3.3 Primate Cooperation

Primates, just as other animals, use interaction via the environment, interaction via sensing and interaction via communication during cooperation. What distinguishes primates from other animals is their sophistication in learning and representing internal goals, plans, dispositions and intentions of others and their ability to construct collaborative plans jointly [Bond 1996]. All primates, humans included, obviously, have the ability to co-construct joint plans with one or more interacting individuals, and flexibly adapt and repair them in real time. In this case the agent must adjust its action selection based on the evolution of the ongoing interaction. In order to achieve interlocking coordination each action may be conditional on the situation, including the successful completion of appropriate actions by collaborators. Each agent attempts different plans, assesses the actions, plans and goals of others, and alters the selection of its own actions and goal to achieve a more coordinated interaction where joint goals are satisfied. Perceived actions and intentions of other primates are obtained by visual and auditory cues. This

provides a communication channel through which joint action can be sought, established and controlled. In the case of non-human primates, much of this comprises passive observation of collaborators. Humans however, make heavy use of explicit communication, and communicative acts can be considered behavioural actions just as much as physical acts.

7.4 COOPERATION IN ARTIFICIAL MULTI AGENT SYSTEMS

We have seen that the three main reasons why animals and humans cooperate are to secure reproductive opportunities [Maynard Smith 1978, Halliday 1994], to promote genes shared with kin [Hamilton 1964, Dawkins 1996] and to barter resources for mutual benefit [Trivers 1971, Axelrod 1984]. Unless artificial agents are endowed with some sort of biological-like reproductive mechanisms, it is unlikely that they will find the first two reasons beneficial. On the other hand, artificial agents can benefit from displaying reciprocal altruism towards each other. So how can we use the lessons learnt from cooperation in biological systems, and apply them to artificial autonomous agent?

We will start by following Franklin's typology of cooperation, shown in Figure 7.1, placing it in the context of multi agent systems and then defining specific types of cooperation [Franklin et al. 1996].

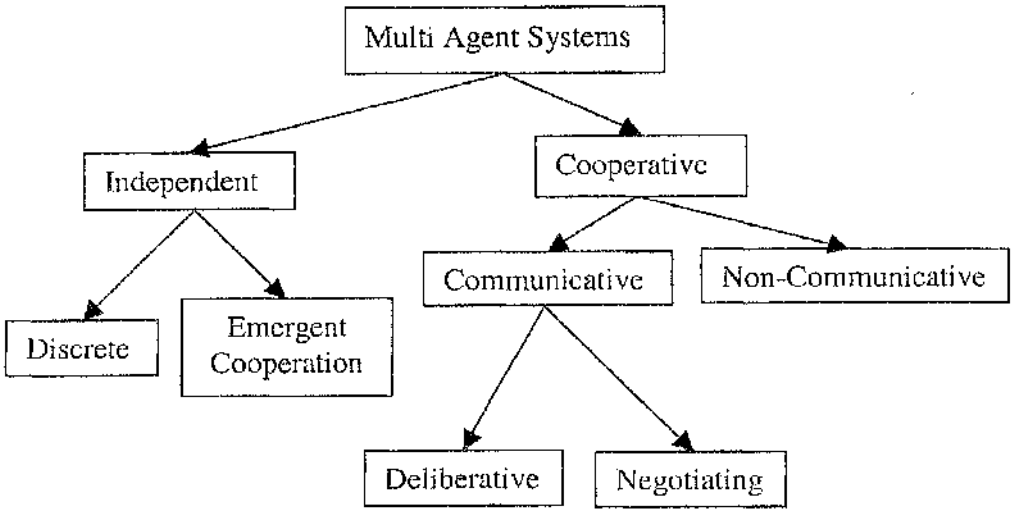

Figure 7.1 Cooperation Typology

A multi-agent system is independent if each agent pursues its own agenda independently from others. A multi-agent system is discrete if it is independent, and if the agendas of the agents bear no relation to one another [Franklin and Graesser 1997]. Discrete systems involve no cooperation. However, agents can cooperate with no intention of doing so. The spacecraft constellation, which will be introduced later, forms an independent system, each following the agenda of recording and downloading data [Radice et al. 1998]. A balanced memory load among the constellation is an emergent behaviour of the system in that, from the observer's point of view, the spacecraft appear to be working together, but from the spacecraft's viewpoint they are not. They are simply carrying out their own individual behaviour. The complement of independent systems are systems in which the agendas of the agents include cooperating with other agents in the system in some way: cooperative systems. Such communication can either be communicative, in that some agents communicate, through the intentional sending and receiving of signals with each other in order to cooperate, or it can be non-communicative. In the latter case, agents coordinate their cooperative activity by each observing and reacting to the behaviour

of others. Intentional communication can take at least two forms: agents can deliberate or they can negotiate. In deliberative systems agents jointly plan their actions so as to cooperate with each other. Negotiating systems are similar to deliberative systems, but have an added aspect of competition.

We have seen how layering arises in biological systems due to the way evolution functions, and noted that some of the same benefits can be had in artificial autonomous agents. The lowest layer will use interaction via the environment, with no explicit communication so that the spacecraft perform their tasks unaware of any neighbour. However, we saw that awareness can increase cooperative task performance, and this will be achieved by a second layer which uses interaction via sensing: the spacecraft will be aware of the presence of one or more neighbouring satellites through some appropriate Inter-Satellite-Link. By using interaction by communication in the third layer, performance can be further enhanced. In this case, the spacecraft will be aware of a neighbouring spacecraft's state and use this information proficiently.

7.5 SELF-ORGANISING SPACECRAFT CONSTELLATION

Self-organisation has three important characteristics. First, a self-organising system can accomplish complex tasks with little and simple behaviour. Secondly, a change in the environment may influence the same system to generate a different task without any change in the behavioural characteristics. Finally, any small differences in individual behaviour can influence the collective behaviour of the system. Therefore, complexity of a system is compatible with simple and identical

individuals, as long as communication among the members can provide the necessary amplifying mechanism. What makes a self-organising system advantageous is the fact that it is based on individual agents requiring simple programming and communication. This collective behaviour will have an "adaptive" character. Such a system is therefore simple, reliable and adaptive, with only a few basic rules needed to define individual behaviour and interactions. Furthermore, the breakdown of one agent will not affect the whole group. A single satellite can provide only partial coverage of the planet it is orbiting. To obtain the global coverage for remote sensing needed in many future planetary missions there is the need to deliver several satellites. Once the geometry and orbits have been determined, so that their coverage, or footprints, overlay the planet we have established a constellation.

The action-selection model we introduced in Chapter 6 for a single satellite, is now expanded to a spacecraft constellation. Sibly and McFarland have successfully proven that adding extra tasks to an autonomous agent using the cue-deficit action selection model is relatively simple [Sibly and McFarland 1976]. The new behaviours are each associated with a deficit, availability and accessibility. The behaviour which will be performed is, as explained in Chapter 3, the one with the highest *drk* product. The spacecraft are now endowed with the ability to transfer stored data between each other. Therefore the single satellite, in addition to the possibility of charging the battery, storing data and transmitting data to the ground station has now the possibility of performing a new behaviour. This new behaviour is to transmit data to a neighbouring satellite as shown in Figure 7.2. A spacecraft with full memory, and not in sight of the ground station, can transmit part of the stored information to a neighbouring spacecraft that has more memory space available.

Sun

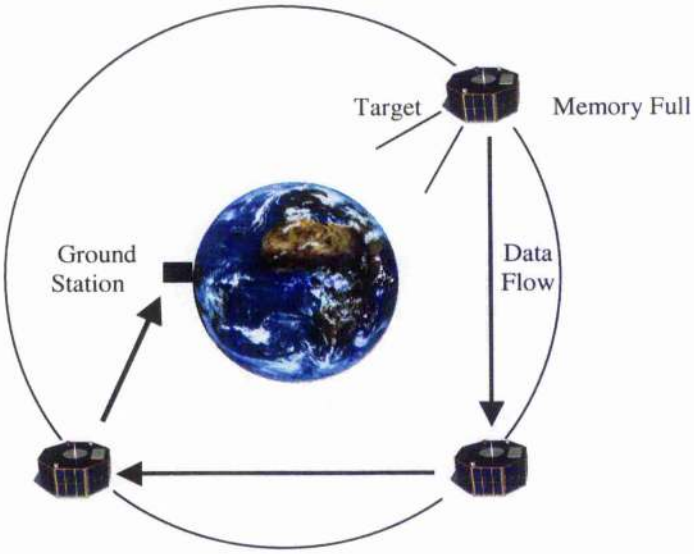

Figure 7.2 Co-operating satellite constellation

The introduction of a new behaviour demands the introduction of the deficit, availability and accessibility associated with it. The new deficit will be termed the satellite deficit and for satellite *i* has the following expression:

$$s_{ij} = \frac{m_i - m_j}{m_{max}} \qquad [7.1]$$

where m_i is the current memory load on satellite *i* and m_j is the memory load on satellite *j*. This deficit will be higher as the difference between the memory loads on the two spacecraft increases. The rate at which the behaviour can be performed is related to the availability associated with this behaviour, as we saw in Chapter 3:

$$\dot{s}_{ij} = -r^{s}_{ij} u^{s}_{ij} \qquad [7.2]$$

with the availabilty r_{ij}^{s} between satellite i and j defined as:

$$r_{ij}^{s} = \begin{cases} 1 & i \text{ visible to } j \\ 0 & i \text{ not visible to } j \end{cases} \qquad [7.3]$$

with $i = 1 - n$ and $j = 1 - n$, where n is the total number of spacecraft in the constellation. The cost function for the i^{th} satellite will therefore be modified by the addition of the satellite deficit:

$$C_i = b_i^2 + t_i^2 + m_i^2 + \sum_j s_{ij} \qquad [7.4]$$

Once again, using Pontriaygin's maximisation method allows us to find the optimal behaviour, which at any time is the one associated with the highest *drk* product. Every spacecraft will now be able to perform one of the following behaviours:

$$\text{Max}[b \cdot r_{\text{sun}} \cdot k_{\text{sun}}] \Rightarrow \text{Charge the battery} \qquad [7.5a]$$

$$\text{Max}[m \cdot r_{\text{target}} \cdot k_{\text{target}}] \Rightarrow \text{Record data} \qquad [7.5b]$$

$$\text{Max}[t \cdot r_{\text{ground station}} \cdot k_{\text{ground station}}] \Rightarrow \text{Transmit to Earth ground station} \qquad [7.5c]$$

$$\text{Max}[s_{ij} \cdot r^{s}_{ij} \cdot k^{s}_{ij}] \Rightarrow \text{Transmit to neighbouring spacecraft} \qquad [7.5d]$$

This leads to a modification of the action selection Simulink model shown in Chapter 5. In Figure 7.3 we can see the new model. Data is passed between satellites through an Inter-Satellite-Link at a rate of 2500 bits/sec and requiring a power consumption of 1 Watt [Wertz 1992].

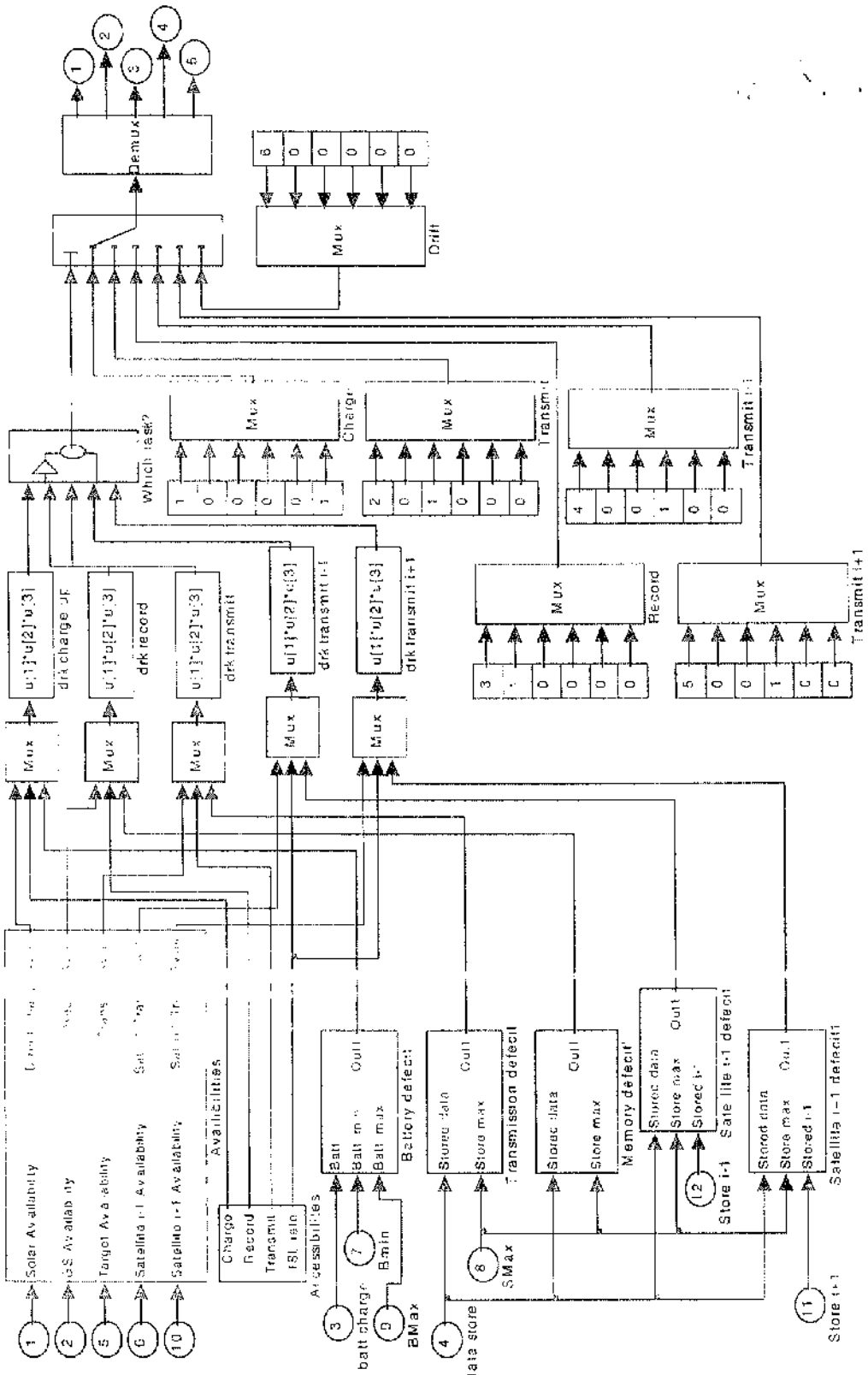

Figure 7.3 Action selection model for spacecraft in constellation

7.6 CASE STUDY

Let us consider the situation of an eight spacecraft constellation orbiting the Earth in a circular polar orbit with a radius of 7000 km. This orbital radius has been chosen since this is the minimum altitude to allow a spacecraft to be in sight of another neighbouring spacecraft and therefore be able to transmit data between each other. In Figure 7.4 we can see the geometrical considerations for this problem.

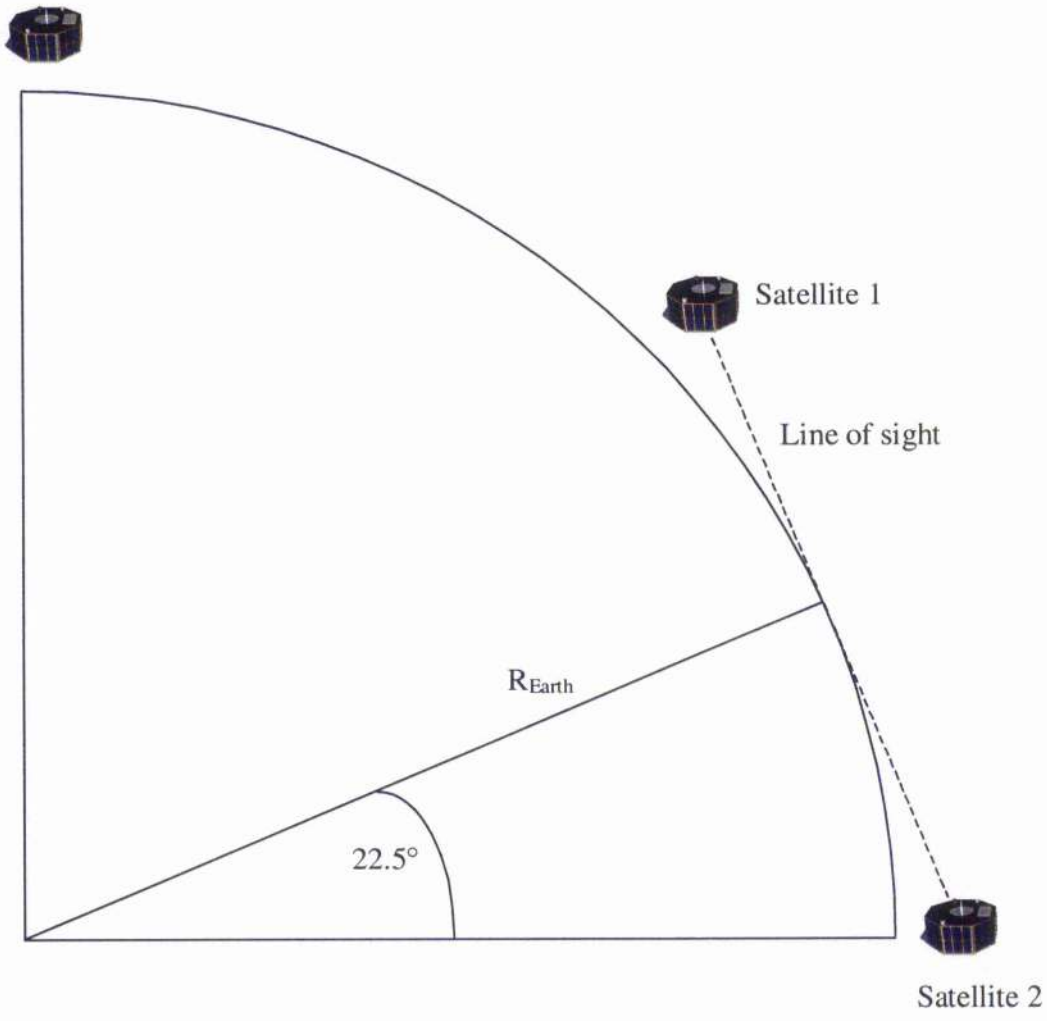

Figure 7.4 Geometrical considerations for spacecraft to spacecraft line of sight

In the case of an equally spaced, eight spacecraft constellation there is a 45° angle between neighbouring satellites. Therefore the minimum altitude requirement is given by the following simple trigonometric relationship:

$$R_{orbit} = \frac{R_{Earth}}{\cos(22.5)} = 6904 \text{ km} \qquad [7.6]$$

where R_{orbit} is the minimum orbital radius required for two neighbouring spacecraft to be in sight of each other, and R_{Earth} is the orbital radius of Earth.

In Tables 7.1-7.3 we can see the orbital, environmental and spacecraft parameters selected for the case study. The simulation runs for 60 orbits. In Figures 7.5-7.8 we can see the results of the simulation.

Parameter	Value
Semi major axis (km)	7000
Eccentricity	0
Inclination (deg)	86
Right ascension (deg)	0
Argument of perigee	0
Orbital period (sec)	5826

Table 7.1 Orbital Parameters

Parameter	Value
Ground station latitude (deg)	40
Ground station longitude (deg)	0
Target latitude (deg)	57
Target longitude (deg)	180

Table 7.2 Ground station and target parameters

Parameter	Value
Maximum battery charge (KJ)	24
Minimum battery charge (KJ)	8
Initial battery charge (KJ)	16
Maximum temperature (K)	350
Minimum temperature (K)	220
Initial temperature (K)	300
Maximum data storage (Mbits)	5
Minimum data storage (Mbits)	0
Initial data storage (Mbits)	0
Battery charge accessibility	1
Recording accessibility	1
Transmission accessibility	1
Spacecraft-to-spacecraft accessibility	1
Moment of Inertia (Kgm^2)	60

Table 7.3 Spacecraft parameters

In Figure 7.5 we can see the total amount of data, which is being transmitted by the spacecraft. As can be appreciated there is an almost constant stream of data being received by the ground station. This can be understood easily by looking at Figure 7.6 which shows see the global availability of the ground station. The global availability is defined as the sum of the ground station availabilities for each individual satellite. The spacecraft start downloading data after approximately 5 orbits: this because each spacecraft has to fill up its internal memory before the *drk* product associated with transmitting the data to a neighbouring spacecraft can 'compete' with the other behaviours. It should also be noted that there is an almost constant flux of information being received by the ground station as at least one spacecraft is always in view of the ground station, again as can be seen from Figure 7.6. It should also be noted how, as was explained in Chapter 5, the availability changes as the spacecraft move in their orbit and the ground station rotates below them with the Earth. Also there are several instances in which two or more spacecraft can view the ground station, highlighted by the increase in amount of data received.

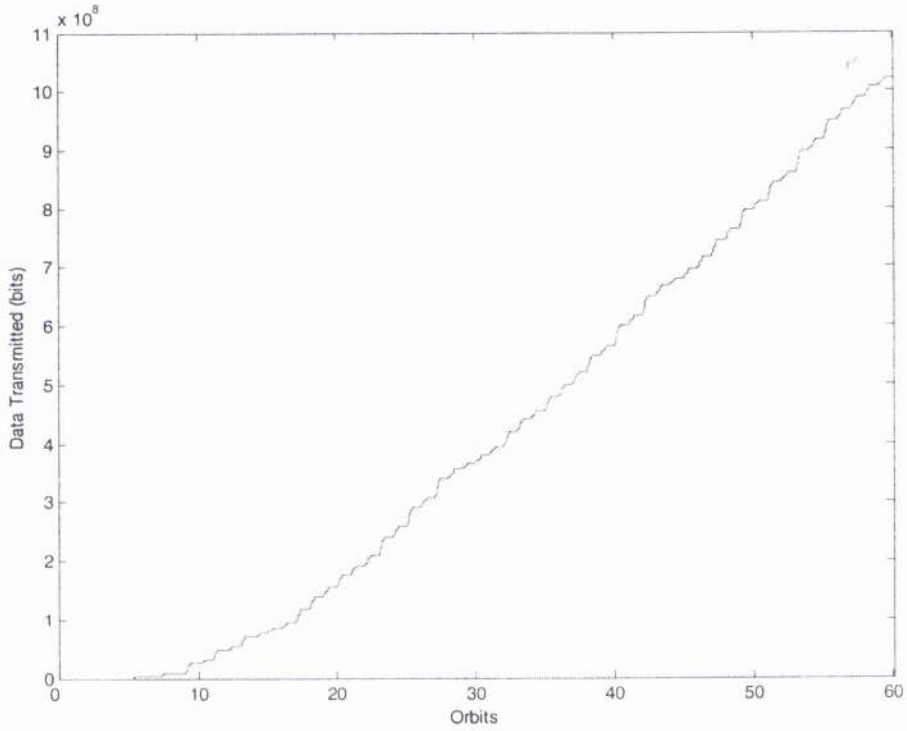

Figure 7.5 Data received by ground station

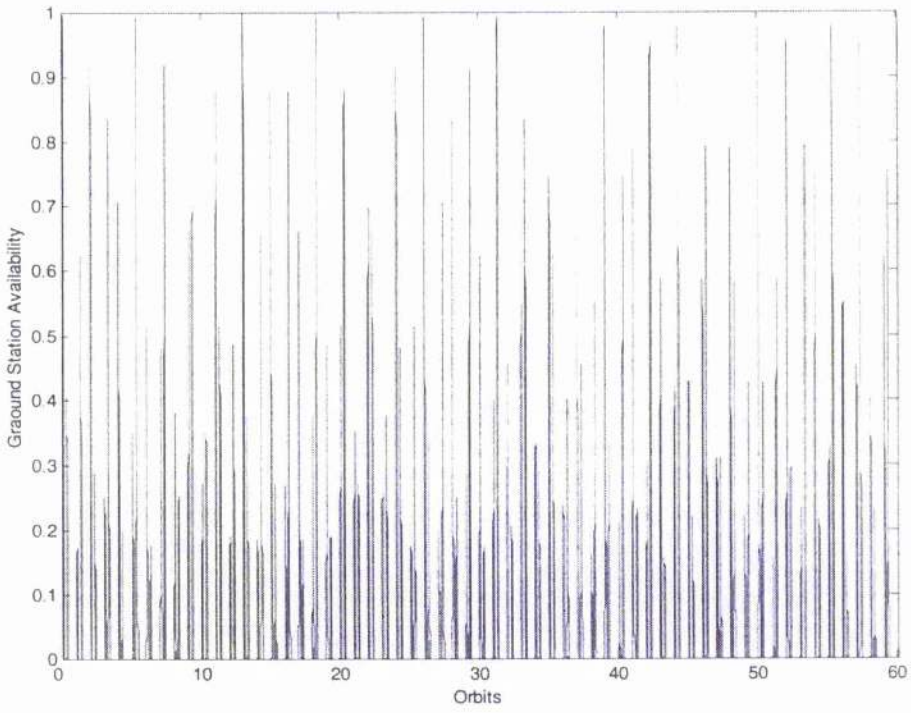

Figure 7.6 Ground station availability for constellation

What is more interesting however is to have a closer inspection of what happens with the individual satellites in Figures 7.7-7.8. Generally, as satellite j transmits data to the Earth ground station, its available memory space increases. This will lead to an increase in the satellite transmission deficits of the two neighbouring satellites s_{j-1} and s_{j+1}. Depending on the magnitude of the other *drk* products the neighbouring satellites will therefore be able to transmit data to satellite j should this behaviour prevail. In the case of Figure 7.7 and 7.8 we can see that satellite 3 has available memory space and satellite 4, not being able to download data to the Earth ground station has the opportunity of decreasing its memory load deficit by transmitting data to it. Similarly as satellite 4 is dumping part of its stored data to satellite 3 its memory load will decrease. This means that its satellite transmission deficit will increase and therefore satellite 5 will have the possibility of reducing its stored memory by transmitting data to satellite 4. This data flow has two positives effects which affect both the individual spacecraft and the overall constellation: the first is reducing the memory load of the individual spacecraft and therefore having a more balanced load throughout the constellation, the second is having an almost constant stream of data reaching the ground station.

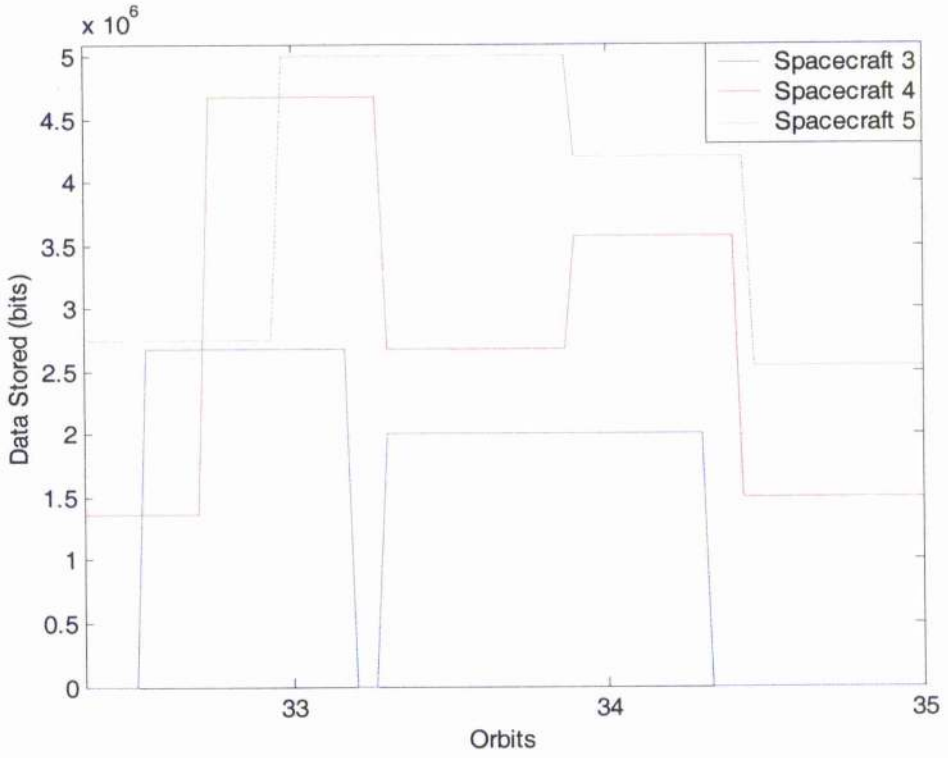

Figure 7.7 Data stored for satellites 3, 4 and 5.

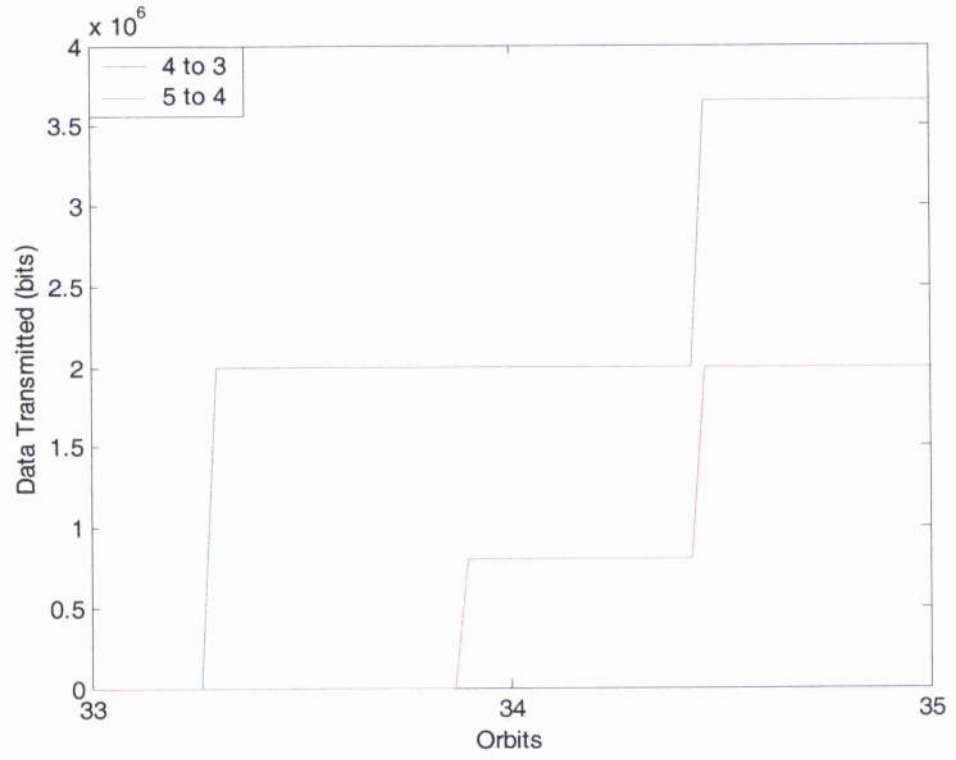

Figure 7.8 Data transmitted from satellite 5 to satellite 4, and satellite 4 to satellite 3

7.7 SPACECRAFT FAILURE

Once again it is vital that the action selection algorithm is tested to determine its robustness. Having considered individual component failures in Chapter 6 we will now look at what happens in the case of a total spacecraft failure within a constellation [Radice et al. 2001]. A mission scenario is proposed, where the orbital, environmental and spacecraft parameters are listed in Tables 7.1-7.3. An eight spacecraft constellation, orbits the Earth in a low polar orbit, of which only two are equipped with a transmitter to down-link data to a ground station. The remaining six spacecraft, equipped with Inter-Satellite-Links only, will therefore have to rely on the two transmitting spacecraft to download all data back to the ground station. It is expected that the behavioural algorithm will be able to account for this situation and successfully schedule the tasks to ensure that as much data as possible is transmitted back to Earth. After just over 40 orbits, one of the two transmitting spacecraft is failed, leaving the six spacecraft to rely solely on the remaining main spacecraft. It is expected that the action selection algorithm will reschedule the sequential behaviour to take into account this new situation, and still manage to accomplish the mission goal of downloading data, while never placing itself in an irrecoverable position. In Figures 7.9-7.10 we can see the results of such a simulation. It would be expected that the two transmitting spacecraft would download a similar volume of data, but we can see that one broadcasts a larger amount than the other in Figure 7.9. However, looking at the situation more closely, this behaviour is consistent with the action selection algorithm; as more data is sent to the ground station the bigger the size of the available memory becomes, into which the neighbouring satellites can transmit part of their load. This behaviour can also be explained and understood by looking at

the availability of the ground station with respect to the two transmitting spacecraft in Figure 7.10. We can see that before the failure, spacecraft 2 has higher average ground station availability than spacecraft 1. This means that, not only the *drk* product associated with the 'transmit' behaviour will be greater, but also that the time spent flying over the ground station will be longer. This has the implication that more data can be downloaded to the ground station by spacecraft 2 compared to spacecraft 1. As a consequence, the available memory space will be larger for spacecraft 2 than for spacecraft 1, meaning that the neighbouring satellites can transmit more of their data to it. After the spacecraft failure we can see that the constellation successfully reschedules itself and that the one remaining transmitting spacecraft is now downloading more data than before the failure. This is obvious, as spacecraft 1 is now the only satellite that can download data to the ground station. Therefore the rest of the satellites have to transmit their stored data to a neighbouring spacecraft until it reaches spacecraft 1 which will then proceed to the downlink. Again this purely emergent behaviour is a result of the interaction of the rules being implemented on each individual spacecraft, and not built-in to the action selection algorithm a priori.

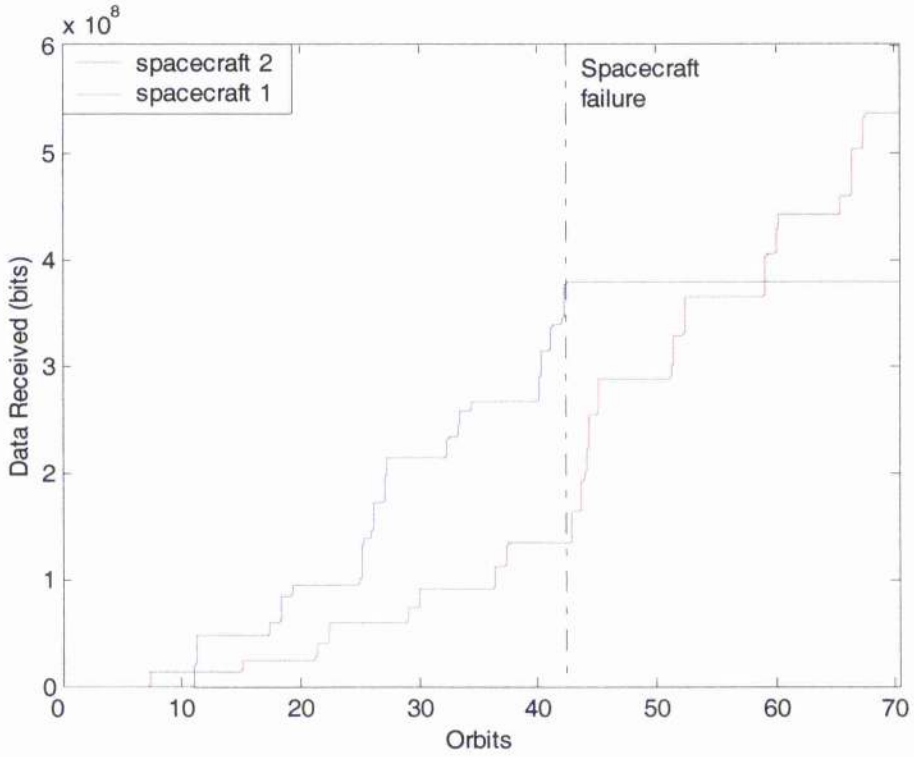

Figure 7.9 Data received by ground station

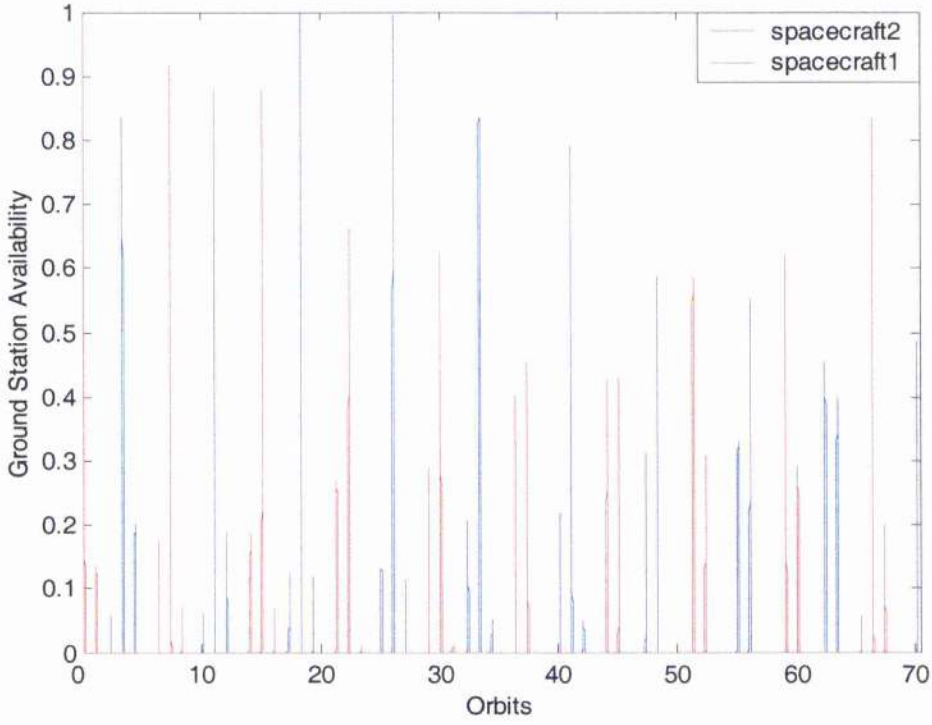

Figure 7.10 Ground station availability

It is interesting to note how this new configuration fares against a traditional constellation, in which all the spacecraft can download data to the ground station. In Figure 7.11 we can see the comparison in the data received by the ground station between a configuration in which eight spacecraft can transmit, and a configuration in which only two spacecraft can transmit data to the ground station. After 40 orbits one of the two transmitting spacecraft is failed leaving the second constellation with only one transmitting satellite. It can be seen that the 'full' constellation performs better than the 'two' constellation, with the ground station receiving approximately $1.5x10^8$ bits of data more just before the spacecraft is failed. This should be expected as in one configuration there is always at least one spacecraft in view of the ground station, while in the other the viewing opportunities are more limited. Together with the reduced ground station availability, which can be appreciated comparing Figures 7.6 and 7.10, we also have to consider that the download time is limited by the fly-by of the spacecraft over the ground station. After just over 40 orbits one spacecraft is failed and the gap in performance between the two constellations increases. The reduction in the performance of the degraded constellation has to be expected, as there is now only one spacecraft that can download data to the ground station. We can see that in less than 30 orbits the difference in downloaded data is increased to $4x10^8$ bits.

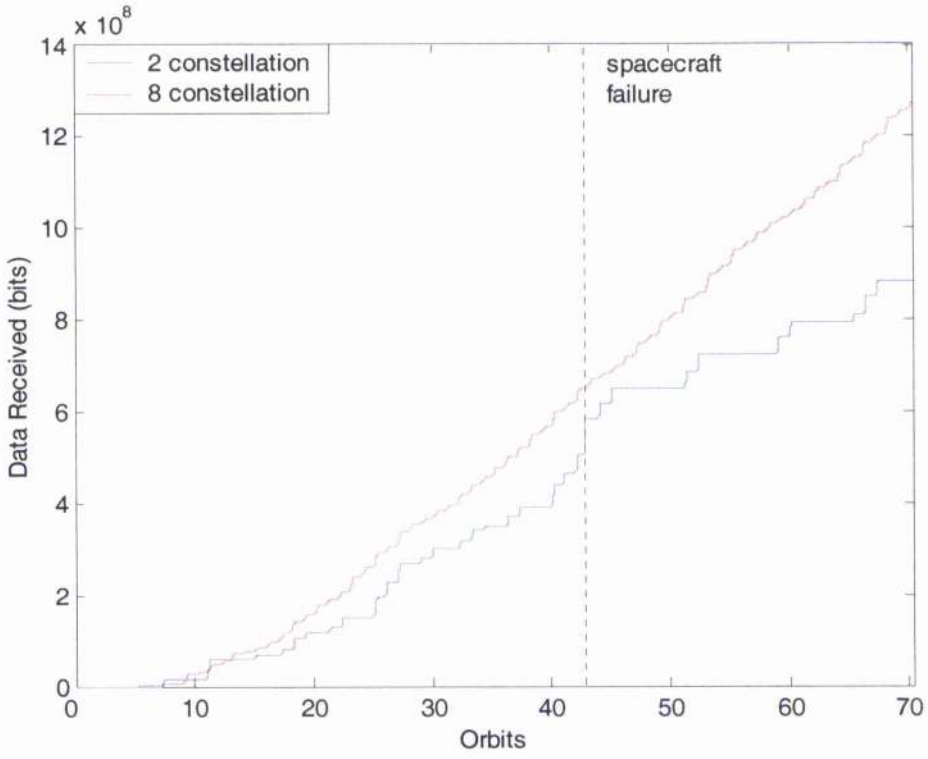

Figure 7.11 Comparison between 8 transmitting spacecraft and 2 transmitting spacecraft constellations.

7.8 COST FUNCTION ANALYSIS

As was done in Chapter 6 for the individual spacecraft, we will now try to determine if the satellite constellation exhibits different overall performances depending on the type of cost function associated with its state space [Radice et al. 2000]. We will choose three different cost functions to determine which one provides the best performance. Once again the best spacecraft performance is here defined as the amount of data received by the ground station, while not placing itself in an irrecoverable position. The spacecraft, environmental and orbital parameters are listed in Tables 7.4-7.6.

Parameter	Value
Semi major axis (km)	7000
Eccentricity	0
Inclination (deg)	0
Right ascension (deg)	0
Argument of perigee	0
Orbital period (sec)	5826

Table 7.4 Orbital Parameters

Parameter	Value
Ground station latitude (deg)	40
Ground station longitude (deg)	0
Target latitude (deg)	180
Target longitude (deg)	0

Table 7.5 Ground station and target parameters

Parameter	Value
Maximum battery charge (KJ)	24
Minimum battery charge (KJ)	8
Initial battery charge (KJ)	16
Maximum temperature (K)	350
Minimum temperature (K)	220
Initial temperature (K)	300
Maximum data storage (Mbits)	5
Minimum data storage (Mbits)	0
Initial data storage (Mbits)	0
Battery charge accessibility	1
Recording accessibility	1
Transmission accessibility	1
Spacecraft-to-spacecraft accessibility	1
Moment of Inertia (Kgm^2)	60

Table 7.6 Spacecraft parameters

We will compare a normal quadratic cost function C_1, with a quadratic cost function that emphasize the work aspect of the spacecraft C_3. As was explained in Chapter 3 the choice of a quadratic function was for mathematical simplicity only, but any convex function could be used. The third cost function C_2, will therefore be of the exponential form.

$$\begin{aligned} C_1 &= b^2 + m^2 + t^2 \\ C_2 &= e^b + e^m + e^t \\ C_3 &= b^2 + \beta(m^2 + t^2) \end{aligned} \qquad [7.7]$$

where $\beta = 10$ is a scaling factor inserted in the cost function equation to increase the weighting on performing useful work. In Figure 7.11 we can see the result of a 50 orbit simulation. It can easily be seen that the cost function C_1, provides the worst spacecraft performance. The quadratic cost function that emphasises work, C_3, downloads close to twice the amount of data than a normal quadratic cost function. This because the spacecraft will, almost always, record and transmit data when flying over the target or ground station. The best performance is however provided by the exponential cost function, C_2. This should have been expected as the cost function is strictly linked to the action selection algorithm through the deficit of a state variable. This is because the cost of possessing the deficit of a state variable increases exponentially, and not quadratically any more, the further away from the homeostatic equilibrium position.

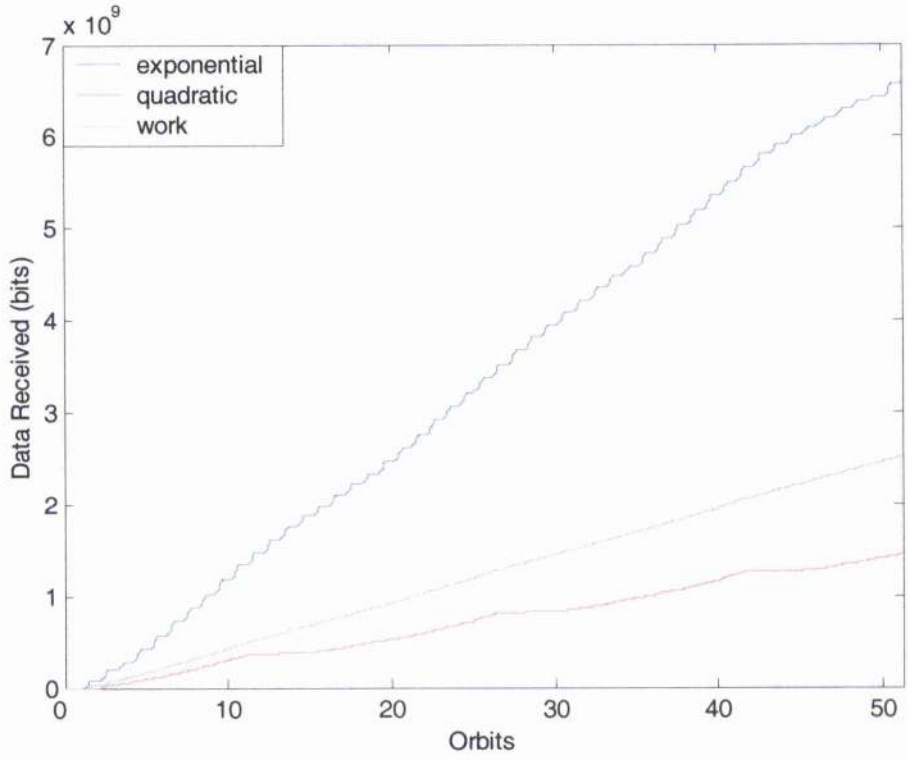

Figure 7.12 Cost function comparison

7.9 CONCLUSIONS

The action selection algorithm has been expanded from a single spacecraft to a constellation of satellites. New deficits, availabilities and accessibilities were introduced to account for the increased number of tasks the spacecraft can perform. It was shown that the action selection algorithm successfully sequences tasks to achieve both mission goals and spacecraft survival. To test the robustness of the action selection algorithm the constellation was subjected to critical failures. It was shown that the constellation successfully reschedules its tasks to account for the spacecraft failure. Finally an investigation of the choice of the cost function affects the performance of the constellation was performed.

CHAPTER VIII

CONCLUSIONS

8.1 REVIEW

A review of spacecraft autonomy, and the approaches to this issue by the main international space agencies, NASA, ESA and ISAS, was initially performed in Chapter 1. Together with this, an overview of current approaches to autonomy ranging from fuzzy logic, to neural networks, through expert systems was provided. The state space analysis was shown to be an appropriate framework for the multi-dimensional problems of autonomous behaviour in Chapter 2. Ethological studies of biological systems allow us to determine the causal factors of behaviour resulting from both the animal's perception of the environment and its internal stimuli. This led to the introduction of the concept of motivational isoclines and switching lines, or surfaces, which separate the candidate states, which are a combination of behavioural tendencies. In Chapter 3 these ethological theories and methods were applied to autonomous agents. Mathematical foundations were introduced with the concept of cost function, availability and accessibility, and the optimal behaviour formalised through Pontryagin's Maximum Principle. A flexible attitude control method was discussed in Chapter 4, where the development of the potential function method from Lyapunov's Second Method and the application to spacecraft attitude control problem was introduced. The potential function method provides a robust, highly flexible

control method, and in addition, stability, and convergence is ensured in a smooth manner. The method was applied in the case of a continuous torque control and a discrete on-off torque control. Multiple pointing constraints in the environment were added, through the introduction of a high potential region, and slewing to multiple intermediate attitudes before the final goal attitude was investigated. The environmental and spacecraft models were presented in Chapter 5. The cue-deficit method together with the potential function method were then used to control a 6 degrees-of-freedom dimensional model of a spacecraft in Chapter 6. To test the robustness of the spacecraft, the subsystems, solar arrays, transmitter and camera, were subjected to various degrees of failure and it was shown that the spacecraft still accomplished mission goals, albeit in a degraded manner. The influence of different types of polynomial cost functions was then considered together with the analysis of different mission orbits. Finally, in Chapter 7, the single satellite model was expanded to a clustered formation and new spacecraft behaviours were introduced. Again to test the robustness of the algorithm, the constellation was subjected to failures, and it was shown that the total failure of a member of the cluster does not compromise the overall success of the mission.

8.2 RECOMMENDATIONS

We have introduced a scheme for sequencing tasks on-board a spacecraft. The action selection algorithm is easily implemented by virtue of its computational simplicity. Moreover, the strategy is derived from optimal control theory. The model is however somewhat simplified, and an actual spacecraft may have several more

operational tasks that may be autonomously controlled or be scheduled or commanded by a ground station. This method however may easily incorporate additional tasks which will either form part of the action selection process, or which can be scheduled at a particular time by setting the *drk* product to equal unity at a fixed time. Adding extra tasks is relatively straightforward; each new behaviour will be given a deficit, availability and accessibility. The resulting behaviour will always be the one with the highest *drk* product. A significant advantage of such a method is that the spacecraft measures environmental parameters (such as the presence of sunlight or ground station) and internal parameters (such as battery charge and memory level). Complex models of the environment are not required to select the appropriate behaviour. Also, it is not necessary to have complex models of the spacecraft and its subsystems. If we consider the battery charge as an example, the model used for it is not directly relevant to the performance of the action selection algorithm; the algorithm uses the *measure* of the battery charge rather than using a *model* of the battery charge. Therefore, we can expect that the addition of more complex and numerous spacecraft subsystems will not change the qualitative behaviour of the algorithm.

Any future progress of this model can be divided into the near-term improvement of the constellation model, the medium-term enhancement of the potential function and action selection methodologies and the long-term development of a physical prototype. Expansion of the model of constellations of co-operating spacecraft to include more satellites, allow for sensor sharing and emergent solutions to achieve mission goals should be the first aim of any future work. We could, for example, envision the situation where advanced knowledge, such as satellite i informing satellite $i-1$ that the target has cloud cover, is available. This would cause

a change in the accessibility of the target for satellite $i-1$, and therefore a change of the *drk* products, so as to ensure that a more useful activity is performed.

With regards to the action selection methodology, rigorous analysis of the mathematical basis of the cue-deficit methodology to investigate extensions to the algorithm, for example to on-line learning, is expected, together with the detailed analysis of competing algorithms, such as fuzzy logic, stochastic methods, finite state machines or traditional scheduling methods. The extension of the methodology to a hybrid system with conventional scheduling algorithm as top-level planner and the reactive behaviour-based system below should be performed to evaluate its performance.

In the long term, with a view to producing reliable flight software, detailed definition of mission scenarios for single spacecraft and constellations, Earth orbiting and planetary missions, will have to be performed. High fidelity simulations of these scenarios will also allow the critical evaluation of the methodologies developed during the course of future work. The method should also be extended to include a detailed model of a generic power system, attitude control actuators and appropriate payloads, SAR, optical and hyperspectral cameras, ultimately leading to future on-orbit flight testing and evaluation.

BIBLIOGRAPHY

Amari S. I., "A Theory of Adaptive Pattern Classifiers", *IEEE Transactions*, Vol. 16, pp 299-307, 1967.

Axelrod R., "*The Evolution of Cooperation*", Basic Books, New York, 1984.

Azoff E. M., "*Neural Network Time Series Forecasting of Financial Markets*", John Wiley & Sons, London, 1994.

Baerends G. P., Brower R., Waterbolk H. T., "Ethological Studies of *Lebistes Reticulatus* (Peters). 1. An analysis of the male courtship patter", *Behaviour*, Vol. 8, pp. 249-334, 1955.

Benzinger T. H., "Heat regulation: Homeostasis of Central Temperature in Man", *Physiological Review*, Vol. 49, pp. 671-759, 1969.

Bernard D., Dorais G., Gamble E., Kanefsky B., Kurien J., Man G. K., Millar W., Muscettola N., Nayak P., Rajan K., Rouquette N., Smith B., Taylor W., Tung Y., "Spacecraft Autonomy Flight Experience: the DS1 Remote Agent Experiment", *AIAA 1999*, Albuquerque, NM, 1999.

Bernard J., Dufour F. Gaudon P., Ceolin T., Kerambrun S., "Rosetta Mission Analysis of the Landing Phase on a Comet", *AIAA/AAS Astrodynamics Specialists Conference*, Monterey, CA, 2002.

Bilgiç T., Türksen I. B., "Measurement of Membership Functions: Theoretical and Empirical Work", *International Handbook of Fuzzy Sets and Possibility Theory*, Kluwer Academic, Dordrecht, 1998.

Blumberg B., "Action-Selection in Hamsterdam: lessons from ethology", *From Animals to Animats 3: Third International Conference on the Simulation of Adaptive Behaviour*, Brighton, United Kingdom, 1994.

Bolles R.C. "*Theory of Motivation*", Harper and Row, New York, 1967.

Bonnet R. M., "European Space Science – In Retrospect and in Prospect", *ESA Bulletin*, No. 81, 1995.

Bond A. H., "An Architectural Model of the Primate Brain", *Department of Computer Science, University of California*, Los Angeles, 1996.

Brooks R., "A Robust Layered Control System for a Mobile Robot", *IEEE Journal of Robotics and Automation*, Vol. 2, pp. 14-23, 1986.

Brown C. E., Phillips M. E., "Expert Systems for Internal Auditing", *Internal Auditor*, Vol. 49, No. 4, pp. 23-28, 1991.

Buchanan B. G., Shortliffe E., "*Computer-based Medical Consultation: the MYCIN Experiment at Stanford*", American Elseiver, New York, 1976.

Buckland R., Johnson J., "The Arthur C. Clarke Mission: Self-Organising Imaging Robot Explorers in the Oceans of Europa", *50th International Astronautical Congress*, Amsterdam, 1999.

Carrara V., Rios Nieto A., "A Neural Network Satellite Attitude Controller with Error Based Reference Trajectory", *XIV Symposium on Space Flight Dynamics*, Brazil, 1999.

Cook R., "Mars Pathfinder Mission Operations: faster, better, cheaper on Mars", *IEEE Aerospace Conference*, Snowass, CO, 1998.

Crespi B. J., Choe J. C., "*The Evolution of Social Behaviour in Insects and Arachnids*", Cambridge University Press, 1997.

Dallas S. S., "Space Interferometry Mission", *IEEE Aerospace Conference*, Snowmass, CO, 1998.

Darwin C., *On the Origin of Species by Means of Natural Selection, or the Preservation of Favoured Races in the Struggle for Life*, Murray, London,1859.

Dawkins R., "*Climbing Mount Improbable*", Penguin Books Ltd., London, 1996.

de LaFontaine J., Buijs J., Vuilleumier P., Van den Braembussche P., Mellab K., "Development of the PROBA Attitude Control and Navigation Software", *4th ESA International Conference on Spacecraft Guidance, Navigation and Control Systems*, Noordwijk, 1999

Dixit A. K., "*Optimization in Economic Theory*", Oxford University Press, 1976.

Duda R., Gaschnig J., Hart P., "Model Design in the Prospector Consultant System for Mineral Exploration", *Expert Systems in the Microelectronic Age*, pp. 153-167, Edinburgh University Press, Edinburgh, 1979.

Elgerd O., "*Control Systems Theory*", McGraw-Hill, New York, 1967.

ESA, "Horizon 2000 Plus Implementation", *ESA Space Science Newsletter*, No. 34, 1998.

ESA, "SMART-1: Mission Overview", http://www.sci.esa.int/smart/

Feigenbaum E. A., Buchanan B. G., Lederberg J., "On Generality and Problem Solving: a case study using the DENDRAL program", *Machine Intelligence*, pp. 105-190, Edinburgh University Press, Edinburgh, 1971.

Fikes R. E., Nilsson N. J., "STRIPS: a new approach to the application of theorem proving to problem solving", *Artificial Intelligence*, Vol. 2, pp. 189-208, 1971.

Fisher R. A., *The Genetical Theory of Natural Selection*, Claredon Press, Oxford, 1930.

Fitzsimons J. T., "La Soif Extracellulaire", *Annals of Nutrition and Alimentation*, Vol.22, pp. 131-144,1968.

Frenster J. H., "Expert Systems and Open Systems in Medical Artificial Intelligence", *Congress on Medical Informatics*, San Francisco, CA, 1989.

Fujita M., Kageyama K., "An Open Architecture for Robot Entertainment", *Proceeding of Autonomous Agents 97*, ACM Press, 1997.

Fukushima K., "Cognitron: A Self-organising Multi-layered Neural Network", Biological Cybernetics, Vol. 20, pp. 121-136, 1975.

Gillies E. A., Johnston G. A. Y., McInnes C. R., "Action Selection Algorithms for Autonomous Microspacecraft", *Journal of Guidance, Control and Dynamics*, Vol. 22, No. 6, pp. 914-916, 1999.

Gorr W. L., Osburn L., Szczypula J., "Comparative Study of Artificial Neural Network and Statistical Models for Predicting Student Grade Point Averages", *International Journal of Forecasting*, Vol. 10, pp. 17-34, 1994.

Grantham W. J., Chingcuanco A. O., "Lyapunov Steepest Descent Control of Constrained Linear Systems," *IEEE Trans. on Automatic Control*, Vol. AC-29, No. 8, 1984.

Grossberg S., "Adaptive Pattern Classification and Universal Recording: Feedback Oscillation, Olfaction and Illusions", *Biological Cybernetics*, Vol.22, pp. 187-207, 1976.

Grudnitski G., Osburn L., "Forecasting S&P and Gold Futures Prices: an application of neural networks", *The Journal of Futures Markets*, Vol. 13, No. 6, pp. 631-643, 1993.

Halliday T. R., "Sex and Evolution", *Behaviour and Evolution*, Cambridge University Press, pp. 150, 1994

Hallman P. J., "*Optical Signals*", Indian University Press, Bloomington, 1977.

Hamilton W. D., "The Evolution of Altruistic behaviour", *American Naturalist*, Vol. 97, pp. 379-384, 1963.

Hamilton W. D., "The Genetical Evolution of Social Behaviour", *Journal of Theoretical Biology*, Vol. 7, pp. 1-52, 1964.

Harris T. J., Stroud R. R., "The Control of Submerged Arc Welding Using Neural Network Interpretation of Ultrasound", *Artificial Neural Networks*, Vol. 2, pp. 1539-1546, North-Holland, Amsterdam and New York, 1992.

Hinde R. A., "Unitary drives", *Animal Behaviour*, Vol. 7, pp. 130-141, 1959.

Höhle U., "A Survey of the Fundamentals of Fuzzy Set Theory", *Handbook of Mechanical Engineering*, CRC Press, Boca Raton, 1997.

Horwitz D., El-Sibaie M., "Applying Neural Nets to Railway Engineering" *AI Expert*, pp. 36-41, January 1995.

Houston A. I., McFarland D. J., "On the Measurement of Motivational Variables", *Animal Behaviour*, Vol. 24, pp. 459-475, 1976.

Houston A. I., McFarland D. J., "Behavioural Resilience and its Relation to Demand Functions", Limits to Action: The Allocation of Individual Behaviour", pp.177-203, 1980.

Hyötniemi H., "Text Document Classification with Self-organising Maps", *Proceedings of Finnish Artificial Intelligence Conference – Genes, Nets and Symbols*, pp. 64-72, 1996.

Johnson A. E., Matthies L. H., "Precise Image-Based Motion Estimation for Autonomous Small Body Exploration", *5th International Symposium on Artificial Intelligence, Robotics and Automation in Space*, Noordwijk, 1999.

JPL, "Space Technology 5", 2000a,
http://nmp.jpl.nasa.gov/st5/about/index.html.

JPL, "*Autonomous Remote Agent*", 1998c,
http://nmp.jpl.nasa.gov/ds1/tech/autora.html.

JPL, "*Integrated Ion and Electron Spectrometer*", 1998b,
http://nmp.jpl.nasa.gov/ds1/tech/spectrometer.html.

JPL, "*Mars Polar Lander Mission*", 1998d,
http://nmp.jpl.nasa.gov/msp98/lander/mission.html.

JPL, "*Nanosatellites*", 2000b,
http://nmp.jpl.nasa.gov/st5/technology/nanosats.html.

JPL, "New Millennium Program: The Program", 1996,
http://nmp.jpl.nasa.gov/

JPL, "*Deep Space 3 - Mission*", 1998e,
http://deepspace3.jpl.nasa.gov/proj/index.html.

JPL, "*Solar Electric (ion) Propulsion*", 1998a,
http://nmp.jpl.nasa.gov/ds1/tech/sep.html.

JPL, "*Space Technology 5*", 2000c,
http://nmp.jpl.nasa.gov/st5/science/index.html.

JPL, "Deep Space 3 - *Technology*", 1998f, http://deepspace3.jpl.nasa.gov/tech/index.html.

Jung D., "Cooperation Between Autonomous Agents", *Proceedings of 1995 Yamabico Symposium*, Tsukuba, Japan, 1995.

Kaiser D., Losick R., "How and Why Bacteria Talk to Each Other", *In Cell*, Vol. 73, No. 5, pp. 873-885, 1993.

Kathman R. M., "Neural Networks for the Mass Appraisal of Real Estate", *Computers Environment & Urban System*, Vol. 17, pp. 372-384, 1993.

Keeton W. T., "The Orientational and Navigational Basis of Homing in Birds", *Advances in the Study of Behaviour*, Vol. 5, pp. 48-132, 1974.

Kerr R. A., "An Icy World Looks Livelier", *Science*, Vol. 274, pp. 478, 1997.

Kirchner F., Hertzberg J., "A Prototype Study of an Autonomous Robot Platform for Sewerage System Maintenance", *Autonomous Robots*, 1997.

Klein R., "Antilock Braking System and Vehicle Speed Estimation Using Fuzzy Logic", *1st Embedded Computing Conference*, Paris, 1996.

Klopf H. A., "*The Hedonistic Neuron: A Theory of Memory, Learning and Intelligence*" Hemisphere, Washington DC, 1982.

Krebs J. R., "Behavioural Aspects of Predation", *Perspectives in Ethology*, pp. 73-111, Plenum Press, New York, 1973.

Kubota T., Hashimoto T., Sawai S., Kawaguchi J., Ninomiya K., "An Autonomous Navigation and Guidance System for MUSES-C Asteroid Landing", *4th IAA International Conference on Low Cost Planetary Missions*, Laurel, MD, 2000.

Lack D., *The Life of a Robin*, Cambridge University Press, 1943.

Lewis J. S., "Satellites of the Outer Planets: Their Physical and Chemical Nature", *Icarus*, Vol. 15, pp. 174-185, 1971.

Likins P. W., Kane T. R., Levison D. A., *Spacecraft Dynamics*, McGraw-Hill, New York, 1983.

Lu C., "Space-Borne CCD Camera System Test", *International NAISO Congress on Information Sciences Innovations*, Dubai, UAE, 2001.

Mackintosh N. J., "Stimulus Selection: Learning to Ignore Stimuli that Predict no Change in Reinforcement", *Constraints on Learning*, pp. 75-100, Academic Press, London, 1973.

Martin W. A., Fateman R. J., "The MACSYMA System", *Second Symposium on Symbolic Manipulation*, Los Angeles, CA, 1971.

Maynard Smith J., "Optimization Theory in Evolution", *Annual Review of Ecology and Systematics*, Vol. 9, pp. 31-56, 1978.

Mayor M., Queloz D., "A Jupiter-Mass Companion to a Solar Type Star", *Nature*, Vol. 378, No. 6555, pp. 355-359, 1995.

McCarthy J., "*LISP 1.5 Programmer's Manual*" MIT Press, Cambridge, 1962.

McCleery R. H., "On Satiation Curves", *Animal Behaviour*, Vol. 25, pp. 1005-1015, 1978.

McCulloch W. S., Pitts W., "A Logical Calculus of the Ideas Immanent in Nervous Activity", *Bulletin of Mathematical Biophysics*, Vol. 5, pp. 115-133, 1943.

McDermott J., "R1: A Rule Based Configurer of Computer Systems", *Artificial Intelligence*, Vol. 19, pp. 39-85, 1982.

McFarland. D. J., Houston A. I., *Quantitative Ethology. The State Space Approach*, Pitman. London, 1981.

McFarland D. J., "Interaction of Hunger and Thirst Motivated in the Barbary Dove", *Journal of Comparative Physiological Psychology*, Vol. 58, pp. 174-179, 1964.

McFarland D. J., "The Effect of Hunger on Thirst Motivated Behaviour in the Barbary Dove", *Animal Behaviour*, Vol. 13, pp. 286-292, 1965.

McFarland D. J., "*Feedback Mechanisms in Animal Behaviour*", Academic Press, London and New York, 1971.

McFarland D. J., "Stimulus Relevance and Homeostasis", *Constraints on Learning*, pp. 141-155, Academic Press, London, 1973.

McFarland D. J., "Form and Function in the Temporal Organisation of Behaviour", *Growing Points in Ethology*, Cambridge Press University, pp. 55-93, 1976.

McFarland D. J., "Decision Making in Animals", *Nature*, Vol. 269, pp. 15-21, 1977.

McFarland D. J., Budgell P., "The Thermoregulatory Role of the Feather Movements in the Barbary Dove (Sterptopelia Risoria)", *Physiology and Behaviour*, Vol. 5, pp. 763-771, 1970.

McFarland D. J., Sibly R., "Unitary Drives", *Animal Behaviour*, Vol. 20, pp. 548-563, 1972.

McFarland D. J., Sibly R. M., "The Behavioural Final Common Path", *Philosophical Transactions of the Royal Society*, (Series B), Vol. 270, pp. 265-293, 1975.

McFarland D. J., "Animals as Cost Based Robots", *International Studies in the Philosophy of Science*, Vol. 6, No. 2, pp.133-153, 1992.

McFarland D. J., Bosser T., *Intelligent Behaviour in Animals and Robots*, MIT Press, Cambridge, MA, 1992

McFarland D. J., Sibly R, M., "The Behavioural Final Common Path", *Philosophical Transactions of the Royal Society (Series B)*, Vol. 270, pp. 265-293, 1975.

McFarland D. J., Spier E., "Basic Cycles, Utility and Opportunism in Self-Sufficient Robots". *Robotics and Autonomous Systems*, Vol. 20. Pp. 179-190, 1997.

McInnes, C. R., "Path Constrained Manoeuvring Using Artificial Potential Functions", *European Space Agency Journal*, Vol. 17, No. 2, pp. 159-169, 1993.

McKay D. S., Gibson E. K., Thomas-Keptra K. L., Vali H., Romanek C. S., Chiller X. D. F., Maechling C. R., Zare R. N., "Search for Past Life on Mars: possible relic biogenic activity in Martian meteorite ALH84001", *Science*, pp. 273:924-930, August 1996.

McKinnon W. B., "Planetary Explorations: sighting the seas of Europa", *Nature*, Vol. 386, pp. 765-767 1997.

McQuade F., McInnes, C. R., "Autonomous Control for On-Orbit Assembly Using Potential Function Methods", *The Aeronautical Journal*, Vol. 101, No. 1008, pp. 255-262, 1997.

Miller W. T., Sutton R. S., Werbos P. J., "*Neural Networks for Control*", MIT Press, Cambridge, 1990.

Milsun J. H., "*Biological Control System Analysis*", McGraw-Hill, New York, 1966.

Minsky M., Papert S., "*Perceptrons*", MIT Press, Cambridge, 1969.

Mishkin A. H., Morrison J. C., Nguyen T. T., Stone H. W., Cooper B. K., Wilcox B. H., "Experiences with Operations and Autonomy of the Mars Pathfinder Microrover", *IEEE Aerospace Conference*, Snowmass, CO, 1998.

Muirhead B., Kerridge S., "The Deep Space 4 – Champollion Mission", *Acta Astronautica*, Vol. 45, No. 4-9, pp. 407-414, 1999.

NASA, "Europa Orbiter Mission Information", 1999,
http://www.jpl.nasa.gov/fire_ice/EO_info.htm

NASA, "SAMPEX", 2002,
http://sunland.gsfc.nasa.gov/smex/sampex/

NASDA, SELenological and ENgineering Explorer, 1998,
http://www.nasda.go.jp/projects/sat/selene/index_e.html

Nayak P. P., Bernard D E., Dorais G., Gamble Jr. E. B., Kanefsky B., Kurien J., Millar W., Muscettola N., Rajan K., Rouquette N., Smith B. D., Taylor W., Tung Y., "Validating the DS1 Remote Agent Experiment", *NMP: DS-1 Technology Validation Symposium*, Pasadena, CA, 2000.

Newell A., "The Knowledge Level", *Artificial Intelligence Journal*, Vol. 18, pp. 87-127, 1982.

Oatley K., Tonge D. A., "The Effect of Hunger on Water Intake in Rats", *Quarterly Journal of Experimental Psychology*, Vol. 21, pp. 162-171, 1969.

Oster G. F., Wilson E. O., "*Caste and Ecology in the Social Insects*" Princeton University Press, Princeton, 1978.

Pasteels J. M., Deneubourg J., Goss S., "Self-organization Mechanisms in Ant Societies: Trail Recruitment to Newly Discovered Food Sources", *From Individual to Collective Behaviour in Social Insects*, Birkauser Verlag, 1987.

Peltorana M., Pfurtscheller G., "Neural Network Based Classification of Non-Averaged Event Related EEG Responses", *Medical and Biological Engineering and Computing*, Vol. 32, pp. 189-196, 1996.

Pontryagin L. S., Boltyanskii V. G., Gamkrelidze R. V., Mishchenko E. F., *The Mathematical Theory of Optimal Processes*, John Wiley and Sons, New York, 1962.

Prosser C. L., "The Nature of Physiological Adaptation", *Physiological Adaptation*, American Physiological Society, Washington DC, 1958.

Prosser C. L., "*Comparative Animal Physiology*", W. B. Saunders, Philadelphia, London, Toronto, 1973.

Radice G., Gillies E.A.,Johnstone G. A. Y., McInnes C.R., "Autonomous Action Selection for Micro-satellite Constellations", *49st International Astronautical Congress*, Melbourne, Australia, 1998.

Radice G., McInnes C.R., "Constrained On-board Attitude Control Using Gas Jet Thrusters", *The Aeronautical Journal*, Vol. 103, No. 1030, pp. 549-556, 2000a.

Radice G., Gillies E.A., McInnes C.R., "Cost Function Analysis for Autonomous Clustered Micro-spacecraft", *51st International Astronautical Congress*, Rio de Janeiro, Brazil, 2000b.

Radice G., Gillies E.A., McInnes C.R., "Autonomous Satellite Constellation for Planetary Exploration", *International NAISO Congress on Information Sciences Innovations*, Dubai, UAE, 2001.

Radice G., McInnes C.R., "Multiple Target Selection and Obstacle Avoidance Using Potential Function Guidance Method", *AAS/AIAA Astrodynamics Specialists Conference*, Quebec City, Canada, 2001.

Rayman M. D., "*Deep Space 1: rocketing the future*", 1998, http://nmp.jpl.nasa.gov/ds1/gen/rocketing_future.html.

Reynolds R. T., Squyres W. T., Colburn D. T., McKay C. P., "On the Habitability of Europa", *Icarus*, Vol. 56, pp. 246-254, 1983.

Rimon E., Koditchek D. E., "Exact Robot Navigation Using Artificial Potential Functions", *IEEE Transactions on Robotics and Automation*, 1992

Roger, A. B., McInnes, C. R., "Safety Constrained Free-Flyer Path-Planning at the International Space Station", *Journal of Guidance, Control and Dynamics*, Vol. 23, No. 6, pp. 971-980, 2000.

Rosen R., "*Dynamical Systems Theory in Biology*", John Wiley, New York, 1970.

Rosenblatt F., "The Perceptron, a Probabilistic Model for Information Storage and Organization in the Brain", *Psychological Review*, Vol. 65, pp. 386-408, 1958.

Rosenblatt F., "*Principles of Neurodynamics: Perceptron and the Theory of Brain Mechanisms*", Spartan Books, Washington DC, 1962.

Roy A. E., *Orbital Motion*, Adam Hilger Ltd., Bristol, 1982.

Rozin P., Kalat J. W., "Specific Hungers and Poison Avoidance as Adaptive Specalizations in Learning", *Physiological review*, Vol. 78, pp. 459-486, 1971.

Ruspini E. H., "On the Semantics of Fuzzy Logic", *International Journal of Approximate Reasoning*, Vol. 5, pp. 45-88, 1991.

Saffiotti A., "The Uses of Fuzzy Logic in Autonomous Robot Navigation: A Catalogue Raisonné" *Soft Computing*, Vol.1, No. 4, pp. 180-197, 1997.

Schoener T. W., "Theory of Feeding Strategies", *Annual Review of Ecological Systems*, Vol. 2, pp. 369-404, 1971.

Schöneberg E., "Stock Price Prediction Using Neural Network: A Project Report", *Neurocomputing*, No. 2, pp. 17-27, 1990.

Schwehm G., Schulz, R., "Rosetta Goes to Comet Wirtanen", *Space Sciences Review*, Vol. 90, pp. 313-319, 1999.

Shin K. G., Cui X., "Design of a Knowledge-based Controller for Intelligent Control Systems", *IEEE Transactions on Systems, Man and Cybernetics*, Vol. 21, No. 2, pp. 368-375, 1991.

Sibly R. M., McFarland D. J., "A State Approach to Motivation", *Motivational Control Systems Analysis*, pp.213-250, Academic Press, London and New York, 1974.

Sibly R. M., "How Incentive and Deficit Determine Feeding Tendency", *Animal Behaviour*, Vol. 23, pp. 437-466, 1975.

Sibly R. M., McFarland D., "A State Space Approach to Motivation", *Motivational Control System Analysis*, Academic Press, London and New York, pp. 213-250, 1974.

Sibly R. M., McFarland D., "On the Fitness of Behaviour Sequences", *The American Naturalist*, Vol. 110, No. 974, pp. 601-617, 1976.

Simon H. A., Newell A., "Heuristic Problem Solving: The Next Advance in Operations Research", *Operations Research*, Vol. 6, pp. 1-10, 1958.

Spier E., McFarland D., "A Finer-Grained Motivational Model of Behaviour Sequencing", *From Animals to Animats 4: Fourth International Conference on the Simulation of Adaptive Behaviour*, Boston, MA, 1996.

Spooner J. T., Passino K. M., "Stable Adaptive Fuzzy Control for an Automated Highway System", *IEEE International Symposium on Intelligent Control*, Monterey, CA, 1995.

Srnivasan M. V., Chahl J. S., Nagle M.G., Weber K., Venkatesh S., Zhang S. W., "Low-level Vision in Insects and Applications to Robot Navigation", *Computational Intelligence: A Dynamic System Perspective*, IEEE Press, pp. 312-226, 1995.

Steels L., "Cooperation Between Distributed Agents Through Self Organisation", *Decentralized A.I.*, North-Holland, Amsterdam, pp. 175-196, 1990.

Steels L., "A Case Study in the Behaviour-Oriented Design of Autonomous Agents", *From Animals to Animats 3: Third International Conference on the Simulation of Adaptive Behaviour*, Brighton, United Kingdom, 1994.

Taipale T., Shigeoki H., "A comparative study of multi-robot systems". *Bulletin of the Electrotechnical Laboratory*, Vol., 56, No. 8, pp. 892-922, 1992.

Takle E. S., "Bridge and Roadway Frost: Occurrence and Prediction by Use of an Expert System", *Journal of Applied Meteorology*, Vol. 29, pp 727-734, 1990.

Tanaka K., Sugeno M., "Stability Analysis and Design of Fuzzy Control Systems", *Fuzzy Sets and Systems*, Vol. 45, pp. 135-156, 1992.

Terai H., "Application of Fuzzy Logic Technology to Home Appliances", *Fuzzy Engineering Toward Human Friendly Systems*, pp. 1118-1119, 1991.

Terano Y., Asai K., Sugeno M., "*Fuzzy Systems Theory and its Applications*", Academic Press, London and New York, 1992.

Teston F., Creasey R., Bermyn J., Mellab K., "PROBA: ESA's Autonomy and Technology Demonstration Mission", *48th International Astronautical Congress*, Turin, 1997.

Tobi T., Hanafusa T., "A Practical Application of Fuzzy Control for an Air-conditioning System", *International Journal of Approximate Reasoning*, Vol. 5, pp. 331-348, 1991.

Trivers R. L., "The Evolution of Reciprocal Altruism", *Quarterly Review of Biology*, Vol. 46, pp. 35057, 1971.

Ujihara H., Tsuji S., "The Revolutionary AI-2100 Elevator Group Control System and the New Intelligent Option Series", *Mitsubishi Electric ADVANCE 5-8*, 1988.

Vadali S.R., Junkins J.L. "Spacecraft Large Angle Rotational Manoeuvres with Optimal Momentum Transfer", *Journal of Astronautical Sciences*, Vol. XXI, No. 2, pp.217-235, 1983.

Walter C., *"Computer Power and Legal Language. The use of Computational Linguistics. Artificial Intelligence and Expert Systems in Law"*, Quorum Books, Newport, 1988.

Weismann A., "The All-Sufficiency of Natural Selection", *Contemporary Review*, Vol. 64, pp. 309-328, 1893.

Werbos P. J., *"Beyond Regression: New Tools for Prediction and Analysis in the Behavioral Sciences"*, Doctoral Thesis, Harvard University, 1974.

Werner R., "Ant Navigation: mini-brains – mega tasks – smart solutions", *International NAISO Congress on Information Science Innovations*, Dubai, UAE, 2001.

Wertz J., *Space Mission Analysis and Design*, Kluwer Academic Publisher, The Netherlands, 1992.

Widrow G., Hoff M. E., "Adaptive Switching Circuits", *Institute of Radio Engineering, Western Electronic Show and Convention*, Convention Record, Part 4, pp 96-104, 1960.

Wilson E. O., *"The Insects Societies: Their Origin and Evolution"*, Narcourt, Brace & Co., New York, 1971.

Wilson E. O., *"Sociobiology: The New Synthesis"*, Harvard, 1975.

Wilson S. W., "The Animat Path to AI", *From Animals to Animats: Proceedings of the First International Conference on Simulation of Adaptive Behaviour*, MIT Press, Cambridge, MA, pp. 115-21, 1991.

Winton A., Gerner J. L., Michel P., Morgan-Owen R., "The Transponder – A Key Element in ESA Spacecraft TTC Systems", *ESA Bulletin*, No. 96, 1996.

Wooton R. J., "A Note on the Nest raiding Behaviour of Male Sticklebacks", *Canadian Journal of Zoology*, Vol. 49, pp. 960-962, 1971.

Yasunobu S., Miyamoto S., "Automatic Train Operation by Predictive Fuzzy Control", *Industrial Applications of Fuzzy Control*, pp.1-18, North Holland, Amsterdam and New York, 1985.

Zadeh L. A., "Fuzzy Sets", *Information Control*, Vol. 8, pp. 338-353, 1965.

Zimmerman R., "Moon Rivers", *The Sciences*, Vol. 37, No. 2, pp. 11, 1997.

APPENDIX I

Mass and Volume First Estimate

The procedure used here is needed to determine the spacecraft's mass, volume and size [Wertz 1992].

STEP	INPUT DATA	PROCEDURE	OUTPUT DATA
1. Payload weight	0.2 kg	Starting point	-
2. Estimate dry weight	Payload weight	Multiply payload weight by 3.3	Dry wgt = 0.66 kg
3. Estimate propellant weight	Dry weight	Normal Range is 25 % of Dry Weight	Prop. wgt = 0 kg, as we assume the control to be performed through inertia wheels
4. Calculate loaded weight	Dry weight and propellant weight	Add	Load wgt = 0.66 kg
5. Estimate volume	Loaded weight	Divide loaded weight by average density of 79 kg/m^3	Volume = 0.008 m^3

Having chosen to model the satellite as a cube we determine that each face will measure 20 cm, which gives us a volume V = 0.2 X 0.2 X 0.2 = 0.008 m^3